PULMONARY IMMUNE ENVIRONMENT DETERMINES THE MANIFESTATION OF EXPERIMENTAL EMPHYSEMA

by
Nathachit Limjunyawong

A dissertation submitted to Johns Hopkins University in conformity with the requirements for the degree of Doctor of Philosophy

Baltimore, Maryland
May, 2015

ABSTRACT

The lung is a complex well-designed organ providing a large surface area for exchanging gas to provide oxygen to the body and eliminate carbon dioxide from the circulation. Because of its exposure to the environment, it is required to have active immunologic defense mechanisms to remove hazardous agents and maintain homeostasis. However, an aberration in this pulmonary immune environment can lead to several pathologic developments. Emphysema is characterized by progressive loss of alveolar surface area with a permanent airspace enlargement, and it is one of the major public health issues leading to serious morbidity and mortality. Disparities in individual immune responses interact with host genetic predispositions and environmental factors in a complex manner that impacts the susceptibility to develop emphysema. The overall goal of this thesis was to study immunological factors that are involved in determining the susceptibility to develop emphysema using a simplified elastase-induced murine model. First, we determined the susceptibility to develop emphysema in two common strains of mice. We found BALB/cJ mice to be much more sensitive to exogenous elastase compared to C57BL/6J mice. Based on gene expression analysis, we found different immunologic mechanisms that might underlie the differential progression of elastase-induced emphysema in these two mouse strains. In addition, MMP-producing macrophages (but not neutrophils or lymphocytes) were identified as the critical cells that mediate the extracellular matrix degradation in emphysema. Furthermore, we use genetically engineered mice to study the importance of several cytokine signaling pathways and transcription factors. We found important roles of IL-17A, IFN-γ, IL-33/ST2/MyD88, STAT6 and STAT3 in activating or modulating the macrophages to become more destructive. Lastly, we also showed that recent viral infections

could impact on the severity of emphysema following the acute elastase injury. In conclusion, the intricacy of genetic and environmental factors together influence immune responses in the lungs to determine the susceptibility to develop emphysema. This knowledge provides new insights into the cellular and molecular mechanisms that may be responsible for the heterogeneity observed in human susceptibility to develop emphysema.

THESIS READERS:

Advisor:

Wayne Mitzner, Professor	Environmental Health Sciences/SPH

Voting members:

Robert Wise, Professor	Medicine (Pulmonary)/SOM
Marsha Wills-Karp, Professor	Environmental Health Sciences/SPH
Alan Scott, Professor	Molecular Microbiology & Immunology/ SPH

Alternates:

Maureen Horton, Associate Professor	Medicine (Pulmonary)/SOM
Wan-Yee Tang, Assistant Professor	Environmental Health Sciences/SPH

ACKNOWLEDGEMENTS

I would like to start by expressing my gratefulness to His Majesty King Bhumibol Adulyadej of Thailand and Her Royal Highness Princess Maha Chakri Sirindhorn, the founder and director of the Ananda Mahidol foundation for granting me this prestigious scholarship to embark on my graduate studies.

My PhD could not have been possible without the extraordinary encouragement, mentorship and dedication from my advisor, Dr. Wayne Mitzner. Over my PhD career, he has fostered the best environment for me to develop as a scientist. His incredible patience, comprehensive support, and great sense of humor will be long remembered. Thank you for letting me work in your lab and being flexible to allow me to work on a diverse research projects. Also, I would like to express my deepest gratitude to Dr. Alan Scott for all of his advice. He is an amazing teacher and I have learned so much from him about science and life. I would like to take this opportunity to thank all the members of my PhD advisory committee, Dr. Marsha Wills-Karp, Robert Wise, MD and Franco D'Alessio, MD for spending their valuable time to provide me their insights, thought provoking questions and professional recommendations. Their presence went beyond the duty of committee members and I am thankful for their support in my future endeavors.

I would like to express my sincere gratitude to all the dedicated past and current members of the Mitzner and Scott labs which consists of some the finest scientists and scientists in the making; including Richard Rabold, Dr. Boris Lande, Dr. Matt Craig, Dr. Daniel Lagassé, Lijie Zhen, Dr. Sandhya Das, Dr. Yan Shang. I would like to especially thank Richard Rabold for all of his assistance and camaraderie with my research, but more importantly for his empathy, and kindness from the very beginning. Also, thanks to Dr. Craig and Dr. Lagassé for helping guide

and troubleshoot throughout each of my projects. You are all the best buddies I have ever had. I am indebted to your infinite patience and all of your countless efforts on my behalf during these past several years. It is an honor for me to work with such an outstanding lab group. Also, I want to thank the program administrator, Ms. Mary Thomas for all her kind help throughout my PhD study.

I am extremely grateful to Dr. Wan-yee "Winnie" Tang, who allows me to share workspace in her laboratory. Without her great support, my research work in molecular biology studies would probably never have gotten off the ground. I would also like to acknowledge Xin Guo for her assistance with all the histology preparation and Alexandra Kearson for her assistance with all quantitative stereology.

A big thank you to my friends Jon Fallica, Cissy Li, Tyna Dao, Lindsey Eldridge, Xiao Xiao, Jessie Huang and Shelly Odwin-Dacosta whom have always been wonderful friends, enhanced my PhD experience and made my journey incredibly enjoyable. I also would like to thank all the terrific faculty, students and staff of the department of Environmental Health Sciences.

Special thanks to Dr. Suchinda Malaivijitnond, my undergraduate advisor, and all faculty members in Biology at Chulalongkorn University. Also, thank you to Dr. Sorachai Srisuma for being a great scientific role model, inspiring me to start my research career and encouraging me to go from my home all the way to the other side of the world to pursue my PhD.

Lastly but certainly not least, I would like to especially thank my family, teachers, friends and passersby who have supported me every step of the way during this adventure and throughout life. Words cannot express how grateful I am for having each and every one of you in my life. Thank you from the bottom of my heart!

TABLE OF CONTENTS

LIST OF TABLES

CHAPTER 1:

CHAPTER 2:

CHAPTER 3:

LIST OF FIGURES

CHAPTER 1:

CHAPTER 3:

CHAPTER 4:

CHAPTER 5:

CHAPTER 6:

CHAPTER 1

GENERAL INTRODUCTION

1.1 Preface

The lung is a complex organ, comprised of a number of different cell types that form the site for gas exchange between oxygen (O_2) in the air and carbon dioxide (CO_2) in the circulation. This pivotal function provides O_2 for cellular respiration, removes toxic CO_2 and maintains whole body homeostasis.

Due to the structure and function of the lung, an extensive area of this organ has to be in direct contact with the external environment, which subjects the conducting and respiratory surfaces to continuous exposure to a broad variety of particles, toxicants and infectious agents in the inhaled air. To limit the harmful consequences from these foreign materials, and to maintain the integrity of gas-exchange, the lung needs a tightly regulated defense mechanism, which is mainly derived from the pulmonary innate and adaptive immune system. Aberrant control of the immune system in response to these agents in genetically susceptible individuals is widely considered a major contributor to the pathogenesis of many pulmonary diseases, including chronic obstructive pulmonary diseases (COPD) characterized by bronchitis and emphysema. The basis of the regulation of pulmonary immunity, and the determination of susceptibility to the development of disease, are key to understanding the underlying mechanisms of disease pathogenesis and to develop novel treatments and interventions.

The focus of the research presented here is to determine, using a mouse model, the immunological pathways responsible for susceptibility to the development and progression of emphysema. This study demonstrates that susceptibility to the development of severe

emphysema is dissimilar in different strains of mice. Furthermore, this susceptibility can be altered in different genetically modified mice, or by pre-exposure to microbial agents.

This first chapter presents known basic background information on the structure and function of the respiratory system, human COPD and emphysema, animal models of emphysema, the assessments of emphysema in murine animals and the key questions on the disease which will be addressed in the remainder of this dissertation.

1.2 Structure and Function of the Respiratory System

The primary function of the mammalian respiratory system is to maintain the body's homeostasis by conducting fresh oxygen-rich air to the alveoli and to facilitate the exchange of O_2 and CO_2 from erythrocytes. . To execute this exchange, air and blood must be brought into intimate contact. The function of the lung, as air conductor and gas exchanger, depends on its very complex structure.

The airways and associated blood vessels are designed as tree-like structures, which branch in concert to reach into all regions of the lung parenchyma. The inspired air, after passing through the nasal passage or mouth, the pharynx, and the larynx (the **upper airways**), enters a series of dichotomous branching tracheobronchial tubular airways leading into the lungs (the **lower airways**). In humans, this branching airway tree begins with the trachea (the so-called generation 0), bifurcating into bronchi (1st generation), bronchioles, terminal bronchioles, respiratory bronchioles, alveolar ducts, and alveolar sacs, in a total (on average) of 23 generations (Fig. 1.1A-B) [1].

In human lungs, the number of branches doubles with each generation, to create 2^{23} or about 8 million end branches [2]. In contrast, in the mouse, there is less airway branching, with only 13 - 17 generations, and no respiratory bronchioles [3].

In humans, from the nose to the terminal bronchioles, the first 16 generations of airways do not participate in gas exchange. These generations form the **conducting zone,** constituting the anatomical dead space whose function is to filter, warm, moisten, and conduct the air into the deeper zone. The remaining 7 generations form the **respiratory zone** that contains the alveoli, which represent the smallest functional units of the lungs.

The alveoli are surrounded by a dense pulmonary capillary network, fed by the pulmonary artery and drained by the pulmonary vein [4, 5]. This capillary network occupies about half the volume of the interalveolar septa, with a very thin wall between the air and blood [6]. In most areas of the respiratory zone, air and blood are separated only by the alveolar epithelium and the capillary endothelium - only about 0.5 μm thick in humans, or one-sixteenth the diameter of an erythrocyte. This narrow distance permits gas to diffuse between the air in the lungs and the erythrocytes in the capillaries (Fig. 1.1C-D).

It is estimated that in the adult human being, there are 480 million alveoli, with a mean diameter of 200 μm, (calculations derived from a direct, unbiased, point-counting stereological approach) [7]. These alveoli provide a total internal surface area of 25-70 m^2, which is about the size of half a tennis court, or about 15-40 times greater than total body surface area (average of 1.7-1.9 m^2) [8-10]. For mice, (adult 20-gram female C57BL/6), the mean alveolar number is estimated to be 2.3 million, which provide a total internal surface

area of 82.2 cm^2 [11]. Alveolar number correlates closely with total lung volume, whereas alveolar size does not [7].

The wall of the alveolar membrane, the important site for gas exchange, consist of two types of epithelial cells. The primary cell type of the alveolar wall is thin, simple, squamous **type I alveolar epithelial cells (type I pneumocytes),** which have large cytoplasmic extensions that forms approximately 95% of the alveolar wall. Gas exchange occurs across the very large surface area formed by these type I pneumocytes, facilitated by their close apposition to the endothelial cells of the capillaries (Fig. 1.1D).

Cuboidal **type II alveolar cells (type II pneumocytes)**, also called septal cells, are interspersed among the type I alveolar epithelial cells. The type II cell represent about 60% of epithelial cells in the alveoli by number, even though they cover only 5% of alveolar surface area. Type II alveolar cells are recognized by abundant lipid-rich lamellar bodies in the cytoplasm and microvilli on the apical surfaces. The microvilli secrete interstitial fluid into the alveoli, thus moistening the surface between the cells and the air. This alveolar fluid contains pulmonary surfactant, a complex mixture of phospholipids and lipoproteins. The surfactant reduces the surface tension of alveolar fluid, thus decreasing the tendency of alveoli to collapse (atelectasis). Moreover, type II alveolar cells are also important in alveolar repair, being capable of both self-renewal, and of giving rise to type I cells through a process of transdifferentiation [12, 13], as well as several other physiologic activities [14, 15].

In addition to alveolar epithelial cells, there are underlying fibroblasts that produce extracellular matrix components including collagen, reticular and elastic fibers, which are the

main components of the basement membrane of the epithelium. The alveoli also contain a variety of other specialized cells, especially immune cells including macrophages, and a small number of dendritic cells, and lymphocytes (Fig. 1.2) [16, 17]. These cells are essential for pulmonary host defense and participate in both innate and adaptive immunity. During unhealthy states such as lung injury, inflammation or pulmonary infection, the amount, proportion and activation status of the immune cells can be markedly altered depending on the nature of the stimuli.

At least three types of macrophages reside in the lung: (i) bronchial macrophages associated with the airway, (ii) alveolar macrophages or dust cells in the alveolar space, juxtaposed with type I or type II alveolar epithelial cells, and (iii) interstitial macrophages, in the interstitial space between the alveoli and the blood vessels. The macrophages function in the innate immune response, to clear fine dust particles, microorganisms, apoptotic cells and other debris from the lungs.

Lung-resident dendritic cells, with many cellular projections, sample foreign antigens in the lumen of the alveoli and conducting airway, and initiate appropriate adaptive immune responses. Typically, dendritic cells that take up antigens in the lungs traffic to the lung-draining lymph nodes (tracheobronchial) and activate B and T lymphocytes to respond to the challenge.

These immune cells require very tight regulation through several mechanisms to balance between maintaining tissue homeostasis and responding to the harmful stimuli. A dysregulation of these responses can be dangerous, and is implicated in pathogenesis of

several common inflammatory lung diseases, including COPD, asthma, acute lung injury, and pneumonia.

Although the best known function of respiratory system is its contribution to homeostasis by providing gas exchange, the respiratory system also plays a vital role in other functions such as regulating blood pH and body temperature, modulating blood pressure by secreting angiotensin converting enzyme, and containing receptors for the sense of smell.

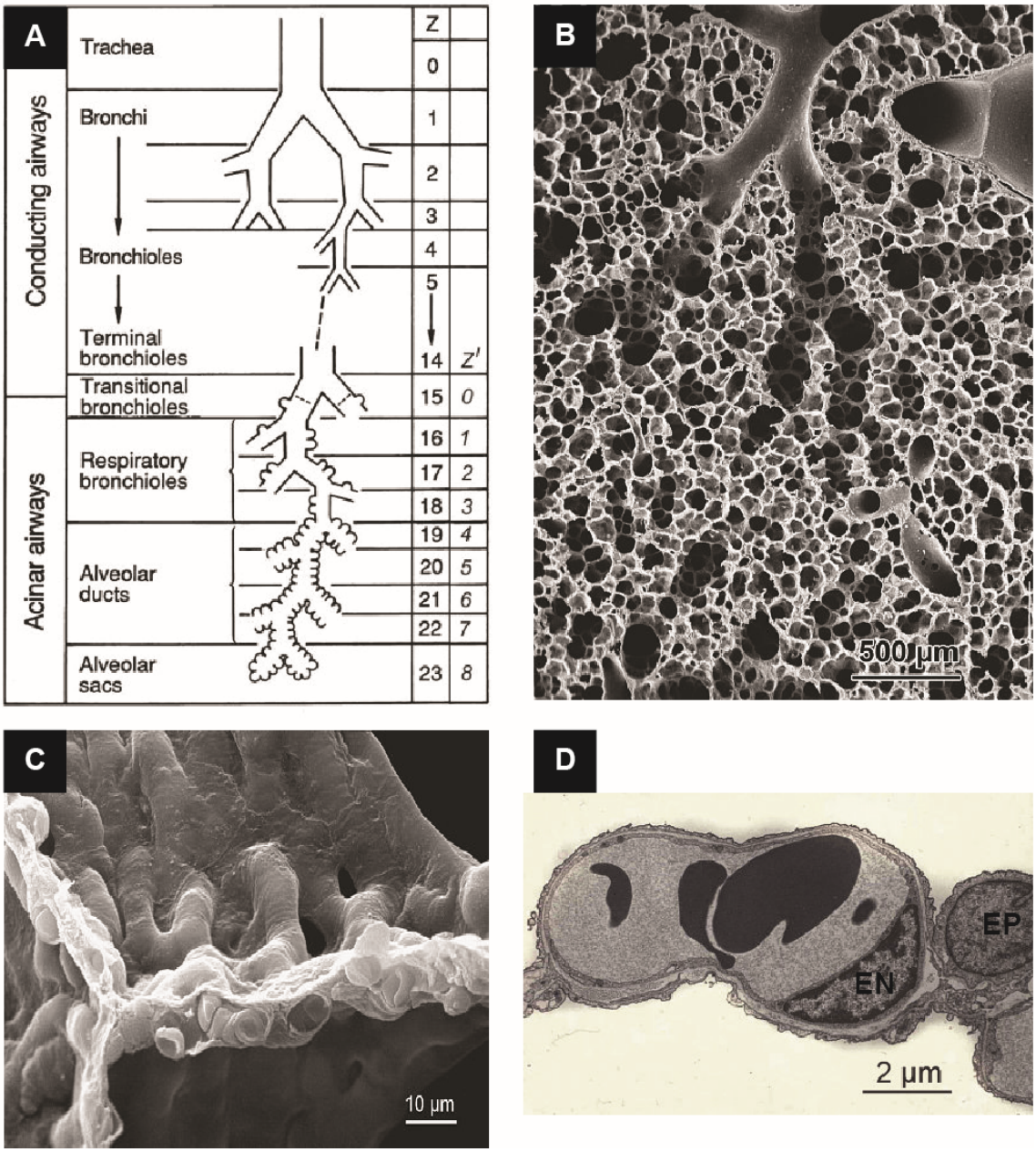

Figure 1.1 Model and electron micrographs of human respiratory structure. (A) Model of airway branching hierarchy in human lung, (B) Scanning electron micrograph of terminal conducting airway which opens into alveoli, (C) Scanning electron micrograph showing thin alveolar barrier separating air and red blood cells in capillaries, (D) Transmission electron micrograph illustrating endothelial cell (EN) lining the capillary bounded by a type I alveolar epithelial cell (EP). Adapted by permission from Basel : EMH Swiss Medical Publishers Ltd.: Swiss medical weekly [5], Copyright (2009).

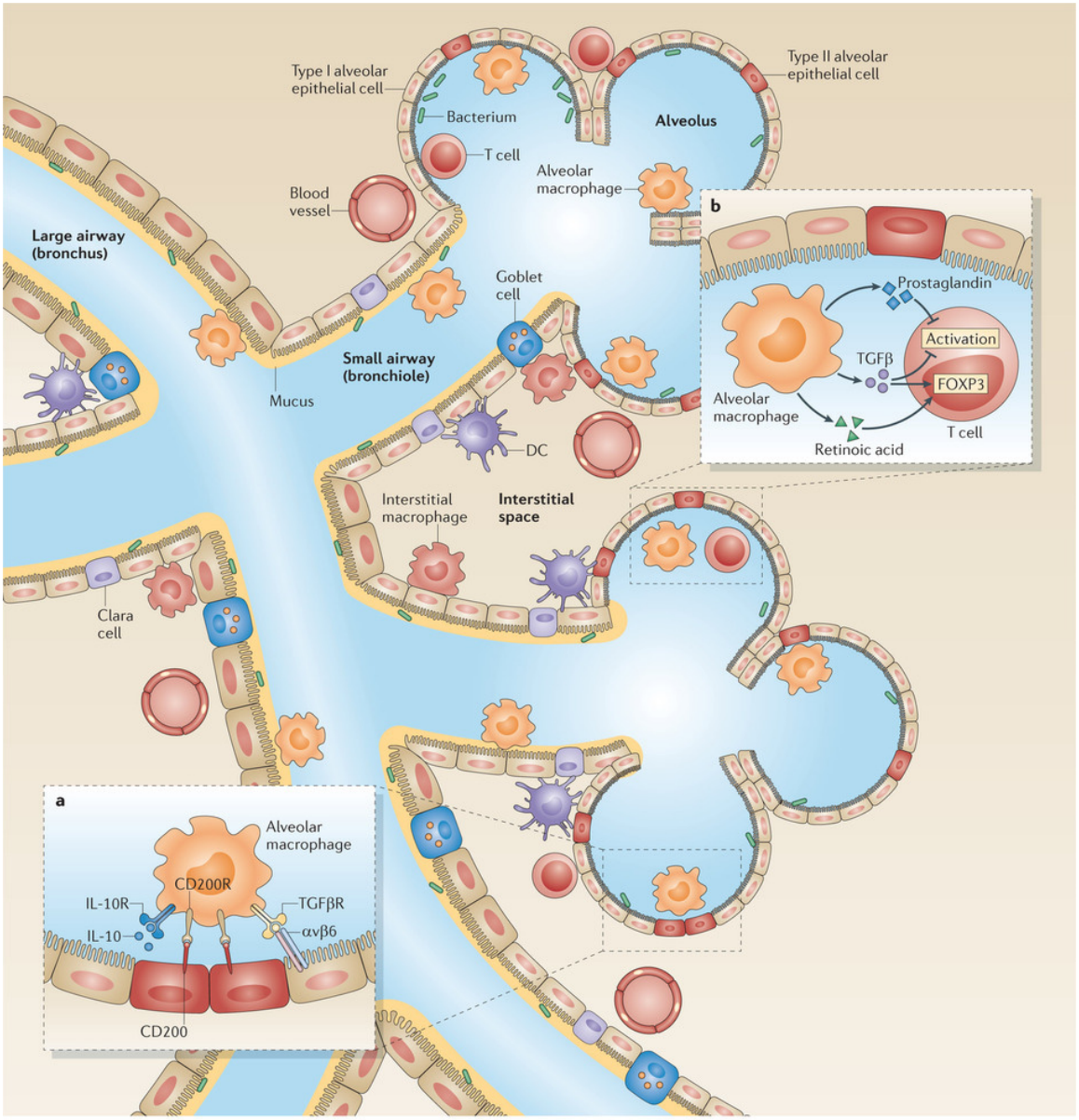

Figure 1.2 Illustration showing structure of peripheral lung tissue and immune-associated cells in the lungs. Reproduced with permission from Nature Publishing Group: Nature Reviews Immunology [16], Copyright (2014).

1.3 Chronic Obstructive Pulmonary Disease (COPD) and Emphysema

1.3.1 Public Health Significance

Chronic obstructive pulmonary disease (COPD) leads to morbidity and mortality, and is a major public health problem, imposing a significant burden on society, the economy and health service resources throughout the world. The burden of COPD is anticipated to increase continually in the next decade, due to continued exposure to risk factors, and aging of the population.

According to the World Health Organization (WHO), COPD became the 3rd leading cause of death globally in 2012, after only heart disease and cancer; (increased from the 4th leading cause of death globally in 2000) [18]. Currently COPD leads to 3 million fatalities per year in North America, which corresponds to 5% of all deaths [18]. Similarly, COPD was ranked as the 3rd leading cause of death in the US in 2011, according to the Centers for Disease Control and Prevention [19]. A further indicator of the public health importance of COPD is the years lost due to disability (YLD's); globally, the rank for COPD has increased from 6th in 1990 to 5th in 2010, with COPD related disabilities affecting more than 60 million people [20]. In North America, the lifetime risk of physician-diagnosed COPD is estimated to be as high as 25% with elevated risk in the age range of 35-80 [21].

The global spending on medicine for COPD, together with asthma, ranks the third highest (behind medicines for cancer and diabetes) [22, 23]. Costs are continually growing for managing this chronic disease among an ever larger patient population. In 2010, the cost associated with COPD in the United States alone was estimated at US$50 billion, comprising $30 billion in direct health care costs (diagnosis, treatment, and rehabilitation), and $20

billion in indirect costs (the morbidity and mortality caused by the disease) [22]. In 2007 the market for COPD drugs was estimated to be valued at over US$5.5 billion worldwide [23]. However, there is still no effective treatment for COPD. None of the available drugs on the market can halt the decline in lung function, reduce the progression of the disease, or have substantial effect on exacerbations, which are the major cause of hospital admission of COPD patients [24].

1.3.2 Definition and Features

COPD is an umbrella term used to describe a complex, heterogeneous and progressive, multi-systemic disease that develops in, and emanates from, the lungs. COPD is classically characterized by persistent airflow limitation measured during forced expiration by spirometry [25]. The disease is associated with an abnormal inflammatory responses in the lung, and is not completely reversible. The pathological characteristics underlying airflow limitation in COPD are: (i) an increase in the resistance of small airways due to **chronic bronchitis** or obstructive bronchiolitis (affecting the conducting airway), and (ii) an increase in lung compliance, or decrease in elastic recoil, due to **emphysema** (affecting the distal airway and respiratory zone) [25-27].

Chronic bronchitis is defined clinically by a chronic cough that produces sputum for at least three months in each of two successive years, which often leads to fibrosis of the large conducting airway [28]. In contrast, emphysema is defined pathologically as progressive destruction of alveolar parenchymal wall, leading to a permanent enlargement of the airspaces distal to the terminal bronchiole, in which there is no apparent pulmonary fibrosis [29].

The principal characteristic respiratory manifestations of COPD are long-lasting cough, sputum production, and breathlessness. The physiological manifestation of COPD is a restriction in airflow. The most reproducible and objective measurement of this airflow limitation is spirometry, which is extensively used for clinical diagnosis. This testing can be done by measuring the forced expiratory flow in one second (FEV_1), and the forced expiratory volume (FVC). COPD is characterized by (i) a persistently low (< 80% of the predicted value) FEV_1, and (ii) a low (< 70%) FEV_1/FVC. In COPD-mediated airflow limitation, low FEV_1 and FEV_1/FVC values are obtained despite the use of bronchodilator medication [30].

The most widely used classification of chronic obstructive lung disease is devised by the Global Initiative for Chronic Obstructive Lung Disease (GOLD) [30, 31]. This classification uses FEV_1 as the most important criterion by which to categorize the degree of COPD, and uses four levels: mild (I), moderate (II), severe (III), or very severe (IV) (Table 1.1). GOLD stage 0 refers to individual with cough, sputum and some history of exposure to risk factors for developing COPD, but without an abnormal FEV_1 and FEV_1/FVC ratio.

Table 1.1 GOLD Classification of COPD (Adapted from [30, 31])

Stage	Severity	FEV_1/FVC	FEV_1 (% predicted)	Characteristics
0	at risk	>70%	≥80%	normal spirometry but with chronic symptoms (cough, sputum production)
I	mild	<70%	≥80%	with/without chronic symptoms
II	moderate	<70%	50 up to <80	with/without chronic symptoms
III	severe	<70%	30 up to <50	with/without chronic symptoms
IV	very severe	<70%	< 30 or < 50	FEV_1 < 30 or FEV_1 < 50 with the presence of respiratory failure or clinical signs of right heart failure.

Due to progressive course of the disease, COPD patients experience a gradual decline in lung function and health throughout their life [32]. The rate of this decline can be accelerated by smoking and aging [32]. While many patients seek health care attention only after substantial symptoms are present, most patients are diagnosed or treated for COPD in the early stage [33]. However, several recent studies show that COPD is commonly underdiagnosed, especially in the early, relatively asymptomatic stages [34-36]. Moreover, COPD is often associated with co-morbidities that may have an impact on prognosis [37]. In the United States, while more than 12.7 million adults have been diagnosed with COPD, there are an additional 24 million undiagnosed adults with impaired lung function consistent with COPD [38].

1.3.3 Risk Factors

COPD is a preventable disease. The primary risk factor for COPD is cigarette smoke, including active, passive and second-hand exposure. Smoking and environmental tobacco exposure are the major causes of COPD deaths [39], accounting for more than 80 % of the risk of developing COPD [40, 41]. However, among individuals with the same smoking history, not all will develop COPD, suggesting that smoking behavior alone is not sufficient to explain all of the etiology of COPD.

There is consistent epidemiological evidence that some non-smokers develop COPD [42]. Environmental risk factors, other than tobacco smoke, which are associated with the onset of COPD include indoor and outdoor air pollution, and occupational exposures (particularly to organic and inorganic dusts, and chemical agents). Differences in genetic predispositions remain important, but maternal smoking, respiratory infections (i.e.

pneumonitis), and other non-respiratory infections (including HIV) have also been linked to emphysema and COPD burden [43-46].

There is a strong, and ever growing, relationship between the increased prevalence of COPD and indoor pollution due to the use of biomass (such as woods, charcoal, crop waste, animal dung and coal) in cooking and heating, particularly in poorly ventilated spaces where there is a high amount of smoke produced [47-52]. For the year 2012, household air pollution caused by biomass fuel cooking was cited as causing 4.3 million deaths, which represent 22% of all deaths due to COPD [53]. This link between COPD and use of biomass fuel for cooking is highly relevant because of the large numbers of people affected. About 3 billion people worldwide are exposed to biomass fuel combustion, especially in low- and middle-income countries; thus the population at risk worldwide is very large [54] The numbers of biofuel users greatly exceeds the number of tobacco smokers, 3 billion versus 1 billion respectively.

Genetic deficiency or mutation in some particular genes are also established etiologic factors for the development of COPD. For example, 1-2% of COPD patients carry homozygosity of the PiZ allele of the *SERPINA1* gene (formerly known as *Pi*), a recessive trait common in Northern Europe [55-58]. This genetic condition results in a marked reduction in production of α_1-antitrypsin (α1-AT) [59-61]. α1-AT, a serine protease inhibitor, is the major inhibitor of neutrophil elastase at steady state. Patients with an inherited deficiency in α1-AT have an elevated level of neutrophil elastase proteolytic activity in the pulmonary tissue, which leads to damage of the alveolar tissue and results in "genetic emphysema".

The balance between proteases and anti-proteases in the lung is widely believe to be one of the common pathologic causes of emphysema, and will be further discussed in section 1.4. Although a variety of other candidate gene loci have been linked to COPD [62-67], convincing evidence proving a genetic risk factor for COPD in humans has only been established for *SERPINA1* gene. Another potential risk factor is exposure to viral infections. Many COPD exacerbations are associated with acute viral infections, and recovery from viral infections may also lead to increased sensitivity to other pathogenic triggers.

Thus, the susceptibility to COPD likely results from a combination of multiple genetic and environmental factors. In this thesis, we employ an animal to provide insights into the enhanced susceptibility to emphysema due to both genetic background and to antecedent viral infection (Chapters 3 and 5).

1.3.4 Pathogenesis of COPD/Emphysema

Experimental and clinical studies have established that multiple types of cells and molecular mediators contribute to the complex pathogenesis of COPD/emphysema. However, there remain key gaps in our understanding of the connection between different events and mediators, the determinants of susceptibility, and identification of the final mediators that perpetuate tissue destruction in emphysema.

The current paradigm holds that the pathophysiological changes in the COPD/emphysema lungs result from imbalance in four critical processes: (i) extracellular matrix proteolysis, (ii)

inflammation, (iii) oxidative stress, and (iv) cell death. Each processes is now reviewed in detail.

1.3.4.1 Protease/antiprotease Imbalance and Extracellular Matrix Proteolysis

The core definition of emphysema is the irreversible destruction of the alveolar wall. This damage has long been considered to be a consequence of proteolytic degradation due to either an abnormal increase in proteases, or a reduction in pulmonary antiproteases - proteins that protect the lung from local proteases [68]. Proteolytic degradation was proposed as a mechanism based on the occurrence of emphysema in humans who were deficient in alpha1-antitrypsin [61, 69] and on experimental animal models in which emphysema was induced by instillation of proteases (such as papain or elastase) into the lung [70, 71].

The most important target of these proteolytic enzymes may be elastin in the connective tissue underlying the epithelium, since loss of lung elasticity is the common feature among COPD patients [72]. Desmosine, a cross-linking amino acid of elastin, and used as a biomarker for elastin degradation, is increased in the blood and urine of COPD patients, and its levels positively correlate with the severity of disease [73-76]. The major endogenous candidates accounting for this tissue degradation are neutrophil elastase (NE) and matrix metalloproteinases (MMPs).

Neutrophil elastase (NE) is an abundant serine protease stored in azurophilic granules in the cytoplasm of the neutrophils, and expressed on the cell surface in response to cytokines [77]. The NE contributes to the regulation of immune responses by acting in combination with

oxygen radicals, to help degrade phagocytized microorganisms [78]. Once secreted in association with neutrophil extracellular traps (NETs), NE destroys virulence factors, kills bacteria, and facilitates the formation of NETs [79]. NE has a wide range of substrates, including most of the extracellular matrix proteins (i.e. elastin, Type III and IV collagens, fibronectin, laminin, and fibronectin). At homeostasis, NE can be inhibited by α1-AT, a serine proteinase inhibitor in the blood.

Neutrophil elastase is considered to be the primary destructive enzyme in emphysema, because patients with inherited α1-AT deficiency develop pulmonary emphysema early in life. Evidence showing that NE (a normally occurring cognate proteinase) can cause emphysema was provided by animal models where human leukocyte elastase was instilled into the lungs of hamsters and dogs [80, 81]. Moreover, elastase was found to bind with connective tissue close to elastic fibers, but not with collagen in the damaged areas of the treated lungs [81]. This spatial association of NE with alveolar interstitial elastin in the emphysematous areas in the animal model was subsequently confirmed in humans [82]. Further evidence for a role for NE comes from the observation that in neutrophil-elastase-null mice, the emphysema induced by chronic exposure to cigarette smoke is significantly less severe than in wild type mice [83]. Mice with reduced α1-AT also developed cigarette smoke-induced emphysema earlier than did wild-type mice [84, 85]. Although many studies have suggested neutrophil elastase as a therapeutic target for treating COPD/emphysema, and several neutrophil inhibitors have been developed and are in clinical trial [86-90], to date none of them are used clinically.

MMPs are a large groups of at least 28 zinc-dependent proteinases that can degrade a variety of matrix components, including collagen, laminin and elastin. The MMPs essentially function in tissue remodeling, repair, and development, as well as in inflammation. The MMP family can be categorized into six groups, based on substrate specificity, amino acid similarity and homology: (i) collagenases (MMP-1, -8, -13, -18), (ii) gelatinases (MMP-2, -9), (iii) stromelysins (MMP-3, -10, -11, -17), (iv) matrilysins (MMP-7, -26), (v) membrane-type MMPs (MT-MMPs, MMP-14, -15, -16, -17, -24, -25), and (vi) other MMPs [91].

Multiple recent studies cite MMPs as the critical proteolytic enzymes involved in the pathogenesis of COPD (Table 1.2). There are increased levels of several MMPs in the blood and BAL from COPD patients. Among all MMPs, MMP-12 has been the most studied as a potential candidate protease associated with pulmonary emphysema, and as a potential target for COPD treatment.

The increased level of MMP-12 in human patients with COPD in some clinical studies [92-94], is supported by the up-regulation of MMP-12 expression in many experimental animal models of emphysema including cigarette smoke [95-103], elastase [104-106], ozone [107] and helminth infection [108]. Additionally, MMP-12 knockout mice are protected from developing emphysema after chronic exposure to cigarette smoke [102]. Orally bioavailable synthetic MMP-9/12 inhibitors decreased inflammation and alveolar destruction in tobacco-exposed guinea pigs [109].

Although strong data from animal models consistently have supported the role of MMP-12 in emphysema, data from human patients is inconsistent. Some studies have failed to detect

elevation of MMP-12 in alveolar macrophages or lung tissue from patients with COPD/emphysema, or find a correlation between the level of MMP-12 with severity of disease [110-112]. Another point that should be taken into the consideration is that MMP-12 also plays an important role in removing microbes from the respiratory tract, and mice deficient in MMP-12 have an increased burden of bacterial infection and increased mortality [113]. This raises a doubt on the benefit of MMP-12 inhibition in treating COPD.

Table 1.2 COPD-associated MMPs and their relevance

Class	MMP	Other name	Substrate	Relevance to COPD
Collagenases	MMP-1	Collagenase-1	Collagens (I–III, VII, VIII, X), gelatin, IL-1β, proteoglycans, pro-MMP-2, pro-MMP-9	• Increased whole lung MMP-1 mRNA and protein in human and guinea pig emphysema [110, 114, 115] • MMP-1 overexpressing mice develop emphysema via degradation of collagen type III [116, 117]
	MMP-8	Collagenase-2, neutrophil collagenase	Collagens (I–III, V, VII, VIII, X), gelatin, fibronectin	• Increased MMP-8 in BAL [118] and sputum which correlated with airflow obstruction [119] • Increased MMP-8 in patients with COPD exacerbation compared to stable COPD and controls [120]
	MMP-13	Collagenase-3	Collagens (I–IV, IX, X, XIV), gelatin, pro- MMP-9	• Increased MMP-13 expression in alveolar macrophages and epithelial cell type II in the COPD patients [121]
Gelatinases	MMP-2	Gelatinase-A	Gelatin, collagen IV–VI, X, elastin, fibronectin	• Increased MMP-2 expression and activity in the COPD patients [122] mainly in alveolar macrophages and airway epithelial cell [115] • Increased MMP-2 in both cigarette smoke-exposed mice [123, 124] and wood smoke-exposed mice [125]

Table 1.2 COPD-associated MMPs and their relevance (continued)

Class	MMP	Other name	Substrate	Relevance to COPD
Gelatinases **(contd.)**	MMP-9	Gelatinase-B	Collagens (IV, V, VII, X, XIV), gelatin, elastin, fibronectin, MBP, pro-MMP-9, pro-MMP-13, IL-1β	• Increased MMP-9 protein and activity in neutrophils, serum, induced sputum of COPD paralleled with severity of the disease [115, 118, 119, 126-129] • Increased MMP-9 expression (mostly associate with increased MMP-12 expression) in both cigarette smoke- and elastase-induced emphysema in murine model [104, 130-135] • Mice overexpressing human MMP-9 in macrophages decrease alveolar wall elastin and develop early-onset emphysema [136] • MMP-9/MMP-12 inhibitor can attenuate smoke-induced emphysema in guinea pigs [109]
Stromelysins	MMP-10	Stromelysin-2	Collagens (III–V), gelatin, casein, elastin, MMP-1, MMP-8	• Increased MMP-10 gene expression in parenchyma with increasing GOLD stage [112]
Other	MMP-12	Macrophage metalloelastase	Collagen IV, gelatin, elastin, casein, fibronectin, MBP, fibrinogen, fibrin	• Increased MMP-12 protein in BAL, induced sputum, bronchial biopsies of COPD [92-94] • Increased MMP-12 production and release in animal model of emphysema induced by cigarette smoke [95-103], elastase [104-106], ozone [107] and hookworm [108] • MMP-12 deficient mice have decreased numbers of macrophages in lungs and do not develop emphysema in response to long-term exposure to cigarette smoke [102] • MMP-9/MMP-12 inhibitor can attenuate smoke-induced emphysema in guinea pigs [109] • Some single-nucleotide polymorphisms in MMP-12 gene are associated with lower risk of developing severe COPD [137-139]

Activity of MMPs can be physiologically inhibited by two main inhibitors: α-2 macroglobulin and tissue inhibitor of the matrix metalloproteinases (TIMP) family (TIMP-1, -2, -3, -4)]. To illustrate the hypothesis of protease/antiprotease imbalance in COPD pathophysiology, most studies observe only relative changes compared to their MMPs substrates. However, association of these inhibitors with COPD pathogenesis, and possible causal connections, are still unclear. A study in humans showed that alveolar macrophages isolated from patients with COPD produced less TIMP-1 than did the alveolar macrophages from healthy smokers and non-smokers [140]. However, in mice exposed to cigarette smoke, TIMP-1 levels were increased [141] or unchanged [142]. Some polymorphisms of the TIMP-2 gene have been identified in COPD patients [143]. Mice exposed to cigarette smoke for 10 days showed an increase MMP-12/TIMP-2 ratio compared to controls. Nonetheless, currently, no study describe the significance of these inhibitors in onset of emphysema in humans.

1.3.4.2 Inflammation

Pulmonary inflammation is a characteristic feature of the COPD patients. Several types of innate and adaptive inflammatory cells are recruited, and many inflammatory mediators are secreted with potential to cause alveolar destruction. The pathophysiological role of each of these types of cells and mediators are not yet fully understood.

Potential role of innate immunity. An elevated number of neutrophils are found in sputum and bronchoalveolar lavage (BAL) fluid of patients with COPD compared to healthy individuals [144, 145]. Furthermore, the severity of pulmonary neutrophilic inflammation and the number of circulating neutrophils, correlate with an acceleration in lung function

decline, suggesting the role of neutrophils in progression of COPD [146, 147]. The elevation in neutrophil count follows the increase in neutrophil chemotactic molecules such as IL-8, growth related oncogene alpha (GROα; also known as CXCL1) and leukotriene B4 (LTB_4) in the BAL fluid or in the sputum from COPD patients [148-151].

Neutrophils are one of the candidate pathogenic cells in COPD because they are a rich source of a range of proteolytic enzymes [such as neutrophil elastase, cathepsin G, several MMPs (MMP-8, MMP-9)] and reactive oxygen species. Typically, activated neutrophils have a very short half-life (about 11.4 hours) [152], and then undergo apoptosis, and get removed by macrophages [153]. However, in COPD, the neutrophils' half-life is prolonged and is associated with a decreased expression of pro-apoptotic genes and an increased expression of anti-apoptotic genes [154].

However, the significance of neutrophils in development of COPD/emphysema remains ambiguous. In experimental animal models, mice depleted of neutrophils or mice deficient in the ability to synthesize the neutrophil chemoattractant LTB_4 were protected from protease-induced pulmonary emphysema [155]. However, in rats, depletion of neutrophils did not lessen the severity of cigarette-smoke induced emphysema [156].

Macrophages are another class of effector cell that produces enzymes that could contribute to lung pathogenesis including MMP-2, MMP-9, MMP-12 (aka macrophage elastase), collagenase 1, and cathepsin K, L and S [93, 115, 157, 158]. The number of macrophages is markedly increased in the sputum, BAL fluid, airway wall and lung parenchyma in COPD patients [145, 159, 160]. The level magnitude of the increase in mononuclear cells is

positively correlated with the severity of COPD [161]. This accumulation of cells can derive from either local proliferation of alveolar macrophages [162, 163], or recruitment of peripheral monocytes into the lung in response to chemokines such as monocyte chemotactic protein 1 (MCP1; CCL2) and GROα [164, 165]. In a rat model of emphysema induced by cigarette smoke, both macrophage count and their elastolytic activity were elevated after 2 months of exposure, and remained elevated for 6 months and the counts and enzymatic activity correlated very strongly with the time course of the histopathological evolution of emphysema [166]. Further, in rats where macrophage accumulation was prevented by neutralizing antibodies, the development of emphysema in cigarette smoke-exposed animals was significantly attenuated [156].

Potential role of adaptive immunity. Adaptive immune response is also appears to be involved in the pathology of COPD/emphysema. Multiple studies have demonstrated an increased in a mix populations of both $CD4^+$ helper T cells and $CD8^+$ cytotoxic T cells in COPD patients. In the peripheral blood, airways, and lungs of COPD patients, lymphocyte polarization was directed towards T helper cell type I (Th1) and T cytotoxic cell type I (Tc1) phenotypes are the predominant $CD4^+$ cells that accumulate [167-169], and there is also an elevated level of Th2 and Th17 cells [170, 171]. The basic features of each T helper cell subpopulation are expressed in Table 1.3. The Th1 cells produce mainly interferon-γ (IFN-γ), which can induce macrophage activation to produce large amounts of pro-inflammatory cytokines [i.e. tumor necrosis factor-alpha (TNF-α), and interleukin (IL)-1β, IL-6] and inducible nitric oxide synthase (iNOS). Not surprisingly, levels of these pro-inflammatory cytokines, along with IFN-γ, were higher in lungs of patients with COPD than in healthy individuals [172].

Transgenic mice overexpressing IFN-γ or TNF-α, specifically in the lung, develop emphysema, possibly due to induction of MMP-12 or MMP-9 in macrophages [173, 174]. Moreover, mice in which there has been gene-targeted knockout of the TNF-receptor, IL-1-receptor and IL-6 develop less severe emphysema than do wild-type mice [105, 175-177].

Although Th2 cells do not predominate in patients with COPD, Th2 cytokines are linked to the pathogenesis of COPD because of their ability to activate proteolytic pathways. Inducible overexpression of IL-13, a potent Th2 cytokine, in transgenic mice activates a number of extracellular matrix degrading enzymes (MMP-2, -9, -12, -13, and -14 and cathepsins B, H, S, K, and L), and results in developing emphysema [178].

There is increasing evidence that Th17 also plays a role in pathogenesis of COPD. Th17 cells are characterized by secretion of IL-17, IL-21, and IL-22 cytokines, which induce the release of GROα, IL-8 and GM-CSF, and orchestrate neutrophilic inflammation [179, 180]. Stable COPD patients have more T cells producing IL-17A$^+$, IL-17F$^+$and IL-22$^+$ in their bronchial and lung biopsies than do control non-smokers [181-184]. Overexpression of IL-17A in lung epithelium in mice promotes lung inflammation, with an induction of MMP-9 and shows a COPD-like phenotype [185]. Mice-deficient in IL-17A or the receptor for IL-17A are protected from both cigarette smoke-induced emphysema and elastase-induced emphysema [186-188].

Collectively, the evidence regarding the role of adaptive immunity in COPD is mixed, with the association of multiple cell populations with COPD. However, the critical function of these cells in the pathogenesis of the disease has not been yet elucidated.

Table 1.3 Effector $CD4^+$ T cell subpopulation (Adapted from [189])

Cell type	Differentiation signals	Transcription factors*	Cell surfaces and cytokine markers	Function
Th1	IFN-γ, IL-12	*Tbet*, STAT1, STAT4, Runx3	IFN-γ, CXCR3	Response to intracellular pathogens and viral infections
Th2	IL-4, IL-2	*GATA-3*, STAT6, STAT5	ST2, IL-4, IL-5, IL-13	Response to extracellular parasites, Involve in allergic response
Th9	TGF-β, IL-4	*PU.1*	IL-9	Involve in tumor immunology or parasites
Th17	IL-6, TGF-β, IL-1β	*RORγt*, AhR, STAT3,Batf	IL-17A, IL-17F, GM-CSF, CD161	Regulator of tissue inflammation, response to extracellular parasites and involved in autoimmunity
Tfh	IL-6, IL-21	*Bcl-6*, Ascl2	CXCR5, IL-21, PD-1	Trigger the formation and maintenance of germinal centers
iTreg	TGF-β, IL-2	*Foxp3*, STAT5	IL-10, TGF-β	Immune suppression, and involve in immune tolerance

* Master transcription factors are shown in *italic*.

Another possible contribution of adaptive immunity to the pathophysiology of COPD/emphysema has been suggested to be though an autoimmune mechanism [190, 191]. Lymphoid follicles with B cells, T cells and follicular dendritic cells are found in both bronchial wall and parenchymal tissue of patients with emphysema [192]. The possibility of the role of autoimmunity in COPD/emphysema was raised with the discovery, in the emphysematous lung, of Th1 and Th17 cytokines, the pivotal cytokine players in autoreactive inflammation [193]. Key evidence of the role of autoimmunity is, in COPD and emphysema patients, the presence of circulating antibodies (produced by B cells) against elastin fragment in COPD, and the responsiveness of CD4+ T cells isolated from COPD lungs to elastin [194]. However, these observations of anti-elastin cannot be reproduced by

other groups [195, 196]. Thus, the involvement of autoimmune response in the pathogenesis of emphysema remains uncertain.

1.3.4.3 Oxidative Stress

Oxidative stress occurs when the redox balance is disturbed by excess reactive oxygen species (ROS) in relation to antioxidant defense mechanisms. The ROS are chemically reactive and unstable molecules or free radicals containing oxygen, which are routinely generated in the cells as a byproduct of aerobic respiration or by oxidoreductase enzymes, and play important roles in intra- and inter-cellular signaling, cell cycle control, homeostasis and host cell defense mechanisms [197]. However, during times of environmental stress (i.e. UV or heat exposure, microbial infection), ROS levels can markedly increase. The imbalance of excess ROS can result in molecular, cellular and tissue damage.

The lung, with its large surface area and dense vascularization, is especially vulnerable to environmental oxidative stress, because it is directly and constantly exposed to multiple foreign materials and pathogens containing oxidants. In smokers and in patients with COPD, there are increased levels of pulmonary and systemic oxidative stress markers in BAL fluid, lung tissue, exhaled breath condensate, serum and urine of smokers [198-204]. Increasing numbers of studies have strongly linked the oxidative stress burden to pathogenesis of COPD.

Increased ROS in the lungs can derive from endogenous cellular activities, (especially release from activated inflammatory cells) and from exogenous oxidants in inhaled air. Cigarette

smoke is likely to be the primary source of oxidants in most cases of COPD. Cigarette smoke is a complex mixture of some 4,700 chemical compounds, which consist of more than 1,000 species of oxidants. In the gas phase there are approximately 10^{15} oxygen free radicals per puff, comprising a variety of organic radicals with different reactivities, such as nitrogen dioxide (NO_2), nitric oxide (NO), hydrogen peroxide (H_2O_2), peroxynitrite ($ONOO^-$), and peroxynitrate (O_2NOO^-). In addition, the particulate matter phase has more than 10^{18} free radicals per gram, which includes hydrogen peroxide (H_2O_2), hydroxyl radicals (•OH) and other organic compounds (e.g. semiquinone, hydroquinone, phenol) [205, 206]. Other gaseous pollutants such as ozone (O_3), sulfur dioxide (SO_2), NO_2, diesel particulates and particulate matter <10 μm (PM_{10}), are also highly reactive and can also cause inflammation in the lung [207-209].

Activated inflammatory cells, including neutrophils or macrophages, and other structural cells such as epithelial and endothelial cells, can be another significant source of ROS in COPD patients. Activated neutrophils or macrophages use the NADPH oxidase system (respiratory burst oxidase) to produce ROS e.g. $O_2^{\bullet-}$, which is rapidly converted to H_2O_2 by superdioxide dismutase (SOD) [206]. The levels of ROS, such as $O_2^{\bullet-}$ and H_2O_2, spontaneously released from BAL macrophages or circulating neutrophils, are higher in smokers than in non-smokers [203, 210-212]. Similarly, neutrophil myeloperoxidase, which can metabolize H_2O_2 to the more reactive hypochlorous acid, accumulates in the lungs of patients with COPD [213]. Cigarette smoke can also activate the generation of oxidants (e.g. $ONOO^-$) via inducible nitric oxide synthase in epithelial cells or endothelial cells, which has been linked to alveolar injury [214].

These ROS are extremely active and can damage all tissues, particularly by oxidizing polyunsaturated fatty acids in cell membranes (lipid peroxidation). The oxidative stress induced by cigarette smoke can cause injury by decreasing cell adherence, and increasing detachment and cell death in human alveolar epithelial cells [215]. Moreover, oxidants can directly damage proteins including those in the lung matrix (such as elastin and collagen) [216], and indirectly through the process called protein carbonylation [217]. This protein modification can alter protein function, disrupting normal cell function and physiological mechanisms. A significant increase in the levels of protein carbonyls correlates with GOLD stage progression in COPD [218]. Particularly important for emphysema, The function of α1-AT can also be inactivated by oxidation with semiquinone extracted from cigarette smoke [219], and the oxidized α1-AT is detectable in BAL fluid of cigarette smokers [220]. Importantly, higher amounts of oxidized DNA, indicated by 8-hydroxydeoxyguanosine in lung tissues, positively correlates with the number of cigarettes smoked per day [221].

Under normal circumstances, the level of oxidants is balanced by several endogenous (enzymatic or non-enzymatic) antioxidant mechanisms. Many classical antioxidant enzymes such as glutathione peroxidase (GPx), superoxide dismutase (SOD), and catalase can prevent initiation of the ROS reaction. Another group of enzymes, including heme oxygenases, peroxyredoxins, thioredoxins and glutaredoxins, neutralize ROS through redox cycle with other protein modifications [222, 223]. The non-enzymatic antioxidants include glutathione, ascorbic acid (vitamin C), α-tocopherol (vitamin E), β-carotene, uric acid, albumin, mucin, bilirubin and lipoic acid. The levels of these antioxidants in COPD patients compared to healthy controls vary among different studies possibly due to variables such as genetics,

smoking histories, severity of the disease, and time interval from last smoke to sampling time [224].

Antioxidants are typically markedly increased in response to cigarette smoke and oxidative stress; however, a question is raised whether this induction of antioxidants is sufficient to deal with the excess of oxidant burdens, particularly in chronic exposure to oxidants. Studies have demonstrated that augmented antioxidant mechanisms, either by direct administration of antioxidant supplementation or by molecular manipulation of antioxidant genes, can ameliorate the severity of emphysema in animal models [217, 225-228]. However, no studies have shown that dietary supplementation with antioxidants results in clinical improvement, nor are the existing antioxidant therapies successful without intolerable side effects [229]. Despite these current significant limitations, development of novel antioxidant drugs and strategies for targeting oxidative stress continue to be pursued as a promising therapeutic approaches to treat COPD [230].

1.3.4.4 Cellular Senescence and Cell death

Another mechanism postulated to result in alveolar wall destruction in emphysema involves failure of the lung maintenance and repair process following repeated injury from chronic exposure to toxicants such as those contained in cigarette smoke [231]. Both an increased number of apoptotic cells and an increase in cell proliferation, particularly septal epithelial and endothelial cells, have been reported in human emphysemic lungs [232-234]. This apoptosis of structural cells in emphysema might be partly due to reduced endothelial cell maintenance factors such as vascular epidermal growth factor (VEGF) [232], as confirmed in both in vitro and animal models [235-237]. Additional evidence that apoptosis could have an

important role in emphysema was provided by the results of experiments where transfection of active caspase-3 into the lung of mice resulted in alveolar wall apoptosis and destruction [238]. However, the exact underlying apoptotic pathway that drive the persistent alveolar destruction associated with emphysema has not yet been identified.

Due to the repeated cell proliferation needed to maintain alveolar integrity during repair, cells with a limited ability to divide might undergo **cellular senescence**, defined as a loss of proliferative capacity which can be determined by a shortening of chromosomal telomeres, and increased expression of senescence-associated cyclin kinase inhibitors (such as $p16^{INK4a}$ and $p21^{CIP1/WAF1/Sdi1}$) and SA-β-gal (senescence-associated-β-galactosidase) [239]. The apparent senescence phenotype of alveolar epithelial and endothelial cells, paralleled with increased levels of senescence markers in peripheral blood leukocytes, is accelerated in COPD patients especially those with emphysema [239, 240]. Some mutations in the essential telomerase (telomere-repeat synthesizing enzyme) genes has been identified as a risk factor of COPD [237]. The finding that genetically modified mice that have short telomeres have increased susceptibility to develop cigarette smoke-induced emphysema [241] also supports the potential importance of cell senescence in the development of emphysema. *In vitro* exposure of human epithelial cells to cigarette smoke results in increased expression of SA-β-gal [242]. Interestingly, lung fibroblasts isolated from patients with emphysema have higher expression of SA-β-gal and reduced proliferative capacity compared with those from healthy smokers [243, 244].

1.3.4.5 Summary Overview of the Pathogenesis of COPD.

Many cells and mediators act together in the pathogenesis of COPD (Fig. 1.3). The key steps are a loss in tissue homeostasis caused by imbalance of several maintenance programs in the lung, including an imbalance in protease/anti-protease activity, inflammatory/anti-inflammatory response, oxidative/anti-oxidative system and regeneration/death or senescence (Fig. 1.4A). It is important to note that these imbalances are not separated entities, but constantly interacting with each other, contributing to the complexity of the progression of COPD (Fig. 1.4B).

The traditional protease/anti-protease model for emphysema requires the recruitment and activation of inflammatory cells including macrophages and neutrophils. A recent study demonstrated a prominent increase of adaptive immune inflammation, (consisting of B cells, $CD4^+$ and $CD8^+$ T lymphocytes and lymphoid follicles) in emphysema patients with the deficiency of α1-AT, suggests that the mechanism underlying emphysema is more complicated than a simple elastase/anti-elastase imbalance [245]. Increased oxidative stress triggered by inhaled environmental toxicants can initiate various early inflammatory events in the lungs including those regulated through NF-κB-dependent pathways [246]. In turn, inflammatory responses result in the production of more ROS, in addition to the alteration of the anti-protease system. Some anti-proteases are susceptible to oxidative damage. The α1-AT activity can be inhibited by oxidation of certain essential methionine residues by H_2O_2, leading to loss of its ability to bind with neutrophil elastase [247]. As a consequence, relatively high levels of proteases are present in excess of the local concentration of their inhibitors. Protease-generated elastin fragments have a chemotactic property for immune cells, and could result in a positive-feedback loop resulting in continuous destruction of

parenchymal tissue [248, 249]. High concentrations of ROS-generated oxidized phospholipids in the plasma membrane of alveolar macrophages can decrease their phagocytic capacity (efferocytosis), resulting in failure to clear microbial infections or apoptotic cells [250]. Impaired efferocytosis can lead to secondary necrosis, sustained inflammation, and inadequate tissue repair in COPD [251]. Apoptosis is notable in areas of high oxidative stress, and inhibiting apoptosis with a broad-spectrum caspase inhibitor markedly reduces expression of oxidative stress markers and inflammation [235, 252]. Caspase-3 activation was directly inhibited by α1-AT, suggesting an anti-apoptosis role of anti-protease protein [253]. Furthermore, senescence is usually increased by DNA damage which can be induced by oxidative stress. This cellular senescence can in turn amplify the oxidative stress, propagate proinflammatory phenotype, diminish repair capacity, and all ultimately drive tissue damage [254, 255].

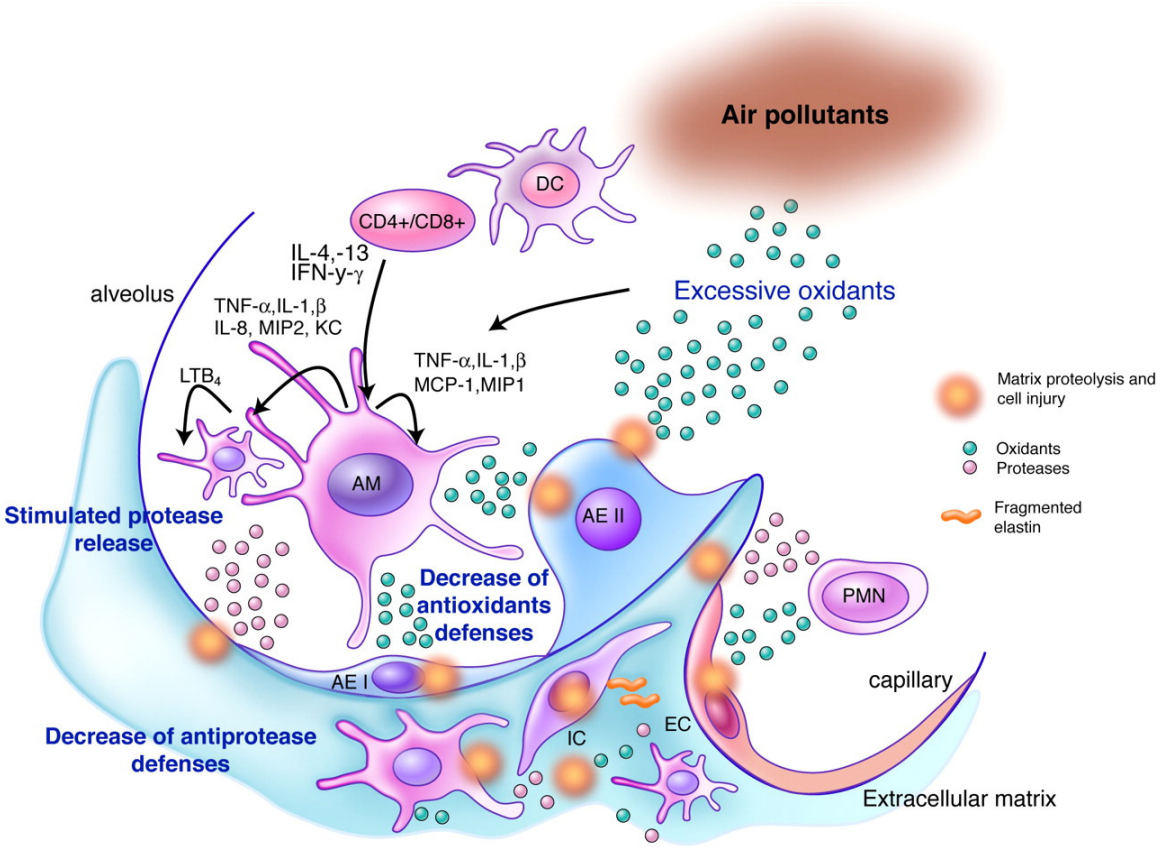

Figure 1.3 Hypothesis of cellular and molecular events underlying pathophysiology of COPD. AEI and AEII: alveolar epithelial cells type I and II, EC: endothelial cells; IC: interstitial cells, AM: alveolar macrophages, PMN: polymorphonuclear cells (neutrophils), DC: dendritic cells, $CD4^+/CD8^+$: $CD4^+/CD8^+$ T lymphocytes.
Reprinted by permission from the American Physiological Society: Physiological Reviews [222], Copyright (2007).

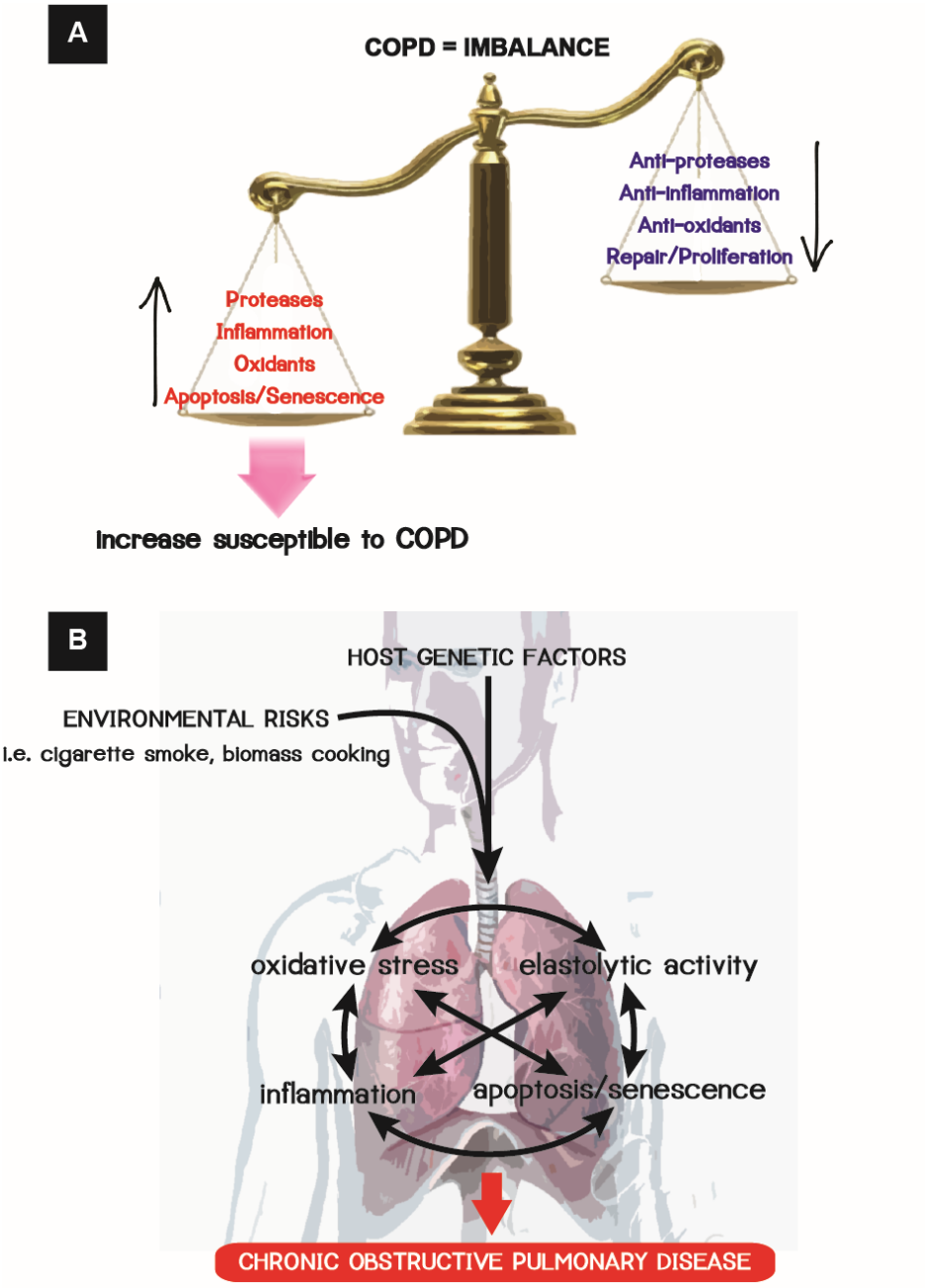

Figure 1.4 Imbalance and interplay model of COPD pathogenesis. (A) COPD is hypothesized to result from imbalances between proteases/anti-proteases, inflammation/anti-inflammation, oxidants/antioxidants and repair/apoptosis. (B) Interplay between protease activity, inflammation, oxidative stress and apoptosis in the overall pathogenesis of COPD, which can be modified by both genetic and environmental factors.

1.3.5 Exacerbation in COPD/Emphysema

COPD is often associated with exacerbations that are a common cause of hospitalization and lead to a large proportion of COPD-associated mortality [256-260]. An exacerbation, as defined by the respiratory physician working group at the Aspen Lung Conference in 1999, "is a sustained episode with acute onset in the natural course of the disease, that deviates from normal day-to-day variations, worsening the patient's symptoms, and requiring a change in medication" [261].

Exacerbations are a primary contributor to both the economic and sociological burdens associated with the management of patients with COPD. Although exacerbations are infrequent in the early stage of COPD, they occur twice a year on average in patients with moderate-to severe disease [262]. The frequency of severe exacerbation is positively correlated with mortality [256].

According to the data from the Healthcare Cost and Utilization Project that studied all hospitalized COPD patients ≥ 40 years of age in the United States in 2008, more than 500,000 patients were hospitalized with acute exacerbation, which cost approximately $3.8 billion in aggregate (which is the main cost driver in this population) [263]. Another study addressed the issue of total annual health care costs and found that the price increased from $11,747 in patients without exacerbation to $14,188 in those with moderate exacerbation and up to $43,042 in the most severe exacerbation group [264].

One of the greatest concerns regarding exacerbations is their long-lasting impact on the speed of the progression and the severity of disease [260, 265]. Thus, one of the main goals of COPD management is to prevent the exacerbation events [31].

Most COPD exacerbations, some 70 – 80%, are caused by bacterial and viral respiratory infections (which may coexist) [266, 267]. Bronchoscopic sampling reveals that more than 50% of COPD patients with exacerbation have high concentration of bacteria in their lower airway, compared to 0-4% of healthy adults [268, 269]. Predominant in the bacterial samples from such patients are new strains of *Haemophilus influenzae, Moraxella catarrhalis, Pseudomonas aeruginosa* and *Streptococcus pneumoniae* [270-274]. The "frequent exacerbators", who experience two or more exacerbations per year, have increased airway colonization with *H. influenzae* and *S. pneumoniae* , more severe symptoms and increased sputum purulence during exacerbation [275].

Employing different approaches studies have reported viruses to be present in one third to two thirds of COPD exacerbations [267, 276, 277]. Although rhinoviruses are the most common identified virus group in COPD patients during exacerbations, influenza virus is the most commonly associated with severe exacerbations requiring hospitalization [260]. Respiratory syncytial virus (RSV) and human metapneumovirus have also been reported as a cause of exacerbation [278, 279].

Other important potential causes include exposure to environmental pollution such as ozone, NO_2 and PM10 [280, 281], and cold weather [282].

Exacerbations profoundly affect the nature of the immune response in the lung, and markedly impact the progression of COPD through several mechanisms. During exacerbations, particularly in patients who have microbial colonization in the respiratory tract, there are often marked increases of inflammatory biomarkers including white blood cell counts, pro-inflammatory cytokines, i.e. TNF-α, IL-6 or IL-8, leukotriene B_4 (LTB_4), C-reactive protein (CRP) and chemokines. Exacerbations have also been linked increased production of ROS, as observed by a persistent increase in 8-isoprostane and hydrogen peroxide in the exhaled breath of COPD patients with exacerbation [202, 283, 284]. There are also elevations of proteases such as neutrophil elastase, MMP-9, but a reduction in protease inhibitor TIMP-1 [285-292].

A variety of conserved molecular motifs within bacteria or viruses, called pathogen-associated molecular patterns or PAMPSs, can be initially recognized by a set of diverse host innate immune-sensor molecules termed "pattern recognition receptors (PRRs)". The Toll-like receptors (TLRs), for instance, are a class of PRRs that detect a broad range of PAMPs including peptidoglycan, lipopolysaccharide (LPS) and flagellin on the bacterial surface, or single-stranded (ss-) and double-stranded (ds-) RNA in the viral genome. The downstream cascade of activation of these receptors can activate multiple signaling pathways, especially the NF-κB-dependent pathways, which activates transcription factors that results in transcription and translation of a spectrum of cytokines, chemokines, and other inflammatory mediators. In a murine model, polyinosinic-polycytidylic acid [poly (I:C)] - a molecule mimicking viral ds-RNA that can activate TLR3 signaling - can augment the effects of cigarette-smoke induced inflammation and apoptosis, and ultimately cause excessive emphysema [293].

Although the cellular and molecular mechanisms of exacerbation are still not well elucidated, most studies have shown that prolonged increases in COPD exacerbations amplify the inflammatory response, proteases, and oxidative stress in the respiratory system. These repeated events further shift the imbalance of COPD-associated mediators (as described in section 1.3.4) towards more susceptibility for COPD progression and severity as shown in Fig. 1.5.

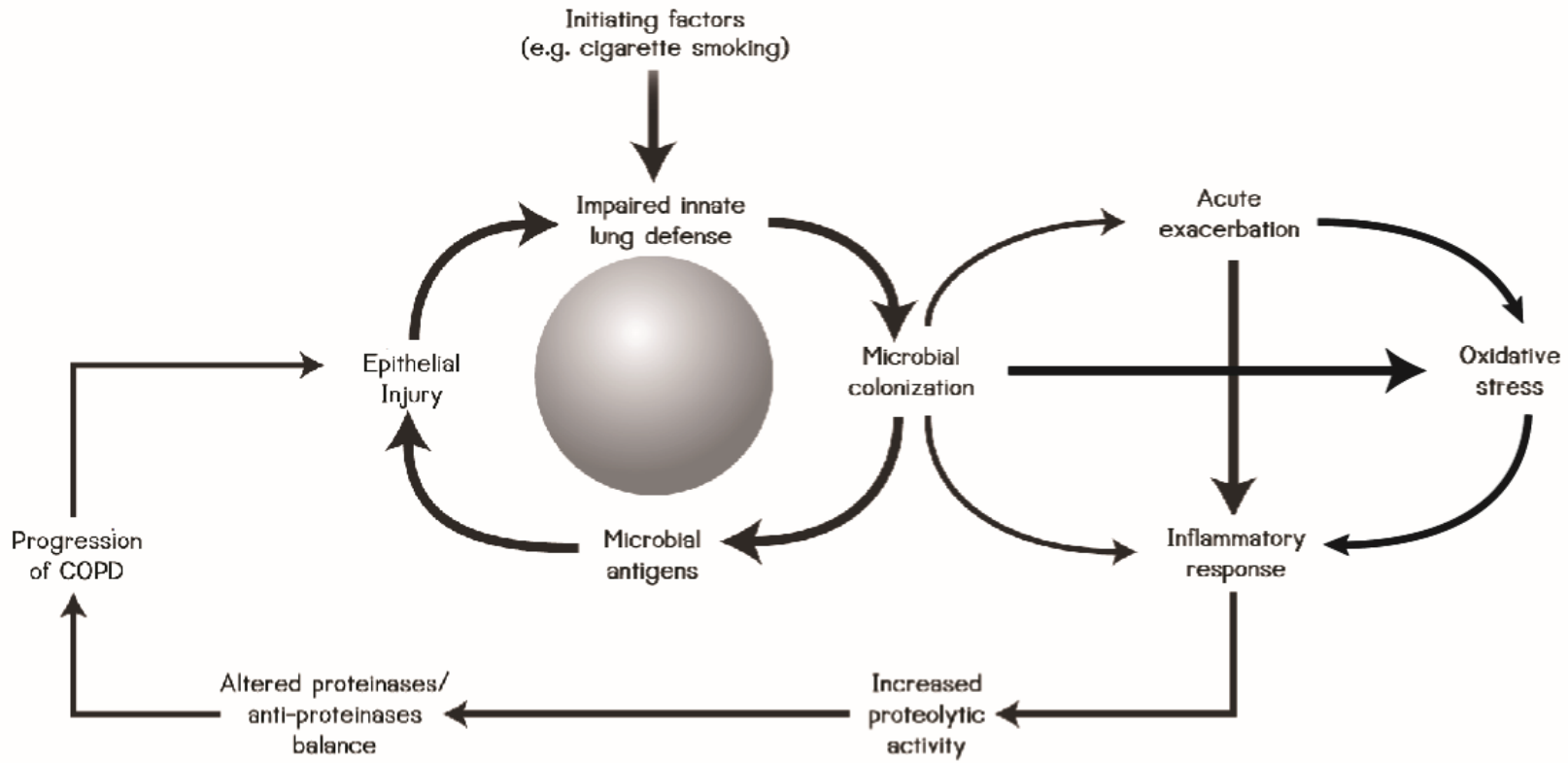

Figure 1.5 Role of microbial infections in exacerbations of COPD.
Modified with permission from New England Journal of Medicine [266], Copyright Massachusetts Medical Society (2008).

1.4 Animal Models of Emphysema

The causes of COPD are not fully understood. Most studies of the pathogenesis of COPD in human patients derive from comparison of human lung tissue or cells between COPD patients with different stages of the disease vs non-COPD patients, or smokers vs non-smokers. However, since COPD is a very complex disease, and usually accompanied by various co-morbidities, such studies have only shown an association of particular events to COPD, causal relationships cannot be determined. Moreover, because human COPD is a slowly progressive disease, it is difficult to follow all the changes in humans. Thus, several animal models of COPD/emphysema have been developed to recapitulate aspects of this disease process, and facilitate understanding of the underlying pathologic mechanisms of the disease. These models also raise the opportunity to test novel drugs and therapies before clinical trials in humans.

One of the complexities of human COPD is that it comprises both chronic bronchitis in the conducting airway, and pulmonary emphysema in the parenchymal tissue. This results in difficulty in using animal models to study both regions of the lung simultaneously. In this thesis, we focus on understanding the pathogenesis of emphysema affecting the destruction of alveolar tissue.

Many of the causative agents of emphysema, including several types of proteases, cigarette smoke, biomass fuels, air pollutants (i.e. ozone), and helminths have been used to induce emphysematous phenotypes in laboratory animals. These animal models play a critical role in our current understanding of emphysema pathogenesis. However, each attempts to model

different aspects of the human disease and have inherent advantages and disadvantages in terms of outcome and human relevance, which will now be reviewed.

1.4.1 Protease-induced emphysema model

In 1965, Gross *et al.* established the first reproducible experimental animal model of emphysema, by intratracheal installation of papain proteinase (a plant protease) into the lungs of rats [71]. This success in developing an animal model closely resembling the human emphysematous phenotype happened shortly after the discovery of an association between α1-AT deficiency and emphysema [58]. From these observations emerged the hypothesis that the development of emphysema was due to the imbalance between proteases and anti-proteases in the lung. While protease activity of papain depends on its purity and source, several other proteases with the capacity to degrade the extracellular matrix in the alveolar wall enzymes have subsequently been used in attempt to induce emphysema in a variety of animal species. These proteases include porcine pancreatic elastase [294, 295], human neutrophil elastase [296, 297], collagenase [298], proteinase 3 [299] and cathepsin B [300].

In rodent models, the most common protease-based approach to induce emphysema is a one-time intratracheal instillation of porcine pancreatic elastase, because of low-cost, good availability, speed, consistency, and impressive airspace enlargement [301-303]. This intratracheal insult causes, in the first few days, edema, hemorrhage and a rapid influx of inflammatory exudates composed of neutrophils and macrophages, with a number of other inflammatory mediators [304]. Within a week after elastase treatment, the hemorrhage and inflammation are typically resolved [155]. One week after treatment, there is an increase in the numbers of adaptive immune cells ($CD4^+$, $CD8^+$ cells), and within 21 days of the insult

there is significant observable enlargement of airspaces [188]. Marked increases of ROS production, other proteases and apoptotic markers can be also detected in the lung after elastase administration [175, 305, 306].

The severity of emphysema progressively evolves for at least 26 weeks after a single insult of pancreatic elastase [70, 304], even though the activity of exogenous enzymes was inhibited by endogenous protease inhibitors within 24 hours following administration [307]. The administration of elastase inhibitors have a protective effect only when given immediately before, or immediately after, elastase challenge; they are not effective if given 4 or 8 hours after challenge [308-310].

This persistent emphysematous change in the animal model corresponds to the characteristics of emphysema in human patients, in which emphysema remains progressive, even after cessation of smoking [311, 312]. Although the mechanism of this progressive changes is not certain, the data suggests that it is the endogenous host responses, triggered by elastase, that cause persistent damage in the lung. It has been suggested that only 20% of the loss of parenchymal tissue after elastase challenge is due to direct attack by instilled elastase: the remaining 80% of the loss results from the host inflammatory or remodeling response [175].

This progressive feature of the elastase model provides a good opportunity to gain insights into the mechanisms underlying the progressive loss of alveolar tissue associated with emphysema and an opportunity to define the roles of repair and remodeling of tissue in response to injury as well as the relationship between altered structure and pulmonary

functions and mechanics in emphysema [188, 313-317]. Ultimately, this model can be a useful tool with which to explore potential drug and intervention therapy to stop emphysema progression [134, 228, 318].

Although instillation of proteases can induce useful and reproducible emphysema-like pathology, and provide valuable information about the mechanisms underlying the progressive phase of emphysema development, these models have several drawbacks. (i) They cannot provide information on upstream events prior to release of excessive proteases in human COPD, particularly when the disease is initially triggered by environmental agents. (ii) It is difficult to explore the role of other proteases that might be involved in the pathogenesis of emphysema, because their proteolytic activities are obscured by the impact of elastase. The question is raised whether the emphysema phenotype induced by a single-dose elastase insult is physiologically comparable to the emphysema in humans, which might involve many proteases and/or more mediators. (iii) Exogenous porcine pancreatic elastase, and endogenous neutrophil elastase, have different primary endogenous inhibitors (α_2-macroglobulin for pancreatic elastase, but α1-AT for neutrophil elastase) [307]. Thus, it is crucial to note whether a particular exogenous inhibitor may not inhibit both of these enzymes. (iv) Unlike the common human emphysema induced by environmental smoke, in which there is development of centrilobular emphysema, elastase produces panacinar emphysema characterized by uniform loss of all portions of the acinus from the respiratory bronchiole to the alveoli, as is typical for inherited α1-AT deficiency emphysema patients [319]. (v) None of these models can totally mimic the entire phenotype seen in human in COPD, because inflammation in the airways and mucus hypersecretion, which might contribute to emphysema development in humans, are not seen in these models. The

extrapolation of the data generated by these models to human diseases therefore has to be done with care.

1.4.2 Cigarette smoke-induced emphysema model

Due to cigarette smoke being the predominant risk factor for development of COPD, smoke-induced animal models have been developed for study of the pathophysiology related to the development of emphysema. Chronic exposure to cigarette smoke in rodents can mimic multiple features of COPD, including accumulation of inflammatory cells and mediators, elevation of oxidative stress, hypersecretion of mucus, decline in lung function, mild emphysema, airway remodeling, pulmonary hypertension, and increased pulmonary inflammation associated with exacerbation [320, 321]. In the rodent model, the cigarette smoke induced centrilobular lesions resemble that seen in human smokers where the pathology begins from the respiratory bronchioles and spreads peripherally [319, 322]. Thus, this experimental model has gained attention for its potential to yield mechanistic insights into the earlier stages of the pathogenesis of emphysema, particularly the roles of inflammation and oxidative stress.

In 1981, Huber *et al.* provided the first description of the morphological and physiological alterations in smoke-induced emphysema in rats [323]. Subsequently, different laboratories have used variations of this system for cigarette smoke-induced animal model of emphysema and no standard exposure protocol is in place. For example, smoke exposure intervals range from 1 to 3 sessions per day, with different numbers of cigarettes smoked in each session (2 to 40 cigarettes a day), 5 to 7 days per week, for 2 to 36 weeks [83, 102, 324-330]. Different routes of exposure have also been used.

To simulate passive smoking, most studies burn the cigarette and passively expose the whole body of the animal. In contrast, some studies use a nose-only smoke exposure system to deliver smoke to the respiratory system only, and avoid the confounding effects of orally-exposed nicotine or tar substances during the animals' self-grooming [328, 331, 332]. Both of these techniques involve using the side stream smoke generated by the burning end of a cigarette (similar to passive smoking) to induce emphysema. To simulate active smoking, investigators have delivered to the animals, the mainstream smoke produced by suction and drawing back of cigarettes by pump or "puffing" [227, 333-335]. However, there are no studies comparing the degree of emphysema produced by these different methods. The smoking chambers are also unique to each group, and not all studies include monitoring of the dose and composition of cigarette smoke to which the animals are exposed. Thus, it is very difficult to make any comparison between the results from different authors.

Recently, a study claimed that multiple injections of cigarette-smoke extracts into the peritoneal cavity of animals resulted in a systemic inflammatory response and the induction of proteases and oxidative stress in lung tissues, which caused pulmonary emphysema within a month [336]. However, the relevance of this approach to human emphysema remain uncertain.

Models of cigarette-smoke induced emphysema have recently been used to investigate the impact of exacerbation by bacterial or viral infection. For instance, mice exposed to cigarette smoke and then infected with influenza virus H1N1 or H3N1 had increased number of BAL immune cells, (especially virus-specific activated $CD8^+$ T cells with altered key cytokine

profiles), compared to smoke or influenza infection only, and had a 10 fold increase in virus titers in the lung at day 3, compared to influenza only mice [337, 338]. Several studies have reported that exacerbation with bacteria (heat-killed non-typeable *Haemophilus influenzae*), virus (rhinovirus), or exposure to a TLR agonist (polyI:C) that mimics virus-induced innate immunity, can accelerate progression of cigarette smoke-induced emphysema in mice [293, 339-341].

Besides the lack of consistency between protocols to induce emphysema by cigarette smoke, other major disadvantages of this model are its high-cost, the need for long-period of exposure to develop the phenotype and the difficulty in using the model to study new therapeutic drugs. Moreover, although the lesions produced in the rodent model are similar to the pathology in humans, the emphysema in the rodent model is only mild, and the emphysema in the rodent does not progress even after smoking ceases, whereas in humans there is progression in symptomatic patients at GOLD stage III or IV. In the animal model, the emphysema from cigarette smoke is stable and non-progressive, with persistent or decreased inflammatory responses after the end of exposure [342-344]. Furthermore, the cigarette smoke-exposed animal model cannot totally explain the susceptibility of human emphysema, since almost all animals develop emphysema, but only 15 - 20% of human develop emphysema. Finally, similar to the elastase model, the cigarette smoke model cannot model the chronic bronchitis seen in human COPD.

1.4.3 Biomass fuel-induced emphysema models

Biomass smoke has been used to induce emphysema in laboratory animals to simulate human disease, particularly that affecting women in developing countries who are exposed to

indoor pollutants from cooking with biomass fuels. Hu and colleagues exposed rats to smoke either generated from 25 gram grain crust (typical biomass fuel used for cooking) or from 10 cigarettes, twice daily with a 4 hour interval, 7 days per week, for 14 weeks. They reported that biomass smoke could induce pulmonary inflammation, systemic oxidative stress and emphysematous damage at levels similar to that of cigarette smoke [345]. Similarly, emphysematous changes were shown to be induced by exposing rabbits to smoke from dried dung [346], and by exposing rats to smoke from cow dung daily for one month [347].

1.4.4 Air pollutant-induced emphysema models

Environmental factors, including gases and particulate matter in polluted air, are involved in the development of COPD. Ground-level ozone, (O_3,) is one of the six commonly found pollutants worldwide (together with particulate matter, carbon monoxide, sulfur oxides, nitrogen oxides, and lead) [348]. In contrast to cigarette smoke, which contains several thousand chemical compounds with a number of ROS species, ozone is a powerful "single" reactive oxidant molecule present in environmental air pollution, which induces pulmonary oxidative stress and triggers adverse health effects. Exposure to high levels of ozone has been associated with worsening of symptoms in patients with asthma and COPD [349-352].

Ozone has long been used in models for asthma, because it can induce neutrophilic lung inflammation and oxidative stress with airway hyperresponsiveness, which are critical features of human asthma [353-355]. Recently, Triantaphyllopoulos *et al.* demonstrated that chronic exposure of mice to ozone at a high concentration (2-3 ppm) for 6 weeks could induce disruptions in alveolar architecture, leading to emphysema-like airspace enlargement [107, 356]. There was increased oxidative stress, an inflammatory response (e.g. increased

BAL cell counts, IL-13, IFN-γ, TNF-α, IL-6 and IL-17), an up-regulation of MMP-12, and increased apoptotic markers (caspase-3 and apoptosis protease activating factor-1). The emphysema-like lesion, and deteriorated lung function did not resolve, even 3 weeks after cessation of exposure [357]. This pattern is similar to that seen in the animal model of cigarette smoke-induced COPD and in human COPD. Thus chronic ozone exposure might be a good model with which to study the role of oxidative stress in initiating the emphysema phenotype. Treatment with N-acetylcysteine (NAC), a therapeutic antioxidant and a mucolytic agent, both before and after the animals were exposed to ozone, could not reverse the ozone-induced emphysema, even though lung inflammation and airway hyperresponsiveness were attenuated [357].

1.4.5 Parasite-induced animal emphysema models

Another interesting novel murine model of emphysema is that in which the disease is induced by infection with the nematode *Nippostrongylus brasiliensis*, which is used in mice and rats as a model for human hookworm infections [358, 359]. The free-living third-stage (L3) larvae of *N. brasiliensis* penetrate, (or injected) the skin and migrate via the circulation to the lungs at around two days post-infection. In the lungs, the L3 larvae reside for 12-48 hours prior to molting to the fourth stage larvae (L4). The L4 migrate up the conducting airways and are swallowed into the small intestine, where parasites complete their develop into adults, mate, and produce eggs deposited in the environment when the rodent defecates [358]. *N. brasiliensis* infection in mice is self-limiting as the adult worms are expelled from the gastrointestinal tract within 9-13 days after infection [358, 360].

Although *N. brasiliensis* larvae reside in the host's lung only for two days, they induce a strong, long-lasting, type 2 immune response, characterized by increasing levels of Th2 cells, IL-4, IL-13, IgE, eosinophils, basophils, mast cells and Type 2 innate lymphoid cells (ILC2s), as well as alternatively-activated (M2) macrophages, which are thought to promote repair of the tissue damage caused by the worms [361-366]. In 2008, Kopf *et al.* showed that *N. brasiliensis* infection left behind a chronic inflammatory response in the lung, causing progressive destruction of alveolar walls, and a marked enlargement of the airspace size, resembling the emphysema phenotype in humans [108]. This prolonged nematode-induced lung damage was associated with hemosiderin positive macrophages, with an alternatively activated (M2) phenotype marked by the induction of *Arg* (Arginase), *Retnla* (Fizz1) and *Chi3l3* (Ym1) expression. These M2 macrophages exhibited substantial up-regulation of MMP-12, (a potential protease candidate that might cause tissue degradation in emphysema pathogenesis), for more than 150 days, suggesting a role of Th2 cells and M2 macrophages in the development of emphysema.

More evidence in support of the role of Th2 cells in this model was demonstrated by injecting *N. brasiliensis* into mice selectively deleted of transforming growth factor-beta receptor type II (TGFβRII) in myeloid cells (including monocytes and macrophages) [367]. This study show that the lack of macrophage-mediated suppressor signaling resulted in an elevation of pro-inflammatory cytokines, an increase in type 2 immunity, excess MMP activity, and a more severe emphysema phenotype. However, these results were in contrast to the findings that mice lacking the capacity to generate Th2 responses, such as mice deficient in the production of the IL-4 receptor, IL-5 receptor, IL-13 or MMP-12, were not

protected from *N. brasiliensis*-induced emphysema. Thus, the mechanism of induction of emphysema by *N. brasiliensis* is still not clear.

1.5 Assessment of Emphysema in Animal Model

A critical step in the investigation of the development of emphysema and the evaluation of the therapeutic interventions in animal models is an efficient and accurate quantitatively assessment of phenotype. The major characteristic features of human emphysema include a decline in lung function over time, alveolar wall destruction, and a loss of elasticity and recoil that results in elevated lung compliance (the change in volume for any given change in distending pressure). Such changes in structure and function need to be evaluated carefully to understand both the pathogenesis and the effects of interventions on the progression of the disease. Several of these pathophysiologic changes can be assessed in animal models using techniques that resemble those used in humans.

1.5.1 Diffusing Capacity for Carbon Monoxide

A test of the diffusing capacity of the lungs for carbon monoxide (DL_{CO}) is one of the most common clinically valuable tests of lung function. In humans it is both convenient and easy to perform. DL_{CO} measures the ability of the lungs to exchange gas, and is directly impacted by a loss of alveolar surface area. It is assessed by measuring the partial pressure difference between inspired and expired carbon monoxide after a 10 second breath hold at the end of a deep inspiration. The uptake of gas during this time reflects ability of the lungs to transfer gas from inhaled air to the red blood cells in the pulmonary capillaries. Because the major pathology of emphysema is the destruction of alveolar membranes and loss of gas-exchange surface area, decreases in DL_{CO} is an excellent index to quantify the anatomic extent of

emphysema. The extent of the fall in DL_{CO} correlates tightly with the degree of emphysema as assessed by a reduction of lung tissue density observed CT imaging [368, 369]. The DL_{CO} also can help separate emphysema from chronic bronchitis in COPD because patients diagnosed with chronic obstructive bronchitis and airway obstruction (but not emphysema) have normal DL_{CO} [370]. To assess this characteristic in mice, our laboratory developed a quick and simple single-breath diffusing capacity measurement which is closely related to the DL_{CO} measurement in humans. This has been shown to be sensitive enough to quantify structural changes in several different lung pathologies including emphysema [371, 372]. The procedure is performed in an anesthetized mouse using a 9 second lung inflation with a gas mixture containing approximately 0.5% neon (tracer gas), 0.5% carbon monoxide. As in humans the gas is then quickly withdrawn and the gas is analyzed for the concentrations of neon and carbon monoxide. However, as there are a number of assumptions in the procedure in the mouse, we call this the diffusion factor for carbon monoxide (DF_{CO}) to distinguish from DL_{CO} in humans.

1.5.2 Pressure-Volume Curve

Lung volumes and lung capacities refer to the amount of air associated with different parts of the respiratory cycle (reviewed in Table 1.4). Measurement of lung volume is an important metric for understanding normal function of the lungs as well as the changes in disease states. Because of the permanent destruction of alveolar walls and the dilation of airspaces in emphysema, the lung loses elasticity and recoil which results in increased lung compliance (or decreased elastance—the reciprocal of compliance). More air can also be trapped within the lung at the end of spontaneous expiration because the peripheral airways tend to collapse in the expiratory phase due to the weakening of interdependent forces between airways and

alveoli. This results in a greater respiratory effort in order to repeatedly open collapsed airways [373-375]. This also leads to the chronic lung hyperinflation, which is manifested by increases in total lung capacity (TLC), functional residual capacity (FRC) and residual volume (RV).

Table 1.4 **Lung volumes and lung capacities definition and their changes in emphysema**

Term	Definition	Change in emphysema
Tidal volume (TV)	the amount of air inspired and expired during normal breathing without conscious effort	decreased
Residual volume (RV)	the volume of air remaining in the lungs after maximum exhalation	increased
Expiratory reserve volume (ERV)	the additional amount of air that can be forcibly exhaled after a normal tidal volume	decreased
Inspiratory reserve volume (IRV)	the additional amount of air that can be forcibly inhaled after a normal tidal volume	reduced
Total lung capacity (TLC)	the maximum amount of air that the lung can hold	increased
Vital capacity (VC)	the total amount of air that can be expired after full inflation to TLC	normal or slightly decreased
Inspiratory capacity (IC)	the maximum amount of air that can be inspired after the end of a normal expiration	decreased
Functional residual capacity (FRC)	the amount of air remaining in the lungs after a normal volume at the end of a normal expiration	increased

In rodents, some of these changes in lung volume and lung compliance can be obtained by determining the quasi-static pressure-volume (P-V) relationship. In our laboratory, this is accomplished by starting at a completely degassed (atelectatic) state and slowly inflating and deflating the lung over a volume range between –10 and +35 mH_2O. An example of the

characteristic of P-V curve in mouse is shown in Fig. 1.6. Since we cannot obtain the maximum lung volume by voluntary effort and the inflation limb of P-V curve never reaches a plateau, TLC has to be determined by using a consistent maximal pressure - we have chosen 35 cmH_2O [376, 377]. The residual volume (RV) can be obtained from the volume of air trapped in the lung due to collapse of airways after the first deflation limb as shown in Fig. 1.6. Moreover, lung compliance (defined as a change in lung volume per unit change in pressure) can be easily phenotyped from the slope of any linear region of the P-V loop (in our laboratory we use the range between 3-8 cmH_2O). In experimental animal models of emphysema, the P-V curve is shifted upward and leftward, resulting in an elevation of TLC, RV, and quasi-static lung compliance compared to naïve control animals (Fig. 1.6).

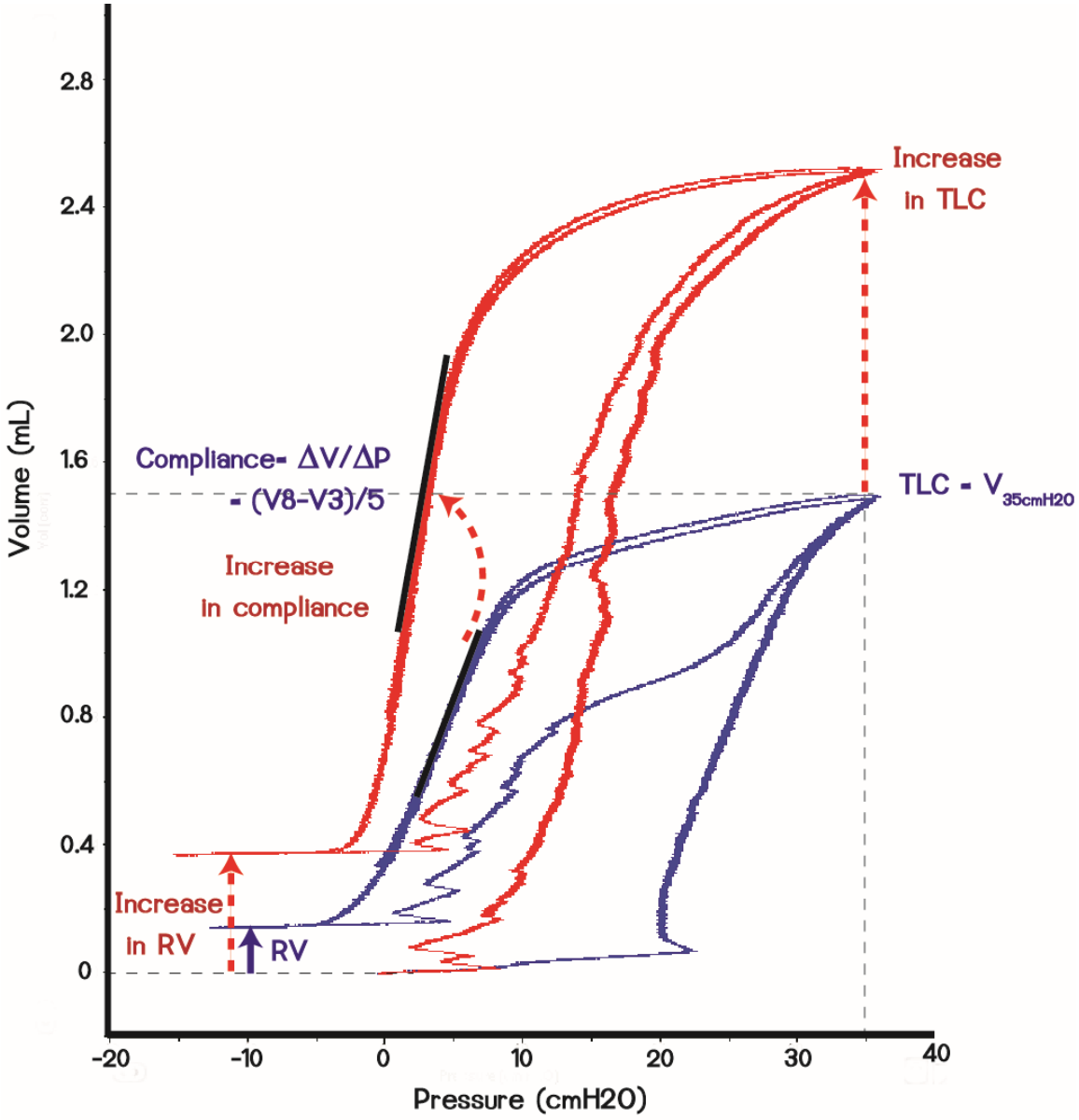

Figure 1.6 Pressure-Volume Relationship. Characteristic P-V curves of naïve BALB/c mouse (blue) and three-unit-elastase-treated BALB/c mouse (red).

1.5.3 Stereological assessment

Emphysema has been defined as the "abnormal permanent enlargement of the airspaces distal to the terminal bronchioles, accompanied by the destruction of their walls" [28]. Lung stereology — unbiased quantitative extraction of the geometry of the irregular three-dimensional (3D) lung structures from microscopy-based two-dimensional (2D) histological section images— was promoted by a joint policy statement from the American Thoracic Society and the European Respiratory Society as the appropriate "gold standard" for assessment lung morphology [378]. A number of different stereological dimensional parameters starting from 0D (number of alveoli), 1D (length or thickness of alveoli), 2D (alveolar surface area), to 3D (alveolar volume or size) can be estimated using this stereological-based approach.

Emphysema in rodent models is commonly quantified in histological samples in terms of the mean linear intercept length (L_m), defined as the mean length of straight line segments (chords) on random test lines spanning the airspace between alveolar walls (Fig. 1.7) [378]. L_m actually derives from measurement of volume-to-internal surface area (V/S) ratio of lung parenchyma [379], but it is commonly used as an index of airspace size [380]. It can also be estimated by intersection and point counting using a suitable coherent stereological test grid [381]. However, it is critical to point out that using L_m to quantify airspace enlargement has several drawbacks. Firstly, L_m is effective only for measuring the convex particles (i.e., where a line traversing the particle can have only one intercept), but alveoli do not always meet this condition (as an example in Fig 1.7) [381]. Also, L_m is a parameter representing only a mean, it cannot give any information regarding the variation on airspace dimension throughout the lung, nor the heterogeneity of pathological changes in the lung that are often found in

pulmonary emphysema. Moreover, L_m is very sensitive to degree of inflation and tissue shrinkage during fixation and sample preparation [376, 382] - in control animals, larger L_m are observed simply with a higher degree of lung inflation [381]. Thus, post-mortem lung fixation must be standardized to ensure a similar inflation state for all samples using a high inflation pressure (20-30 cmH_2O) with a rapid inflow. However, it is not sufficient to conclude that the airspace enlargement observed by increased L_m always means emphysema, unless there is evidence showing destruction of alveolar walls. It is easy to generate increased L_m by inflating a lung without destruction of alveolar walls. Thus, it is important to obtain an estimate of tissue destruction, such as a decrease in total alveolar wall volume, total alveolar surface area, total capillary length, or total number of alveoli as well. [378, 383-385]

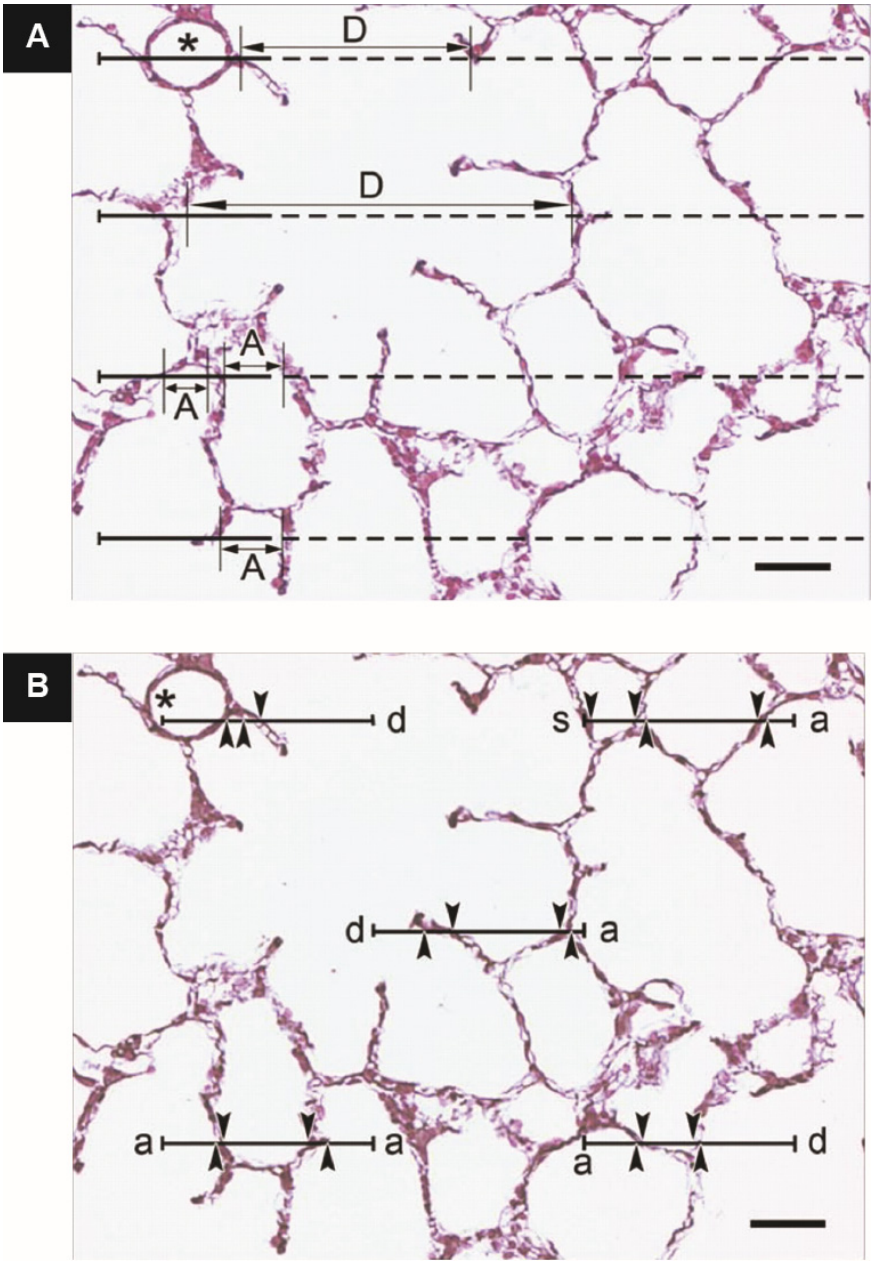

Figure 1.7 Two approaches to estimate mean linear intercept (chord) length (L_m).
Direct method based on intercept distribution. The distance (chord length) between intercepts of two alveolar walls is measured. A: alveolar airspace, D: alveolar duct, *: blood vessel.
Indirect method based on point and intercept counting. L_m can be estimated indirectly by simple point and intersection counting using a coherent test line system. Points overlying on alveolar air space (a), ductal air space (d), septal tissue (s), and blood vessel (*).

1.5.4 Imaging-based techniques

In clinical practice, although emphysema can typically be diagnosed by physical examinations and pulmonary function tests (PFTs), including DL_{CO}, spirometry or P-V relationships, these PFTs have a low sensitivity to detect the early stages of emphysema. Since they lack the ability to discriminate at the regional level, the PFT results are at the whole lung level and reflect the variable pathologic changes in all lung compartments – some of which may not be related to emphysema. Indeed, more than 30% of patients with emphysema have no detectable functional abnormalities [386]. However, imaging-based techniques, such as high-resolution computed tomography (CT), are noninvasive and have sufficiently high resolution and sensitivity to depict the presence and characteristic of emphysema *in vivo*. In rodents, X-ray micro-CT scanning on anesthetized animals has been used to study the progression of emphysema *in vivo* [387]. Vasilescu *et al.* applied the principles and methods of design-based stereology used for histological sections to the mouse lung parenchymal images obtained from micro-CT methods. They found no difference in most stereological parameters (i.e. volume fraction of parenchymal and non-parenchymal tissue, mean linear intercept, number of alveoli) between quantitative analysis of traditional histological sections and micro-CT images [388]. Recently, several types of magnetic resonance imaging (MRI) modalities such as proton MRI, and hyperpolarized ^{3}He- or ^{129}Xe-diffusion MRI, have been applied successfully for the detection of emphysema in animal models [389-393]. Moreover, Jobse *et al.* recently illustrated that the V/Q (ventilation/perfusion) SPECT (single-photon emission computed tomography) imaging can detect lung structural changes in mice exposed to cigarette smoke as early as 8 weeks before CT scanning can detect any changes [394].

While the technology for small animal imaging has been developing, each of these techniques have advantages and limitations. The ability to be non-invasive allows *in vivo* imaging, and this is an obvious advantage compared to *ex vivo* histological techniques, since it can preserve the integrity of lung tissue while allowing three-dimensional (3D) reconstruction of the anatomy, whereas histological-based techniques physically destroy the lung's 3D structure during the fixation and sectioning processes [388]. However, these imaging techniques are costly, requiring expensive instruments and highly trained technicians. Also, the histological sections can be further analyzed for biological insight, particularly for differentiation of cell/tissue structure and immuno-staining, which is not possibly with the *in vivo* imaging.

1.6 Thesis Summary, Hypothesis and Specific Aims

Emphysema is a fundamental component of COPD. Emphysema is characterized by a long-term, progressive loss of alveolar tissue, and airspace enlargement. The studies that have been carried out to define the pathogenesis of emphysema suggest that the mechanisms underlying the development of the disease are very complicated, and not completely understood.

Several key mechanisms contributing to the pathophysiology of emphysematous changes remain unsolved. (i) Although cigarette smoke is the primary risk factor for COPD/emphysema, only 15 - 20% of smokers develop the disease. This statistic suggests that beyond the factors in cigarette smoke that promote emphysema there are complex underlying genetic, environmental and biological factors that dictate susceptibility to the disease. In animal models, different species, and different strains within the same species, when exposed to the same emphysema-inducing factors, develop different degrees of emphysema. (ii) Even though smoking cessation is a recommended therapeutic intervention to slow the decline in lung function, in most cases cessation does not stop the progression of the disease. This continuous decline is also commonly seen in murine models. This data indicates that individual initiating factors, such as cigarette smoke, cannot fully explain the pathogenesis of the disease. Aberrant, self-perpetuating, inflammatory or repair mechanisms, perhaps enhanced or triggered by initiating factors, might play important roles in the progression of emphysema. However, the nature and regulation of the proposed aberrant mechanisms are still poorly understood. Thus, identification of the associated cellular and molecular processes driving the persistent development of the disease is still required. (iii) Many types of respiratory infections can exacerbate emphysema. However, there is scarce

literature exploring the mechanisms by which these infections can alter or promote the progression of emphysema in humans and experimental animals. Moreover, the studies that have considered the effect of infection on the severity of emphysema, none have investigated the impact that a history of viral infection has on the progression and severity of emphysema.

To date, there are several animal models of emphysema, but none satisfactorily model all aspects of human emphysema. Even though arguably the cigarette smoke animal model has merit for its use of a proven risk factor, this model is costly, takes a long time and results in a weak and high variability outcome. For this research project, we selected the elastase-induced emphysema animal model because it has several advantages over the cigarette-smoking animal model. The elastase model is relatively simple, inexpensive to implement, disease development is rapid, consistent, reproducible and the results replicate several aspects of the human disease. The degree of emphysema can easily be controllable by changing the dose of the elastase enzyme, (in contrast, in the cigarette smoke model, it is difficult to control the severity of emphysema, or produce severe emphysema). Moreover, the elastase model shares many similar mechanisms with the cigarette smoke model, such as proteolytic damage, matrix remodeling, and inflammatory responses. Lastly, the elastase model allows us to study the mechanisms that define the key characteristics of human emphysema disease – the progressive loss of alveolar epithelium – an aspect of emphysema that is not reproduced in the cigarette smoke model. This should be beneficial for development of novel therapeutic drugs to stop or reverse the progression of the disease.

The overall goal of the present research is to explore - using elastase-induced murine model - the factors, particularly the immunological factors that contribute to the susceptibility to, and the regulation of, the development of emphysema. The severity of the emphysematous outcomes will be assessed by a combination of approaches, including pulmonary function tests such as diffusion factor for carbon monoxide (DF_{CO}), pulmonary mechanics tests (lung volume and compliance), and quantitative stereology on histological sections, as well as several inflammatory biomarkers.

We hypothesize that: (i) the susceptibility to the develop elastase-induced disease is different in two strains of mice (Chapter 3); (ii) immune mechanisms mediate this difference (Chapter 4); and (iii) the disease can be altered by pre-infection with viruses (Chapter 5). The results should provide insight into the pathogenesis of emphysema, and help determine the roles of each mediator in the disease mechanism, thus providing potential targets for novel therapeutic intervention.

To test our three hypotheses, we have established three specific aims, each of which will be addressed in an individual chapter.

<u>Specific Aim 1</u>: Compare the susceptibility to elastase-induced emphysema in two commonly-used mouse strains: C57BL/6 and BALB/c

To identify a genetic basis for differential susceptibility to develop emphysema of two commonly-used strains of mice, C57BL/6 and BALB/c, were exposed to varying doses of elastase and at different time points. The levels of lung damage were assessed by performing functional tests, mechanical tests, histology, inflammatory analysis and gene expression.

<u>Specific Aim 2</u>: Explore the immunological responses that contribute to susceptibility to, and progression of, elastase-induced emphysema

To determine the role of various immunological mediators in the development of emphysemic damage, genetically modified mice deficient in specific mediators were challenged with elastase and the degree of emphysema was assessed by performing functional tests, mechanical tests, and histology.

<u>Specific Aim 3</u>: Determine the impact of viral infection on development of elastase-induced emphysema

To investigate the role of viral infection on emphysema development, two types of viruses, (vaccinia and influenza), were delivered at different time points either before or after elastase challenge. To determine the degree of emphysema, we performed the functional tests, mechanical tests, and histology, comparing the infected mice to uninfected control mice.

CHAPTER 2

MATERIALS and METHODS

2.1 Animals

Male wild type (WT) BALB/cJ, wild-type C57BL/6J, RAG-1$^{-/-}$ (on both BALB/c and C57BL/6 genetic background) and MyD88$^{-/-}$ (C57BL/6 background) were purchased directly from The Jackson Laboratory (Bar Harbor, ME). Breeder pairs of IFN-$\gamma^{-/-}$ (both on BALB/c and C57BL/6 background) and STAT6$^{-/-}$ (BALB/c background) mice were also obtained from The Jackson Laboratory. ST2$^{-/-}$ mice were originally generated and backcrossed onto a BALB/c background by Dr. Andrew McKenzie (Medical Research Council, United Kingdom) as previously described [395, 396] and provided to us by Dr. DeLisa Fairweather. IL17A$^{-/-}$ (BALB/c background) mice were generated by Dr. Yoichiro Iwakura (University of Tokyo, Japan) [397] and kindly donated by Dr. Noel Rose. Conditional deleted STAT3 in myeloid cells (Cre-Lyz/STAT3$^{fl/fl}$) and in CD4 cells (Cre-CD4/STAT3$^{fl/fl}$) mice were gifts from Dr. Cynthia Sears (Johns Hopkins School of Medicine). All knockout mice were bred and housed under specific pathogen-free conditions at the Johns Hopkins School of Public Health. The animals were provided filtered air (60-70% relative humidity) at 22-26ºC and maintained on a 12-hour light/dark cycle with *ad libitum* access to autoclaved food and filtered water. All experiments were performed using adult 8-10 week-old male mice according to the Institutional Animal Care and Use Committee of the Johns Hopkins University's guidelines for all procedures.

2.2 Intratracheal Elastase Administration

To induce pulmonary emphysema, mice were anesthetized with a mixture of ketamine (100 mg/kg)/xylazine (15 mg/kg) via intraperitoneal (i.p.) injection and suspended supine on a 15º sloped platform by their upper teeth using silk thread. A small incision on the neck was made to visualize the trachea. A 20-gauge IV catheter (Jelco Optiva®, Smith Medical,

Dublin, OH) with a manually bent tip was inserted into the trachea by gently pulling out the tongue and inserting the cannula toward the ventral surface of the mouse. A single dose of either 1.5, 3, 6 or 9 units (U) of porcine pancreatic elastase (EC-134, Elastin Products Company, Owensville, MO) dissolved in 50 μL of sterile 1X phosphate-buffered saline (PBS) was injected into the lung through the inserted catheter. To promote the distribution of the solution into the lung, mice were then immediately ventilated through the cannula for 10 seconds with room air at 0.1 mL tidal volume and 150 strokes/minute using a MicroVent Ventilator (Model 848, Harvard Apparatus, Holliston, MA). Control animals obtained an equal volume of sterile PBS only. After removing the cannula, the incision was closed by applying a small amount of cyanoacrylate tissue adhesive (Vetbond™ 3M™). Mice were allowed to recover at least 2 days, and were studied at various time points (2 days up to 5 months) after elastase challenge as indicated in each experiment.

2.3 Vaccinia and Influenza Infections

To test the role of viral infection on the susceptibility of emphysema progression, either vaccinia virus (VV) or influenza A virus (IAV) was used in this study. Attenuated Modified Vaccinia Ankara (MVA) strain of VV was kindly provided by Drs. Maureen Horton and Jonathan Powell at the Johns Hopkins School of Medicine. The VV was generated and passaged as previously described [398]. This strain of VV was genetically modified to contain ovalbumin protein sequence in the construct for facilitating the antigen-specific anti-viral immune response, while lacking lytic ability. Stock of VV at 1 x 10^8 plaque-forming units (pfu) was stored at -80ºC. To inoculate VV into mice, mice were anesthetized by inhalation of 3% isoflurane mixed in an oxygen vaporizer, and then administered intranasally (i.n.) with 2 x 10^6 pfu. The mock vaccinated mice were given with 20 μL of PBS. At 7 or 21 days after

immunization with vaccinia, the mice were challenged i.t. with either PBS or elastase (1.5, 3 or 6 U) as described above.

For IAV-infected mice, mouse-adapted influenza A virus, A/Puerto Rico/8/34 (PR8: H1N1), was obtained from Dr. Sabra Klein, who originally obtained it from Dr. Maryna Eichelberger at the Food and Drug Administration. Mice were anesthetized by i.p. injection of a mixture of ketamine-xylazine (100 mg/kg and 15 mg/kg, respectively) and then i.n. inoculated with 20 μl of a sublethal dose of PR8 (50 $TCID_{50}$ (50% tissue culture infective dose) units/mouse) diluted in Dulbecco's modified Eagle's medium (DMEM; Invitrogen) [399]. This dose of PR8 was chosen based on preliminary experiments showing that this dose did not kill any animals at least for 5 weeks after infection. The mock infected mice received an equal amount of vehicle (DMEM). All mice were maintained in microisolater cages and handled using biosafety level 2 (BSL2) practices and procedures. Body weights of mice were measured daily throughout the experiments. At 14 days after infection, mice received either PBS or elastase as appropriate for each specific experiment.

2.4 Pulmonary Functions and Structure Phenotyping

2.4.1 Diffusion Factor for Carbon Monoxide (DF_{CO}) Measurement

The complete procedure for measuring DF_{CO} in mice was described in our recent publication [372]. Briefly, on the harvest day, mice were anesthetized with a ketamine/xylazine mixture (i.p.) prior to tracheostomy with an 18G stub needle cannula. Then, mouse lungs were quickly inflated with 0.8 mL of gas mixture containing approximately 0.5% carbon monoxide (CO), 0.5% neon (insoluble inert tracer gas) and balance room air. After a 9 second breath hold, 0.8 ml was quickly withdrawn from the lung

and diluted to 2 mL with room air. The dilution to 2 mL was needed to ensure that the tubing connection in the system was cleared with the sample gas. The diluted exhaled gas was allowed to mix for at least 15 seconds and was then injected into a Micro GC gas chromatograph (INFICON, Micro GC Model 3000A, East Syracuse, NY) to measure the concentrations of Ne and CO. This process was repeated at least twice and the averages of these Ne and CO concentration were used to calculate the DF_{CO} for each animal. The DF_{CO} was calculated as $1– (CO_9/CO_C)/(Ne_9/Ne_C)$, where "9" subscript refers to gases after the 9 seconds of being held by the animal and "C" subscript refers to the calibration gases [371].

2.4.2 Pulmonary Mechanics and Quasi-static Pressure-Volume Relationships

After DF_{CO} measurements, mice were paralyzed with an intramuscular injection of succinylcholine at a dose of 75 mg/kg body weight. Then, animals were immediately connected to a flexiVent™ ventilator (Scireq, Montreal, QC, Canada) which provided a constant-volume ventilation to the mice with 100% oxygen at a tidal volume of 10 mL/kg, a rate of 150 breaths per minute, and a positive end-expiratory pressure (PEEP) of 3 cmH_2O. Following at least 3 minutes of this ventilation, the lungs were inflated to 30 cmH_2O for 5 seconds and returned to normal ventilation for 1 minute. Measurement of respiratory mechanics was then performed under closed chest conditions by applying an oscillatory pressure (the forced oscillation technique (FOT)), to the animal's lungs and measuring the flow responses to the applied pressures. Before doing the FOT measurement, conventional single-compartment mechanics was first measured with 2 seconds of a 2.5-Hz sinusoidal oscillation (Snapshot-150) to obtain respiratory system resistance (*R*rs), dynamic compliance (*C*rs) and elastance (*E*rs) [400]. Next, the broadband FOT maneuver (Quick prime-3) was

performed and analyzed using the constant phase model, which provided Newtonian airway resistance (R_n), tissue damping (G), and tissue elastance (H) [401].

Following the FOT maneuver, the stopcock connected to the cannula was closed to seal the mouse's lung for 4 minutes, which allowed the animal to absorb all gas from the lung. After complete degassing, the lung volume was zero, and quasi-static pressure-volume (P-V) curves were immediately generated with a system detailed in previous studies [377]. Briefly, the system consists of a 5 mL air-filled glass syringe with an initial volume set at 3 ml mounted on a dual infusion-withdrawal syringe pump (model 55-2226, Harvard Apparatus, Holliston, MA). Delivered air volume to the lung was measured with a linear displacement transformer (model 244-000, Transtek, Ellington, CT), while airway pressure was measured with a differential-pressure transducer (PX-137, Omega Engineering, Stamford, CT). Airway pressure and volume were measured and the generated P-V curve was recorded on a PowerLab digital data acquisition system (ADInstruments, Colorado Springs, CO). To avoid excessive pressures during initial recruitment of the degassed lung, the first inflation was acquired at a slow flow rate (1 mL/min). Until reaching the pressure of 35 cmH_2O, the flow rate was increased to 3 mL/min and the pump was instantly reversed to deflate the lung till a pressure of -10 cmH_2O. Then, two more sequential P-V loops between 0 – 35 cmH_2O were performed to ensure no leak or obstruction in the system and in the lung. Total lung capacity (TLC) and residual volume (RV) of each mouse were defined as the volume at 35 cmH_2O and –10 cmH_2O respectively, and quasistatic compliance of the respiratory system (Cstat) was defined as the slope of the most linear part of second deflation limb (between 3 and 8 cmH_2O).

2.4.3 Lung Harvesting and Fixed Left Lung Volume Measurement

After finishing the pulmonary mechanics measurements, the chest wall and diaphragm were exposed and the right mainstem bronchus was tied off with suture. The four right lobes of the lung (cranial, middle, caudal including accessory lobes) were removed, snap frozen in liquid nitrogen and stored at –80°C for RNA and protein analysis. The left lobe was then inflated with zinc-buffered formalin (Z-Fix, 174, Anatech, Battle Creek, MI) at a constant pressure of 30 cmH_2O for at least 10 minutes. Next, the trachea was tied, the heart and left lung *en bloc* were excised from the chest cavity and kept submerged in Z-fix for at least 24 hours. Then non-lung tissues were removed, and the fixed left lung volume was measured by the water immersion technique (Archimedes principle) [402]. Finally, the left lung was stored in 70% ethanol for further histologic processing.

2.4.4 Lung Histology and Morphometry

To measure the quantitative stereologic parameters of the lung, the left lung was cut transversely to the long axis into three pieces and then embedded in paraffin. Five-micron-thick sections were cut from each of the pieces, and the sections were stained with hematoxylin and eosin (H&E) to assess lung architecture and inflammatory cells. Photos of parts of these sections were taken using a systematic uniform random sampling method [378] with a Nikon Eclipse 80i (Nikon, Tokyo, Japan) at ×200 magnification. Fifteen to twenty digital images were obtained from each of the 3 lung sections. Each of these images was then analyzed by overlaying them with a sample grid line using Nikon's NIS Elements software. The stereological metric of airspace size was determined by the mean linear intercept (L_m) and alveolar surface area (S). These quantitative assessments of emphysematous changes in the lung were performed with a traditional system of

quantification [381] using counts of the number of intercepts with alveolar walls, and identifying where the end points of each line fell. From this sampling data, we then calculated the following:

Alveolar surface area (S) = $4(Vp \cdot Ialv) / (d \cdot Pair)$;

$L_m = 4Vp/S$,

where Vp = parenchymal volume (which can be calculated from parenchymal fraction (Fpar) x fixed lung volume (from water displacement method),

Ialv = number intercepts with alveolar septal walls,

d = length of a single test line,

and Pair = number of points hitting air spaces in alveoli and ducts.

2.5 Bronchoalveolar Lavage (BAL)

2.5.1 Collection of BAL

To assess cellular and protein profiles in the interalveolar space, lungs were slowly lavaged three times with 0.8 mL of cold PBS containing complete protease cocktail inhibitor tablets (Roche Applied Science, Indianapolis, IN). For each lavage, the withdrawn lavage was stored on ice. This process was repeated with a fresh 0.8 mL volume of cold PBS. The first recovered BAL fluids from each sample were centrifuged at 300 g at 4ºC for 10 minutes to pellet cells. The supernatant was collected and stored at -80ºC for later BAL total protein and cytokine measurement. The cell pellet from the first wash was pooled with the second wash and centrifuged. The supernatant was discarded, and the remaining cells were re-suspended with 1 mL of cold PBS and aliquoted into two separate tubes (0.5 ml each). One aliquot was used to determine the hemoglobin content, whereas another was processed to identify total and differential cell counts.

2.5.2 Hemoglobin Content

To quantify hemorrhage from alveolar epithelium-endothelium leakage into the BAL, we indirectly determined hemoglobin [403], by spectrophotometric analysis. Hemoglobin shows maximum light absorbance peak between 400-420 nm and absorbance at 405 nm correlates linearly with amount of erythrocytes in both lysed and intact cell suspension form [404]. Thus, one aliquot of 0.5 mL BAL from each sample was centrifuged and the supernatant was discarded. Cells in the pellet were lysed with 0.5 mL hypotonic distilled water for 5 minutes. Absorbance measurements of 0.2 mL cell lysates in replicate were taken at 405 nm using an Epoch Micro-Volume Spectrophotometer (BioTek, Winooski, VT).

2.5.3 Differential Cell Count

Another BAL aliquot was centrifuged to pellet the cells. After removing the supernatant, 0.1 mL of Ammonium-Chloride-Potassium (ACK) lysis buffer (118-156-721, Quality Biological, Gaithersburg, MD) was added to the pellet at room temperature to lyse erythrocytes for 5 minutes. Then, 0.4 mL of cold 1X PBS was added to the lysates. Ten microliters of total white blood cells in BAL were stained with Turk's solution (EMD Millipore) prior to counting on a hemocytometer (Cambridge Instruments, Buffalo, NY) using a 20X objective of a Nikon Eclipse 80i (Nikon, Tokyo, Japan). Cells were also adhered to a glass microscope slide by cytocentrifugation (Cytospin 2; Shandon Instruments, Pittsburg, PA), fixed, and stained with Hema3™ (Fisher Scientific, Waltham, MA). BAL cells were identified and counted using morphological criteria under a light microscope with evaluation of ≥400 cells/slide.

2.5.4 Protein Concentration Measurement

Total protein in BAL supernatant was determined with a bicinchoninic acid (BCA) protein assay (Pierce Thermo Scientific, Rockford, IL) according to the manufacturer's protocol. In brief, 25 μl of BAL fluid was added to 200 μL of a mixture of alkaline cupric (Cu^{2+}) solution and BCA, and incubated at 37°c for 30 minutes. The absorbance of purple-colored reaction products of this assay was measured at 562 nm with Epoch Micro-Volume Spectrophotometer (BioTek). The total protein in BAL fluid was determined by calculating the optical density of samples using standard curves generated with serial dilutions of known concentrations of bovine serum albumin (BSA) and expressed as micrograms per milliliter. The limit of detection was 5 μg/mL.

2.6 RNA Extraction, Reverse Transcription, and Real-Time PCR

Small pieces of snap-frozen right lung tissue were homogenized at 4000 rpm for 30 seconds in 1 mL Trizol Reagent (Ambion RNA Life technologies, Carlsbad, CA) in pre-filled Zirconium Beads Tubes (Denville Scientific, South Plainfield, NJ) using a Bead Bug microtube homogenizer (Benchmark Scientific, Edison NJ). Then, RNA was extracted from the aqueous phase of a Trizol and 1-bromo-2-chloropropane (BCP) mixture, precipitated with 100% isopropanol, washed with 75% ethanol in Diethylpyrocarbonate (DEPC)-treated water, and suspended in 100-200 μL of DEPC-treated water. Lung RNA concentration and purity were assessed by a ratio of absorbance at 260 nm and 280 nm using the Take3 session mode on the Epoch Micro-Volume Spectrophotometer (BioTek). This lung RNA was stored at -80ºC until used.

One μg of total RNA from lung homogenates was reverse-transcribed into complementary DNA (cDNA) with oilgo-dT and random primers using an iScript cDNA synthesis kit (Bio-Rad, Hercules, CA) following the manufacturer's instruction. Reaction tubes were incubated at 25°C for 5 minutes, then at 42°C for 60 minutes, and finally with stopped reaction at 85 °C for 5 minutes. The cDNA was then used for amplification and real-time detection in a 96-well format using the Applied Biosystems 7500 real-time PCR system with TaqMan Gene Expression Assays-On-Demand, and TaqMan Universal Master Mix (Life Technologies, Grand Island, NY) following the manufacturer's recommendation. Briefly, 15 μL reactions were used containing 2 μL of cDNA, 0.5 μl commercially available gene expression Taqman fluorogenic primer/probes set as mentioned in Table 2.1 (Life Technologies), 7.5 μL of Taqman Universal Master Mix (Life Technologies), and 5 μL of DEPC-treated water. The PCR reaction was performed with the following thermal profile: 50ºC for 2 minutes, 95ºC for 10 minutes, and then 40 cycles of 95ºC (15 seconds), followed by 60ºC (1 minute). Analysis of gene expression was performed using the Applied Biosystems 7500 system SDS software package (Life Technologies). The relative expression ratio (RER) of the real-time PCR products was calculated by the $2^{-\Delta\Delta Ct}$ method [405] which represents the fold difference in gene expression normalized to a housekeeping gene control (*Actb*: β-actin) from the same sample. The relative expression was compared to the average of naïve Day 0 or PBS/media control treated groups. The average CT value of control groups was arbitrarily assigned an abundance value of 1.

Table 2.1 List of Taqman gene expression Assays-on-Demand primer/probe sets used in this study.

Gene Name	Gene Symbol	Entrez Gene ID	Taqman Assay ID
Actin, beta	*Actb*	11461	*Mm00607939_s1*
Interferon, gamma	*Ifng*	15978	*Mm01168134_m1*
IL-1, alpha	*Il1a*	16175	*Mm00439620_m1*
IL-1, beta	*Il1b*	16176	*Mm00434228_m1*
IL-4	*Il4*	16189	*Mm00445259_m1*
IL-5	*Il5*	16191	*Mm00439646_m1*
IL-6	*Il6*	16193	*Mm00446190_m1*
IL-10	*Il10*	16153	*Mm01288386_m1*
IL-13	*Il13*	16163	*Mm00434204_m1*
IL-17A	*Il17a*	16171	*Mm00439618_m1*
IL-18	*Il18*	16173	*Mm00434225_m1*
IL-23, alpha subunit p19	*Il23a*	83430	*Mm01160011_g1*
IL-33	*Il33*	77125	*Mm00505403_m1*
Interleukin 1 receptor-like 1, ST2, T1/ST2	*Il1rl1*	17082	*Mm00516117_m1*
Amphiregulin	*Areg*	11839	*Mm00437583_m1*
Epidermal growth factor receptor (EGfr)	*Egfr*	13649	*Mm00433023_m1*
Foxp3	*Foxp3*	20371	*Mm00475162_m1*
Heme Oxygenase (decycling) 1 (HO-1)	*Hmox1*	15368	*Mm00516005_m1*
Inducible nitric oxide synthase 2 (iNOS)	*Nos2*	18126	*Mm00440502_m1*
Arginase, liver (Arg-1)	*Arg1*	11846	*Mm00475988_m1*
Chitinase-like 3 (Ym1)	*Chil3*	12655	*Mm00475988_m1*
Resistin like alpha (RELMa, Fizz1)	*Retnla*	57262	*Mm00445109_m1*
Matrix Metalloproteinase 2 (MMP-2)	*Mmp2*	17390	*Mm00439498_m1*
Matrix Metalloproteinase 9 (MMP-9)	*Mmp9*	17395	*Mm00442991_m1*
Matrix Metalloproteinase 12 (MMP-12)	*Mmp12*	17381	*Mm00500554_m1*
Alpha-1-antitrypsin (α1-AT)	*Serpina1a*	20700	*Mm02748447_g1*
Alpha-2-macroglobulin	*A2m*	232345	*Mm00558642_m1*
Tissue inhibitor of metalloproteinase 1 (TIMP-1)	*Timp1*	21857	*Mm00441818_m1*
Tissue inhibitor of metalloproteinase 2 (TIMP-2)	*Timp2*	21858	*Mm00441825_m1*
Tissue inhibitor of metalloproteinase 3 (TIMP-3)	*Timp3*	21859	*Mm00441826_m1*
Tissue inhibitor of metalloproteinase 4 (TIMP-4)	*Timp4*	110595	*Mm01184417_m1*
Signal Transducer and Activator of Transcription 3 (STAT3)	*Stat3*	20848	*Mm01219775_m1*
CD200 antigen (OX2)	*Cd200*	17470	*Mm00487740_m1*
CD200 receptor 1	*Cd200r1*	57781	*Mm00491164_m1*
Transformation related protein 63 (p63)	*Trp63*	22061	*Mm00495793_m1*
Antigen identified by monoclonal antibody Ki 67	*Mki67*	17345	*Mm01278617_m1*

2.7 Protein isolation and Enzyme-Linked Immunosorbent Assays (ELISAs)

To isolate protein for ELISA analysis, all four right lobes of the lung from each mouse were homogenized at 4000 rpm for 45 seconds in 1 mL cold PBS plus complete protease cocktail inhibitor (Roche Applied Science) in the pre-filled Zirconium Beads Tubes (Denville Scientific) using a Bead Bug microtube homogenizer (Benchmark Scientific). Homogenates were then centrifuged at 10,000g at 4ºC for 10 minutes. The supernatants were transferred to a new tube and stored at -80ºC until used. Levels of IFN-γ and IL-33 were determined in homogenized supernatant using Duoset® ELISA development system kits (R&D System, Minneapolis, MN) according to the manufacturer's instructions. Level were expressed as pg/mL/right lung. The limits of detection were 15.6 pg/mL for IL-33, and 31.25 pg/mL for IFN-γ

2.8 Western Blotting

For Western blot analysis of STAT3 and STAT6 phosphorylation, pieces of snap-frozen right lungs were homogenized at 4000 rpm for 45 seconds in 0.5 mL ice-cold 1X radio-immunoprecipitation assay (RIPA) lysis buffer (Sigma Aldrich, St. Louis, MO) containing protease cocktail inhibitors (Roche Applied Science), 100 mM phenylmethylsulfonyl fluoride (PMSF) solution, and both serine/threonine and tyrosine protein phosphatase inhibitors (Sigma Aldrich). Homogenates were then centrifuged at 10,000g at 4ºC for 10 minutes, and the lysates were stored at –20°C until required. Protein concentrations were determined by BCA protein assay (Pierce Thermo Scientific) as described in section 2.5.4. All samples were heated at 70°C for 10 minutes in 25 μL NuPAGE® Lithium Dodecyl Sulfate (LDS) Sample Buffer containing NuPAGE® reducing agent (Life Technologies). Then, denatured protein (50 μg) was loaded and separated by electrophoresis on a pre-cast 4-12% Bis-Tris

polyacrylamide gel using Bolt® mini gel tank system (Life Technologies), and subsequently transferred onto 0.2 μm polyvinyl difluoride (PVDF) membranes for 7 minute using iBlot® Dry Blotting system (Life Technologies, Grand Island, NY). Membranes were blocked in Odyssey® blocking buffer (Li-cor Biosciences, Lincoln, NE) overnight at 4°C. Afterwards, the membranes were incubated with the following primary antibodies (in 0.2% Tween-20 in blocking buffer) for 1 hour at room temperature (also see in Table 2.2): phospho-STAT3 (Tyr705) (1:1500, Cell Signaling Technology, Beverly, MA), STAT3 (1:200, Santa-Cruz Biotechnology, Dallas, TX), phospho-STAT6 (Tyr641) (1:500, Santa-Cruz Biotechnology, Dallas, TX), STAT6 (1:500, Santa-Cruz Biotechnology), or anti-β-actin (1:1000, Cell Signaling Technology). Membranes were then washed four times with 1X PBS and 0.1% Tween® 20 (Sigma Aldrich) and incubated for 30 minutes at room temperature with appropriate IRDye® fluorescently-labeled secondary antibody (in 0.2% Tween® 20 plus 0.02% SDS in blocking buffer at 1:10000 dilution, Li-cor Biosciences). Blots were washed again, rinsed with PBS and imaged using an Odyssey® Classic Infrared Imaging system (Li-cor Biosciences). Densitometric analysis of the immunoreactive signal was analyzed with Image Studio Lite (Li-cor Biosciences). The data were expressed as a ratio between arbitrary units (A.U.) of phospho-protein and total STAT3 or STAT6 protein.

2.9 Nuclear Protein Extraction and STAT3 Transcription Factor Activity Assay

To quantify the activation and translocation of STAT3 into the nucleus, nuclear extracts from a piece of frozen right lung were prepared using a nuclear extract kit (Active Motif, Carlsbad, CA). Briefly, the tissue was homogenized in ice-cold 1X hypotonic buffer containing phosphatase and protease inhibitors supplemented with dithiothreitol (DTT) and detergent using a 7-mL dounce tissue grinder (Wheaton, Millville, NJ). The lysate was then

centrifuged at 850 g at 4°C for 10 minutes. The pellet containing cells was re-suspended in 1X hypotonic buffer with detergent, vortexed at high speed, and centrifuged at 14000 g at 4°C for 30 seconds to pellet the nuclear fraction. The supernatant with the cytoplasmic fraction was discarded, and the pellet containing the nuclear components was lysed in lysis buffer plus DTT and protease inhibitor cocktail, vortexed, incubated on ice for 30 minutes, and centrifuged at 14,000 g at 4°C for 10 minutes. The nuclear extract in this final supernatant compartment was aliquoted, and its protein content was measured using the BCA assay as mentioned above, and then store at -80°C until used.

The lung nuclear extract was used to determine the specific binding of STAT3 to its respective consensus binding site (5'-TTCCCGGAA-3') using TransAM® STAT3 transcription factor activity assay kit (Active Motif). The colorimetric result was developed using anti-STAT3 primary antibody and an HRP-conjugated secondary antibody system, whose absorbance could be measured at 450 nm with a reference wavelength of 655 nm (Epoch Micro-Volume Spectrophotometer - BioTek). Nuclear extracts from human liver cancer Hep G2 cells treated with IL-6, a well-known STAT3 activator, were used as positive controls. Specificity was monitored by adding STAT3 binding competitors, using either wild-type or mutated (no ability to compete binding with STAT3) consensus oligonucleotide.

Table 2.2 List of antibodies used in this study.

Antibody	Company	Catalog No.	Origin	Type*	Application **	Dilution
Ly-6-G (1A8)	BioXcell	BE0075-1	rat	mAb	Neutrophil depletion	500 μg/mouse
β-actin (8H10D10)	Cell Signaling	3700	mouse	mAb	WB	1:1000
Phospho-STAT3 (Tyr705) (D3A7)	Cell Signaling	9145	rabbit	mAb	WB	1:1500
STAT3 (C-20)	Santa-Cruz	sc-482	rabbit	pAb	WB	1:200
Phospho-STAT6 (Tyr641)	Santa-Cruz	sc-11762-R	rabbit	pAb	WB	1:500
STAT6 (D1)	Santa-Cruz	sc-374021	mouse	mAb	WB	1:500
Anti-rabbit IgG IRDye® 800CW	Li-cor	926-32213	donkey	2° Ab	WB	1:10000
Anti-mouse IRDye® 680RD	Li-cor	926-68070	goat	2° Ab	WB	1:10000
SiglecF-PE	BD Biosciences	552126	rat	mAb	FL	1:100
CD11b-PerCP-Cy5.5	BD Biosciences	550993	rat	mAb	FL	1:100
CD11c-APC	Miltenyi Biotec	130-091-844	hamster	mAb	FL	1:50
CD4-FITC	eBioscience	11-0042-82	rat	mAb	FL	1:100
CD8-PE	eBioscience	12-0081-82	rat	mAb	FL	1:100
CD3-PerCP-Cy5.5	eBioscience	45-0031-82	hamster	mAb	FL	1:100
B220-APC	BD Biosciences	553092	rat	mAb	FL	1:100
NKp46-FITC	eBioscience	11-3351-82	rat	mAb	FL	1:100
CD49b-PE	BD Bioscience	553858	rat	mAb	FL	1:100
NKG2D-APC	eBioscience	17-5882-81	rat	mAb	FL	1:100
Ly6G-FITC	eBioscience	11-5931-82	rat	mAb	FL	1:100
CD64-PE	BD Biosciences	558455	rat	mAb	FL	1:100
Ly6C-APC	BD Biosciences	560595	rat	mAb	FL	1:100
gdTCR-APC	eBioscience	17-5711-81	hamster	mAb	FL	1:100
IL-10-PE	eBioscience	12-7101-81	rat	mAb	FL	1:100
Isotype-PE	eBioscience	12-4031-81	rat	mAb	FL	1:100
CD25-PE-Cy7	eBioscience	25-0251-81	rat	mAb	FL	1:100
Foxp3-AlexaFluor647	BD Biosciences	560402	rat	mAb	FL	1:100
IFN-g-APC	eBioscience	17-7311-81	rat	mAb	FL	1:100
Isotype-APC	eBioscience	17-4301-81	rat	mAb	FL	1:100
IL-33 propeptide	R & D	AF5010	sheep	pAb	IF	1:20
Prosurfactant protein C	Abcam	ab90716	rabbit	pAb	IF	1:200
Alexa Fluor® 555 Anti-Sheep IgG	Molecular Probes	A21436	donkey	2° Ab	IF	1:200
Alexa Fluor® 488 Anti-Rabbit IgG	Molecular Probes	A11008	goat	2° Ab	IF	1:200

*mAb indicates monoclonal antibody, whereas pAb indicates polyclonal antibody. 2° Ab = secondary antibody.
**WB: Western Blotting, FL: Flow Cytometry, IF: Immunofluorescence

2.10 Flow Cytometry Analysis

Single-cell suspensions from whole lungs were generated as previous described [406]. Briefly, lungs were perfused with 10 mL of room temperature sterile Dulbecco's PBS via the right ventricle of the heart, then carefully removed from the chest (excluding non-lung tissue), minced thoroughly into fine pieces, and digested in a 5 mL RPMI 1640 medium (Life Technologies) containing 1 mg/mL collagenase type II (1701-015, Life Technologies) and 30 μg/mL DNase I (10104159001, Roche Applied Science) at 37°C for 30 minutes. Minced tissues were then filtered through a 100-μm mesh nylon cell strainer (352360, BD Falcon, Bedford, MA) to form a single-cell suspension. These single-cell suspensions were pelleted at 1500g at 4°C, washed and re-suspended in ACK lysis buffer (Quality Biological) at room temperature for 5 minutes to lyse any contaminating erythrocytes. The remaining cells were passed through a new cell strainer, washed twice in FACS staining buffer [1X PBS with 2% heated-inactivated fetal calf serum (35-011-CV, Mediatech, Inc., Manassas, VA)], and treated with anti-mouse CD16/CD32 Fc Block (553142, BD Biosciences, San Jose, CA) for 10 minutes prior to incubating in the dark with appropriate fluorochrome-conjugated surface marker staining antibodies on ice for 20 minutes.

If intracellular cytokine staining (ICS) was needed, prior to the blocking and surface staining, isolated cells were stimulated for 4 hours at 37°C with 50 ng/mL phorbol 12-myristate 13-acetate (PMA, P1585, Sigma-Aldrich), 1 μg/mL ionomycin (I0634, Sigma-Aldrich) in the presence of cytokine secretion blocker Brefeldin (00-4506, eBioscience). Then, these stimulated cells were blocked, surface stained as above, washed in FACS staining buffer, fixed and permeabilized with the BD Cytofix/Cytoperm™ solution kit (555028, BD

Bioscience), and finally stained with fluorescently-labeled specific intracellular staining antibodies. Staining with control isotype antibodies was included in each sample.

All stained samples were then washed twice and analyzed on a BD FACSCalibur flow cytometer equipped with CellQuest Pro software (BD Bioscience). Total live cell numbers were counted on a hemocytometer using standard tryphan blue (15250-061, Life Technologies) dead cell exclusion test. All flow cytometry data were analyzed and plotted with FlowJo software (TreeStar, Inc., Ashland, OR).

2.11 Immunofluorescent histochemistry

To localize IL-33 expressing cells in the lung, unstained formalin-fixed, paraffin-embedded histological sections of 5 μm thickness were deparaffinized with 3 soakings in xylene for 5 minutes each, followed by rehydrating in a series of ethanol concentration (100%, 95%, 70%) for 3 minutes each, and then placed in running distilled H_2O. Antigen retrieval was then done by heating the slides in 10 mM citrate buffer (pH 6.0) (S2369, Dako, Carpentaria, CA) to 90°C in a microwave for 10 minutes. Tissue sections were outlined with a hydrophobic barrier Dako pen (Dako) and blocked in the mixture between 2.5% normal goat serum (S-1012, Vector Labs, Burlingame, CA) and 2.5% donkey serum (D9663, Sigma Aldrich) in PBS for 1 hour at room temperature. Then, primary antibodies, including sheep polyclonal anti-IL-33 propeptide antibody (1:20, R&D) and rabbit polyclonal anti-prosurfactant protein C antibody (1:200, Abcam, Cambridge, MA) in blocking solutions, were added to the slides and incubated overnight at 4°C. Sections were subsequently rinsed three times with 1X PBS and 0.05% Tween® 20 (Sigma Aldrich) prior to incubating 1.5 hours with secondary antibodies including Alexa Flour® 555 donkey anti-sheep antibody

(1:200, Molecular Probe, Grand Island, NY) and Alexa Flour® 488 goat anti-rabbit antibody (1:200, Molecular Probe) at room temperature. After 3 additional 5 minute washes, the sections were mounted with a medium containing the nuclear dye 4',6-diamidino-2-phenylindole (DAPI) (Vectashield® mounting medium, H-1200, Vector Labs). Epifluorescent images were taken with a Nikon Eclipse 80i fluorescent camera (Nikon, Tokyo, Japan).

2.12 Statistical Analysis

Data were analyzed using GraphPad Prism Software (GraphPad, La Jolla, CA) by either a two-tailed unpaired Student *t* test (two groups) or a two-way analysis of variance (ANOVA) for multiple group analysis following by a post-hoc Tukey's multiple comparison test to compare differences between groups as specified in each figure legends. Comparisons of Kaplan-Meier survival curves between groups were analyzed with a log-rank test. All of the data were expressed and plotted as means ± standard error of mean (SEM). Statistical differences between groups were considered significant if $p \leq 0.05$.

CHAPTER 3

BALB/cJ mice are more susceptible to develop elastase-induced emphysema than C57BL/6J mice

3.1 Abstract

Emphysema, one of the major components of COPD, is characterized by the progressive and irreversible loss of alveolar lung tissue. Even though more than 80% of COPD cases are associated with cigarette smoking, only a relatively small proportion of smokers develop emphysema, suggesting a potential role for genetic factors in determining individual susceptibility to develop emphysema. Although strain-dependent effects have been shown in several animal models of emphysema, the molecular basis underlying this intrinsic susceptibility is not fully understood. In this present study, we investigated emphysema development using the elastase model in two commonly used mouse strains, C57BL/6J and BALB/cJ. The results demonstrate that mice with different genetic backgrounds show disparate susceptibility to the development of emphysema. BALB/cJ mice were found to be much more sensitive than C57BL/6J to elastase insults in both a dose-dependent and time-dependent manner, as measured by a significantly higher mortality, greater body weight loss, greater decline in lung function and mechanics, as well as a greater loss of alveolar tissue. The more susceptible BALB/cJ strain also showed persistence of inflammatory cells in the lung, especially macrophages and lymphocytes. A comparative analysis of gene expression following elastase-induced injury showed BALB/cJ mice elevated levels of IL-17A and alternatively-activated macrophages (M2) markers, whereas the C57BL/6J mice demonstrated augmented level of IFN-γ. These findings suggest a possible role for these cellular and molecular mediators in modulating the severity of emphysema, and the possibility that they might contribute to the heterogeneity observed in clinical emphysema outcomes.

3.2 Introduction

Chronic obstructive pulmonary disease (COPD) is the 3rd leading cause of death in the Unites States and its prevalence and mortality is also steadily increasing globally. COPD is comprised of two key components, chronic bronchitis and emphysema, and both lead to persistent airflow limitation [18, 25]. Emphysema is anatomically defined as a condition with irreversible airspace enlargement along with a slow progression of the alveolar wall destruction [29]. The mechanistic basis underlying its pathogenesis is very complex, involving a combination of recurrent inflammation, oxidative stress, proteases, and cell death, and all of these can be modified by both environmental exposures and host genetics [222, 407]. Cigarette smoking has been identified to be the most important environmental risk factor in developing emphysema, accounting for more than 80% of the cases [39-41]. Although clinical studies have shown that all smokers demonstrate a degree of pulmonary inflammation, only 15 - 20% of smokers develop emphysema [408]. This underscores the importance of susceptibility factors, which are almost certainly controlled by host genetic predisposition.

Experimental mice are now commonly used to study the pathogenesis of many diseases, and the availability of inbred strains has provided many insights into the genetic basis of resistance or susceptibility to developing a number of different human diseases including emphysema. It has been documented that the development of emphysema in cigarette smoke-exposed mice is strain-dependent [409, 410]. Another common way to establish experimental emphysema is the use of an intratracheal instillation of an elastolytic protease into the lung, although the genetic basis underlying the sensitivity to elastase-induced progressive emphysemic change has not been studied.

C57BL/6 and BALB/c are two well-characterized laboratory inbred murine strains that have been widely used to model a number of different human diseases, in addition to being used as background strains to generate many types of genetically-engineered mice. They have been shown to have different phenotypic outcomes under various experimental conditions, emphasizing the important role of genetic backgrounds in the susceptibility to diseases [411]. In terms of immune responses, it has been well documented that genetic differences in the regulation of type 1 and type 2 cytokine-mediated immune responses between C57BL/6 and BALB/c mice play key roles in determining the resistance or susceptibility to many diseases, ranging from microbial infections to asthma. BALB/c mice have been widely shown to exhibit strong Th2-biased immunity, with eosinophilia and high levels of IgE, IL-4, IL-5, and IL-13 in response to allergens or parasitic infection [412-414]. On the other hand, C57BL/6 mice display Th1-based immunity, recognized by high levels of IgG2a, IFN-γ and TNF-α in response to parasite infection (e.g. *Leishmania major*) and greater susceptibility to atherosclerosis or organ-specific autoimmune disease [415-418]. In addition to this differential T cell polarization, macrophages from C57BL/6 are much also more capable of producing nitric oxide as a result of classical activation (M1 activation) in response to IFN-γ and lipopolysaccharide (LPS) [419]. This contrasts with the preferential alternative activation (M2 activation) with a Th2 cytokine milieu in BALB/c mice [420, 421]. However, the pattern of the polarization of Th1/Th2 or M1/M2 phenotypes in these two mouse strains can vary widely depending on the specific type of infection or stimuli.

In the present work we aimed to investigate whether these two common inbred mouse strains, (C57BL/6J and BALB/cJ) also show a differential in susceptibility to progressive emphysema induced by elastase instillation. Differences in the response of the two strains

could help identify candidate genes and pathways contributing to the discordant phenotypes, and such information might have implications for the design of the therapeutic intervention for human emphysema.

3.3 Results

3.3.1 Effects of elastase administration on the lifespan and body weight in C57BL/6J and BALB/cJ mice

In order to obtain a measure of the differential sensitivity to elastase injury in C57BL/6J and BALB/cJ male mice, we intratracheally administered porcine-derived pancreatic elastase and observed survival as well as changes in body weight. Fig. 3.1 show the survival of the mice treated with elastase at doses of 6 (panel A) and 9 (panel B) enzymatic units (U). The proportion of surviving animals with elastase injury was significantly higher in male C57BL/6J mice than in male BALB/cJ mice. Approximately 40% of BALB/cJ mice challenged with 6U elastase (Fig. 3.1A) and more than 80% of those that received 9U elastase (Fig. 3.1B) failed to survive beyond 3 days after the elastase insult. In contrast, there was only 50% mortality in C57BL/6J mice given 9U of elastase and less than 10% with 6U of elastase in the first three days. The differences in survival between the two strains were significant ($p < 0.05$) at both doses. No further mortality was found in either C57BL/6J or BALB/cJ mice beyond 3 days. The early deaths of elastase-treated mice at these relatively high doses suggest marked acute lung injury that cannot be resolved in a certain fraction of the mice. No animals treated with 3U of elastase died at any time during the 21-day monitoring period (data not shown).

Fig. 3.1C-D shows the changes in body weight of mice receiving 3U or 6U of elastase. No weight losses were found in the saline-treated control groups. During the first few days post-elastase challenge the animals treated with 3U and 6U of elastase exhibited a marked weight loss in both C57BL/6J and BALB/cJ mice. As expected, the decrease in body weight of the mice from both strains treated with 6U of elastase (Fig. 3.1D) was greater than in the 3U groups. C57BL/6J mice tended to show an earlier recovery from this early weight loss compared to BALB/cJ mice. At 3U and 6U, the body weight of C57BL/6J mice recovered to the level of saline controls by day 5 (Fig. 3.1C) and by day 8 (Fig. 3.1D), respectively. In BALB/cJ mice body weight returned to baseline levels at 8 days with 3U elastase, but still hadn't caught up with the controls by 21 days. BALB/cJ that received 6U of elastase had still not recovered to their starting weight by day 21 (Fig. 3.1D).

These survival and weight loss data clearly indicate that the BALB/cJ mice are much more sensitive to acute lung injury caused by elastase and they recovered slower after elastase challenge compared to C57BL/6J mice.

3.3.2 Effect of elastase on the development and severity of progressive emphysema in C57BL/6J and BALB/cJ mice

To address the dose-responsiveness of elastase on the lungs of these two strains of mice, we measured several variables of pulmonary function as well as lung mechanics and lung histology. Mean values of lung gas exchange function assessed by the DF_{CO} in control C57BL/6J and BALB/cJ mice were not significantly different. However, there were dose-dependent declines in DF_{CO} in the elastase-treated groups in both strains. The fall in DF_{CO} was found to be significant at the lower dose of enzyme and to a greater degree in BALB/cJ

mice compared to C57BL/6J mice (Fig. 3.2A). These drops in gas exchange ability were supported by changes in lung mechanics assessed by air-filled pressure-volume measures of total lung capacity, residual volume and quasistatic compliance (Fig. 3.2B-D). Control BALB/cJ mice had larger lung volumes and compliance compared to C57BL/6J mice. Increasing doses of elastase resulted in dose-dependent increases in TLC, residual volume, and lung compliance in both strains, but the changes were much more pronounced in BALB/cJ mice than C57BL/6J mice. Similar patterns were also found in several dynamic mechanical measurements obtained from the Flexivent ventilator, including compliance (Crs), elastance (Ers), tissue damping (G), and tissue elastance (H) (Table 3.1). However, elastase did not alter either of the measurements of resistance [respiratory system (Rrs) or airway resistance (Rn)].

To examine the structural changes in the lungs, we assessed the morphology of lung parenchyma with histological sections (Fig. 3.3). Microscopic examination of histological sections of lungs at day 21 post-challenge with 1.5U, 3U, 6U or 9U of elastase showed substantial enlargement of alveoli in both strains of mice. However, at each dose of elastase the changes in the BALB/cJ were much greater than those in C57BL/6J.

3.3.3 Time course of elastase-induced emphysema development in C57BL/6J and BALB/cJ mice

Based on the survival results (Fig. 3.1) and the dose-response effects of elastase (Fig. 3.2-3.3), we selected a dose that induced minimal mortality in both mouse strains (3U) to be used for the remainder of the experiments.

On the first day after instillation of 3U in both C57BL/6J and BALB/cJ mice we observed prominent hemorrhage consistent with acute lung injury. Much of the hemorrhage was resolved by the day 2 in C57BL/6J mice, but evidence of hemorrhage remained until day 4 in BALB/cJ mice (Fig. 3.4). The degree of hemorrhage was quantified by colorimetric assessment of hemoglobin in BAL (Fig. 3.11A) andthe results confirmed that BALB/cJ had more severe and prolonged hemorrhage. In addition to sustaining elevated and persistent hemorrhage, starting at day 14, the overall size of the BALB/cJ lungs was visually larger than the C57BL/6J lung.

Fig. 3.5 shows that both C57BL/6J and BALB/cJ mice treated with 3U of elastase exhibited a significant decrease in DF_{CO} as early as day 4. However, the decrease in DF_{CO} in BALB/cJ mice was much greater than in C57BL/6J mice, and a further gradual decline of DF_{CO} after day 21 was found only in BALB/cJ mice. Much higher increases in TLC and RV in BALB/cJ mice mirrored what seen in DF_{CO} (Fig. 3.6-3.7). More than 40% and 100% increases total lung capacity were observed in BALB/cJ mice on day 7 and day 96, respectively, compared to only approximately 10% and 20% increases in C57BL/6J mice at the same time points. Although BALB/cJ mice had significantly reduced quasistatic compliance during the first week after elastase challenge (likely due to edema and inflammation in the lung), the compliance recovered quickly. After this recovery, compliance was increased over control and the percent increases were found to be higher than in the C57BL/6J mice beyond the first month post-elastase (Fig. 3.8). The higher increase in Crs and greater decreases in Ers, G, and H in BALB/cJ mice compared to C57BL/6J mice (Table 3.2) are all consistent with more emphysematous damage in the lungs of BALB/cJ mice.

Histologic assessment of the lung structure confirmed the more pronounced emphysematous changes in the BALB/cJ mice (Fig. 3.9). Quantitative morphometric analysis showed significant increases in L_m as early as day 2, and the L_m continued to progress rapidly, reaching a 360% increase by day 21 in BALB/cJ mice. In C57BL/6J mice a significant increase (30%) of L_m was not observed until day 21 (Fig. 3.10).

3.3.4 Inflammatory cell influx into the lungs of C57BL/6J and BALB/cJ mice in response to elastase

To determine the inflammatory response in the lungs of C57BL/6J and BALB/cJ mice in response to 3U of elastase, we assessed the number of total inflammatory cells in bronchoalveolar lavage fluid. As shown in Fig. 3.11B, the number of total cells in the BAL was significantly increased to the same degree in both strains 2 days after the acute elastase insult. However, the number of total BAL cell in C57BL/6J mice began to decline by day 4 and returned to baseline level on day 7, whereas the number of cells in BALB/cJ mice remained elevated above baseline even at 21 days post-elastase challenge. These remaining BAL cells in BALB/cJ mice correlated with the increased hemoglobin levels (Fig 3.11A), suggesting an instability of the alveolar epithelial-endothelial barrier, consistent with the increased acute damage of pulmonary tissue seen in this strain. To further characterize the cellular content of the BAL, we performed differential cell counts using Diff-Quik staining. The number of macrophages in BAL was increased after elastase administration in both strains. The macrophages were significantly increased by day 2 in BALB/cJ mice compared to day 4 in C57BL/6J, and this increase persisted above baseline in the long-term only in BALB/cJ mice (Fig. 3.11C). We observed a huge influx of neutrophils on day 2 in both strains, however these were cleared from the BAL in the first week, and no significance was

found between two strains of mice (Fig. 3.11D). Interestingly, as illustrated in Fig. 3.11E, the elastase insult recruited lymphocytes into the lung, and there was a markedly higher number of recruited lymphocytes in the first week after the insult in BALB/cJ mice compared to C57BL/6J mice. On the other hand, the number of eosinophils tended to be higher in C57BL/6J mice than BALB/cJ mice after elastase administration, but this increase in eosinophil count did not reach a significance level of 0.05 compared to naïve animals in either strains (Fig. 3.11F).

We characterized the lymphocyte population in whole lung tissue using cell surface marker staining (NK cells: $CD3^{-}CD49b^{+}$, NKT cells: $CD3^{+}$ $CD49b^{+}NKp46^{+}$, $CD4^{+}$ cells: $CD3^{+}CD4^{+}CD8^{-}$ and $CD8^{+}$ cells: $CD3^{+}CD4^{-}CD8^{+}$), and analysis by flow cytometry. BALB/cJ had more of NK cells and $CD4^{+}$/$CD8^{+}$ lymphocytes even at baseline (Fig. 3.12). Both NK cells and $CD8^{+}$ cell numbers were further elevated in response to elastase by day 14 in both strains, whereas there was an increase in NKT cells from day 14 to 21 only in BALB/cJ mice. No significant changes in the number of $CD4^{+}$ cells was detected after elastase either strain.

3.3.5 Levels of IFN-γ and IFN-γ-producing cells in C57BL/6J and BALB/cJ mice after elastase instillation

In order to characterize the pathways underlying the difference in sensitivity to developing emphysema in C57BL/6J and BALB/cJ mice, we first compared levels of IFN-γ expression following elastase injury. The rationale is that C57BL/6J mice are well-known to be biased toward Th1 responses with high production of IFN-γ [417]. The mRNA expression level of

Ifng in whole lung tissue was significantly increased after day 7 and remained elevated at day 21 after elastase challenge in C57BL/6J mice (Fig. 3.13A). This increase in mRNA correlated with an increase in its protein level by day 21 (Fig. 3.13B). In contrast, BALB/cJ mice showed no changes in either IFN-γ mRNA or protein expression over the 21-day sampling period. To identify the cells that produce IFN-γ in response to elastase, we performed intracellular staining of IFN-γ in combination with several surface markers of potential IFN-γ-producing cells and analyzed the cells by flow cytometry. The results showed that, although both mouse strains have increases in total IFN-γ-positive cells in the lungs at day 14 following elastase challenge, the increase was significantly greater in C57BL/6J relative to BALB/cJ (Fig. 3.13C). This disparity in the number of IFN-γ^+ cells at this time point was mainly due to greatly increased expansion of IFN-γ^+ NK cells in C57BL/6J mice (Fig. 3.14A-B). While there were increases of IFN-γ^+ NKT cells and IFN-γ^+ $CD8^+$ cells in BALB/cJ mice at day 14, these were not significantly different from the increased levels in documented in C57BL/6J mice (Fig. 3.14C, E). No significant increases in the number of IFN-γ^+ $CD4^+$ cells were noted in either strain (Fig. 3.14D).

3.3.6 Gene expression profiles of other T cell-associated genes in C57BL/6J and BALB/cJ mouse lungs following an elastase insult

While C57BL/6J mice are Th1-biased, BALB/cJ mice are Th2-biased and associated with production of IL-4, IL-5 and IL-13 [412]. We thus looked for differences in gene expression of Th2 cytokines. Although there was a gradual upregulation of *Il4* and *Il5* expression in both C57BL/6J and BALB/cJ mice after instillation of elastase, we did not find any significant differences in *Il4*, *Il5,* and *Il13* mRNA expression between the two strains (Fig.

3.15A-C). The same profile was also observed with expression of *Il10* and *Foxp3*, two genes associated with regulatory T cells, lymphocytes with the ability to suppress other immune response (Fig. 3.15D-E). However, BALB/cJ mice did show a much greater increase in expression of *Hmox1*, gene encoding for heme oxygenase I, particularly at day 4 (Fig. 3.15F). Increased expression of heme oxygenase I (a stress-inducible enzyme with ability to catalyze the degradation of heme with potential anti-inflammatory effects) in BALB/cJ mice might be associated with the increased levels of iron from erythrocytes needing to be recycled after the increased hemorrhage in this strain (Fig. 3.15F) [422].

Interestingly, on days 7 and 14 following elastase treatment, expression of the *Il17a* gene encoding for IL-17A was nearly 20-fold higher in BALB/cJ mice relative to C57BL/6J mice (Fig. 3.16A). This increase was accompanied by higher mRNA expression of *Il6* (in the early days), *Il1b* (at a various time points) and *Il18* (at the same times). These are genes encoding cytokines that are known to drive Th17 differentiation and promote IL-17A production (Fig. 3.16C- E) [423, 424]. Thus, the data suggest a possible role for the IL-17A signaling pathway in modulating the severity of elastase-induced emphysema. Complicating this picture, however, is that finding that mRNA levels of IL-23a (important for Th17 maintenance) was higher in C57BL/6J mice at day 1, and no alteration in STAT3 expression (an induced transcription factor involved in Th17 differentiation) was seen in either strain (Fig. 3.16B, F).

3.3.7 Macrophage activation in C57BL/6J and BALB/cJ mice following elastase challenge

Macrophages are key cells in the immune response, and our results have shown that they are the only immune cell type that persists in the BAL at days 14 and 21 following elastase challenge (Fig. 3.11). For this reason, we sought to further characterize the activation status of macrophages. Generally, classical activation of macrophages (M1) is recognized by increased production of inducible nitric oxide synthase, and this activation is involved mainly in type I inflammation that can kill intracellular pathogens [425]. In contrast, alternatively activated macrophages (M2) which can be divided into several subtypes with different stimuli, play a role in type II inflammation, which includes immunoregulation, wound healing, and tissue remodeling. Our gene transcriptional profiles of whole lung tissue indicate that the majority of genes in BALB/cJ affected by elastase are involved in M2 macrophage activation (*Arg1*, *Chil3*, *Retnla*, *Mmp2 and Mmp12*) (Fig. 3.17). There was a 15-fold induction of *Arg1* and a 20-fold induction of *Retnla* at day 2. There was also a 4-fold increase of *Mmp2* and a 40-fold increase of *Mmp12* at 7 and 21 days post-elastase administration in BALB/cJ. On the other hand, *Chil3* and *Mmp2* expression were significantly up-regulated in C57BL/6J lungs only at day 7 (Fig. 3.17B, D). Although BALB/cJ had greater expression at baseline of the M1 activation marker, *Nos2*, compared to C57BL/6J mice, the overall trend of its expression following elastase instillation was not different between the two strains (Fig. 3.18A).

CD200 is a receptor that is highly expressed on the surface of alveolar macrophages. CD200 ligands can be found on a variety of cells, with notably elevated expression especially on alveolar epithelial cells [426]. An engagement of CD200 receptor with the CD200 ligand has

been shown to inhibit classical macrophage activation and is likely is likely to play a role in the induction of alternatively activated macrophages [427]. We observed a drop in expression of *Cd200* in BALB/cJ mice, which may reflect increased epithelial cell death. Related to this decreased in CD200, we found increased expression of *Cd200r1* at the later time points, where the tissue repair function of M2 macrophages is likely increased (Fig. 3.18B-C). Overall, these data implicate a role for M2 macrophages in causing the differential severity of emphysema in these two mouse strains.

3.3.8 Cell proliferation and alarmin-associated gene expression in C57BL/6J and BALB/cJ mice following elastase challenge

To determine if there was proliferation of cells in the lung after elastase injury, we assessed the expression level of *Mki67*, a marker of cell proliferation. The data show that both C57BL/6J and BALB/cJ mice had increases in this cell proliferation marker within the first week. A greater level, however, was observed in BALB/cJ mice suggesting more robust repair response in this strain (Fig. 3.17D). Moreover, we also determined the level of *p63* expression, which was recently shown to be an essential marker of stem cells in the lung parenchyma [428]. We did not detect any changes in *p63* expression in either strain (Fig. 3.18E).

We also assessed the expression of a subset of epithelial cell alarmins, a group of constitutively produced molecules released in response to cellular stress or injury and with an ability to promote immune responses to restore tissue homeostasis [429]. Elastase injury resulted in a sudden increase in expression of *Il33*, followed by *Il1rl1* (the gene encoding for IL-33 receptor; aka ST2), but these increases were similar between the two strains (Fig.

3.19A-B). To further pursue the effects of IL-33, we looked at its downstream signaling pathway. In the first week *Areg,* which codes for amphiregulin, was significantly up-regulated, while *Egfr* (the Areg receptor) was down-regulated (Fig. 3.19D-E). Interestingly, the baseline level of *Il1a* was about 6-fold higher in BALB/cJ mice when compared to C57BL/6 (Fig. 3.19C). *Il1a* transcription levels rebounded by day 4 and remained elevated to day 21 (Fig. 3.19C). Intriguingly, there was no change in *Il-1a* expression in the lungs from C57BL/6J mice (Fig. 3.19C).

3.3.9 Expression profile of anti-proteases in C57BL/6J and BALB/cJ mice following elastase challenge

Since anti-proteases are a pivotal component in the protease/anti-proteases mechanism that can protect tissue destruction by ablating proteolytic activity, we measured the level of several anti-protease genes (Fig. 3.20). *Serpina1a*, encoding for α1-antitrypsin (α1-AT), was significantly higher in naïve BALB/cJ relative to naïve C57BL/6J, but the levels were decreased in both strains after the mice received elastase. In contrast, naïve C57BL/6J mice had higher levels of *A2m*, which encodes for α2-macroglobulin, but the level of *A2m* was elevated in response to elastase in both strains. No differences in *Timp1*, *Timp2*, *Timp3, or Timp4* were found in C57BL/6J and BALB/cJ mice at baseline. Only *Timp1* levels rapidly increased after elastase insult to a much greater degree in BALB/cJ mice. In contrast, *Timp2*, *Timp3,* and *Timp4* levels dropped during first few days in BALB/cJ mice, but not in C57BL/6J mice, and the level gradually increased after these early days. However, we did not see any differences between the two strains of mice.

3.4 Discussion

A single intratracheal administration or aerosol inhalation of porcine-derived pancreatic elastase has long served as an effective approach to rapidly induce acute lung injury leading to subsequent pulmonary emphysema in a wide variety of experimental animals. One proposed mechanism for the development of emphysematous changes involves the concept of a protease/anti-protease imbalance. This notion emerged following studies of emphysema patients with severe alpha1-antitrypsin deficiency [58]. Most of the older animal studies were performed in Syrian golden hamsters, and it was thought that this species developed severe emphysema following elastase because of its relatively low α1-antitrypsin level, low acute lung injury response, and depletion of glutathione-related antioxidant enzymes in the early phase [430-432]. Recently, mice C57BL/6 have been used to model elastase-induced experimental emphysema. Most of the work has been carried out in C57BL/6 mice taking advantage of the fact that complete information on its genome is known and many genetically engineered strains have been produced on this genetic background. However, as noted in the mouse model for allergic asthma [433], there is likely to be important strain difference in the response to elastase. In the present work, our aim was to compare the emphysematous phenotype in C57BL/6J mice and another commonly used mouse strain in immunologic studies, BALB/cJ mice. The hypothesis is that these differential responses could be used to provide new insights on the cellular or molecular processes contributing to the pathogenesis of the progressive stage of the disease.

To this end we assessed various phenotypic endpoints, including mortality, body weight, pulmonary function, lung mechanics, and lung structure in both strains exposed to intratracheal elastase. Our data clearly show that at a given exposure level BALB/cJ mice are

more susceptible to elastase-induced pulmonary emphysema. Our results are consistent with the previous observation of differential susceptibility to emphysema induced by *Nippostrongylus brasiliensis* hookworm infection between BALB/c and C57BL/6 strains [108]. The strain-dependent effect has also been demonstrated in cigarette smoke-induced emphysema [84, 131, 410, 434, 435]. In these studies, C57BL/6 mice were considered as a "moderately sensitive" strain to develop emphysematous lesions after smoke exposure, because this strain of mouse showed more pathologic changes in response to cigarette smoke compared to the less sensitive mouse strains studied, the outbred ICR strain and inbred NZW strain. However, cigarette smoke only caused mild pathologic emphysema in the C57BL/6 strain as evidenced by only a 13-18% increase in mean linear intercept after 5-6 months of exposure. This increase was less than in other more sensitive strains studied, i.e., AKR, SJ/L, A/J, and C3H. Only one study [434] compared the effect of cigarette smoke exposure on the C57BL/6J and BALB/cJ strains we studied here. They found that smoke-exposed BALB/cJ mice did not show a significantly greater mean linear intercept, but they did find significantly more blood vessel muscularization compared to smoke-exposed C57BL/6J mice [434]. Similar levels of emphysematous injury between C57BL/6 and BALB/c mice were also observed in a chronic ozone-induced emphysema model [107]. Nevertheless, these models of emphysema induced by chronic exposure to cigarette smoke or ozone cause only relatively very mild damage in alveolar tissue, which is not enough to magnify the inter-strain differences that can be observed with elastase or hookworm infection.

The differential susceptibility between C57BL/6 and BALB/c mice that has been shown in a variety of other disease models can be attributed to differences in the immune responses.

Therefore, we sought to identify the differences in the immune milieu in response to elastase injury between the two strains. Our temporal evaluation of BAL cells showed that BALB/cJ mice had more lymphocytes in the first two weeks after elastase treatment and more persistent macrophages throughout the three weeks after the insult. These results suggest a potential role of these two cell types in determining susceptibility. Therefore, we also measured the alteration of several cytokines and activation markers associated with lymphocytes and macrophages. The instillation of elastase in the lungs recruited more IFN-γ producing cells, particularly NK cells with higher IFN-γ expression in C57BL/6J mice when compared with BALB/cJ mice. This result agrees with a number of published studies showing that C57BL/6 mice are Th1-prone and have the ability to produce elevated IFN-γ [416, 417]. However, elastase-treated BALB/cJ mice did not demonstrate the greater Th2 response (IL-4, IL-5 and IL-13) that was shown in allergic or the parasitic infection model [413, 414]. Interestingly, in BALB/cJ mice there was a 20-fold upregulation of IL-17A, which was not found in C57BL/6J mice. Moreover, there was higher expression of IL-18 in BALB/cJ mice relative to C57BL/6J, both at baseline and after elastase administration. While mice overexpressing either IFN-γ or IL-18 specifically in the adult lung displayed an emphysema-like phenotype accompanied with high level of proteases such as MMP-12 and cathepsins [173, 436], it was also reported that IL-17A-deficient mice developed less pulmonary inflammation with reduced severity of emphysema after 3.5U elastase [188]. Moreover, transgenic IL-18-overexpressing mice had enhanced expression of IFN-γ and IL-17A together with elevated numbers of IFN-γ and IL-17A positive cells in the lung [436]. These studies suggest a potential role of these cytokines in causing emphysematous damage triggered by elastase, but the mechanism remains unclear. Collectively, we hypothesize that

C57BL/6J and BALB/cJ mice have different mechanisms underlying the initial destruction of the alveolar tissue, and that the higher inductions of IL-17A and IL-18 are involved in the mechanism that results in an increased susceptibility to develop emphysema in BALB/cJ mice.

Another potentially important difference in elastase-treated BALB/cJ mice and C57BL/6J mice is the prolonged presence of alternatively activated macrophages (M2 phenotypes) in the lung BAL. Such M2 macrophages participate in the resolution of inflammation, wound healing and tissue remodeling by producing a broad array of extracellular matrix proteases such as MMP-2, MMP-9 and MMP-12 (macrophage elastase) [425, 437]. To maintain tissue homeostasis, the activation of these macrophages has to be tightly regulated. In chronic inflammatory states, persistent activation of macrophage-derived MMPs is involved in remodeling the extracellular matrix, to the extent that such excessive stimulation can lead to subsequent loss of matrix integrity and mechanical failure as seen in periodontal disease or arthritis [438-440]. Several studies that have indicated a significant contribution of MMP-12 protease in degradation of extracellular matrix in alveolar walls, and this is supported by a study that showed mice lacking MMP-12 have an attenuated severity of cigarette smoke-induced emphysema [102]. Therefore, MMP-12 is commonly measured in experimental emphysema models to correlate with the severity of the pathology. Consistent with previous studies, we showed that the susceptible BALB/cJ mice had a greater elevation and prolonged production of MMP-12 in the lung in response to elastase injury than the resistant C57BL/6J strain. The polarization of macrophages toward M2 phenotypes with MMP-12 elevation has also been observed in the hookworm infection model of emphysema [108], the acute ozone exposure model [441], the mouse cigarette smoke model [442, 443], and

possibly in human emphysema patients [444]. Interestingly, in addition to the expression signature for M2 macrophages, we also found the higher expression of inducible nitric oxide synthase (iNOS), a typical marker for classical activated macrophages (M1 phenotype) at baseline and after elastase insult in the BALB/cJ strain. This data is similar to several previous human studies showing the increased expression of iNOS in alveolar macrophages and lung tissue from COPD patients [445-447]. This classical activation of macrophages have been linked to the increase in production of reactive oxidation species (ROS) and nitric oxide (NO) as well as the enhanced release of several proinflammatory cytokines (e.g. IL-1β, IL-6, IL-8 and TNF-α) which have been shown to be important contributors to the pathogenesis of COPD [133, 448-450]. We also reported higher elevated expression of both IL-1β and IL-6, possibly due to greater M1 activation in BALB/cJ mice following to elastase challenge than C57BL/6J mice. Deficiency of either IL-1β or IL-6 were shown to protect the elastase-induced emphysema in mice [105, 176]. Overall, similar to the data from human COPD patients, our present work displayed mixed M1/M2 activation of macrophages in elastase-induced emphysema animals. The mixed M2/M1 phenotype could reflect a unique fixed activation status of the lung macrophages, a plastic phenotype that is dependent on changes in the local lung environment or it could represent the presence of multiple distinct populations of macrophages. It is possible that genetic factors contribute significantly to the changes in the lung environment that in turn influences a dynamic activation and metabolic phenotype of macrophages that ultimately promotes the progression of emphysema

To completely understand the impact that a protease has on the progression of emphysema, also it is important to considered the expression dynamics of the endogenous and inducible inhibitors that regulate the overall level of protease activity in the lungs. Our results

illustrated that the control BALB/cJ mice have lower expression levels of α2-macroglobulin, a major endogenous anti-protease that can bind to porcine pancreatic elastase. Thus, if the up-regulation in the lung tissue after elastase was smaller in BALB/cJ mice relative to C57BL/6J mice, it could account for the increased emphysema in the BALB/cJ. However, α2-macroglobulin is produced mainly by hepatocytes in the liver, and only in small amounts by cells in the lungs [451]. Moreover, a primary role of α2-macroglobulin is to rapidly trap excess proteinases, but not to inactivate them, so proteases can still be released after binding α2-macroglobulin [307, 452]. Unlike α2-macroglobulin, α1-AT is more likely to be a physiological inactivator of elastase. Interestingly, our data showed a greater level of α1-AT in BALB/cJ mice when compared to C57BL/6J mice. This data is consistent with Martonana *et al.* who reported that there was higher mRNA levels of α1-AT expression in the liver tissue of BALB/c than C57BL/6 and pallid mice, corresponding with higher serum α1-AT level and more elastase inhibitory capacity [453]. The pallid mice, which have a marked reduction in α1-AT levels, were shown to spontaneously develop an emphysema-like phenotype at early ages of life, as well as having an increased susceptibility to develop more emphysema when exposed to the neutrophil chemotactic peptide FMLP [453, 454]. The fact that BALB/cJ mice have higher levels of α1-AT suggests that the increased susceptibility of this strain to progressive emphysema is more likely a result of other mechanisms, rather than anti-proteases activities.

One of the outstanding questions regarding the pathogenesis of emphysema is the role of persistent chronic inflammation, and how it may lead to the continual alveolar tissue destruction in the lungs. In addition, there is often a gradual decline in lung function in

human patients, even in the absence of the risk factors as seen in smokers who have quit yet emphysema continues to progress [311]. This observation implies that the mechanisms underlying the initiation phase of human emphysema might be different from the mechanism driving the progression phase. This progression of immune-mediated pathology in humans cannot be reproduced in animals exposed to chronic cigarette smoke. This aspect of the human disease is perhaps better modeled in the BALB/cJ model of elastase-induced experimental emphysema, especially in BALB/cJ mice. A single insult that quickly heals leads to progressive tissue destruction over many months. Originally, as mentioned earlier, the hamster was reported to be susceptible to the development of emphysema induced by elastase presumably because of its low level of serum α1-antitrypsin and in low elastase inhibitory capacity [430]. Nevertheless, the hamster was shown to still have the ability to eliminate the exogenous elastase from the lung within 24 hours [307]. This situation is mimicked in our mouse model as evidenced by exogenous elastase-associated acute lung injury (e.g. mortality, hemorrhage, massive neutrophil infiltration) only in the first few days post challenge. Although this is a simple insult to produce, the model is clearly not mechanistically simple. The mechanism requires other endogenous mediators that may have many similarities to the human situation. Due to the fact that many emphysema patients are typically not diagnosed until they are symptomatic and in a relatively late stage of the disease [34, 36], studies utilizing the elastase-induced emphysema in BALB/cJ mice might turn out to be very beneficial for studying the mechanisms that are associated with progression of the disease at early stages, for evaluating potential therapeutic interventions to slow or stop the disease perpetuation and identify markers that could be used for early diagnosis.

In conclusion, differences in strain-associated susceptibility to develop elastase-induced emphysema is documented here. We provided data in support of the hypothesis that the disparity in immune responses between the two strains studied results in part from differences in production of IFN-γ, IL-17A and alternative activation of macrophages. However, more experiments have to be performed to elucidate the mechanistic linkage between this immune response and the susceptibility of emphysema.

3.5 Acknowledgements

At the Johns Hopkins School of Public Health: The flow cytometric analysis of lymphocytes and IFN-γ producing cell populations in Fig. 3.12-3.14 were carried out by Dr. Daniel Lagassé. All histological tissue preparation were assisted by Xin Guo and the measurement of L_m from tissue sections were performed by Alexandra Kearson. This work was supported by grant from National Heart, Lung, and Blood Institute Grant # P01HL10342.

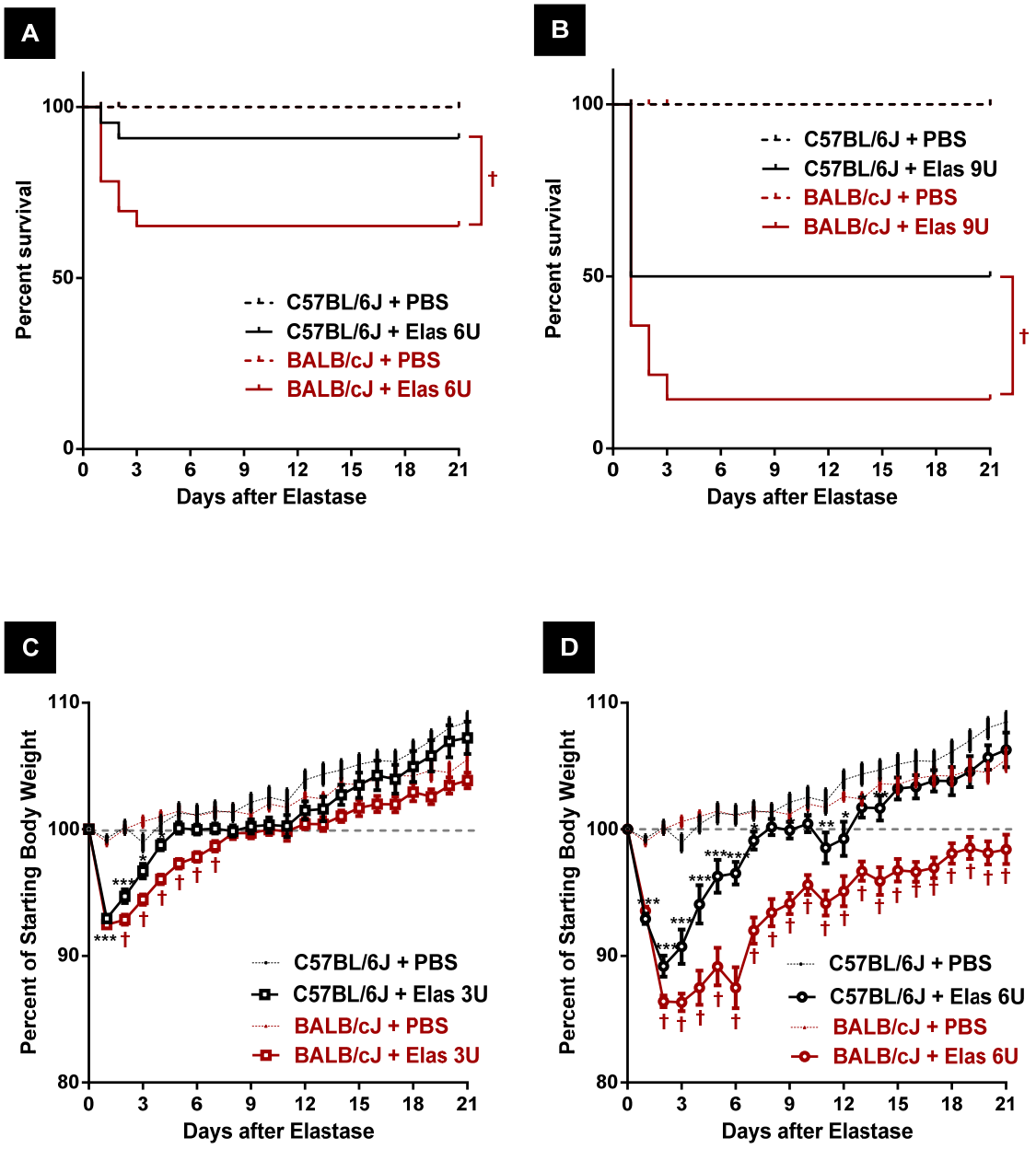

Figure 3.1 Survival rate and body weight of C57BL/6J and BALB/cJ mice following elastase challenge. (A-B) Survival after intratracheal instillation of C57BL/6J and BALB/cJ mouse lungs with 6 units (A) or 9 units (B). (C-D) Weight loss after intratracheal instillation of C57BL/6J and BALB/cJ mouse lungs with 3 units (C) or 6 units (D). ($n \geq 12$ mice per group). † = $p < 0.05$ by log-rank test (A-B) or one-way ANOVA (C-D) comparing BALB/cJ with C57BL/6J at the same dose. * = $p < 0.05$, ** = $p < 0.01$, *** = $p < 0.001$ by one-way ANOVA comparing elastase-treated group to PBS.

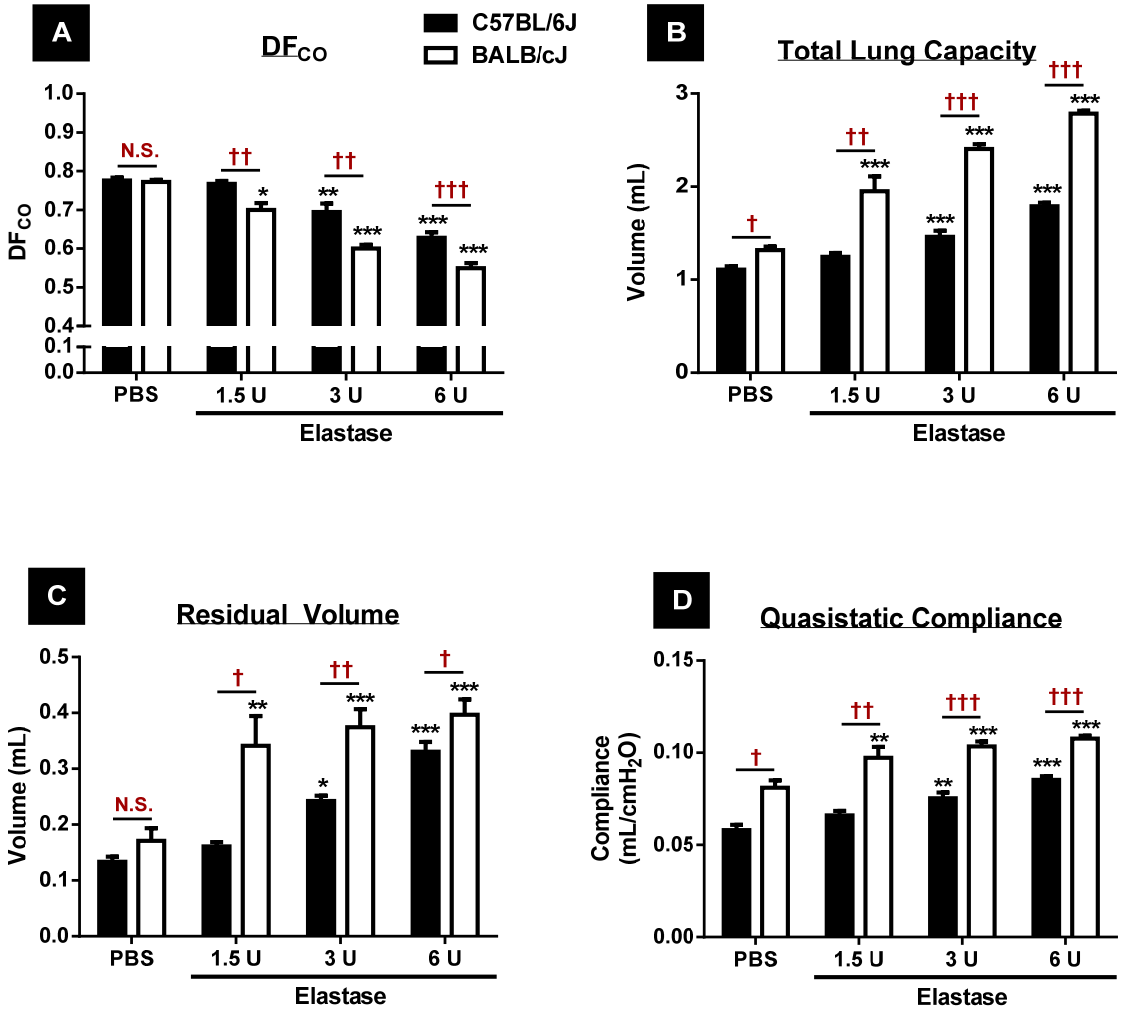

Figure 3.2 Diffusion capacity and PV parameters in C57BL/6J and BALB/cJ mice following increasing doses of elastase. (A) Diffusion factor for carbon monoxide; (B) Total lung capacity; (C) Residual volume and (D) Quasistatic compliance of C57BL/6J and BALB/cJ mice after intratracheal challenge with elastase at the doses of 1.5, 3, and 6 units. (n = 5-14 mice per group). Two-way ANOVA analysis: * = $p < 0.05$, ** = $p < 0.01$, *** = $p < 0.001$ comparing elastase-treated group to PBS. † = $p < 0.05$, †† = $p < 0.01$, ††† = $p < 0.001$ comparing BALB/cJ with C57BL/6J at the same dose.

Table 3.1 Baseline values for lung mechanics parameters in both mouse strains before elastase and at 21 days after different time points after 1.5. 3U, or 6U elastase. Parameters measured are: respiratory system resistance (Rrs), elastance (Ers), compliance (Crs), airway resistance (*Rn*), tissue damping (*G*), and tissue elastance (*H*) displayed at different doses of elastase of both mouse strains.

Treatment	Rrs (cmH_2O s/mL)	Crs (mL/cmH_2O)	Ers (cmH_2O/mL)	Rn (cmH_2O s/mL)	G (cmH_2O/mL)	H (cmH_2O/mL)
PBS						
C57BL/6J	0.821 ± 0.058	0.038 ± 0.0004	26.369 ± 0.263	0.450 ± 0.039	4.503 ± 0.144	25.669 ± 0.570
BALB/cJ	0.819 ± 0.075	0.052 ± 0.0004†††	19.190 ± 0.165†††	0.549 ± 0.059	3.528 ± 0.094†††	18.573 ± 0.404
Elastase 1.5U						
C57BL/6J	0.691 ± 0.029	0.042 ± 0.0010	24.117 ± 0.529**	0.361 ± 0.028	4.186 ± 0.238	21.600 ± 0.722***
BALB/cJ	0.621 ± 0.019	0.072 ± 0.0037†††	13.944 ± 0.694***†††	0.358 ± 0.022	2.935 ± 0.120*†††	10.983 ± 0.957***†††
Elastase 3U						
C57BL/6J	0.767 ± 0.044	0.052 ± 0.0015***	19.464 ± 0.508***	0.441 ± 0.033	4.098 ± 0.123*	15.311 ± 0.507***
BALB/cJ	0.717 ± 0.033	0.080 ± 0.0014***†††	12.603 ± 0.219***†††	0.435 ± 0.030	2.916 ± 0.062**†††	8.900 ± 0.281***†††
Elastase 6U						
C57BL/6J	0.697 ± 0.036	0.059 ± 0.0013***	16.999 ± 0.359***	0.398 ± 0.028	3.741 ± 0.093***	12.620 ± 0.502***
BALB/cJ	0.889 ± 0.090	0.080 ± 0.0009***†††	12.561 ± 0.150***†††	0.579 ± 0.071	2.872 ± 0.041***†††	8.654 ± 0.161***†††

Results are expressed as mean ± SEM (n = 5-14 mice per group). Two-way ANOVA analysis: * = $p < 0.05$, ** = $p < 0.01$, *** = $p < 0.001$ comparing elastase-treated group to PBS. † = $p < 0.05$, †† = $p < 0.01$, ††† = $p < 0.001$ comparing BALB/cJ with C57BL/6J at the same dose.

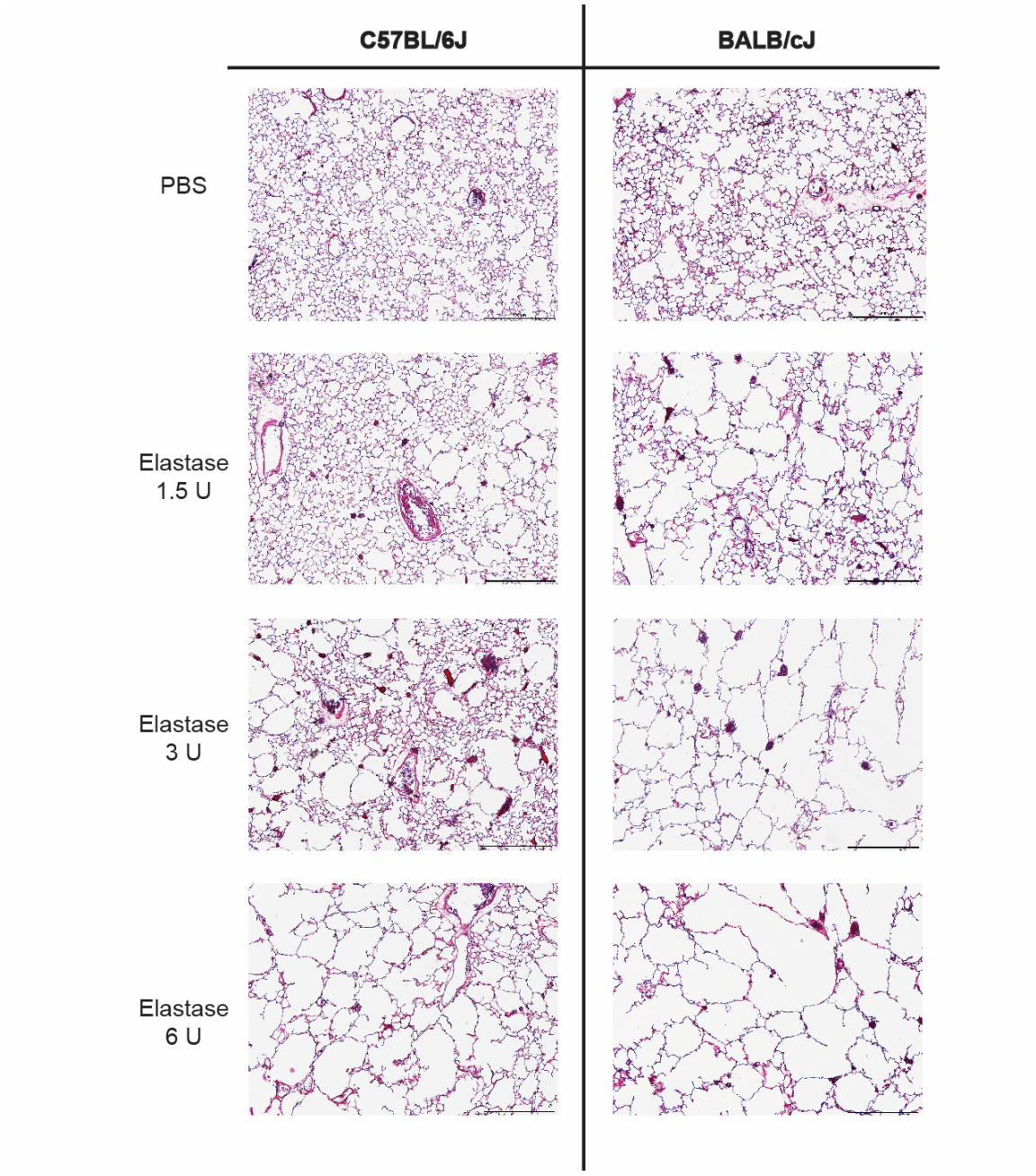

Figure 3.3 Photomicrographs of C57BL/6J and BALB/cJ lung parenchyma after treatment with 1.5, 3, and 6U elastase or vehicle. Representative H&E-stained lung sections from C57BL/6J (*left panel*) and BALB/cJ (*right panel*) mice before elastase and at day 21 after 1.5, 3, or 6U elastase. Original magnification x40. Scale bar = 500 μm.

Figure 3.4 Gross appearance of C57BL/6J and BALB/cJ lungs following elastase challenge. Representative gross pathology of air-inflated lungs from C57BL/6J (*left panel*) and BALB/cJ (*right panel*) mice at days 1, 2, 4, 7, 14 and 21 post-elastase (3 units) challenge compared to naïve control lung.

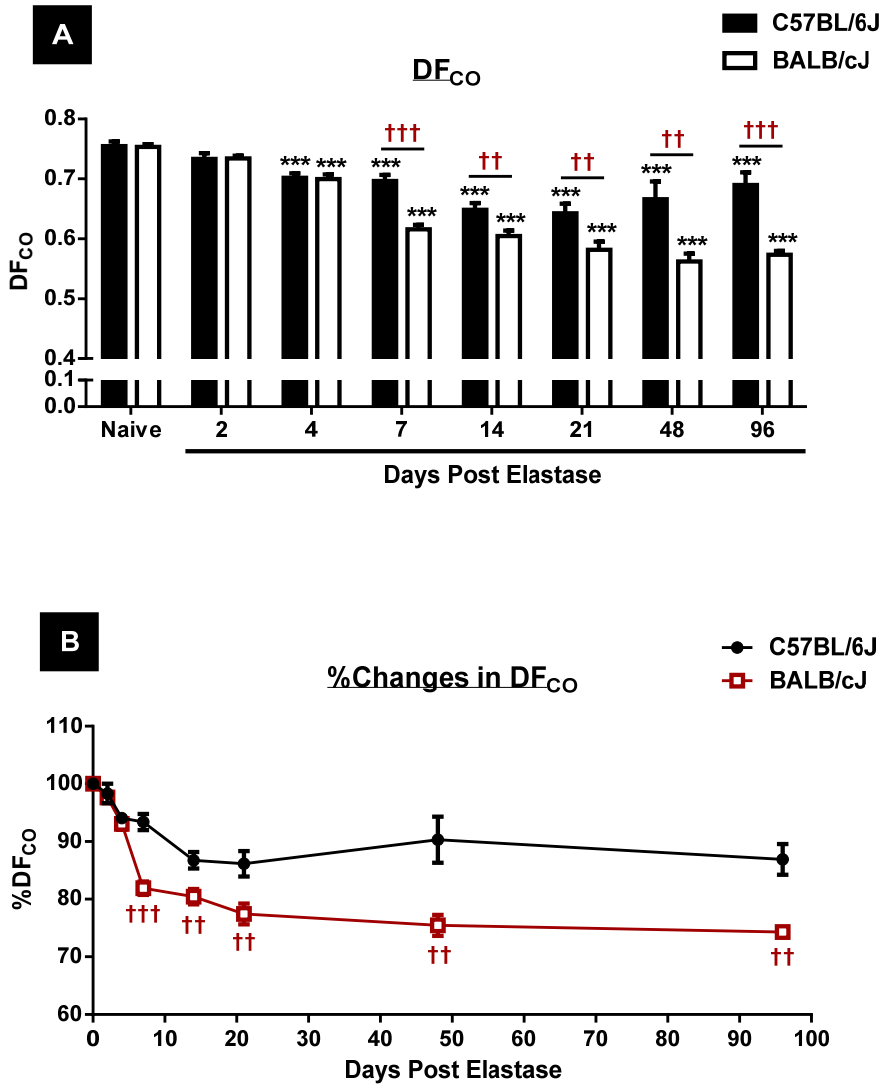

Figure 3.5 Time course of decline in diffusion capacity between two mouse strains following 3U elastase. (A) Diffusion factor for carbon monoxide and (B) Percentage change of DF_{CO} in C57BL/6J and BALB/cJ mice at days 2, 4, 7, 14, 21, 48 and 96 following 3 units elastase. (n = 5-10 mice per group). Two-way ANOVA analysis: * = $p < 0.05$, ** = $p < 0.01$, *** = $p < 0.001$ comparing elastase-treated group to naïve animals. † = $p < 0.05$, †† = $p < 0.01$, ††† = $p < 0.001$ comparing BALB/cJ with C57BL/6J at the same time point.

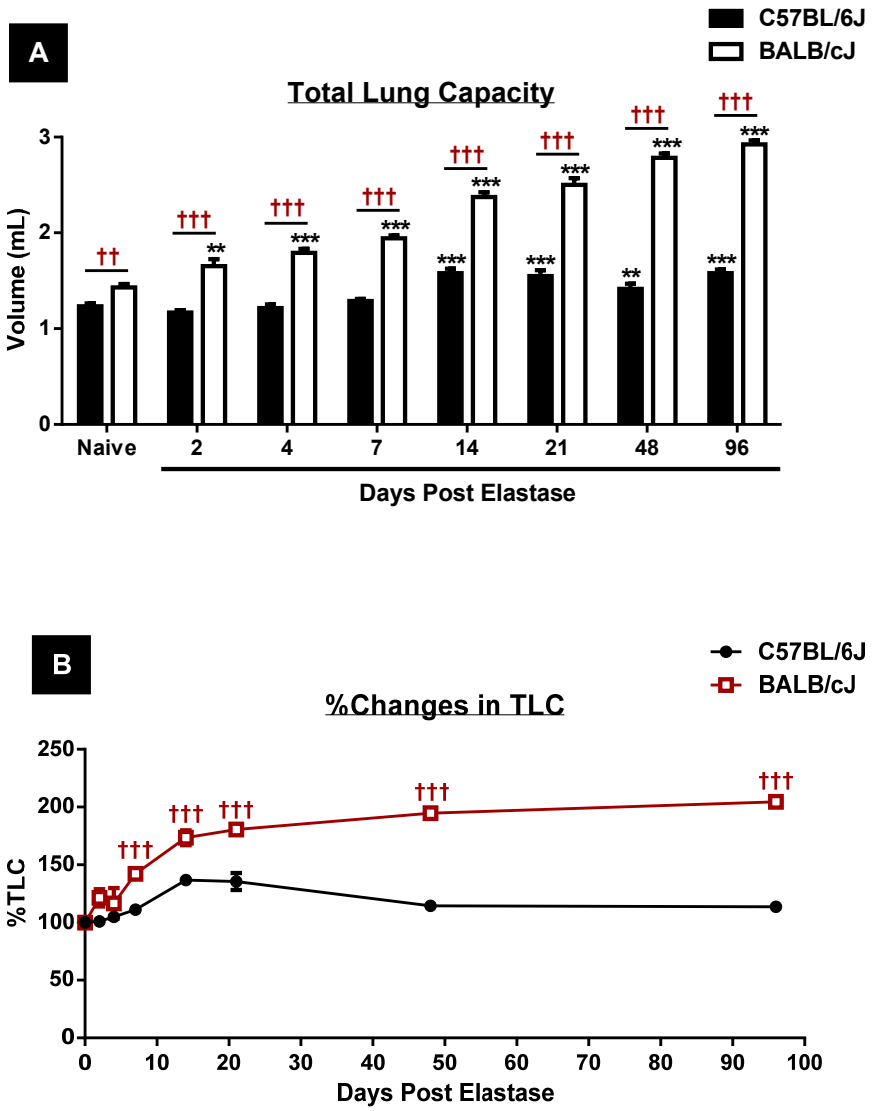

Figure 3.6 Time course of increase in total lung capacity between two mouse strains following 3U elastase. (A) Total lung capacity and (B) Percentage change of TLC in C57BL/6J and BALB/cJ mice at days 2, 4, 7, 14, 21, 48 and 96 following 3 units elastase. (n = 5-10 mice per group). Two-way ANOVA analysis: * = $p < 0.05$, ** = $p < 0.01$, *** = $p < 0.001$ comparing elastase-treated group to naïve animals. † = $p < 0.05$, †† = $p < 0.01$, ††† = $p < 0.001$ comparing BALB/cJ with C57BL/6J at the same time point.

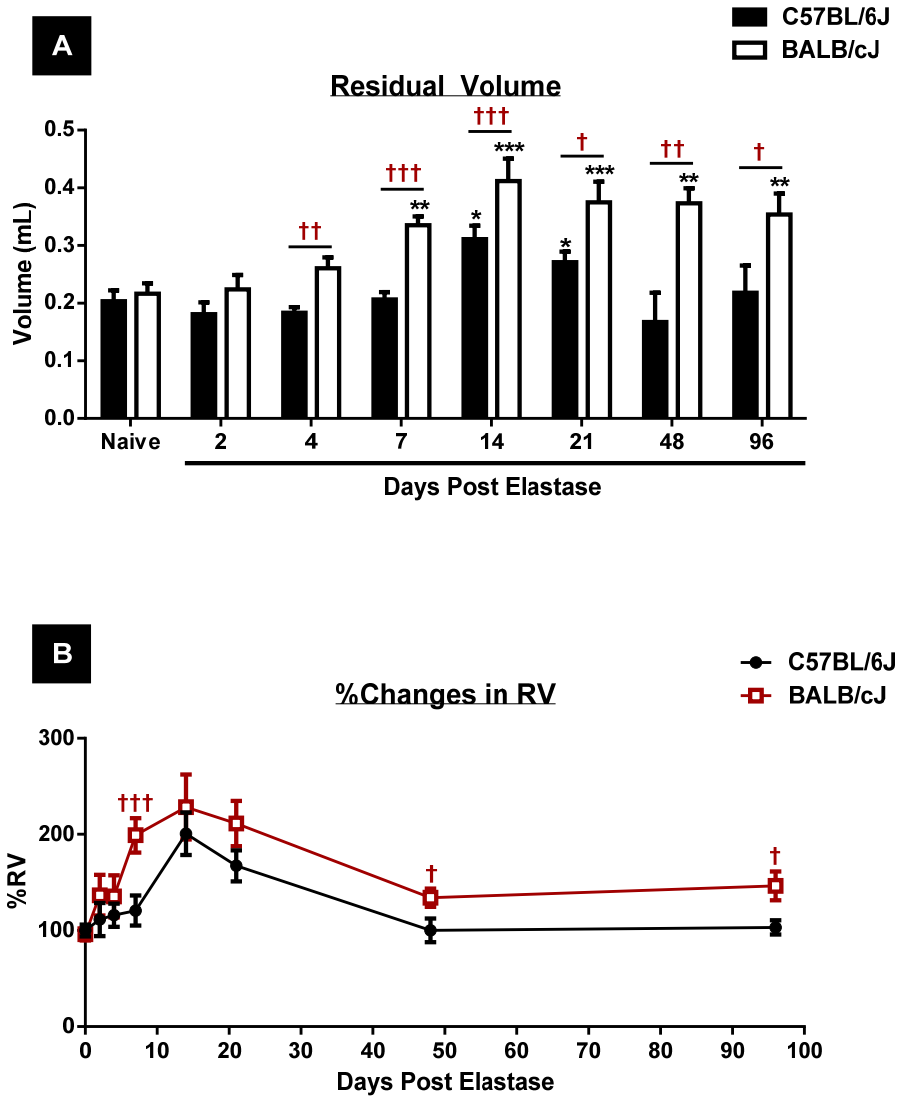

Figure 3.7 Time course of increase in residual volume between two mouse strains following 3U elastase. (A) Residual volume and (B) Percentage change of RV in C57BL/6J and BALB/cJ mice at days 2, 4, 7, 14, 21, 48, and 96 following 3 units elastase. (n = 5-10 mice per group). Two-way ANOVA analysis: * = $p < 0.05$, ** = $p < 0.01$, *** = $p < 0.001$ comparing elastase-treated group to naïve animals. † = $p < 0.05$, †† = $p < 0.01$, ††† = $p < 0.001$ comparing BALB/cJ with C57BL/6J at the same time point.

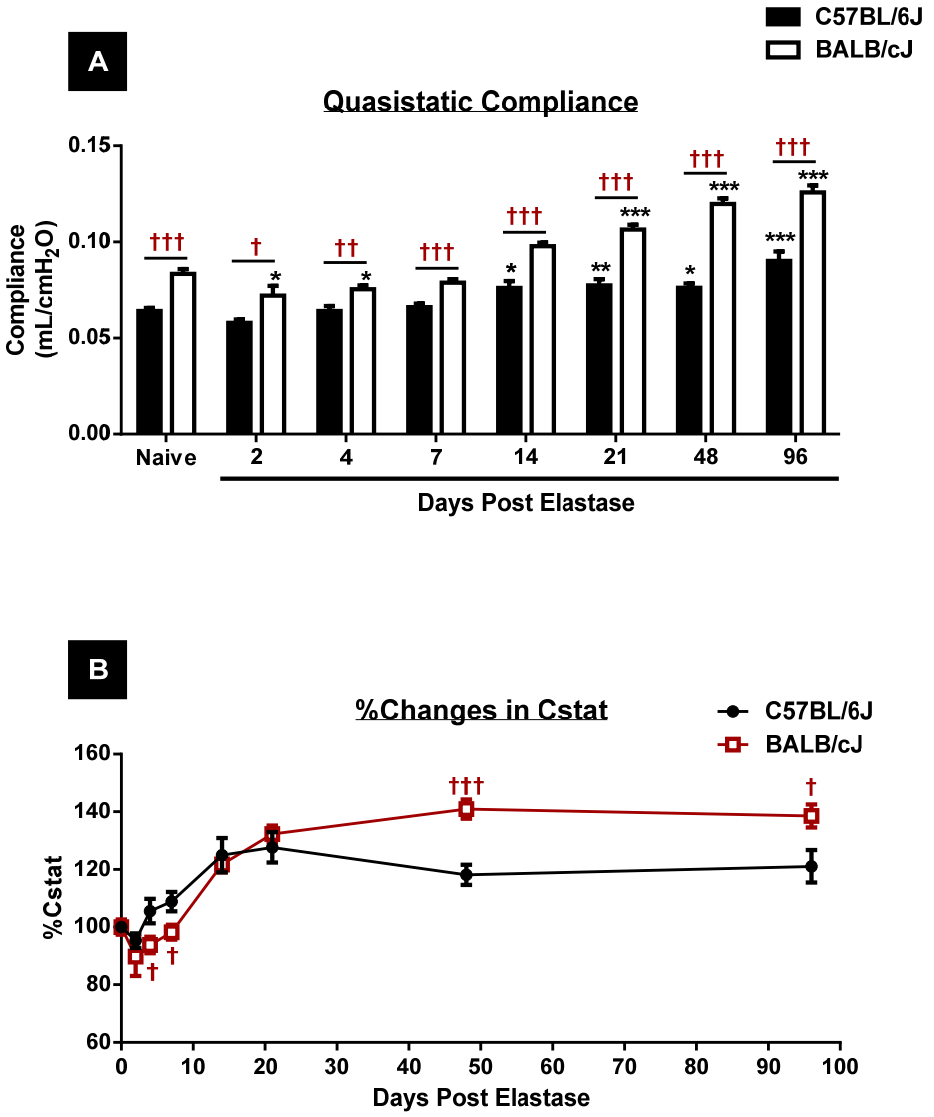

Figure 3.8 Time course of increase in lung quasi-static compliance between two mouse strains following 3U elastase. (A) Quasi-static compliance and (B) Percentage change in Cstat from C57BL/6J and BALB/cJ mice at days 2, 4, 7, 14, 21, 48, and 96 following 3 units elastase. (n = 5-10 mice per group). Two-way ANOVA analysis: * = $p < 0.05$, ** = $p < 0.01$, *** = $p < 0.001$ comparing elastase-treated group to naïve animals. † = $p < 0.05$, †† = $p < 0.01$, ††† = $p < 0.001$ comparing BALB/cJ with C57BL/6J at the same time point.

Table 3.2 Baseline values for lung mechanics parameters in both mouse strains at different time point following 3U elastase. Parameters measured are: respiratory system resistance (Rrs), elastance (Ers), compliance (Crs), airway resistance (*Rn*), tissue damping (*G*), and tissue elastance (*H*).

Treatment	Rrs (cmH_2O s/mL)	Crs (mL/cmH_2O)	Ers (cmH_2O/mL)	Rn (cmH_2O s/mL)	G (cmH_2O/mL)	H (cmH_2O/mL)
Naive						
C57BL/6J	0.756 ± 0.041	0.040 ± 0.0007	25.345 ± 0.432	0.449 ± 0.033	4.262 ± 0.144	24.922 ± 0.535
BALB/cJ	0.806 ± 0.074	0.054 ± 0.0009†††	18.767 ± 0.268†††	0.534 ± 0.056	3.540 ± 0.132†††	17.995 ± 0.524†††
Day 2						
C57BL/6J	0.723 ± 0.029	0.041 ± 0.0005	24.521 ± 0.315	0.360 ± 0.0019	4.468 ± 0.084	21.011 ± 0.469***
BALB/cJ	0.753 ± 0.048	0.053 ± 0.0033††	19.753 ± 1.333††	0.427 ± 0.036	3.760 ± 0.270†	15.303 ± 1.445††
Day 4						
C57BL/6J	0.703 ± 0.088	0.043 ± 0.0017	23.724 ± 1.223	0.298 ± 0.027	4.676 ± 0.262	18.028 ± 0.570***
BALB/cJ	0.639 ± 0.038	0.059 ± 0.0007†††	16.882 ± 0.195†††	0.365 ± 0.033	3.493 ± 0.197††	12.589 ± 0.538***†††
Day 7						
C57BL/6J	0.633 ± 0.026	0.047 ± 0.0009**	21.438 ± 0.400***	0.361 ± 0.036	4.029 ± 0.122	17.597 ± 0.812***
BALB/cJ	0.785 ± 0.047†	0.063 ± 0.0015***†††	15.906 ± 0.372*†††	0.485 ± 0.054	3.319 ± 0.062†††	10.917 ± 0.300***†††
Day 14						
C57BL/6J	0.721 ± 0.030	0.054 ± 0.0023***	18.880 ± 0.922***	0.420 ± 0.032	3.952 ± 0.131	15.149 ± 1.065***
BALB/cJ	0.703 ± 0.032	0.075 ± 0.0013***†††	13.312 ± 0.225***†††	0.423 ± 0.035	2.998 ± 0.063†††	9.070 ± 0.163***†††
Day 21						
C57BL/6J	0.815 ± 0.067	0.053 ± 0.0023***	19.224 ± 0.755***	0.483 ± 0.049	4.155 ± 0.194	15.047 ± 0.759***
BALB/cJ	0.717 ± .0033	0.080 ± 0.0014***†††	12.603 ± 0.219***†††	0.435 ± 0.030	2.916 ± 0.062†††	8.900 ± 0.281***†††
Day 48						
C57BL/6J	0.813 ± 0.075	0.048 ± 0.0023*	20.885 ± 1.057**	0.411 ± 0.056	4.219 ± 0.215	17.126 ± 1.193***
BALB/cJ	0.719 ± 0.080	0.084 ± 0.0012***†††	11.939 ± 0.177***†††	0.447 ± 0.080	2.878 ± 0.047†††	8.334 ± 0.153***†††
Day 96						
C57BL/6J	0.676 ± 0.050	0.053 ± 0.0024***	19.004 ± 0.804***	0.385 ± 0.022	4.024 ± 0.207	15.209 ± 0.663***
BALB/cJ	1.090 ± 0.180	0.090 ± 0.0021***†††	11.129 ± 0.267***†††	0.820 ± 0.159**††	2.600 ± 0.097*†††	8.350 ± 0.071***†††

Results are expressed as mean ± SEM (n = 5-10 mice per group). Two-way ANOVA analysis: * = $p < 0.05$, ** = $p < 0.01$, *** = $p < 0.001$ comparing elastase-treated group to naïve animals. † = $p < 0.05$, †† = $p < 0.01$, ††† = $p < 0.001$ comparing BALB/cJ with C57BL/6J at the same time point.

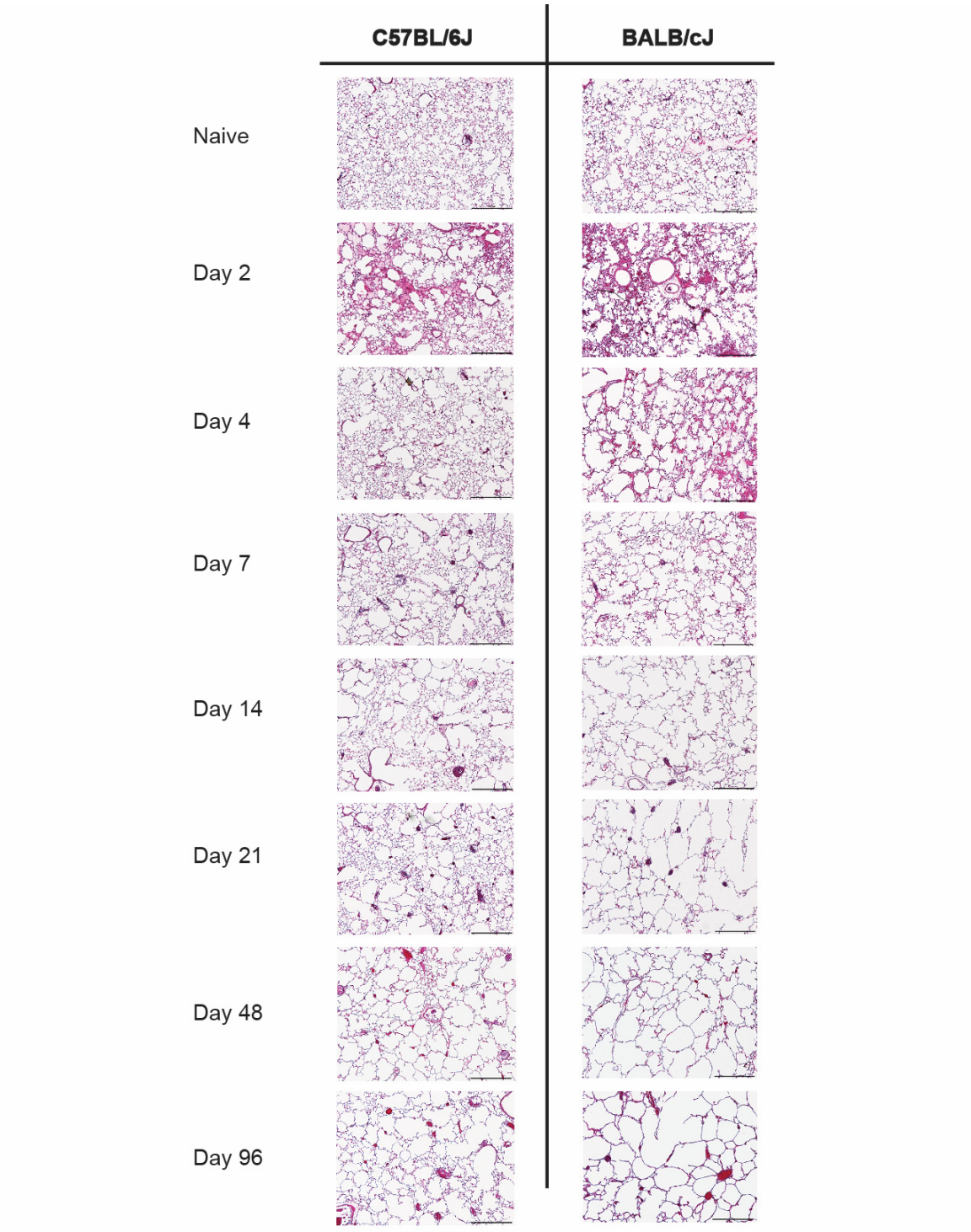

Figure 3.9 Representative photomicrographs of C57BL/6J and BALB/cJ lung parenchyma after treatment with 3U elastase at different time points. H&E-stained lung sections from C57BL/6J (*left panel*) and BALB/cJ (*right panel*) mice prior to and at days 2, 4, 7, 14, 21, 48, and 96 after elastase. Original magnification x40. Scale bar = 500 μm.

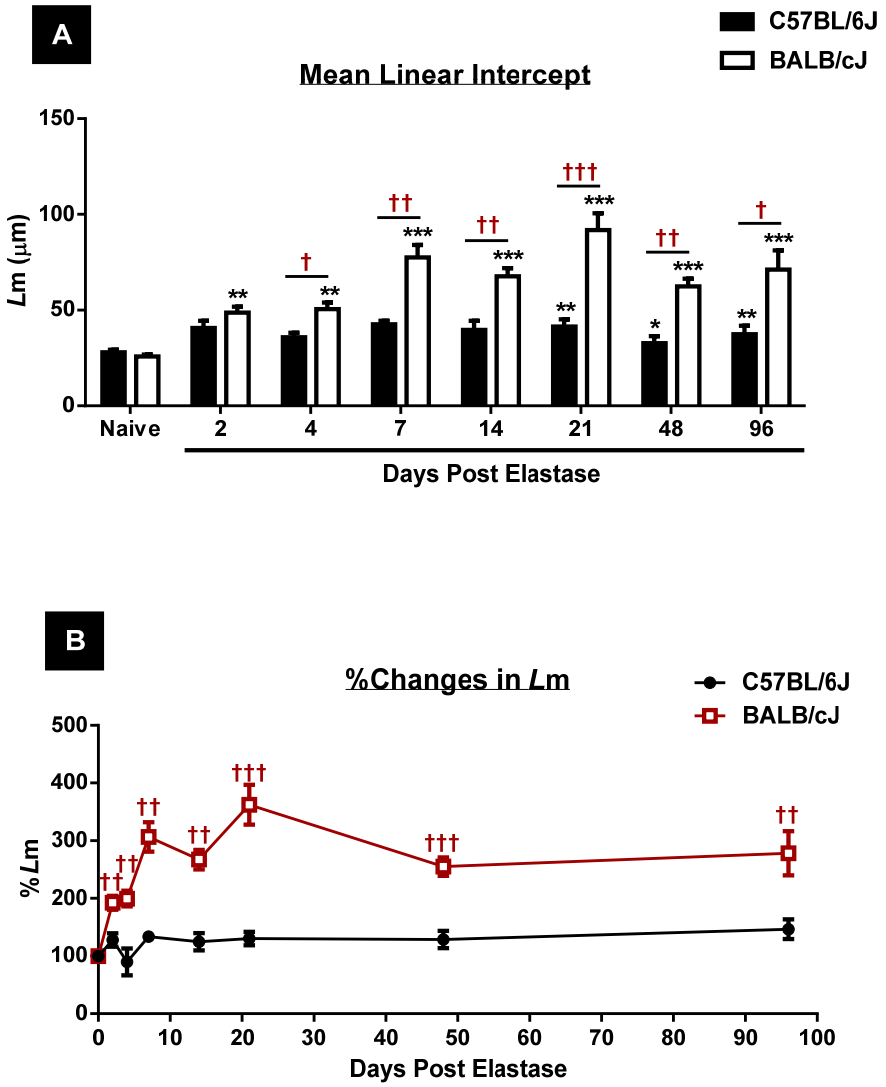

Figure 3.10 Time course of increase in mean linear intercept between two mouse strains following 3U elastase. (A) Mean linear intercept and (B) Percentage change of L_m in C57BL/6J and BALB/cJ mice at days 2, 4, 7, 14, 21, 48, and 96 following 3 units intratracheal elastase. (n = 5-10 mice per group). Two-way ANOVA analysis: * = $p < 0.05$, ** = $p < 0.01$, *** = $p < 0.001$ comparing elastase-treated group to naïve animals. † = $p < 0.05$, †† = $p < 0.01$, ††† = $p < 0.001$ comparing BALB/cJ with C57BL/6J at the same time point.

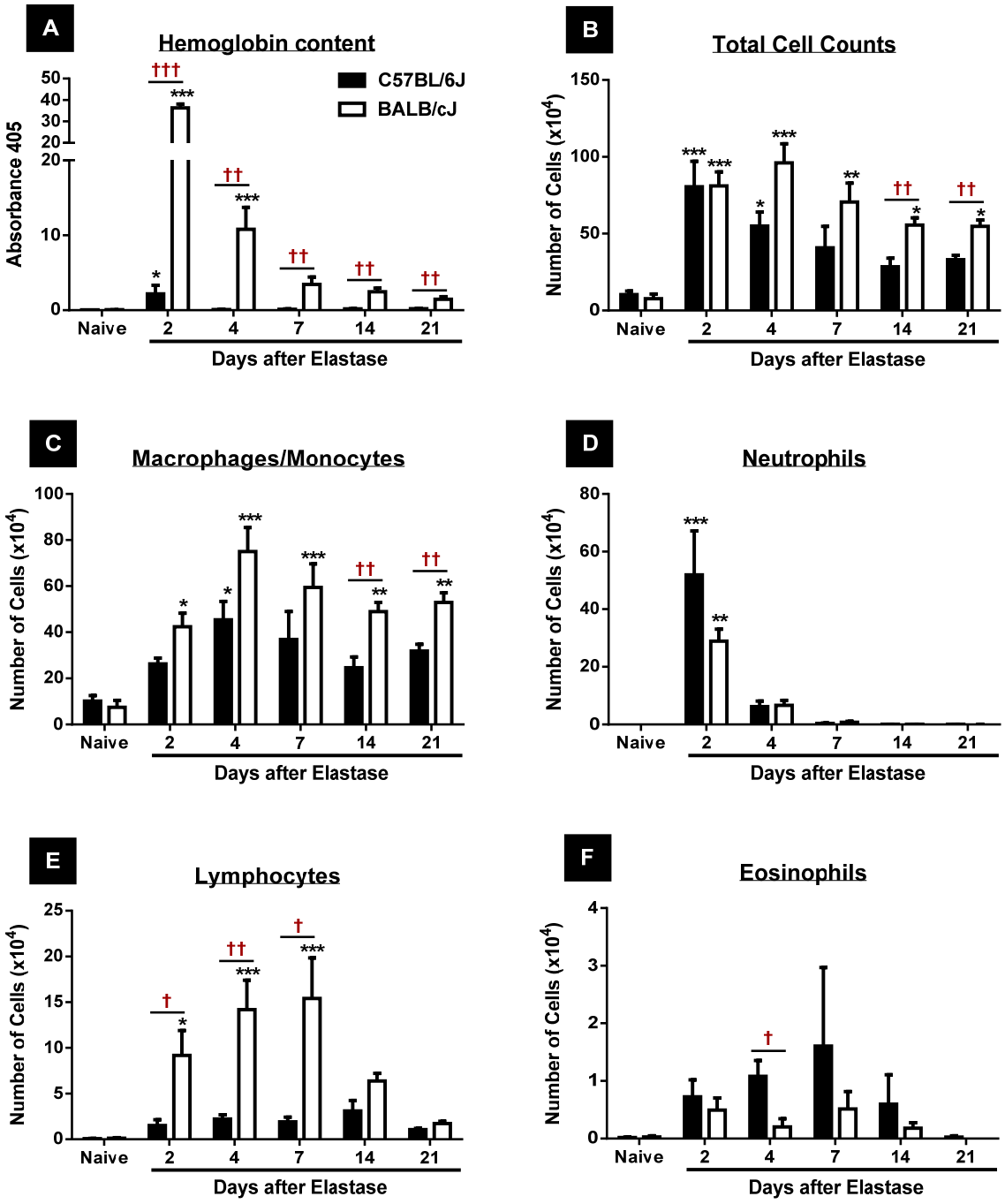

Figure 3.11 Analysis of bronchoalveolar lavage from C57BL/6J and BALB/cJ mice following 3U elastase. (A) Hemoglobin content; (B) Total cell counts; (C) Macrophage and monocyte counts; (D)Neutrophil counts; (E) Lymphocyte counts; and (F) Eosinophil counts from BAL of C57BL/6J and BALB/cJ mice at days 2, 4, 7, 14, and 21 following 3U elastase. (n = 4-5 mice per group). Two-way ANOVA analysis: * = $p < 0.05$, ** = $p < 0.01$, *** = $p < 0.001$ comparing elastase-treated group to naïve animals. † = $p < 0.05$, †† = $p < 0.01$, ††† = $p < 0.001$ comparing BALB/cJ with C57BL/6J at the same time point.

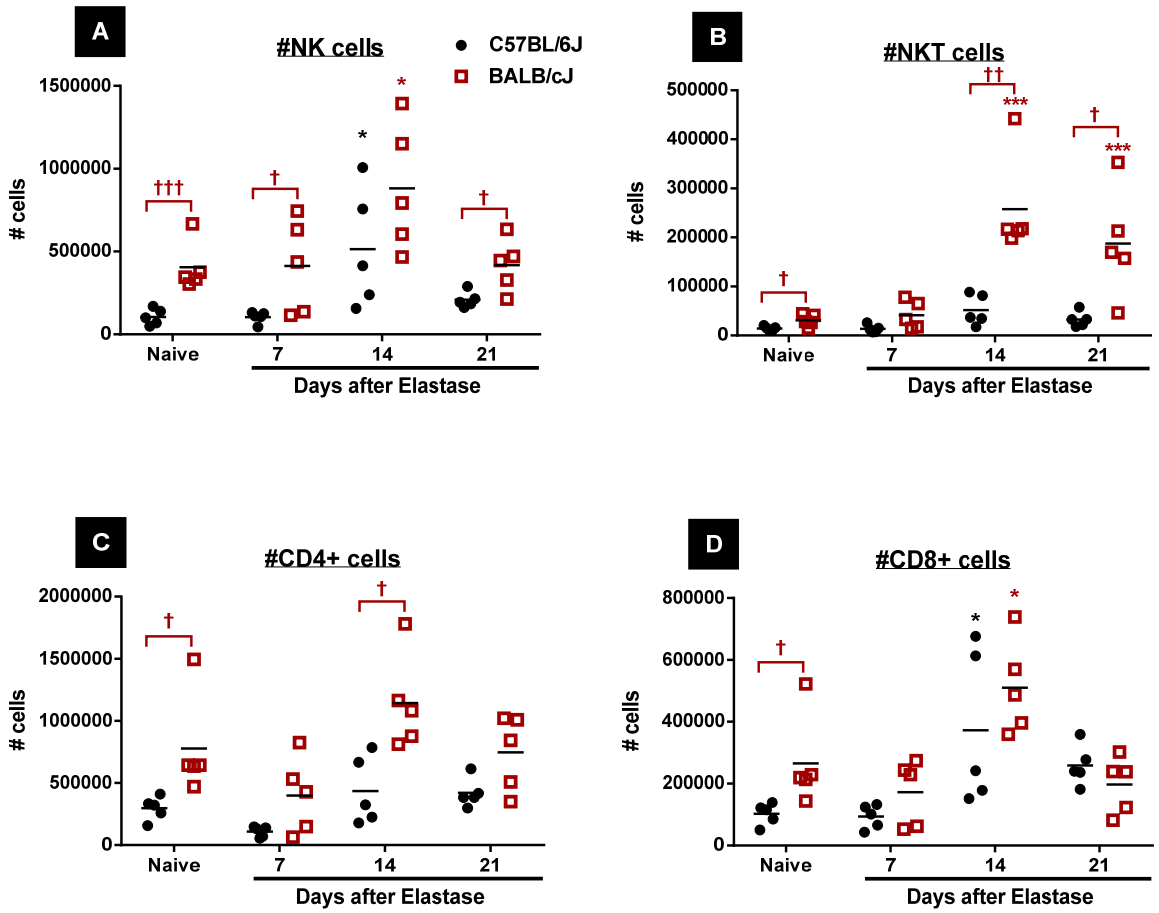

Figure 3.12 Flow cytometry analysis of NK, NKT and T cells from whole lung of C57BL/6J and BALB/cJ mice following 3U elastase. Number of (A) NK cell; (B) NKT cells; (C) $CD4^+$ cells; and (D) $CD8^+$ cells per lung in C57BL/6J and BALB/cJ mice at days 7, 14, and 21 after challenge with 3U elastase. (n = 5 mice per group). Two-way ANOVA analysis: * = $p < 0.05$, *** = $p < 0.001$ comparing elastase-treated group to naïve animals. † = $p < 0.05$, †† = $p < 0.01$, ††† = $p < 0.001$ comparing BALB/cJ with C57BL/6J at the same time point.

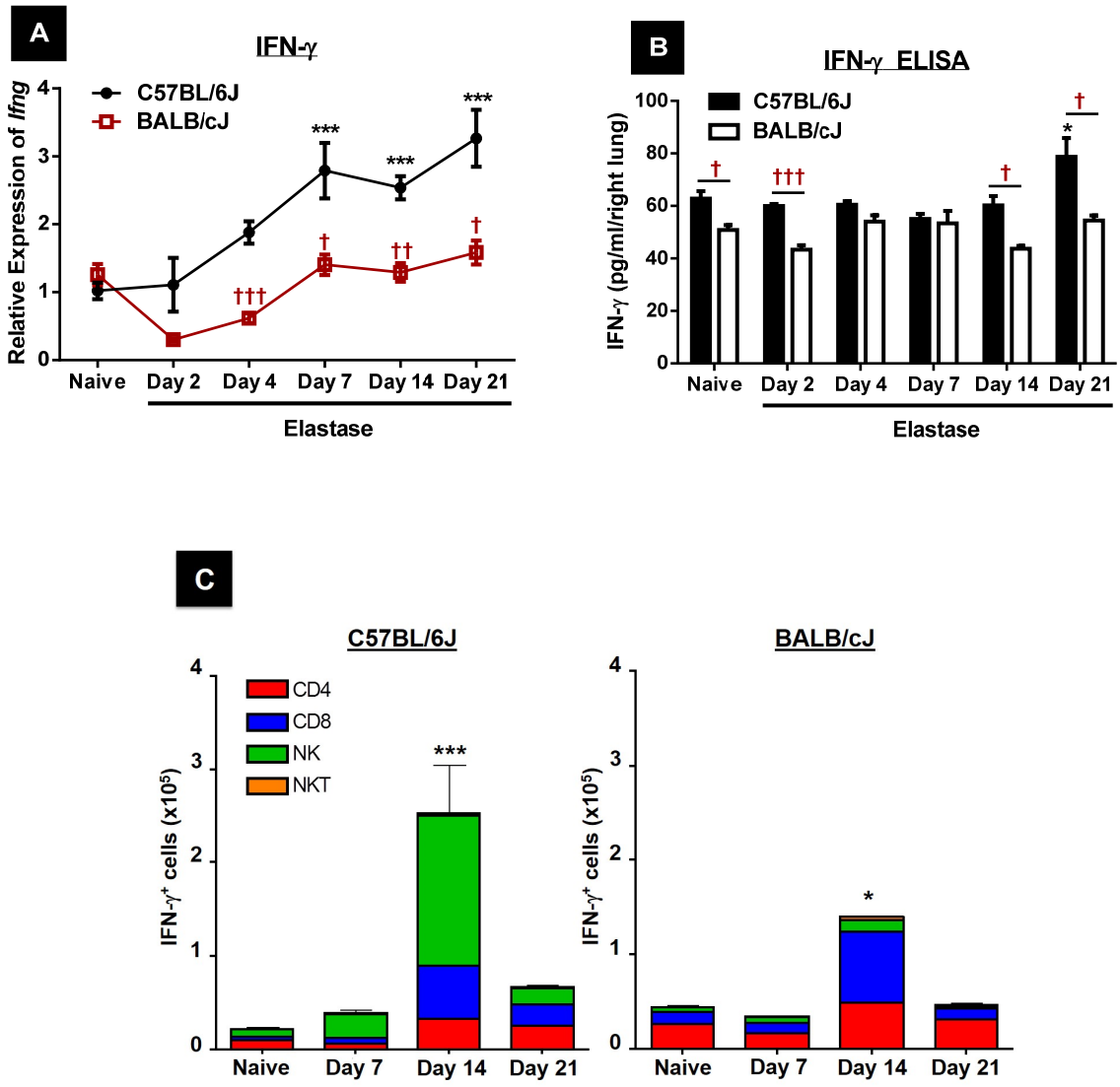

Figure 3.13 Expression of IFN-γ and number of IFN-γ-producing cells from C57BL/6J and BALB/cJ mice following 3U elastase administration. (A) Real-time RT-PCR; (B) ELISA analyses of IFN-γ mRNA and protein levels; and (C) Flow cytometry analysis of the number of IFN-γ positive cells per lung in C57BL/6J and BALB/cJ mice following intratracheal challenge with 3U elastase at days 2, 4, 7, 14 and 21. (n = 4-5 mice/group). Two-way ANOVA analysis: * = $p < 0.05$, *** = $p < 0.001$ comparing elastase-treated group to naïve animals. † = $p < 0.05$, †† = $p < 0.01$, ††† = $p < 0.001$ comparing BALB/cJ with C57BL/6J at the same time point.

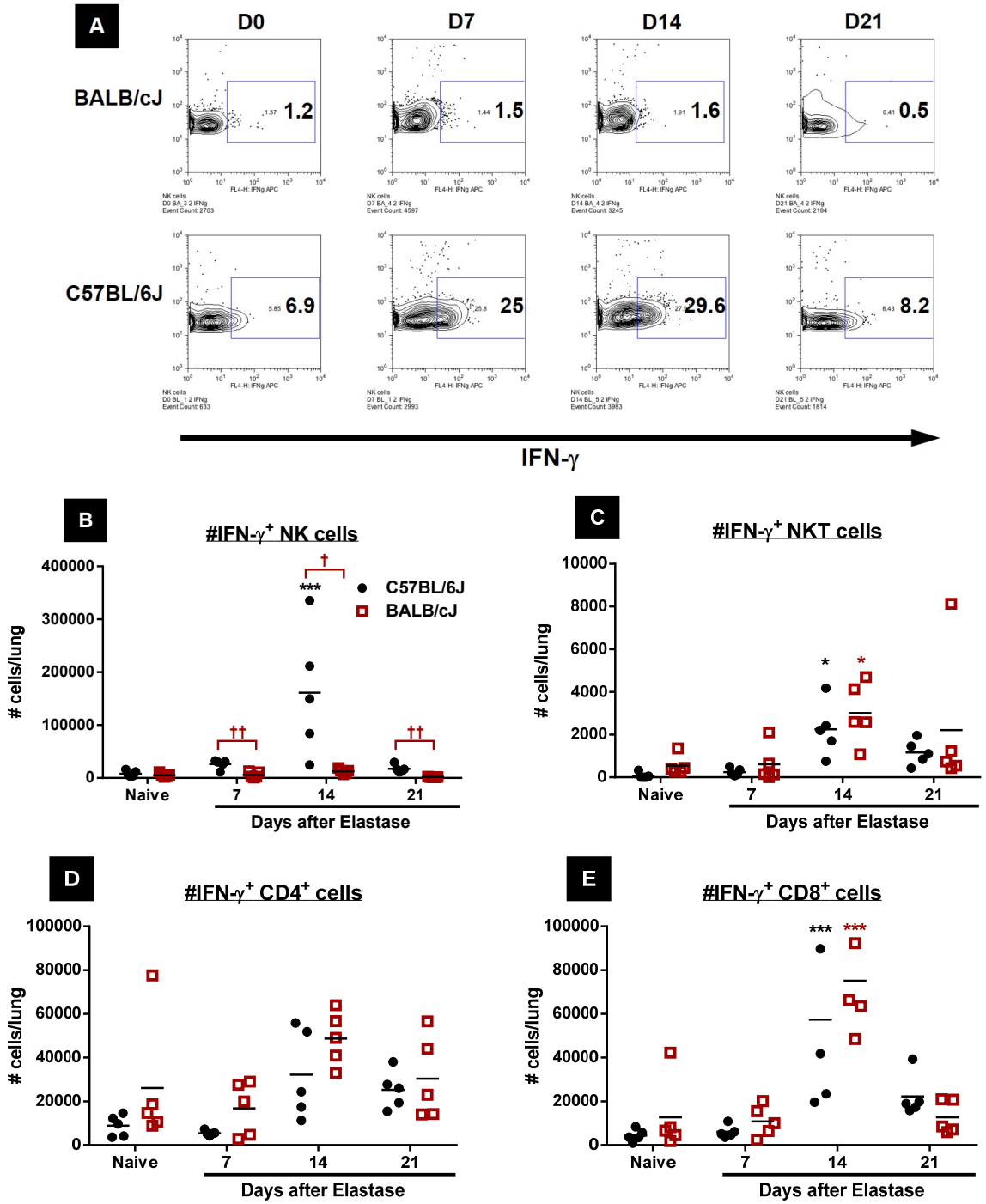

Figure 3.14 Pulmonary sources of IFN-γ in C57BL/6J and BALB/cJ mice following 3U elastase administration. (A) Representative flow plot showing the percentage of IFN-γ^+ cells gated on $CD3^-NKp46^+$ (NK cells) and number of IFN-γ^+ ; (B) NK cells; (C) NKT cells; (D) $CD4^+$ cells; and (E) $CD8^+$ cells per lung in C57BL/6J and BALB/cJ mice at days 7, 14 and 21 after challenge with 3U elastase. (n = 5 mice per group). Two-way ANOVA analysis: * = $p < 0.05$, *** = $p < 0.001$ comparing elastase-treated group to naïve animals. † = $p < 0.05$ comparing BALB/cJ with C57BL/6J at the same time point.

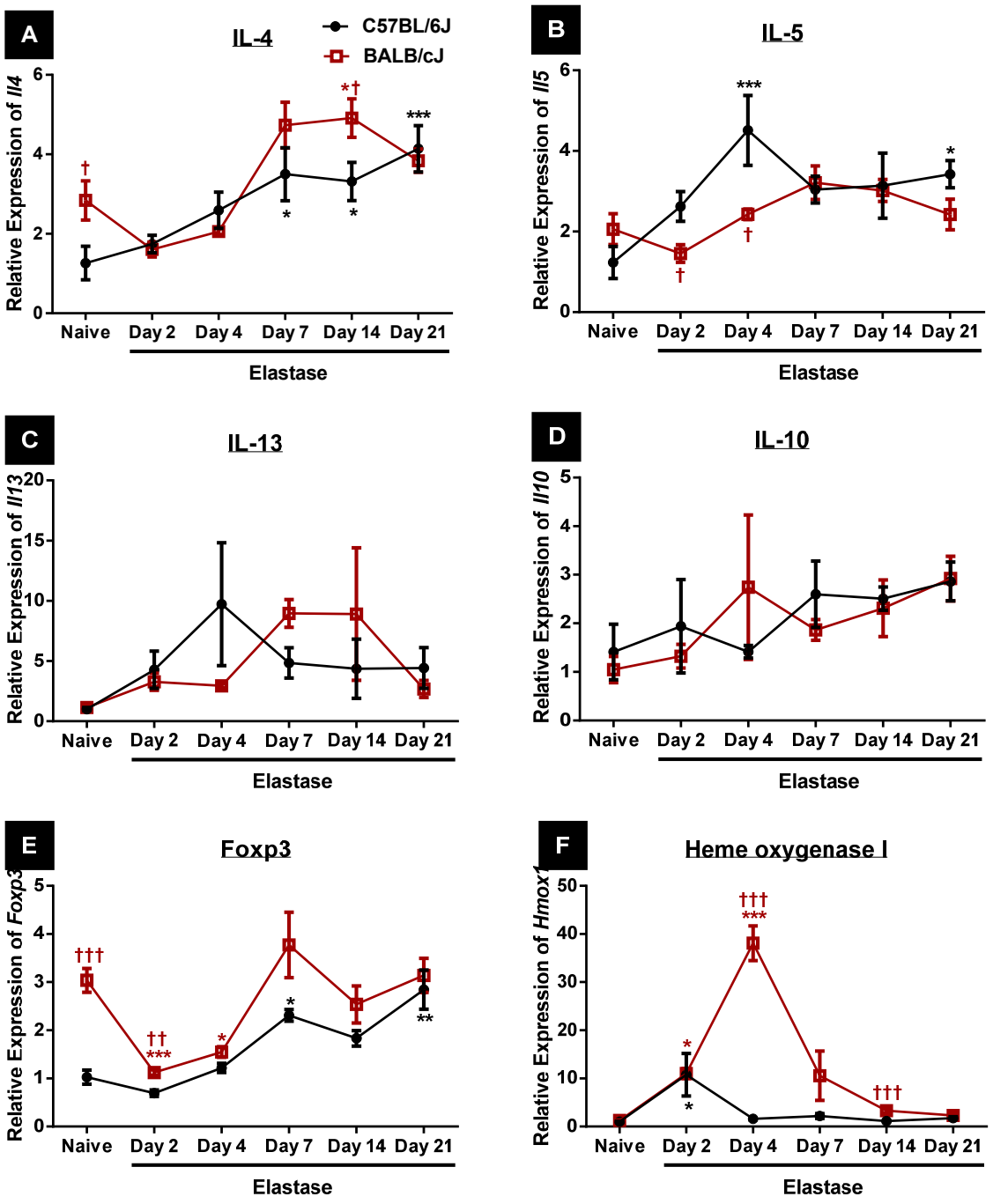

Figure 3.15 Th2- and Treg-associated gene expression profiles in the lungs obtained from 3U elastase-treated C57BL/6J and BALB/cJ mice. Real-time PCR analysis of lung mRNA levels of (A) IL-4, (B) IL-5, (C) IL-13, (D) IL-10, (E) Foxp3, and (F) Heme oxygenase I in C57BL/6J and BALB/cJ mice at days 2, 4, 7, 14, and 21 after challenge with 3U elastase. (n = 4 mice per group). All data are compared with naïve C57BL/6J group and normalized to β-actin expression. Two-way ANOVA analysis: * = $p < 0.05$, ** = $p < 0.01$, *** = $p < 0.001$ comparing elastase-treated group to naïve animals. † = $p < 0.05$, †† = $p < 0.01$, ††† = $p < 0.001$ comparing BALB/cJ with C57BL/6J at the same time point.

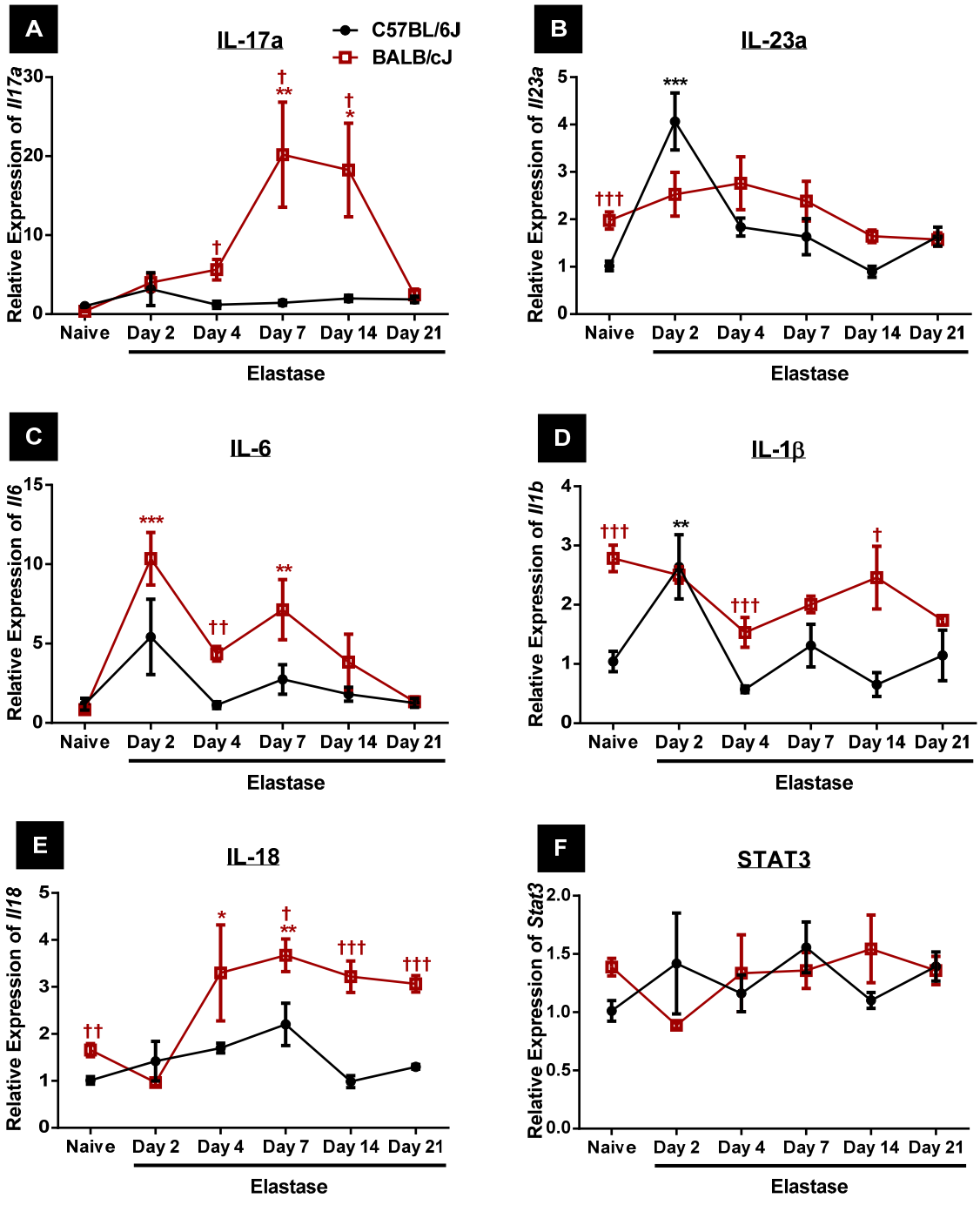

Figure 3.16 Th17-associated gene expression profiles in the lungs obtained from 3U elastase-treated C57BL/6J and BALB/cJ mice. Real-time PCR analysis of lung mRNA levels of (A) IL-17a, (B) IL-23a, (C) IL-6, (D) IL-1β, (E) IL-18, and (F) STAT3 of C57BL/6J and BALB/cJ mice at days 2, 4, 7, 14 and 21 after challenge with 3U elastase. (n = 4 mice per group). All data are compared with naïve C57BL/6J mice and normalized to β-actin expression. Two-way ANOVA analysis: * = $p < 0.05$, ** = $p < 0.01$, *** = $p < 0.001$ comparing elastase-treated group to naïve animals. † = $p < 0.05$, †† = $p < 0.01$, ††† = $p < 0.001$ comparing BALB/cJ with C57BL/6J at the same time point.

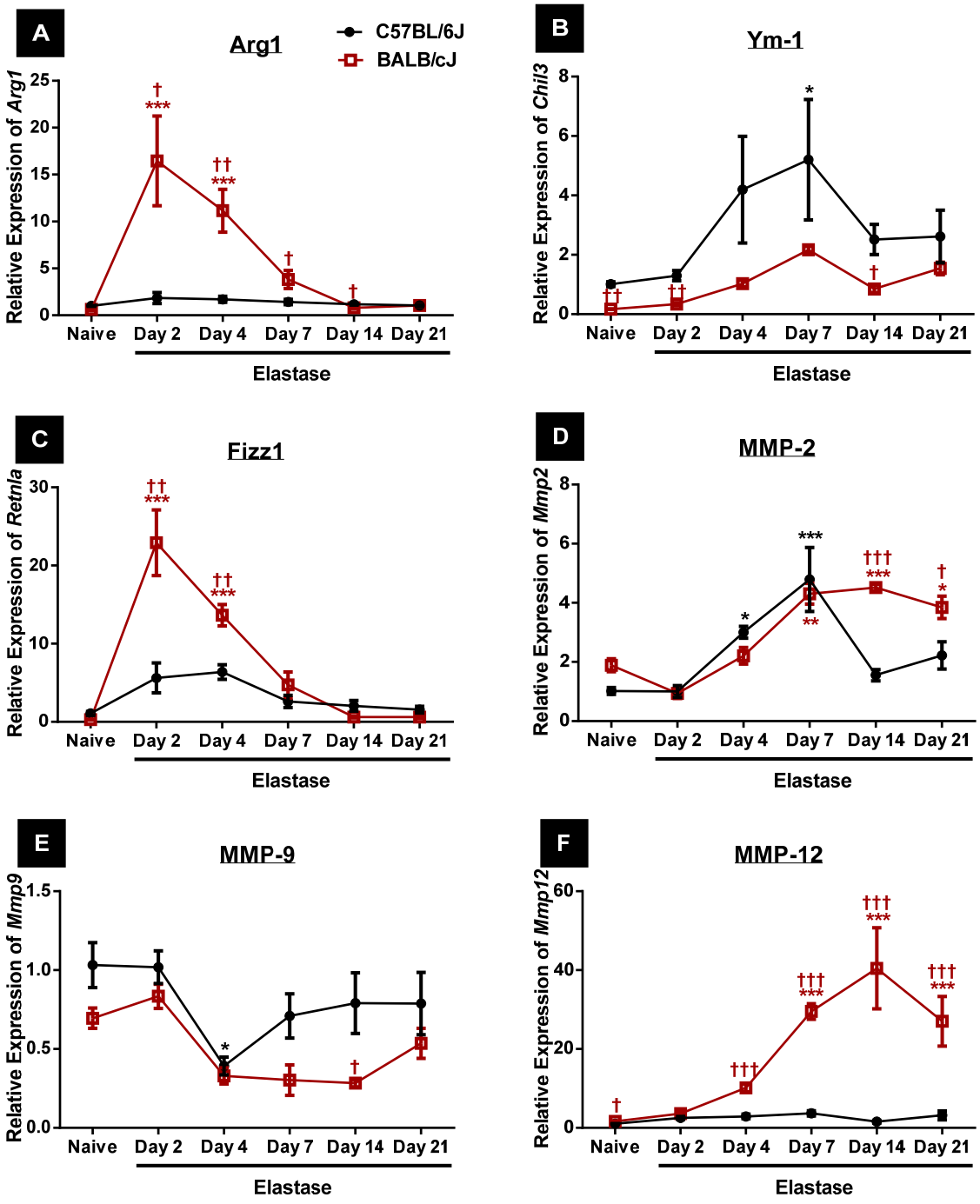

Figure 3.17 M2 macrophage-associated gene expression profiles in the lungs obtained from 3U elastase-treated C57BL/6J and BALB/cJ mice. Real-time PCR analysis of lung mRNA levels of (A) Arginase1, (B) Ym1, (C) Fizz1, (D) MMP-2, (E) MMP-9, and (F) MMP-12 in C57BL/6J and BALB/cJ mice at days 2, 4, 7, 14 and 21 after challenge with 3U elastase. (n = 4 mice per group). All data are compared with naïve C57BL/6J group and normalized to β-actin expression. Two-way ANOVA analysis: * = $p < 0.05$, ** = $p < 0.01$, *** = $p < 0.001$ comparing elastase-treated group to naïve animals. † = $p < 0.05$, †† = $p < 0.01$, ††† = $p < 0.001$ comparing BALB/cJ with C57BL/6J at the same time point.

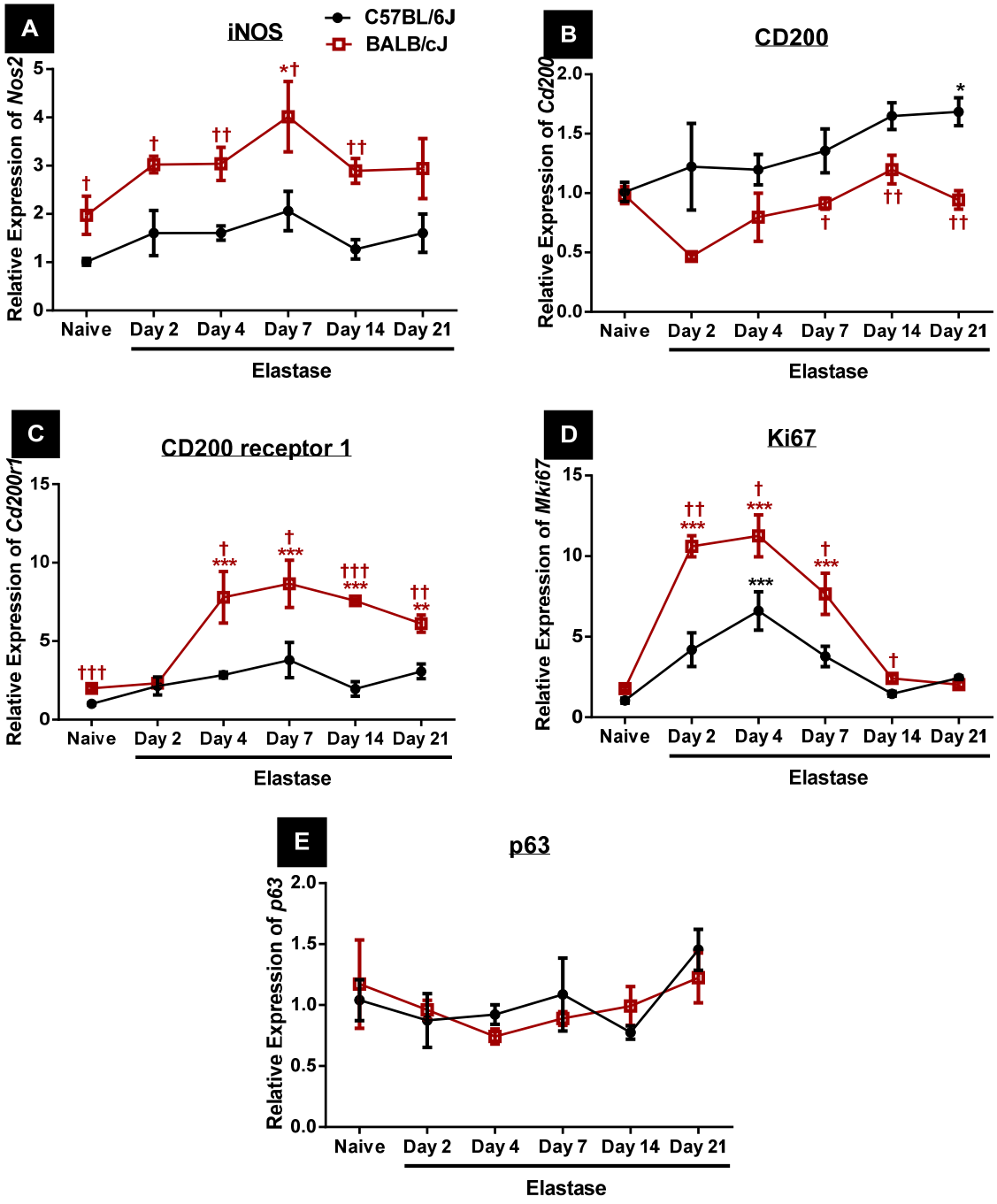

Figure 3.18 M1 macrophage and stem cell proliferation-associated gene expression profiles in the lungs obtained from 3U elastase-treated C57BL/6J and BALB/cJ mice. Real-time PCR analysis of lung mRNA levels of (A) iNOS, (B) CD200, (C) CD200r1, (D) Ki67 and (E) p63 in C57BL/6J and BALB/cJ mice at days 2, 4, 7, 14 and 21 after challenge with 3U elastase. (n = 4 mice per group). All data are compared with naïve C57BL/6J group and normalized to β-actin expression. Two-way ANOVA analysis: * = $p < 0.05$, ** = $p < 0.01$, *** = $p < 0.001$ comparing elastase-treated group to naïve animals. † = $p < 0.05$, †† = $p < 0.01$, ††† = $p < 0.001$ comparing BALB/cJ with C57BL/6J at the same time point.

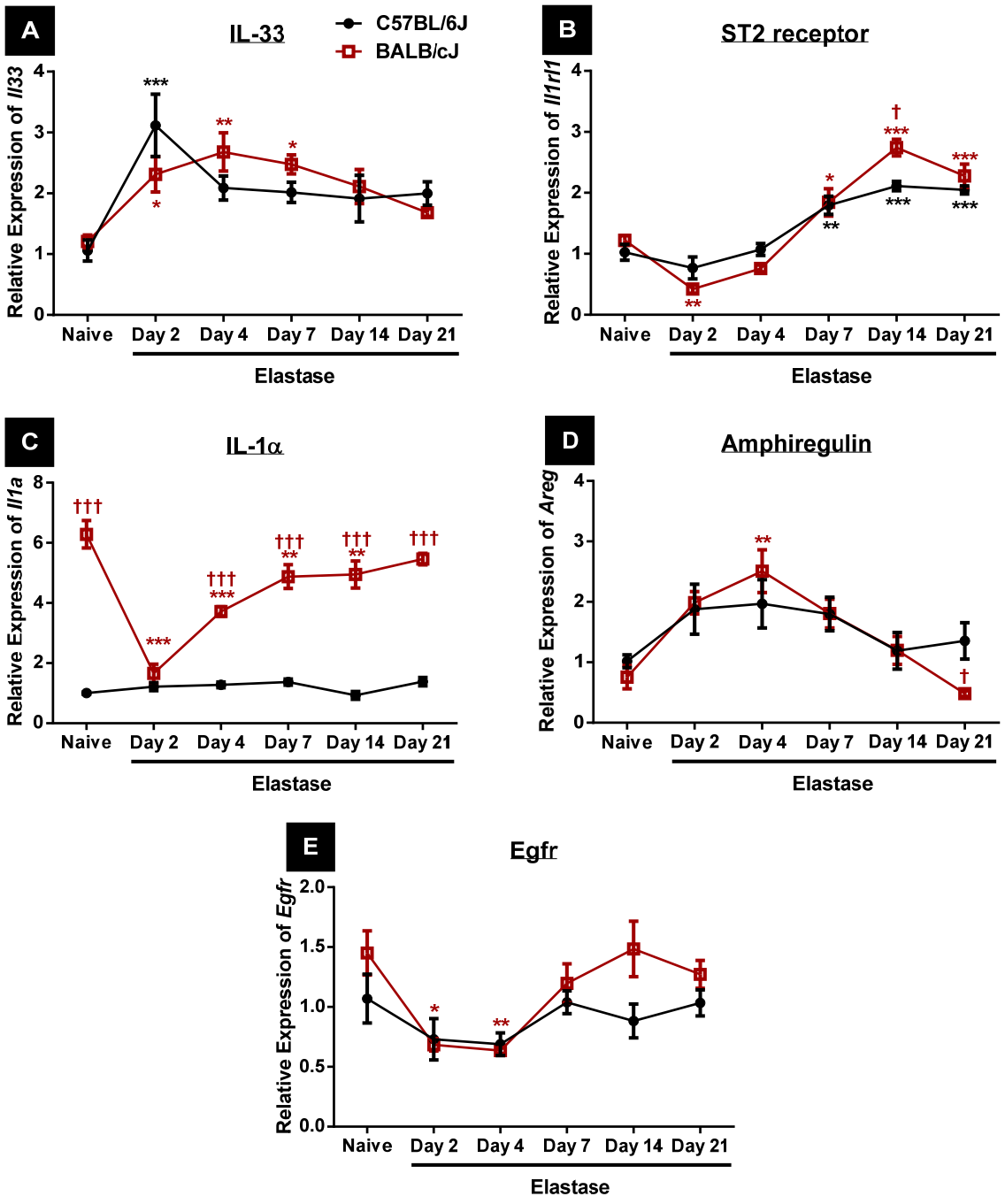

Figure 3.19 Alarmin-associated gene expression profiles in the lungs obtained from 3U elastase-treated C57BL/6J and BALB/cJ mice. Real-time PCR analysis of lung mRNA levels of (A) IL-33, (B) ST2, (C) IL-1α, (D) Amphiregulin, and (E) Epidermal growth factor receptor in C57BL/6J and BALB/cJ mice at days 2, 4, 7, 14 and 21 after challenge with 3U elastase. (n = 4 mice per group). All data are compared with naïve C57BL/6J mice and normalized to β-actin expression. Two-way ANOVA analysis: * = $p < 0.05$, ** = $p < 0.01$, *** = $p < 0.001$ comparing elastase-treated group to naïve animals. † = $p < 0.05$, †† = $p < 0.01$, ††† = $p < 0.001$ comparing BALB/cJ with C57BL/6J at the same time point.

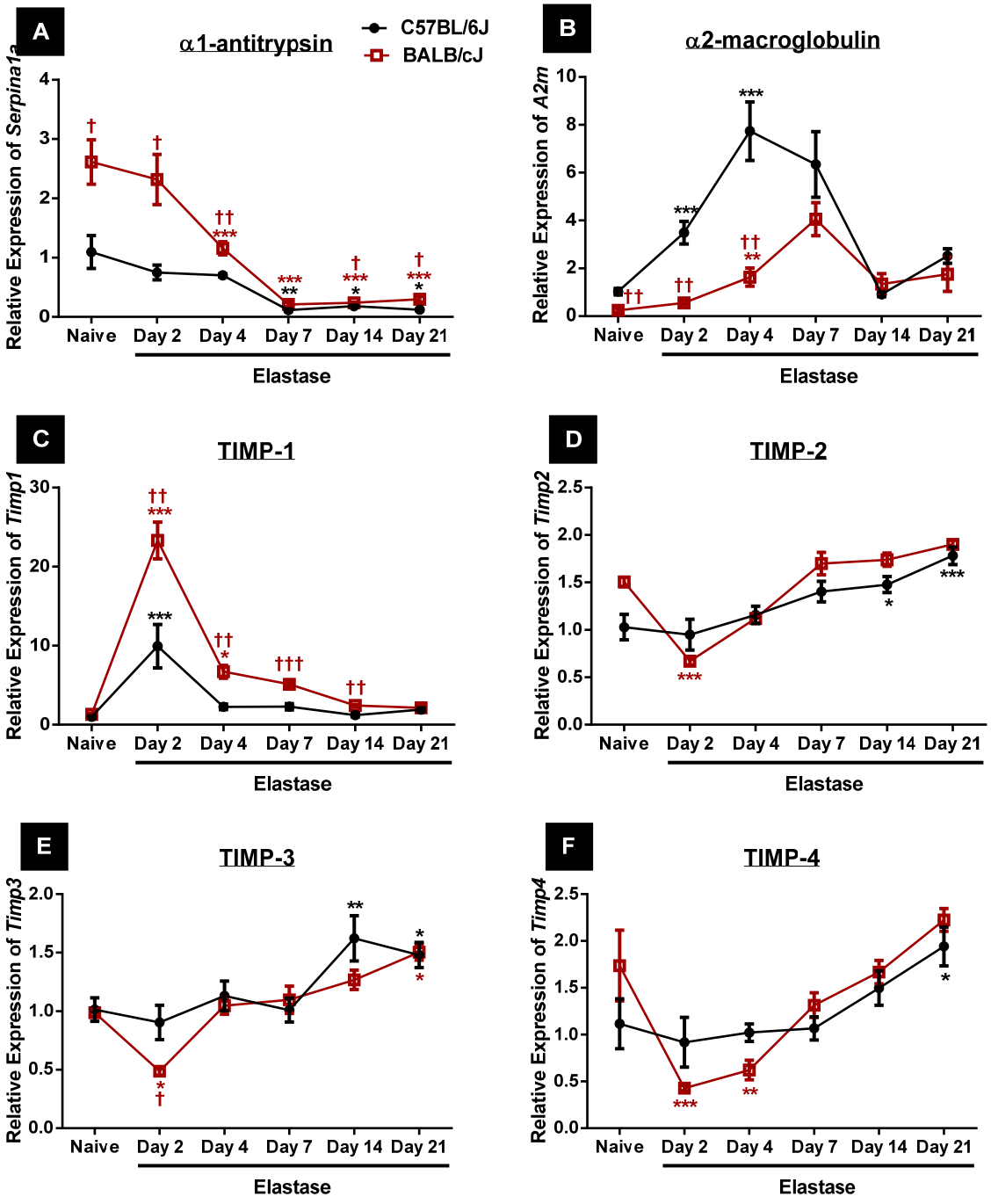

Figure 3.20 Anti-protease gene expression profiles in the lungs obtained from 3U elastase-treated C57BL/6J and BALB/cJ mice. Real-time PCR analysis of lung mRNA levels of (A) α1-antitrypsin, (B) α2-macroglobulin, (C) TIMP1, (D) TIMP2, (E) TIMP3, and (F) TIMP4 in C57BL/6J and BALB/cJ mice at days 2, 4, 7, 14 and 21 after challenge with 3U elastase. (n = 4 mice per group). All data are compared with naïve C57BL/6J mice and normalized to β-actin expression. Two-way ANOVA analysis: * = $p < 0.05$, ** = $p < 0.01$, *** = $p < 0.001$ comparing elastase-treated groups to naïve animals. † = $p < 0.05$, †† = $p < 0.01$, ††† = $p < 0.001$ comparing BALB/cJ with C57BL/6J at the same time point.

CHAPTER 4

Determining immune-mediated mechanisms contributing to the susceptibility and the progression of elastase-induced emphysema

4.1 Abstract

Prominent inflammatory infiltrates in the alveolar space are often recognized as one of the major features during development of emphysema in both human patients and experimental animals. This involves the recruitment and activation of several types of inflammatory cells, particularly neutrophils, lymphocytes and macrophages. However, the relationship between the activation status of these cells and the destruction of alveoli and enlargement of airspaces resulting in emphysema are not well understood. In this chapter, we investigated the effects of inhibiting immune cell recruitment and activation on the severity of emphysema induced by elastase. We found that although a marked increase in the number of neutrophils and lymphocytes in the BAL was observed following elastase administration, the absence of these cells did not alter the severity of emphysema progression. These findings do not support the hypothesized potential role of neutrophils and lymphocytes in the pathogenesis of emphysema at least in this elastase experimental model. However, deficiency of IFN-γ or IL-17A mitigated the severity of elastase-induced emphysema. Moreover, the hindrance of alternative activation of macrophages by either abrogate of STAT6, STAT3 or IL-33 signaling pathway diminish the progression of emphysema as well. From these data, we conclude that macrophages which are alternatively activated via these pathways in response to elastase-induced injury as well as IFN-γ and IL-17A contribute to the development of emphysema in this model, whereas neutrophils and lymphocytes do not. Given the persistent presence of these activated macrophages in injured lungs, they might serve as a potential therapeutic target to cease the progression of emphysema.

4.2 Introduction

Persistent pulmonary inflammation is one of the prominent features of chronic obstructive pulmonary disease (COPD). Inflammation has been hypothesized to make a critically important contribution to the pathophysiological process of emphysema, a primary component of COPD. A persistent elevation of certain inflammatory cells together with increased expression of a number of inflammatory mediators including cytokines, chemokines, inflammatory enzymes, and adhesion molecules in BAL, sputum and lung tissue have been shown to associate with the severity of the disease [145, 146, 148, 150, 151]. However, most studies have only established a firm correlation between this immunological phenotype and the severity of disease. Some aspects of this emphysema-associated immune responses can be seen in animal models of emphysema including cigarette smoke inhalation, elastase-induced experimental emphysema, ozone exposure, hookworm (*Nippostrongylus brasiliensis)* infection and various models of gene overexpression and gene deficiency. While these models have provided partial insight into the immunopathologic mechanisms underlying the disease [107, 108, 455], a coherent cellular and molecular mechanism that accounts for the pathogenesis of emphysema is yet to be defined.

Neutrophils or polymorphonuclear cells (PMNs), macrophages and T-lymphocytes are the most common inflammatory cells proposed to be involved in the pathogenesis of emphysema, as they are typically elevated in the lungs of patient with emphysema [456]. Neutrophil infiltration is often an early response following pulmonary injury. Emphysema is one of the most studied diseases that exhibits a marked pulmonary neutrophilia [457]. The rapid influx of circulating neutrophils into the lungs has been demonstrated in most animal models of emphysema as well [107, 155, 458]. Neutrophils are attractive candidates for

contributing to tissue destruction in emphysema because of their capacity to produce a variety of potential effector molecules that can damage tissue, particularly proteases (e.g. neutrophil elastase, cathepsins and several matrix metalloproteinases MMPs) and reactive oxygen species (ROS) [457]. However, neutrophils have been shown to play an important role in wound healing and tissue repair [459, 460]. The phagocytic capacity of neutrophils removes necrotic cells generated during tissue injury to limit further damage and facilitate proper repair [461, 462]. Also, recent studies have shown that neutrophils can also release neutrophil extracellular traps (NETs), extracellular web-like fibril matrices which are able to trap infectious agents and scavenge cellular debris [463]. Thus, the role of neutrophils in the pathogenesis of emphysema remains unclear.

Similar to neutrophils, macrophages are another major effector cell in innate host defense and can release a number of tissue-damaging mediators, predominantly MMPs and collagenase [115]. There is mounting evidence that an increase in the number of macrophages in the BAL fluid, sputum, alveolar space and lung parenchymal tissue in COPD patients, due in part to an increased macrophage proliferation and prolonged macrophage survival [145, 159, 160, 464, 465]. Interestingly, macrophages are also found at the site of alveolar tissue destruction in patients with emphysema [466, 467]. It is likely that the pulmonary immune environment during COPD development drives the differentiation of a heterogeneous population of macrophages that display characteristics of both classically- (M1) and alternatively- (M2) activated cells. This mixed phenotype is represented by the simultaneous elevation of inducible nitric oxide synthase (iNOS) and arginase activity, typical markers of M1 and M2, respectively [468-470]. While M1 macrophages express high levels of pro-inflammatory genes relevant to innate and adaptive cell-mediated immunity, M2

polarization is typically associated with wound-healing, tissue remodeling and immunoregulatory function [420, 425]. Both populations of macrophages might play a role in the development of emphysema, however, a better understanding of the relative contribution of these M1 and M2 macrophages is likely to enhance our understanding of the pathogenesis of progressive stage of emphysema.

Cells of the adaptive immune response are also associated with emphysema. There is an infiltration of multiple subsets of T-lymphocytes into the airways and lung parenchyma of patients with COPD accompanied by their canonical cytokines and chemokines [168, 170, 464, 471]. IFN-γ-producing type 1 T helper (Th1) $CD4^+$ and type 1 cytotoxic (Tc1) $CD8^+$ cells are predominant among all population of lymphocytes [167]. Indeed, studies in experimental animals demonstrated that cigarette smoke-exposed CD8-deficient mice fail to develop emphysema, whereas IFN-γ-overexpressing mice develop spontaneous emphysema at an early age [173, 472]. While cigarette smoking has been shown to induce IFN-γ-producing Th1 or Tc1 responses, it also appears to promote IL-17A-producing Th17 or Tc17 responses in mice [187, 473]. Moreover, a recent study revealed the persistence of elevated IFN-γ in the BAL and an increase in the number of Th17/Tc17 cells in the lung tissue of 24-week cigarette smoke-exposed mice; changes that were maintained even after 12 weeks of smoking cessation [474]. A number of other publications have identified the presence of IL-17A-producing Th17, Tc17 and γδ cells in COPD subjects [181-184, 475]. The IL-17 cytokine can induce other pro-inflammatory cytokines and chemokines from several cell types and in turn recruit neutrophils to the site of inflammation, which might enhance pathologic outcomes associated with neutrophils [476]. Moreover, either IL-17A or

IL-17 receptor deficiency in mice resulted in a mitigated degree of smoke-induced pulmonary inflammation and emphysema. In contrast, lung epithelial cell-specific overexpression of IL-17A in transgenic mice exaggerated the effects of cigarette smoke [186, 187]. Antigen-presenting cells isolated from the lungs of patients with emphysema stimulated T lymphocytes to secrete significant amounts of IFN-γ and IL-17A, but not IL-4, in co-culture experiments [477]. Data presented in Chapter 3 demonstrates that IFN-γ and IL-17A are also elevated in the elastase-induce experimental emphysema model. Overall, these studies reveal the potential role of IFN-γ and IL-17A in emphysema, but the exact function of these cytokines in the mechanism that results in the destruction of alveolar walls has not been fully explored yet.

Here, the goal was to test the role of neutrophils, macrophages as well as the IFN-γ and IL-17A signaling pathways in the elastase-induced experimental emphysema model. In contrast to the cigarette-smoke induced emphysema model, the intratracheal elastase model causes progressive immune-mediated emphysema which allows for a more accurate means to tease out the underlying mechanisms involved in the development of alveolar tissue destruction and airspace enlargement.

4.3 Results

4.3.1 IFN-γ deficiency alters the development of elastase-induced emphysema

Drawing on our data demonstrating that C57BL/6J mice had higher expression of IFN-γ following the elastase injury than BALB/cJ mice (Fig. 3.13 – 3.14), we sought to determine the role of IFN-γ in the pathogenesis of emphysema by utilizing IFN-γ-deficient mice on

both C57BL/6 and BALB/c backgrounds. The elastase-treated IFN-$\gamma^{-/-}$ mice on C57BL/6 background (IFN-$\gamma^{-/-\ B6}$) had improved pulmonary function as shown by a higher diffusion capacity than elastase-treated C57BL/6J WT animals (Fig. 4.1A). Although no statistically significant differences were detected, which might be due to the IFN-$\gamma^{-/-\ B6}$ mice having larger lungs at the baseline, the elastase insult resulted in a less than 10% increase in total lung capacity in IFN-$\gamma^{-/-\ B6}$ mice compared to almost a 50% increase in WT mice (Fig. 4.1B). A slightly smaller increase in residual volume and compliance in IFN-$\gamma^{-/-\ B6}$ mice were also observed (Fig. 4.1C-D). We attempted to confirm these data with IFN-$\gamma^{-/-}$ mice on a BALB/c background (IFN-$\gamma^{-/-\ BALB}$). The absence of IFN-γ in BALB/c mice also protected them from elastase-induced emphysema, as evidenced by significantly lower TLC, RV and compliance values. These results implicate IFN-γ contributing to the development of elastase-induced emphysema.

4.3.2 IL-17A contributes to the severity of elastase-induced emphysema in a neutrophil-independent fashion

As opposed to the IFN-γ up-regulation in C57BL/6J mice, the susceptible BALB/cJ mice had almost a 20-fold higher induction of IL-17A expression in the lung after challenge with elastase (Fig. 3.16A). To evaluate whether IL-17A is involved in dictating the severity of elastase-induced emphysema, BALB/c mice deficient in IL-17A production, were used for this study. Twenty one days after elastase treatment, significantly higher DF_{CO} accompanied by lower TLC, RV and compliance were found in IL-17A$^{-/-\ BALB}$ mice compared to BALB/cJ WT mice, highlighting a reduction of elastase-induce emphysema in the knockout animals (Fig. 4.3). These results were confirmed by histological analysis that demonstrated

significantly less alveolar destruction and airspace enlargement in the lungs from IL-17A$^{-/-}$ ^{BALB} mice compared to the WT controls (Fig. 4.4).

IL-17A has been shown to mediate inflammation by enhancing the recruitment of neutrophils into the inflammatory site [476]. In addition, we found marked migration of circulating neutrophils into the lung after elastase injury (Fig. 3.11). To investigate the role of neutrophils in the elastase-induced experimental emphysema model, an antibody-mediated depletion strategy was employed. Fig 4.5A-B shows that a single intraperitoneal injection of 500 mg of an anti-Ly6G (Clone 1A8) antibody successfully depleted neutrophils within the peripheral blood within 24 hours and that the percentage of circulating neutrophils relative to total leukocytes remained constantly low for at least 6 days following injection. Moreover, 1A8 treatment could also mitigate the infiltration of neutrophils into the lungs following to the elastase insult (Fig. 4.5B). These results indicated that our approach could successfully block neutrophil infiltration within the window of regular neutrophil influx observed after an elastase insult. The number of macrophages and lymphocytes in the BAL were not appreciably changed in response to neutrophil depletion by 1A8 treatment (data not shown). However, neutrophil depletion failed to influence the severity of elastase-induced pulmonary emphysema, as no significant alterations to DF_{CO}, TLC, RV, compliance or a quantitative histological assessment of airspace enlargement were observed in 1A8-treated BALB/cJ mice 21 days after elastase challenge (Fig. 4.6 – 4.7).

4.3.3 T and B cells do not significantly alter the severity of elastase-induced emphysema

We next sought to explore the importance of adaptive immune cells, particularly T and B cells, in the progression of elastase-induced emphysema by utilizing mice lacking functional recombination activation gene-1 (*Rag-1*). The RAG-1 protein mediates immunoglobulin and T cell receptor V(D)J recombination, which is required for B and T lymphocyte development. As such, RAG-1 knockout mice are entirely devoid of T and B cells [478]. We treated RAG-1-deficient mice on both C57BL/6 (RAG-$1^{-/-\,B6}$) and BALB/c (RAG-$1^{-/-\,BALB}$) backgrounds with 3U elastase. RAG-$1^{-/-\,B6}$ mice developed the same degree of emphysema observed in WT animals (Fig. 4.8). While the absence of T and B lymphocytes in RAG-$1^{-/-\,BALB}$ mice can significantly lessened the TLC elevation caused by elastase, no significant changes in DF_{CO}, RV and compliance were observed between WT and the genetically-modified mice (Fig. 4.9). Of note, both RAG-$1^{-/-\,B6}$ and RAG-$1^{-/-\,BALB}$ mice had slightly smaller lungs than the WT control animals as indicated by lower TLC values, an observation that has yet to be described in the literature. Furthermore, assessment of lung histology showed that there was no significant difference in extent of airway damage (Fig. 4.10A) or L_m values (Fig. 4.10B) between the elastase-challenged RAG-$1^{-/-\,BALB}$ mice and their WT controls.

4.3.4 Macrophage activation during the development of elastase-induced emphysema

Owing to the failure to diminish the severity of elastase-induced emphysema in mice lacking either neutrophils or lymphocytes, we hypothesized that macrophages might be the key effector cells causing emphysematous damage in our model. We have previously shown a

correlation between the persistent increase in macrophage number recovered from the BAL, sustained alternative activation of macrophages (M2 phenotype) and the progression of emphysema in the sensitive BALB/cJ strain in Chapter 3. Therefore, we sought to test the hypothesis that blocking the ability of macrophages to develop an M2 activation phenotype diminishes the severity of emphysema. Signaling though the Signal Transducer and Activator of Transcription (STAT) 6 protein has been shown to be essential for the differentiation and proliferation of alternatively-activated macrophages [479], as STAT6-deficient mice have displayed defective M2 expansion in a variety of studies [480, 481]. In this way, we compared the extent of emphysematous changes in the lungs in response to intratracheal elastase administration between $STAT6^{-/-}$ mice and WT BALB/cJ controls. Fig. 4.11 illustrates that the absence of STAT6 significantly diminishes the severity of pulmonary emphysematous changes at 21 days post-elastase administration as assessed by all of the pulmonary function and mechanics measurements. In agreement with these physiological findings, intratracheal elastase caused noticeably fewer emphysematous lesions in histological sections obtained from $STAT6^{-/-}$ mice compared to WT controls by gross inspection (Fig. 4.12A) and quantified by mean linear intercept (Fig. 4.12B).

In addition to STAT6-dependent M2 activation, STAT3 signaling downstream of IL-6 or IL-10 receptor-engagement has been reported to up-regulate the expression of several genes associated with M2-like phenotypes [482, 483]. We first examined whether STAT3 was activated via phosphorylation in response to elastase injury. Immunostained Western blots demonstrated that there was a significant increase in phosphorylation of the tyrosine-705 residue of STAT3, an indication of STAT3 activation, in the lungs during first 4 days after elastase challenge, while there was no change in total STAT3 levels (Fig. 4.13A-B). Since

phosphorylated STAT3 can translocate into the nucleus and bind to STAT3-responsive elements in the promoter regions of its target genes, we next confirmed its activation by extracting the nuclear protein fractions from the lung tissue of mice receiving elastase at different time points and evaluating their ability to bind to oligonucleotides containing the STAT3 consensus binding site. Similar to the patterns observed by the immunostained Western blots, intratracheal elastase administration led to a significant elevation of STAT3 DNA binding activity in the lung from day 1 to day 4 post-elastase treatment (Fig. 4.13C). Due to the fact that whole body STAT3 deletion is embryonic lethal, we assessed the significance of STAT3 activation in our model using conditional knockout mice where the STAT3 gene is specifically ablated in either myeloid cells (Cre-LyZ/Stat3$^{fl/fl}$) or CD4 cells (Cre-CD4/Stat3$^{fl/fl}$) on a C57BL/6 background. These mice were challenged with elastase in comparison to Stat3$^{fl/fl}$ control animals. Only myeloid-specific STAT3-deficient mice, not CD4-specific mice, showed a reduction in elastase-induced lung damage as seen by the lower values for lung function and airspace enlargement (Fig. 4.14 – 4.15).

4.3.5 Blocking the IL-33 signaling pathway can attenuate the progression of elastase-induced emphysema

IL-33 is an innate cytokine that is rapidly released following damage to the mucosal epithelium [484]. It functions via binding to a heterodimeric membrane receptor complex of ST2 and IL-1 receptor accessory protein (IL-1RAcP), which is constitutively expressed or inducible on a variety of cell types including IL-13-secreting type 2 innate lymphoid cells and macrophages [485-487]. As such, IL-33 has been shown to enhance the polarization of macrophages towards the M2 phenotype [488]. We first attempted to identify the cellular source(s) of IL-33 by immunofluorescence staining assay, and we found it to be primarily co-

localized with cells expressing pro-surfactant protein C, suggesting that a major source of IL-33 in our model is alveolar type II cells in the lungs (Fig. 4.16) [489]. Based on its known function and these findings, it was interesting to test if targeted disruption of the IL-33 signaling pathway can modulate the development of elastase-induced lung injury. As shown in Fig. 4.17, higher DF_{CO} was associated with lower TLC, RV, and compliance suggesting significantly abrogated elastase-induced emphysematous damage in $ST2^{-/-}$ mice compared with WT mice. Similarly, quantitative histomorphometric assessment indicated that deletion of the IL-33 receptor significantly inhibited the increase in L_m typically observed for BALB/cJ mice (Fig. 4.18). Furthermore, mice lacking MyD88, an essential adaptor protein downstream of IL-33 receptor engagement and key for the signaling cascade, also developed a lesser degree of elastase-induced emphysema when compared to C57BL/6J WT controls (Fig. 4.19).

4.4 Discussion

Emphysema is well-known to correlate with an increased number of inflammatory cells in the pulmonary system, predominantly neutrophils, macrophages and lymphocytes. Controversy remains whether neutrophil or macrophages are involved in the destruction of alveolar tissue seen in emphysematous lung since both of them can secrete a number of elastolytic enzymes associated with the pathology. Mixed subsets of T lymphocytes are found in human emphysema subjects and can produce different mediators that modulate the function of neutrophils and macrophages. In light of the existing evidence, our goal here was to address the impact of these cells in a model of protease-induced loss of lung tissue.
In an attempt to clarify the impact of neutrophils, we used a 1A8 antibody to systemically deplete neutrophils. This 1A8 antibody is an antibody against Ly6G which is specifically

expressed on neutrophils and has been successfully used to deplete neutrophils from the circulating blood [490]. In our hands, a single dose of intraperitoneal injection of 1A8 antibody was sufficient to significant reduce the number of neutrophils in both the peripheral blood and to limit the recruitment of neutrophils into the lung even in the context of elastase-induced inflammation. We did not see a rebound in neutrophil counts for at least for 6 days after elastase administration, suggesting efficient depletion at least during the period when we typically observe the marked influx of neutrophils during the response to elastase. In our hands, neutrophil depletion did not alter the degree of elastase-induced emphysematous damage in the lung. This result is consistent with the study from Ofulue and Ko showing no effects of neutrophil depletion on cigarette-smoke induced emphysema [156]. However, our data is conflicting with work by Shim *et al.* demonstrating that emphysema induced by elastase could be ameliorated by alleviating neutrophil inflammation [155]. One possibility that might lead to these contrary results is a potential difference in the antibodies used to deplete neutrophils. While our antibody treatment with the 1A8 anti-Ly6G clone selectively depletes neutrophils, and we did not observe any changes in other leukocyte counts, Shim and colleagues' study specified only that they used an anti-Ly6G antibody from BioXCell, which could include the 1A8 Clone we utilized or the RB6-8C5 Clone as both are anti-Ly6G antibodies. However, the RB6-8C5 antibody clone not only recognizes Ly6G but also binds with low affinity to Ly6C, which also results in the depletion of blood-derived inflammatory monocytes [490-492], plasmacytoid dendritic cells (pDCs) [493, 494], and $CD8^+$ T cells [495, 496]. In addition, intranasal elastase markedly increased lung volume, compliance and chord length in their study, and the effects of neutrophil depletion on these parameters of emphysema were minimal (less than 10% reduction of lung volume and chord length). Together, it is reasonable to speculate that the minor protective

effect observed in their study might be a result from non-specific depletion of monocytes or other immune cells.

Historically, based on observations in patients with severe α1-antitrypsin (α1-AT) deficiency, neutrophils were suggested to be a potential candidate for driving the pathogenesis of emphysema [58]. Lacking enough functional α1-AT, these patients exhibited high levels of neutrophil elastase activity which correlated with the extent of their emphysema [497]. Also, mice with low levels of α1-AT (such as pallid mice) display a certain degree of airspace enlargement at 12-months of age and develop smoke-induced emphysema earlier than wild-type mice [84, 85, 453]. However, it is worth noting that α1-AT does not only function to inhibit neutrophil elastase activity, since some studies have shown a suppressive effect of α1-AT on the number of inflammatory cells in the BAL as well as TNF-α and MMP-12 production by alveolar macrophages following cigarette smoke exposure [101, 498]. Moreover, although neutrophils have the ability to secrete a number of enzymes causing elastolytic damage, emphysema was not detectable in other pulmonary diseases such as cystic fibrosis where chronic neutrophil inflammation is even more apparent [72]. Additionally, neutrophils are short-lived and are present only in the first few days after elastase administration, whereas the tissue damage progresses over months. In this regard, we suspect that increased number of recruited neutrophils seen in the lung shortly after elastase challenge is only the consequence of the elastase-induced tissue damage, which compromises the integrity of the alveolar-capillary barrier, increases microvascular permeability, and induces the release of neutrophil chemotactic factors. Nevertheless, we did not see an appreciable role of neutrophils per se in the degradation of alveolar tissue in this

model. This does not necessarily mean that neutrophils have no effect on the development of emphysema in COPD patients, who display chronic inflammation with persistent presence of neutrophils in the lungs. Moreover, neutrophils might have even bigger roles during microbial infection-induced exacerbation in these patients because neutrophils can release several other mediators (e.g. highly reactive oxygen species, proteases, etc.) in order to destroy invading microorganisms. However, these mediators might be deleterious to the host tissue as well.

Next we sought to evaluate the involvement of lymphocytes in the pathogenesis of emphysema. Experimentally, both cigarette smoke and elastase models of emphysema show significant elevation of lymphocyte counts in the lungs [104, 344] (also shown in Chapter 3). However, our data from RAG-$1^{-/-}$ mice showed that lymphocytes are not required for the progression of disease in the elastase-triggered airspace enlargement. This is in agreement with D'hulst and colleagues who showed that severe combined immunodeficiency (*scid*) mice, which also lack functional B and T lymphocytes, developed pulmonary emphysema at comparable levels to WT mice when exposed to cigarette smoke [499]. Our assumption is that the elevation of lymphocytes observed might be in response to foreign antigen derived from the exogenously-administered porcine elastase and/or modified self-antigens derived from damaged host proteins after elastase-induced injury, but in any case these responses do not appear to have a significant impact on progressive alveolar tissue destruction per se. These observations do not support the notion for a causal role for the adaptive immune response in the progression of emphysema as well as the suggestion that chronic emphysema is mechanistically an autoimmune disease [190, 193].

Having been unable to determine a clear role for neutrophils and lymphocytes in our elastase-induced experimental emphysema model, we then hypothesized that macrophages could play a significant role in the progression of this disease. Ofulue and Ko showed that while depletion of neutrophils did not protect the lung from cigarette-smoke induce emphysema in rats, the depletion of macrophages/monocytes clearly did [156]. Moreover, several recent studies strongly support the impact of macrophages in mouse models of smoke-induced emphysema, for example, mice lacking macrophage elastase (MMP12) did not develop emphysema [102]. Together with our data in Chapter 3, macrophages appear to be the only inflammatory cell type in BAL that remains elevated even two weeks after the initial elastase insult, a time frame that corresponds with ongoing tissue destruction and progressive emphysema. This suggests that macrophages, rather than neutrophils, may be the effector cells causing alveolar tissue degradation in this model. However, we have yet to definitively show the effects of macrophage depletion on elastase-induced emphysema, but these studies are currently ongoing. A member of our group, Dr. Daniel Lagassé, attempted to selectively deplete macrophages in the lungs using intratracheal administration of clodronate-loaded liposomes. Although he could successfully deplete about 90% of macrophages in naïve animals, the efficacy of depletion fell to only 40 – 60% when the animals had previously received elastase.

While troubleshooting our approach to macrophage depletion, we instead decided to validate the importance of macrophages in the development of emphysema by focusing on their activation status using knockout mice which possess altered expression of interesting genes relevant to macrophage activation. In terms of activation status and phenotype, macrophages display a high level of plasticity depending on the dictates of their

microenvironment [500]. Classical pro-inflammatory M1 macrophages versus alternative M2 macrophages were originally distinguished from each other based on the Th1/Th2 cytokines mediating their activation *in vitr*o [501, 502]. However, a number of recent studies have illustrated that macrophage polarization in vivo is much more complex [503]. M2 macrophages are of particular interest to the work herein since prior global gene expression analyses of alveolar macrophages isolated from COPD smokers, healthy nonsmokers and healthy smokers revealed the up-regulation of immunomodulatory and repair-associated M2-related genes but a deactivation of M1-related pro-inflammatory genes [469]. For example, the expression of MMP12, which is associated with extracellular matrix remodeling and has been repeatedly linked to emphysema progression in mice, was shown to be favored by M2 activation [504]. Interestingly, helminth parasitic infection, which is also marked by a heavily Th2/M2-skewed immune response, results in the development of progressive emphysema as well [108]. In Chapter 3, we also found an elevation of M2 markers (*Arg1*, *Chil3*, *Retnla* and *Mmp12*) together with *Il4* (a major driver of M2 phenotype) in response to elastase injury. We further investigated the role of alternatively activated macrophages using STAT6-decifient mice, since STAT6 is a transcription factor that responds to IL-4 and IL-13 signaling and is essential to skew towards the M2 phenotype [480, 481, 505]. We found that deficiency in STAT6 decreased the severity of elastase-induced emphysema, a result that is consistent with the spontaneous development of an emphysema-like phenotype accompanied by elevated MMP-12 expression in mice overexpressing IL-13 [178]. This IL-13-mediated pulmonary emphysema could be rescued by eliminating MMP-12 [506].

In addition, ST2 receptor knockout mice and MyD88 knockout mice, genes involved in the IL-33 signaling pathway, that is known to amplify IL-13-dependent M2 activation both *in*

vitro and *in vivo* [488], also exhibited reduced progressive damage of alveolar tissue. As shown in Chapter 3, the expression of IL-33 mRNA was significantly increased during the first week after elastase insult, which was then followed by the concurrent up-regulation of ST2 and MMP12 mRNA on days 7 and 21(Fig. 3.18 – 3.19). We hypothesize that IL-33 is released from injured epithelial cells following elastase injury, becomes subsequently activated by proteases in the inflamed lung, and ultimately binds to ST2 on the surface of macrophages to push them towards the M2 phenotype. Also, type 2 innate lymphoid cells (ILC2), which are resident in the lung and are known to express the ST2 receptor, might respond to IL-33 by releasing IL-13 [507]. The released IL-13 from ILC2 can in turn drive the M2 activation of alveolar macrophages via STAT6 [508]. Of note, Couillin and his group showed that both IL-1R1$^{-/-}$ mice and MyD88$^{-/-}$ mice are protected from elastase-induced emphysema [176]. However, we could only reproduce their results in MyD88$^{-/-}$ mice but not in IL-1R1$^{-/-}$ mice. Furthermore, MyD88 is an adaptor protein shared by a number of Toll-like receptor (TLR) and IL-1 receptor family members including ST2 [509]. Thus, we suspect the protective effect of MyD88$^{-/-}$ might be due to the lack of IL-33 signaling, rather than the loss of IL-1β signaling, as speculated in their study. Overall, given the sustained presence of alternatively activated macrophages in elastase-treated lungs, these cells may in fact perpetuate the degradation of extracellular matrix components and promote chronic emphysema progression.

In addition to STAT6, STAT3 phosphorylation is also predominant in alternatively activation macrophages [505]. Again, we obtained a protective effect in mice which had the STAT3 gene conditionally deleted in myeloid cells. STAT3 is the key transcription regulator of both IL-6 and IL-10. Fernando and colleagues demonstrated that IL-6 can enhance the

expression of several M2 markers (*Arg1*, *Retnla*, *Chil3*) in bone marrow derived macrophages when co-treat with IL-4/IL-13 [483]. This enhancement of M2 phenotype by IL-6 was shown to be STAT3-dependent. Furthermore, IL-6 can stimulate the expression and the release of IL-10 [510]. IL-4/IL-13-induced M2 macrophages treated with IL-6 spontaneously produce significant amount of IL-10 [483]. IL-10 derived from M2 macrophages themselves can also induce STAT3 activation and can drive and perpetuate M2 polarization [482]. Again, we showed in Chapter 3 that there was an up-regulation of IL-4 expression following elastase insult. This increased IL-4 can skew macrophage toward an M2 phenotype, which would be enhanced by IL-6- and IL-10-mediated STAT3 activation. Thus, depletion of STAT3 in macrophages can block the IL-6/IL-10/STAT3 axis and in turn diminish the alternative activation and ultimately abrogate the tissue destruction.

Based on the observation that IFN-γ expression was higher in the less susceptible C57BL/6J strain of mouse, and the fact that IFN-γ is known to skew towards the M1 macrophage phenotype and away from the potentially pathogenic M2 phenotype, we hypothesized that IFN-γ may be a protective molecule in our system. Instead, we found that IFN-γ deficiency resulted in an attenuation of elastase-induced emphysema in both C57BL/6 and BALB/c mice, implicating IFN-γ in the pathogenesis of the disease. Although contrary to our hypothesis, these results are consistent with data from Wang *et al.* who reported that IFN-γ overexpressing transgenic mice displayed spontaneous airspace enlargement and larger lung volume [173]. In addition, Ma *et al.* showed an amelioration of the emphysema-like phenotype induced by cigarette smoke in IFN-γ-null mice [511]. In Fig.3.14, we showed increases in the number of both IFN-γ^+ NK cells and IFN-γ^+ $CD8^+$ cells following elastase

administration. However, since emphysema remained unchanged in the absence of T lymphocytes including $CD8^+$ cells in $RAG1^{-/-}$ mice, NK cells are potentially the critical source of IFN-γ in our model. Interestingly, transgenic overexpression of IFN-γ significantly increased the number of macrophages in the BAL as well as the expression of a number of proteases including MMP-12, MMP-9 and cathepsins, possibly via up-regulation of chemokine receptor CCR5 and its ligands [173, 511]. However, the mechanisms by which IFN-γ modulates the function of macrophages and the release of these elastolytic enzymes particularly during progression of emphysema are not well understood.

Having observed a much greater increase in the expression of IL-17A in the elastase-susceptible BALB/cJ strain (data shown in Chapter 3), we also explored the role of IL-17A by using $IL\text{-}17A^{-/-}$ mice on a BALB/cJ background. The data show that deletion of IL-17A could ameliorate the extent of elastase-induced emphysema. This result resembles a recently published study done with $IL\text{-}17A^{-/-}$ mice on C57BL/6 background by Kurimoto *et al.* [188]. However, it is critical to note that a past study in our laboratory failed to find this protective effect in IL17A-deficient mice on C57BL/6J background following elastase treatment. In both the previous study and our present work, IL-17A was undetectable in the BAL fluid, and the level of IL-17A in lung tissue was not significantly altered from saline controls. This raises some doubt about whether C57BL/6 mice mount a substantial IL17A response to elastase injury. In looking at other animal models of emphysema, protection from emphysema development was also found in cigarette smoke-exposed IL-17A and IL-17 receptor knockout mice, and conversely, overexpression of IL-17A in lung epithelial cells was found to enhance the severity of emphysema from cigarette smoke [186, 187]. However, knockout of IL-17R (C57BL/6 strain) did not mitigate the extent of ozone-induce

emphysema [512]. This contradiction likely reflects different underlying mechanisms in the pathogenesis of emphysema between a complex mixture of substances (cigarette smoke) and a single oxidizing molecule (ozone). With regards to its function, IL-17A is well-known to mediate inflammation by promoting neutrophil chemoattractant chemokines and cytokines [476, 513]. The number of neutrophils was attenuated in the BAL of IL-17A$^{-/-}$ mice exposed to either or cigarette smoke and elastase when compared to that of wild-type animals [187, 188]. Nevertheless, unlike deficiency in IL-17A, the depletion of neutrophils did not significantly impact the extent of emphysema in either cigarette smoke or elastase models. This suggests that IL-17A modulates the development of emphysema in a neutrophil-independent fashion. Shan and colleagues showed that the receptor for IL-17A was expressed on the surface of lung macrophages and treating lung macrophages with recombinant IL-17A induced the expression of macrophage-specific MMP-12 [477]. Interestingly, cigarette smoke-exposed or elastase-treated IL-17A$^{-/-}$ mice did not exhibit a reduced influx of neutrophils, but did have fewer macrophages and lower expression of MMP-12 compared to exposed wild-type mice [187, 188]. Moreover, overexpression of IL-17A in the lung increased the number of macrophages and enhanced the expression of MMP-12 in response to cigarette smoke [187]. Collectively, we suspect that IL-17A modulates the severity of emphysema via the activation of macrophages.

Another important outstanding question is the cellular source of IL-17A during the development of emphysema. Although IL-17A was initially reported to be predominantly expressed in activated CD4^{+} Th17 cells [514], our results in RAG-1$^{-/-}$ mice suggests that these cells are not likely to be the critical source of IL-17A in our model. Furthermore, STAT3 is known to be required for the differentiation of naïve CD4^{+} cells into Th17 cells

[515], and yet mice specifically deleted of STAT3 in CD4 cells developed the same degree of pulmonary emphysema as wild-type animals receiving elastase. All of this evidence suggests cells other than Th17 cells are the important source of IL-17A in our system. Recently, some innate non-lymphoid cells such as monocytes, NK cells, NKT cells and lymphoid tissue inducer (LTi)-like cells have been shown to have the capacity to rapidly produce IL-17A [516], and further investigations into these cells is warranted.

In summary, data from the present study strengthen the critical role of MMP-secreting macrophages, rather than neutrophil and lymphocytes in the pathogenesis of emphysema. The function of these macrophages can be modified by a variety of cytokines, including IFN-γ, IL-17A, and those that signal through STAT6 and STAT3, all of which we have shown can alter the severity of elastase-induced emphysema. Furthering our knowledge towards understanding the mechanisms associated with macrophage polarization in the context of the emphysemic lung might be beneficial for identifying macrophage-targeted diagnostic and therapeutic manipulations of this disease.

4.5 Acknowledgements

The neutrophil depletion experiments in Fig. 4.5 were performed by Dr. Matt Craig and Catherine Bradley of the Johns Hopkins School of Public Health. All histological tissue preparation was assisted by Xin Guo and the quantitative morphometric analyses of lung tissues were done by Alexandra Kearson. We also thank Dr. DeLisa Fairweather for providing the $ST2^{-/-}$ mice, Dr. Noel Rose for providing IL-$17A^{-/-}$ mice and Dr. Cynthia Sears for providing the Cre-LyZ/$Stat3^{fl/fl}$, Cre-CD4/$Stat3^{fl/fl}$ mice. This work was supported by National Heart, Lung, and Blood Institute Grant # P01HL10342.

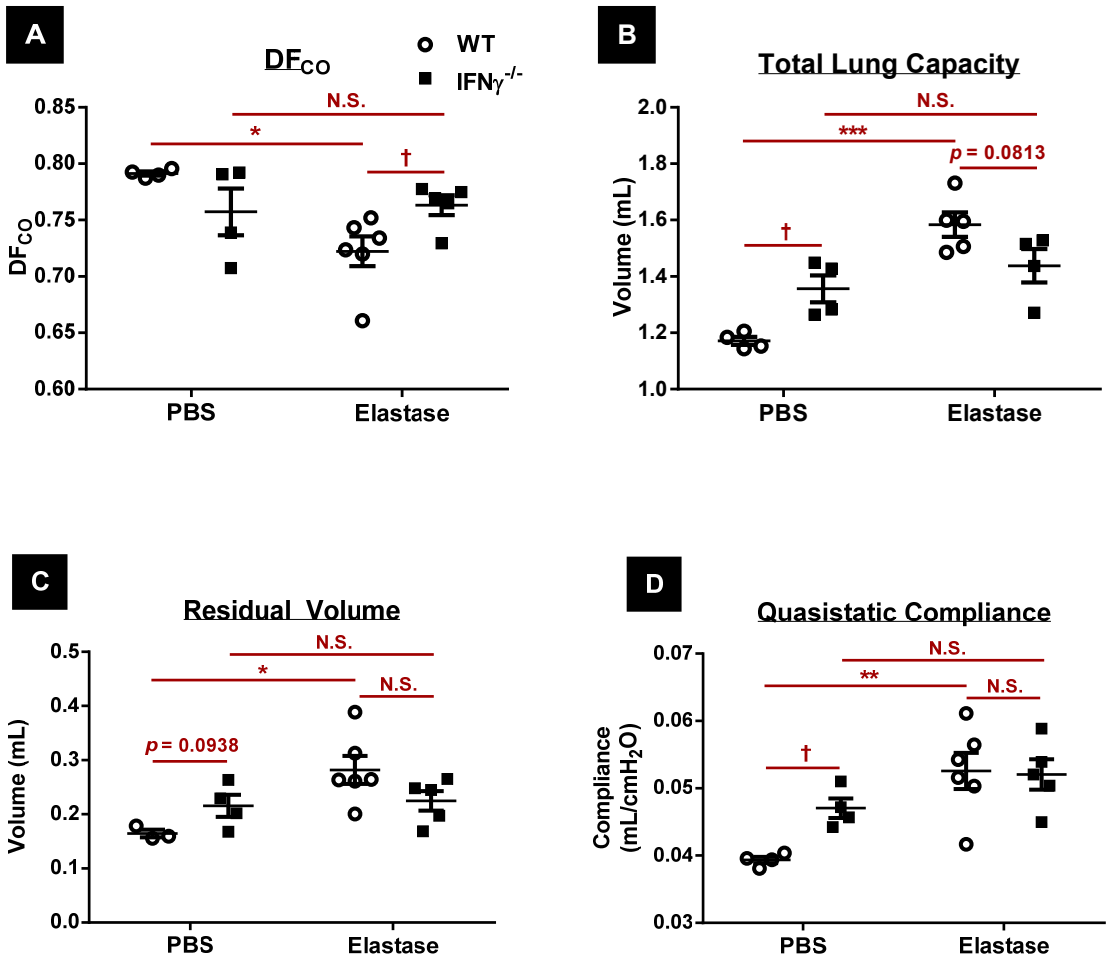

Figure 4.1 Properties of lungs from IFN-γ-deficient (C7BL/6 background) and C57BL/6J mice following 3U elastase. (A) Diffusion capacity (B) Total lung capacity (C) Residual volume and (D) Compliance of respiratory system of IFN-$\gamma^{-/-}$ and wild-type (WT) C57BL/6J mice on Day 21 after intratracheal administration of 3U elastase. (n = 4-6 mice per group). Two-way ANOVA analysis: N.S. = not significant, * = $p < 0.05$, ** = $p < 0.01$, *** = $p < 0.001$ comparing elastase-treated group to PBS-treated animals on the same genotype. † = $p < 0.05$ comparing IFN-$\gamma^{-/-}$ mice with WT mice.

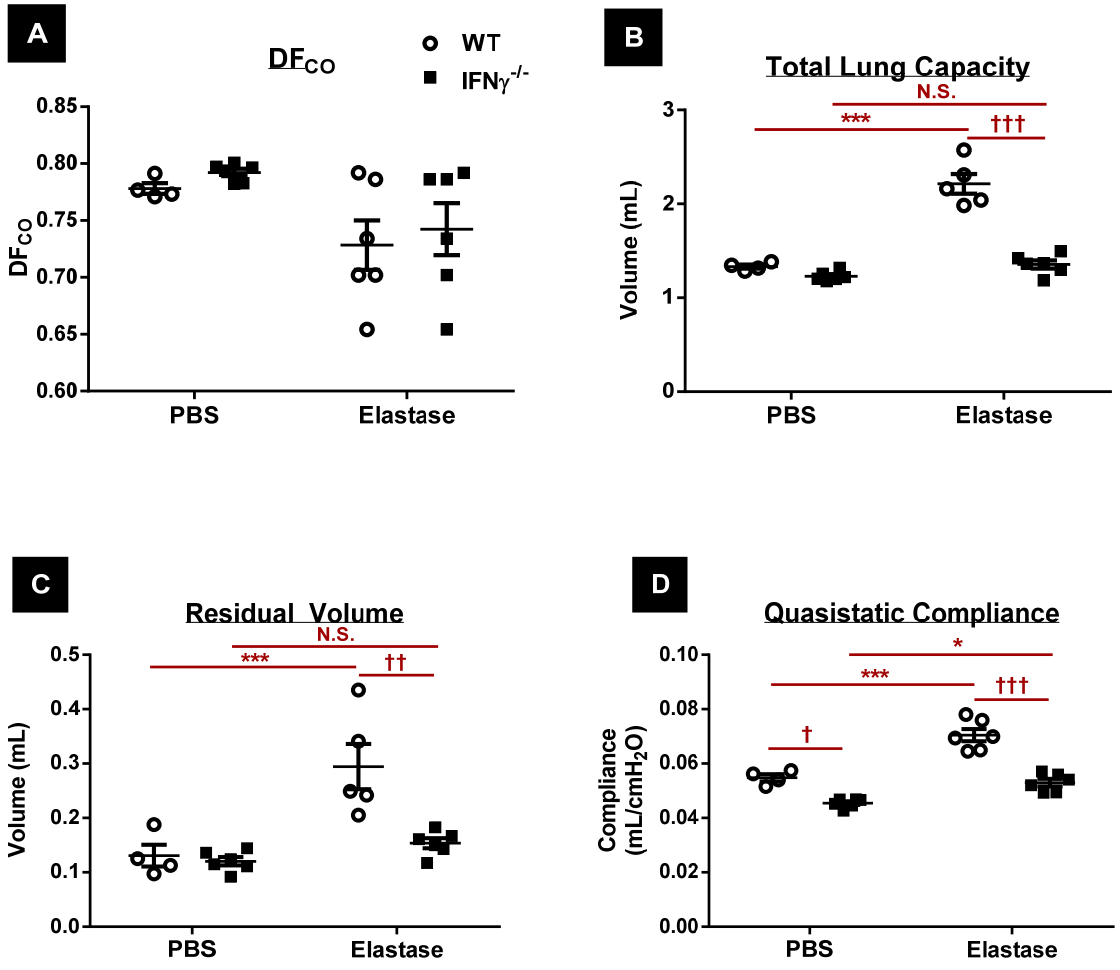

Figure 4.2 Properties of lungs from IFN-γ-deficient (BALB/c background) and BALB/cJ mice following 3U elastase. (A) Diffusion capacity (B) Total lung capacity (C) Residual volume and (D) Compliance of respiratory system of IFN-$\gamma^{-/-}$ and wild-type (WT) BALB/cJ mice on Day 21 after intratracheal administration of 3U elastase. (n = 4-6 mice per group). Two-way ANOVA analysis: N.S. = not significant, * = $p < 0.05$, *** = $p < 0.001$ comparing elastase-treated group to PBS-treated animals on the same genotype. †† = $p < 0.01$, ††† = $p < 0.001$ comparing IFN-$\gamma^{-/-}$ mice with WT mice.

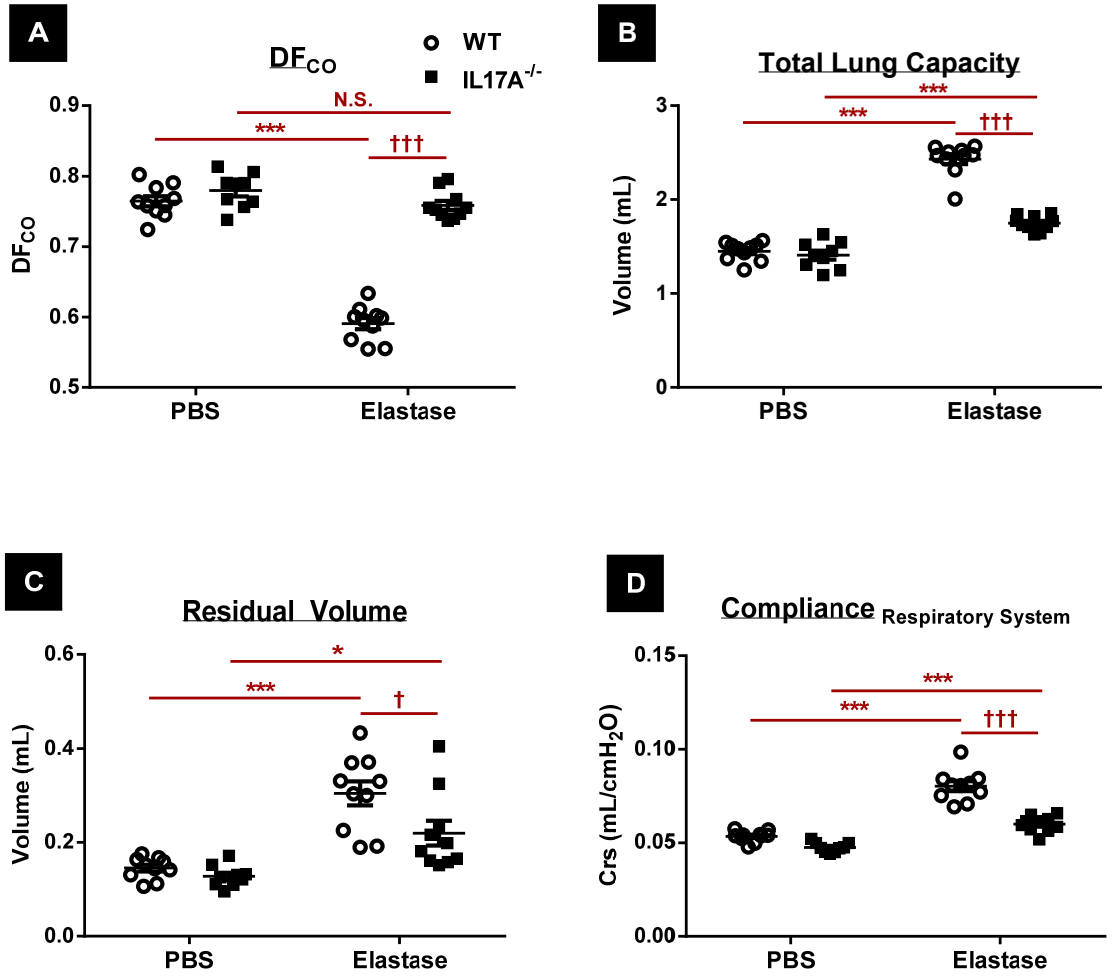

Figure 4.3 Properties of lungs from IL-17A-deficient (BALB/c background) and BALB/cJ mice following 3U elastase. (A) Diffusion capacity (B) Total lung capacity (C) Residual volume and (D) Compliance of respiratory system of IL-17A$^{-/-}$ and wild-type (WT) BALB/cJ mice on Day 21 after intratracheal administration of 3U elastase. (n = 9-10 mice per group). Two-way ANOVA analysis: N.S. = not significant, * = $p < 0.05$, *** = $p < 0.001$ comparing elastase-treated group to PBS-treated animals on the same genotype. † = $p < 0.05$, ††† = $p < 0.001$ comparing IL-17$^{-/-}$ mice with WT mice.

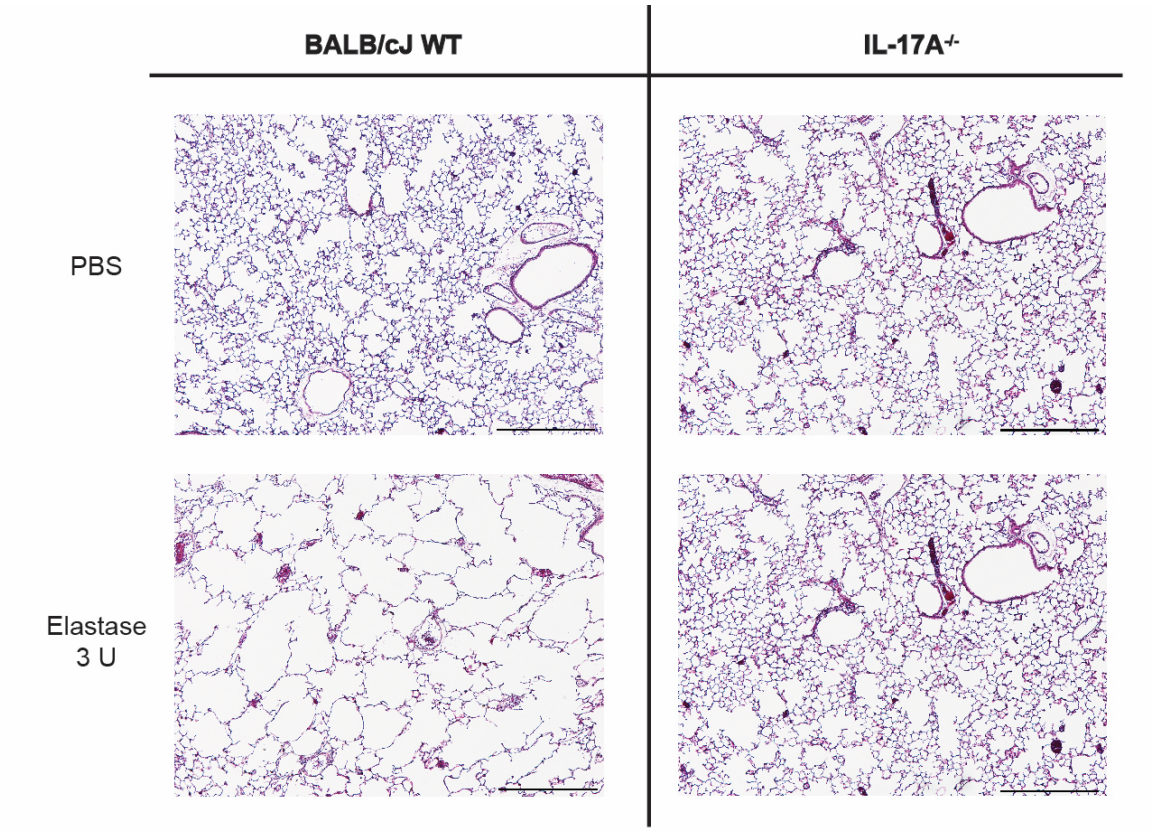

Figure 4.4 Histologic assessment of lungs from IL-17A-deficient and BALB/cJ mice following 3U elastase. Representative H&E-stained lung sections from wild-type (WT) BALB/cJ (*left panel*) and IL-17A$^{-/-}$ (*right panel*) mice on day 21 after 3U elastase or PBS control. Original magnification x40. Scale bar = 500 μm.

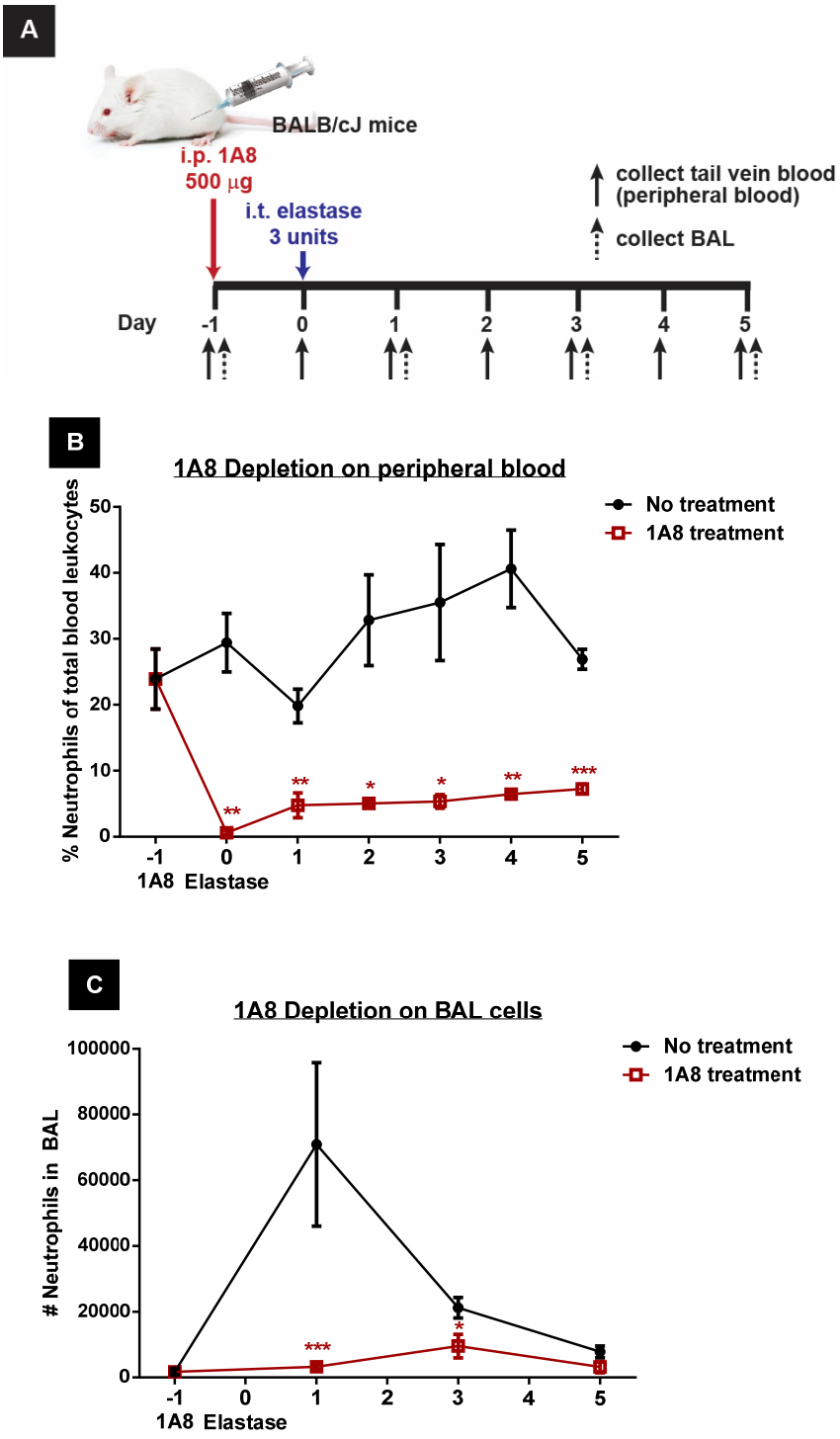

Figure 4.5 Neutrophil depletion with 1A8 antibody in BALB/cJ mice. (A) Schedule of treatment with 1A8 antibody, elastase challenge and tissue harvesting. (B) Percentage of neutrophils in peripheral blood, and (C) number of neutrophils at different time points in BAL fluid after 1A8-mediated systemic neutrophil depletion following 3U elastase. (n = 3 mice/group). Unpaired *t*-test: * = $p < 0.05$, ** = $p < 0.01$, *** = $p < 0.001$ for 1A8 treated group compared to untreated animals.

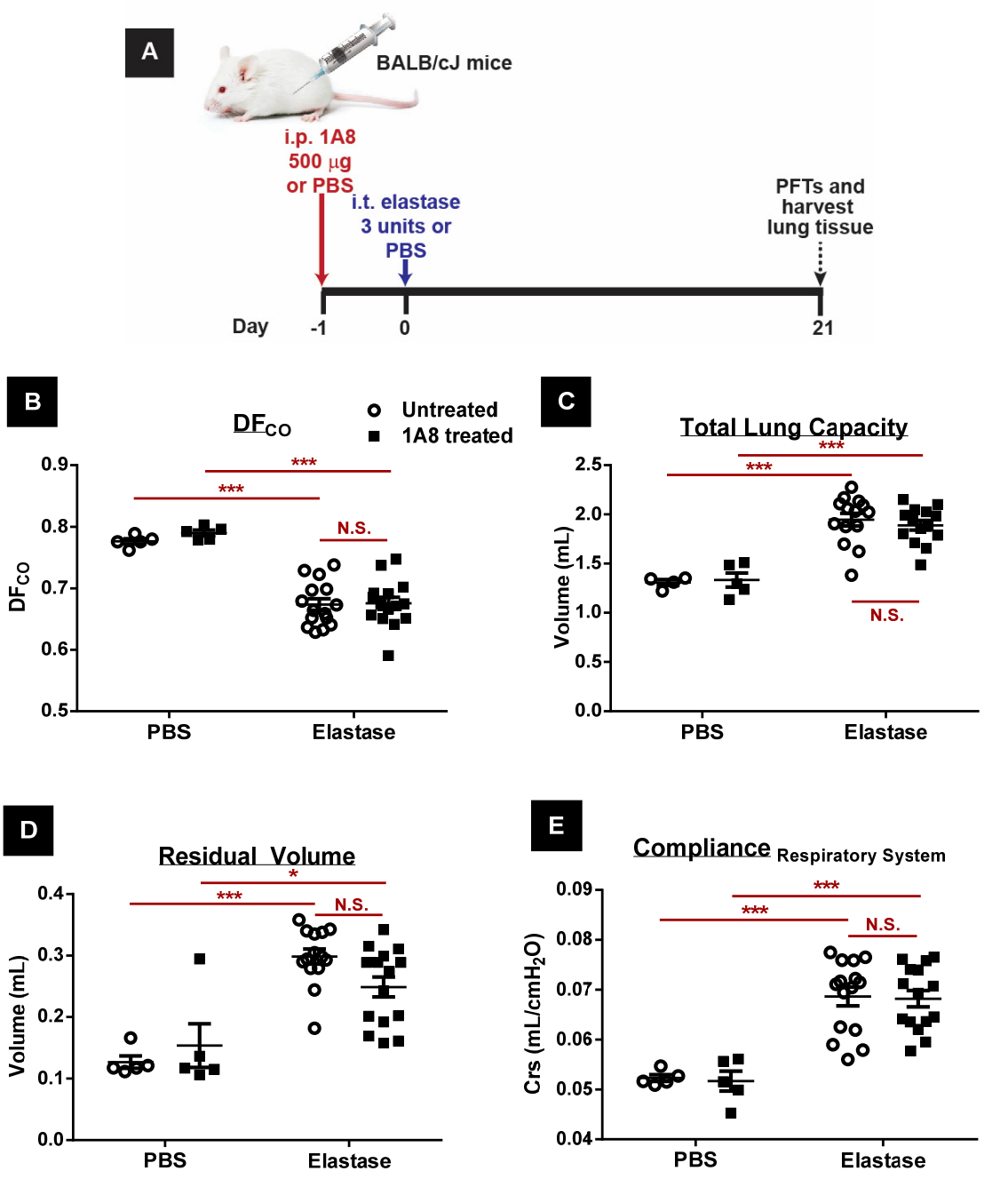

Figure 4.6 Effect of systemic neutrophil depletion on the development of emphysema induced by 3U elastase in BALB/cJ mice. (A) Schedule of treatment with 1A8 antibody, elastase challenge and tissue harvesting. (B) Diffusion capacity. (C) Total lung capacity. (D) Residual volume, and (E) Compliance of respiratory system of BALB/cJ mice treated with 1A8 antibody or untreated one day prior to giving 3U elastase or PBS. All data were collected on day 21 after administration of 3U elastase or PBS. (n = 5 for PBS-treated group, n = 15 for elastase-treated group). Two-way ANOVA analysis: * = $p < 0.05$, *** = $p < 0.001$ comparing elastase-treated group to PBS-treated animals. N.S. = no significant different were found comparing between elastase-treated animals with or without 1A8 injection.

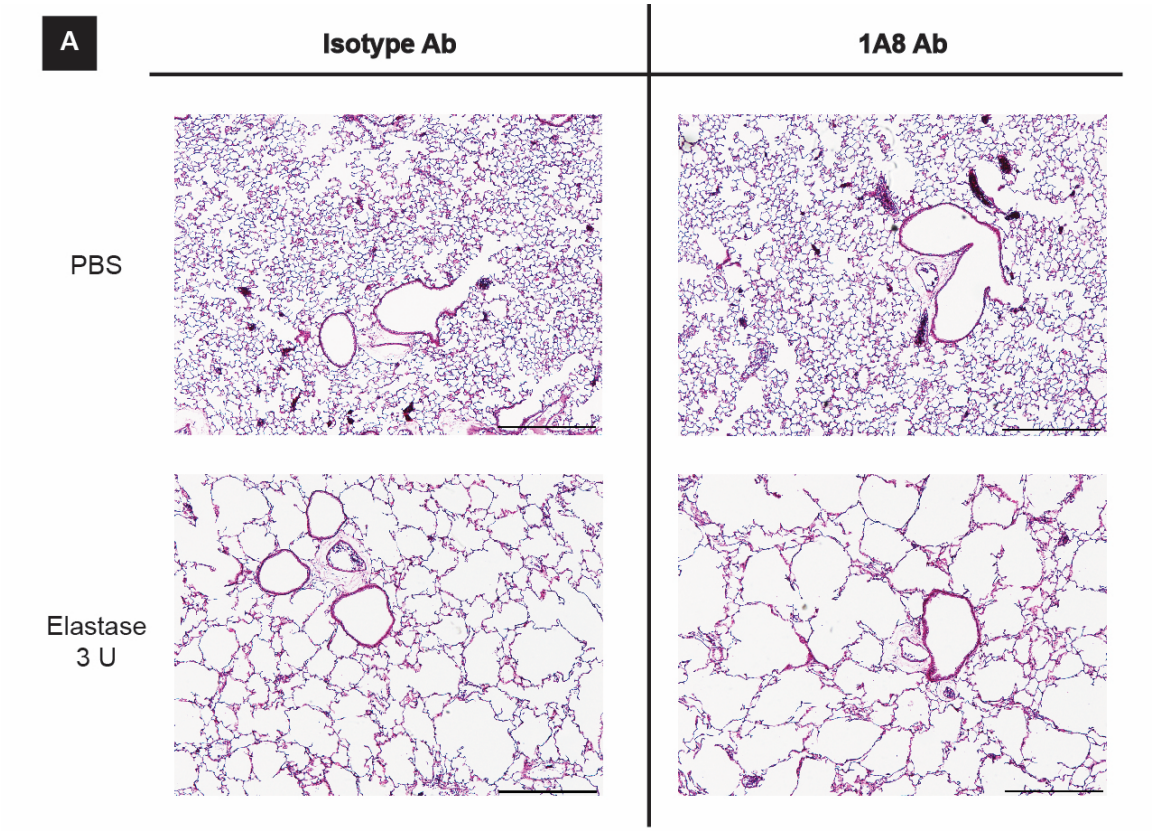

Figure 4.7 Histologic assessment of lungs from either neutrophil-depleted or non-depleted BALB/cJ mice following 3U elastase. (A) Representative H&E-stained lung sections from untreated (*left panel*) and 1A8-treated (*right panel*) BALB/cJ mice on day 21 after 3U elastase or PBS control. Original magnification x40. Scale bar = 500 μm. (B) Mean linear intercept of histological sections from untreated and 1A8-treated BALB/cJ mice. Two-way ANOVA analysis: *** = $p < 0.001$ comparing elastase-treated group to PBS-treated animals. N.S. = no significant different were observed comparing between untreated vs 1A8-treated group.

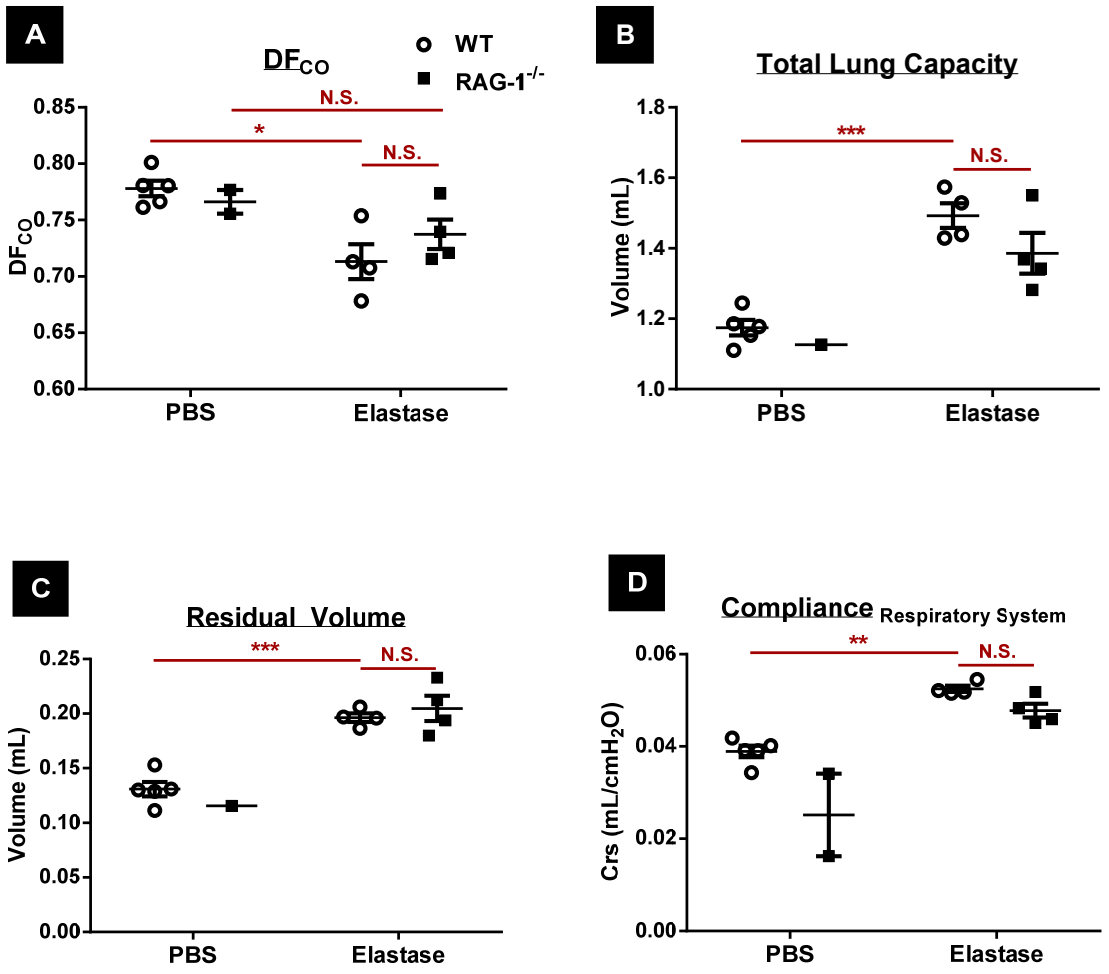

Figure 4.8 Properties of lungs from RAG-1-deficient (C57BL/6 background) and C57BL/6J mice following 3U elastase. (A) Diffusion capacity (B) Total lung capacity (C) Residual volume and (D) Compliance of respiratory system in RAG-$1^{-/-}$ and wild-type (WT) C57BL/6J mice on Day 21 after intratracheal administration of 3U elastase. (n = 2-5 mice per group). Two-way ANOVA analysis: * = $p < 0.05$, ** = $p < 0.01$, *** = $p < 0.001$ comparing elastase-treated group to PBS-treated animals on the same genotype. N.S. = not significant.

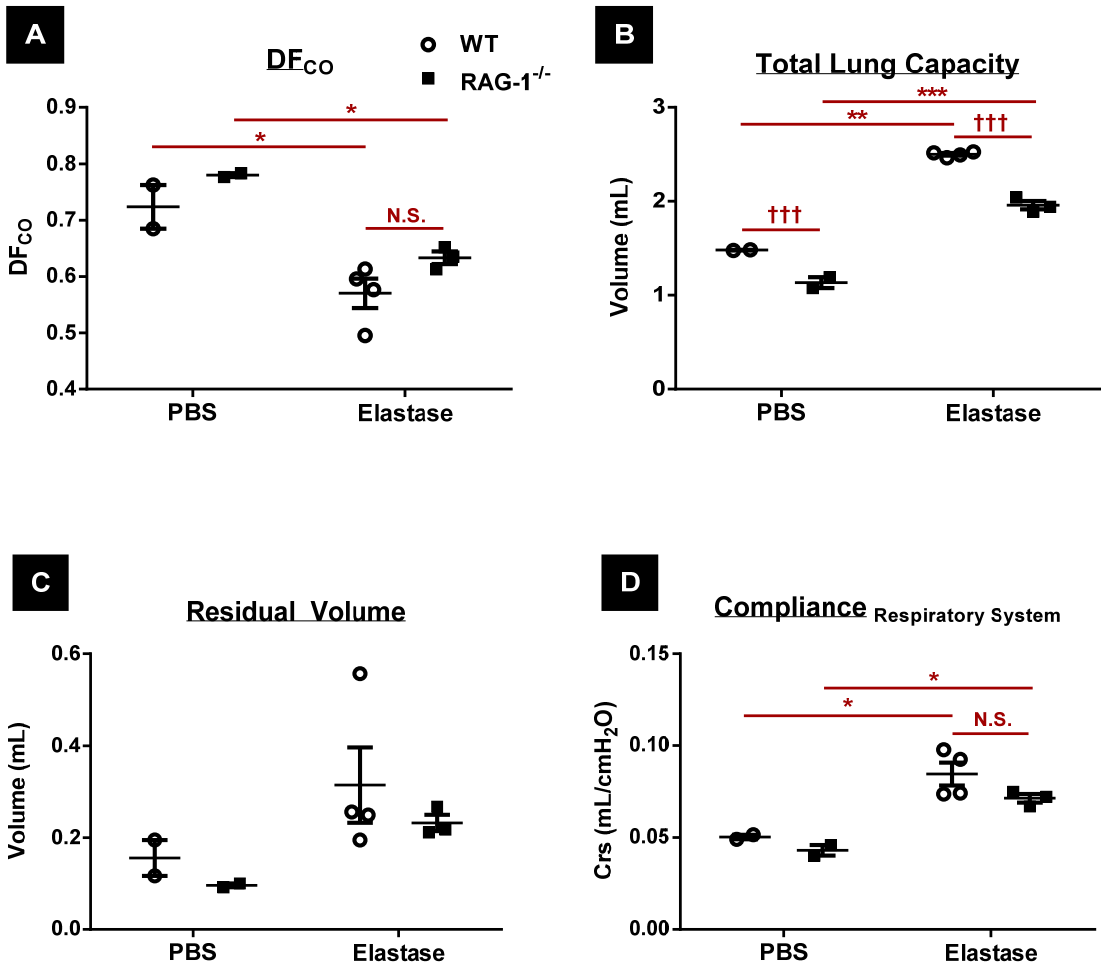

Figure 4.9 Properties of lungs from RAG-1-deficient (BALB/c background) and BALB/cJ mice following 3U elastase. (A) Diffusion capacity (B) Total lung capacity (C) Residual volume and (D) Compliance of respiratory system in RAG-1$^{-/-}$ and wild-type (WT) BALB/cJ mice on Day 21 after intratracheal administration of 3U elastase. (n = 2-4 mice per group). Two-way ANOVA analysis: * = $p < 0.05$, ** = $p < 0.01$, *** = $p < 0.001$ comparing elastase-treated group to PBS-treated animals on the same genotype. ††† = $p < 0.001$ comparing Rag-1$^{-/-}$ mice with WT mice. N.S. = not significant.

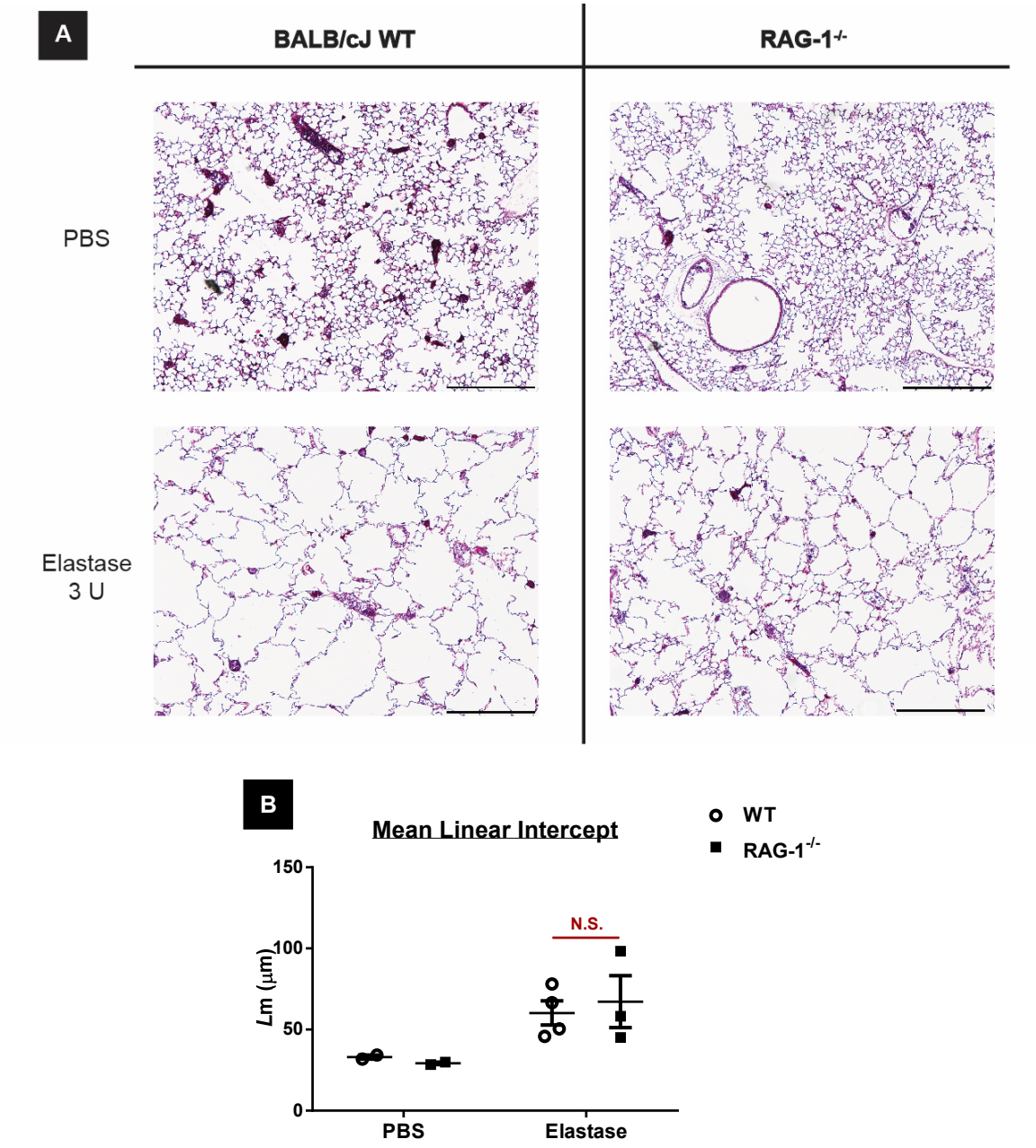

Figure 4.10 Histologic assessment of lungs from RAG-1-deficient and BALB/cJ mice following 3U elastase. (A) Representative H&E-stained lung sections from wild-type (WT) BALB/cJ (*left panel*) and RAG-$1^{-/-}$ (*right panel*) mice on day 21 after 3U elastase or PBS control. Original magnification x40. Scale bar = 500 µm. (B) Mean linear intercept of histological sections from RAG-$1^{-/-}$ and wild-type (WT) BALB/cJ mice. Two-way ANOVA analysis: N.S. = no significant different were observed comparing between elastase-treated RAG-$1^{-/-}$ to elastase-treated WT animals.

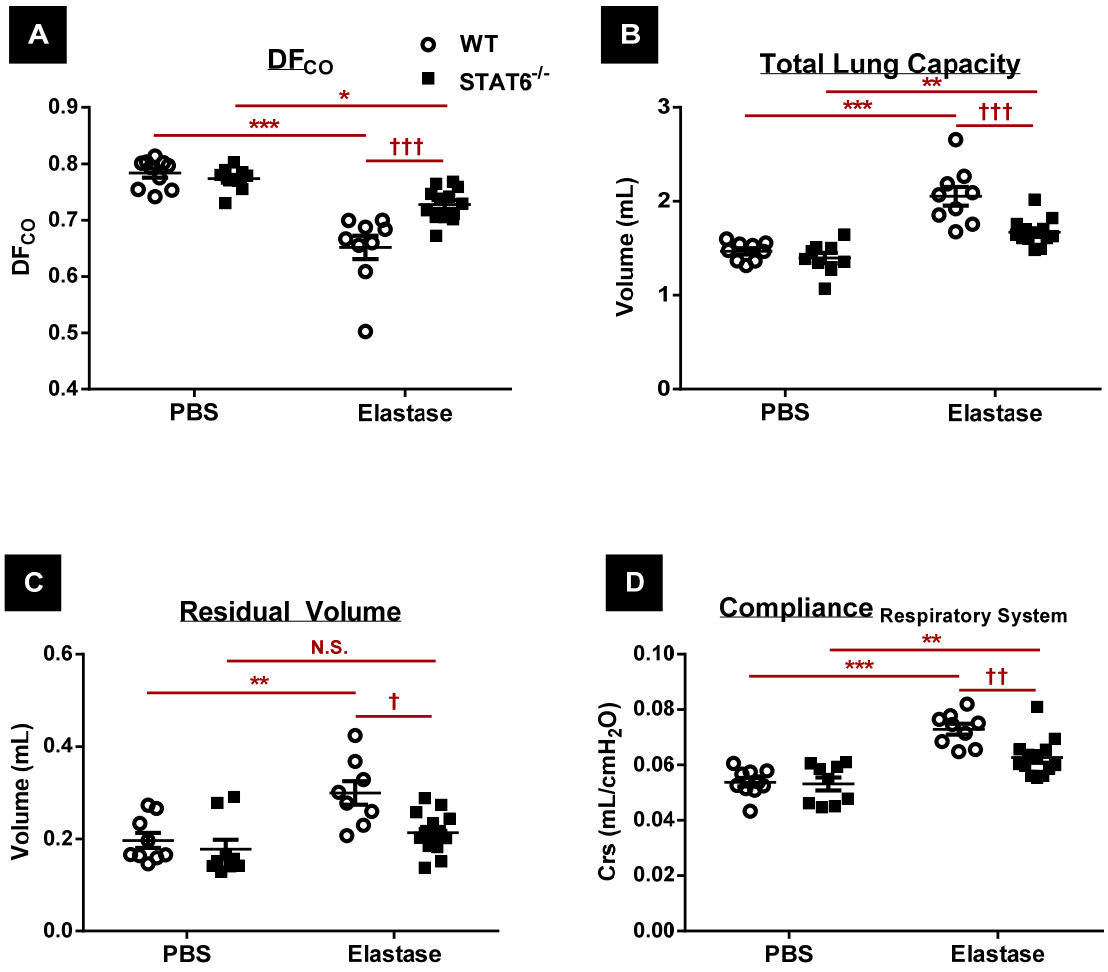

Figure 4.11 Properties of lungs from STAT6-deficient (BALB/c background) and BALB/cJ mice following 3U elastase. (A) Diffusion capacity (B) Total lung capacity (C) Residual volume and (D) Compliance of respiratory system of STAT6$^{-/-}$ and wild-type (WT) BALB/cJ mice on Day 21 after intratracheal administration of 3U elastase. (n = 9-13 mice per group). Two-way ANOVA analysis: * = $p < 0.05$, ** = $p < 0.01$, *** = $p < 0.001$ comparing elastase-treated group to PBS-treated animals on the same genotype. † = $p < 0.05$, †† = $p < 0.01$, ††† = $p < 0.001$ comparing STAT6$^{-/-}$ mice with WT mice.

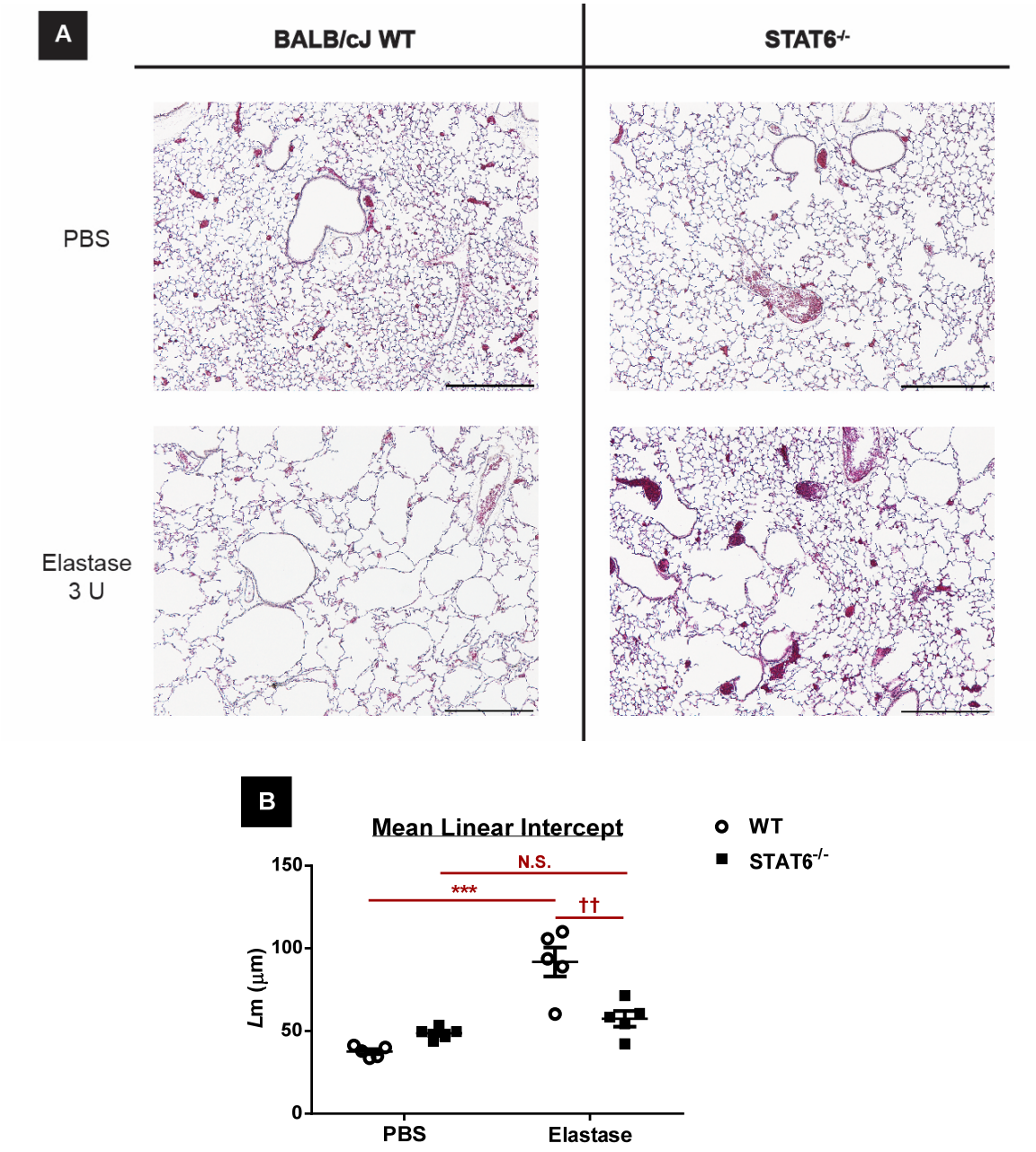

Figure 4.12 Histologic assessment of lungs from STAT6-deficient and BALB/cJ mice following 3U elastase. (A) Representative H&E-stained lung sections from wild-type (WT) BALB/cJ (*left panel*) and STAT6$^{-/-}$ (*right panel*) mice on day 21 after 3U elastase or PBS control. Original magnification x40. Scale bar = 500 µm. (B) Mean linear intercept of histological sections from STAT6$^{-/-}$ and wild-type (WT) BALB/cJ mice. (n = 5 mice per group). Two-way ANOVA analysis: N.S. = not significant, *** = $p < 0.001$ comparing elastase-treated group to PBS-treated animals on the same genotype. †† = $p < 0.01$ comparing STAT6$^{-/-}$ mice with WT mice.

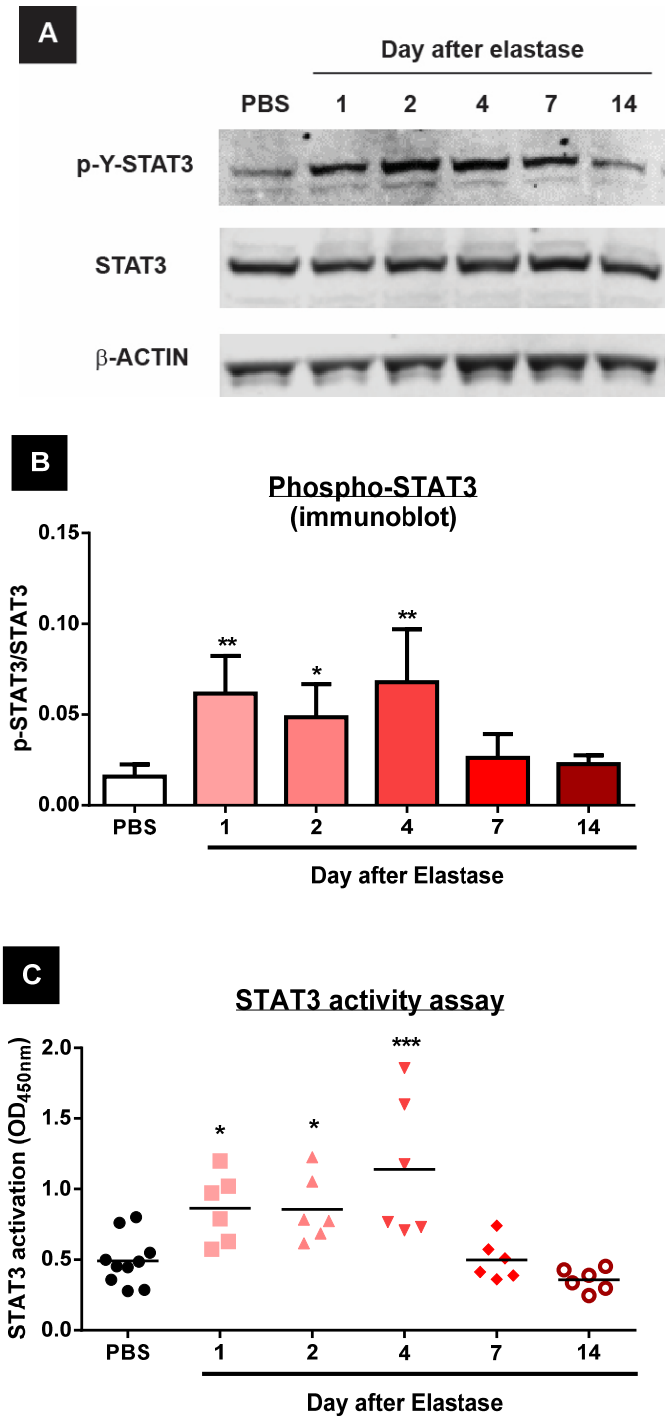

Figure 4.13 Time course of STAT3 activation in lung tissue from C57BL/6J mice following 3U elastase. (A) Representative western blot images for expression level of p-STAT3, STAT3 and β-actin (B) Graph showing the ratio of the relative density of p-STAT3 and STAT3 and (C) Level of STAT3 DNA binding activity in the lungs of C57BL/6J mice at various time points following administration of 3U elastase or PBS control. ($n \geq 6$ mice per group). One-way ANOVA analysis: * = $p < 0.05$, ** = $p < 0.01$*** = $p < 0.001$ comparing elastase-treated group to PBS-treated animals.

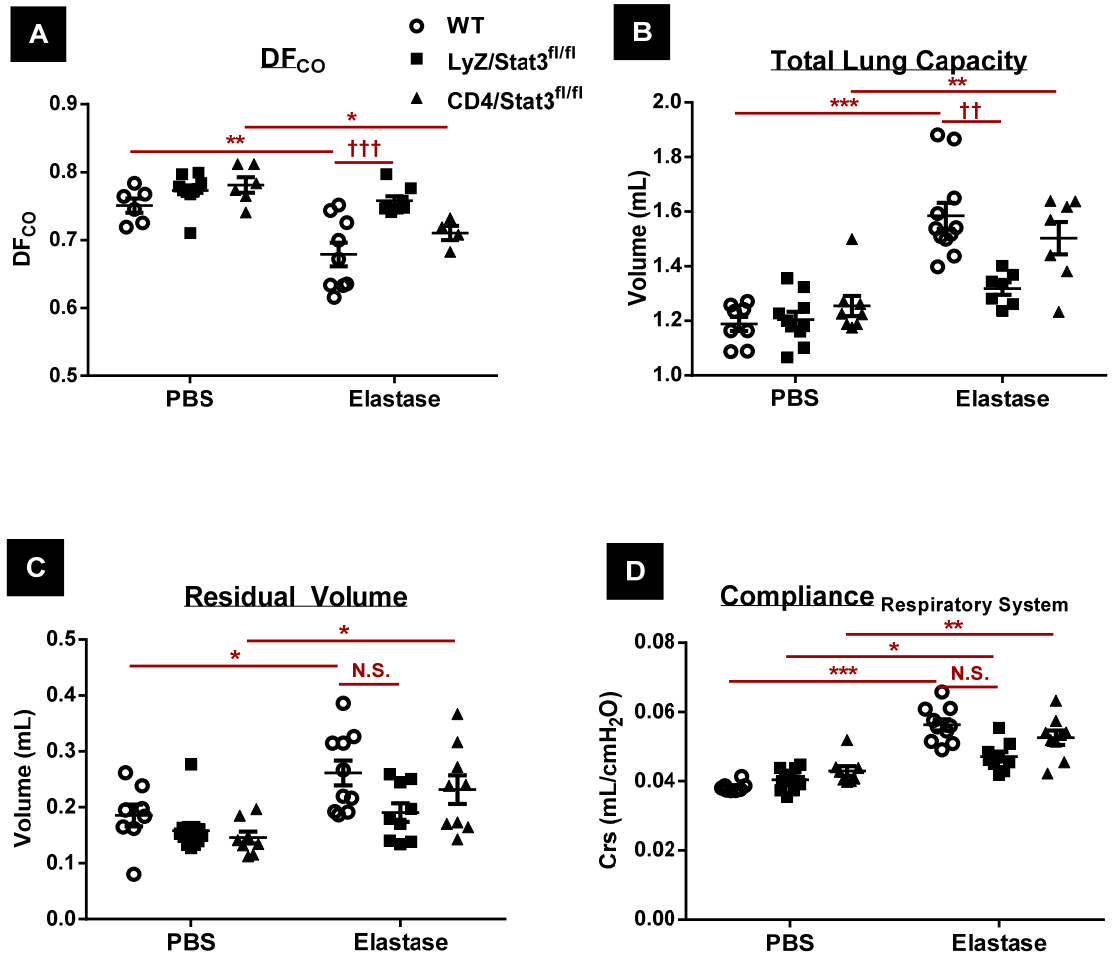

Figure 4.14 Properties of lungs from STAT3-deficient in either myeloid or CD4 cells mice and C57BL/6J mice following 3U elastase. (A) Diffusion capacity (B) Total lung capacity (C) Residual volume and (D) Compliance of respiratory system of Cre-LyZ/Stat3$^{fl/fl}$, Cre-CD4/Stat3$^{fl/fl}$ and wild-type (WT) C57BL/6J mice on Day 21 after intratracheal administration of 3U elastase. (n = 4-10 mice per group). Two-way ANOVA analysis: * = $p < 0.05$, ** = $p < 0.01$, *** = $p < 0.001$ comparing elastase-treated group to PBS-treated animals on the same genotype. †† = $p < 0.01$, ††† = $p < 0.001$ comparing STAT3-defeicient mice with WT mice.

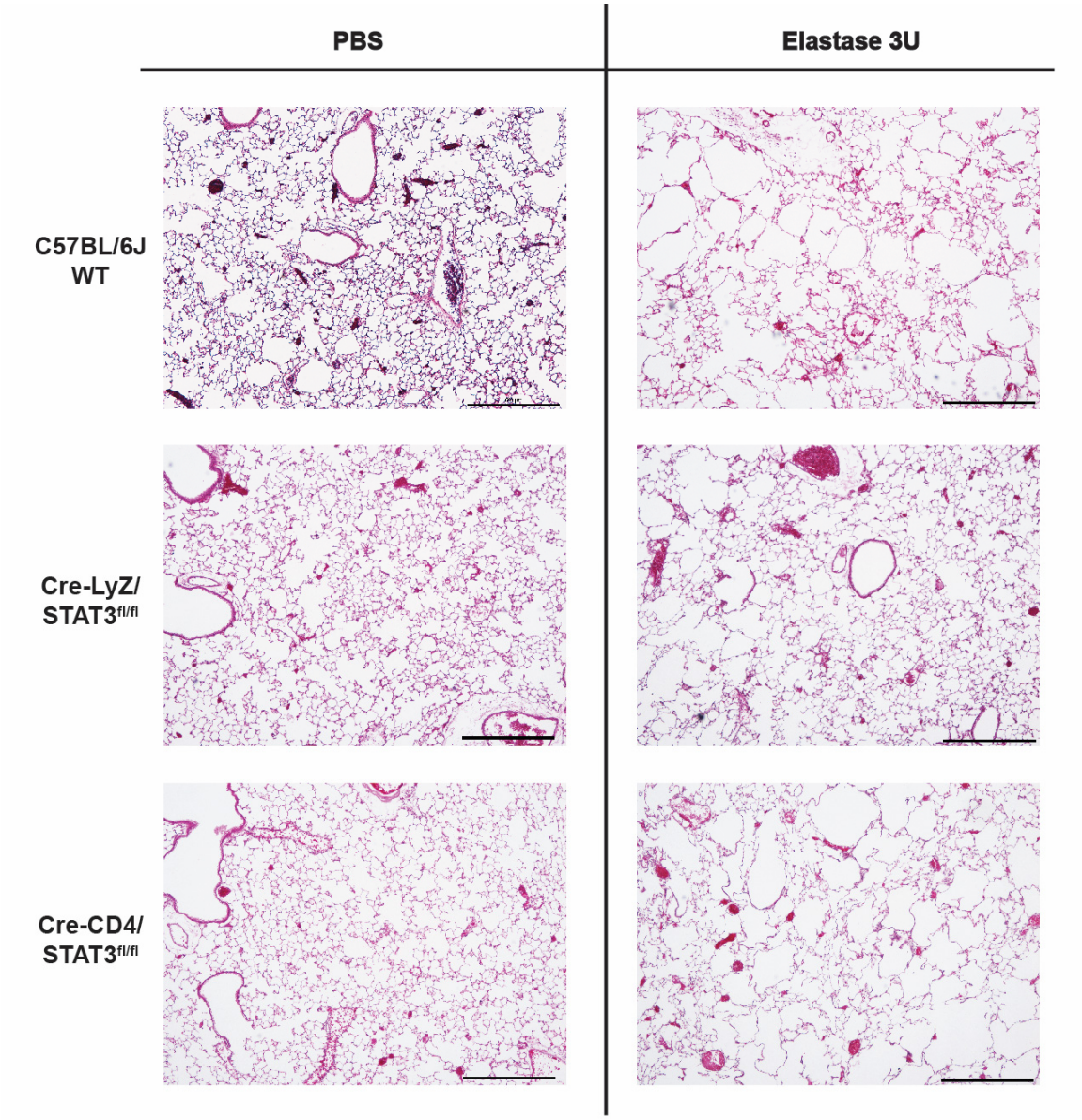

Figure 4.15 Histologic assessment of lungs from STAT3-deficient in either myeloid or CD4 cells mice and C57BL/6J mice following 3U elastase. Representative H&E-stained lung sections from wild-type (WT) C57BL/6J (*upper panel*), Cre-LyZ/Stat3$^{fl/fl}$ (*middle panel*) and Cre-CD4/Stat3$^{fl/fl}$ (*lower panel*) mice on day 21 after 3U elastase or PBS control. Original magnification x40. Scale bar = 500 μm.

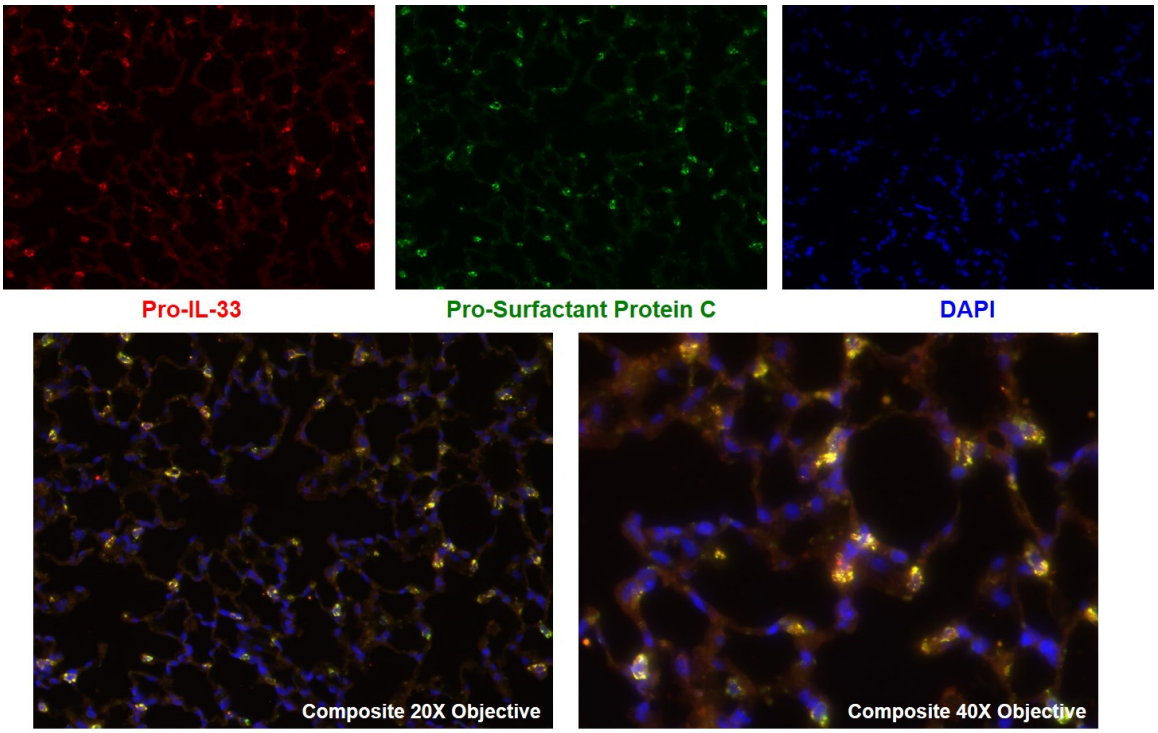

Figure 4.16 Localization of IL-33 protein in the lungs of BALB/cJ mice. (*Upper panel*) Representative immunofluorescence stained lung sections for pro-IL-33, pro-surfactant protein C and DAPI (nuclear stain) of BALB/cJ mice. (*Lower panel*) Composited images showing co-localization of pro-IL-33 and pro-surfactant protein C. Original magnification 20x or 40x objective lens.

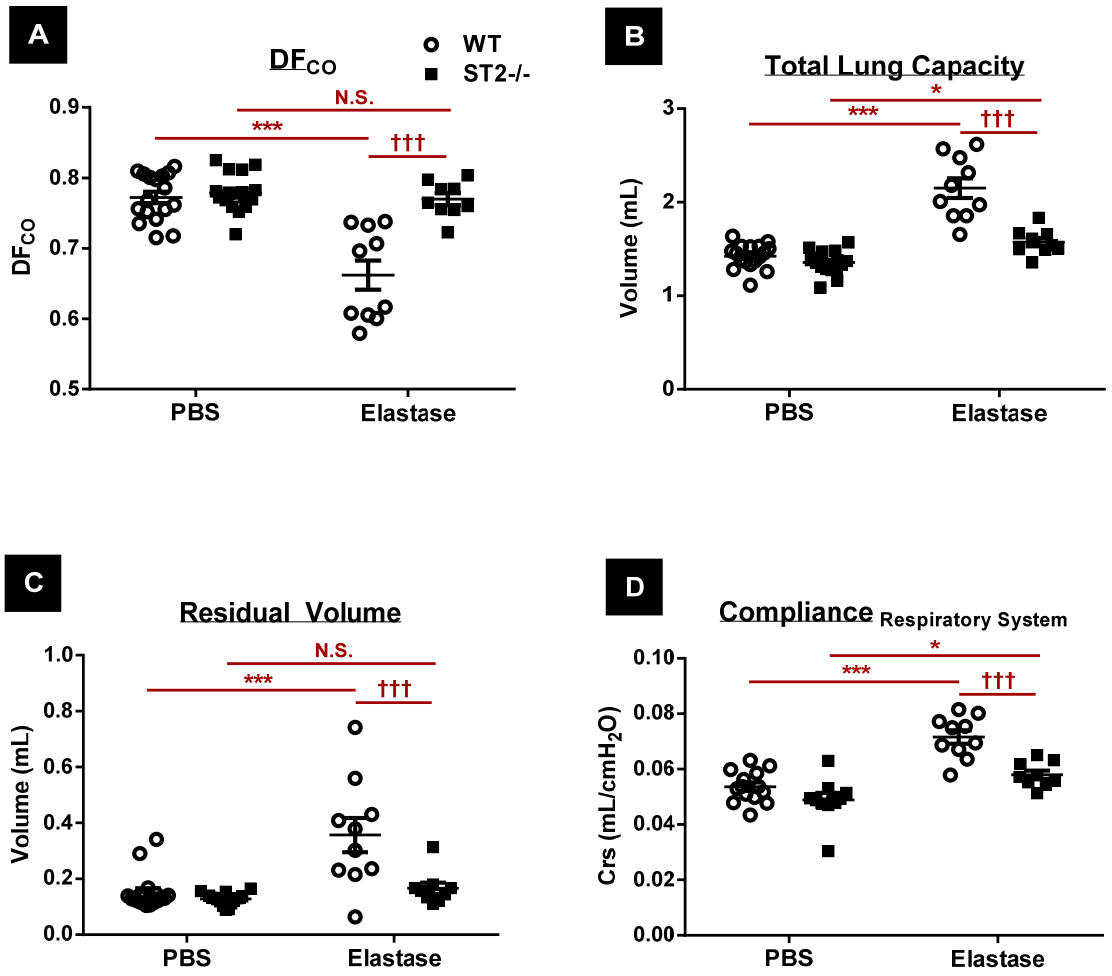

Figure 4.17 Properties of lungs from ST2-deficient (BALB/c background) mice and BALB/cJ mice following 3U elastase. (A) Diffusion capacity (B) Total lung capacity (C) Residual volume and (D) Compliance of respiratory system of $ST2^{-/-}$ and wild-type (WT) BALB/cJ mice on Day 21 after intratracheal administration of 3U elastase. (n = 10-17 mice per group). Two-way ANOVA analysis: *** = $p < 0.001$ comparing elastase-treated group to PBS-treated animals on the same genotype. ††† = $p < 0.001$ comparing ST2-defeicient mice with WT mice.

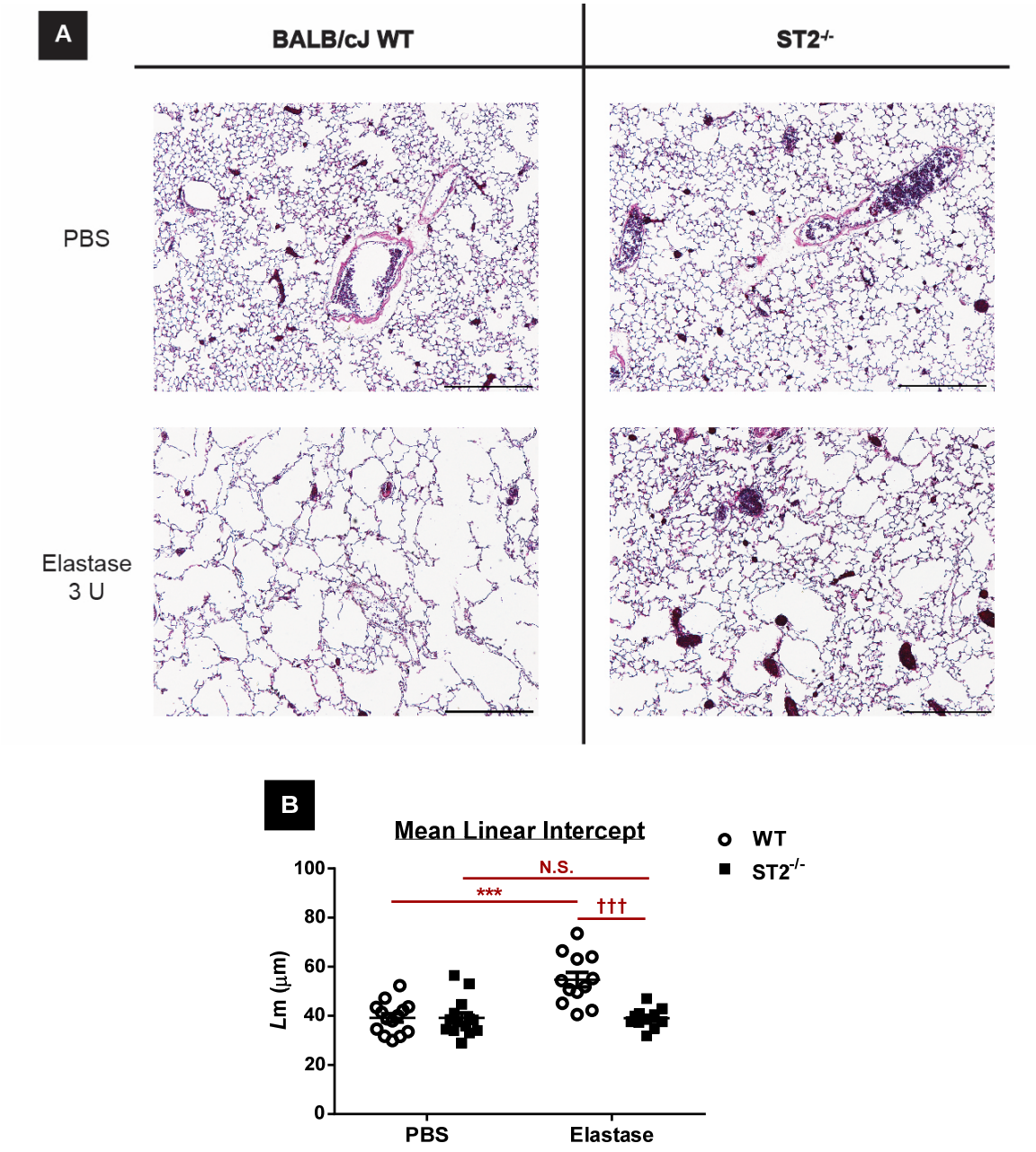

Figure 4.18 Histologic assessment of lungs from ST2-deficient and BALB/cJ mice following 3U elastase. (A) Representative H&E-stained lung sections from wild-type (WT) BALB/cJ (*left panel*) and ST2$^{-/-}$ (*right panel*) mice on day 21 after 3U elastase or PBS control. Original magnification x40. Scale bar = 500 µm. (B) Mean linear intercept of histological sections from ST2$^{-/-}$ and wild-type (WT) BALB/cJ mice. (n = 10-14 mice per group). Two-way ANOVA analysis: N.S. = not significant, *** = $p < 0.001$ comparing elastase-treated group to PBS-treated animals on the same genotype. ††† = $p < 0.001$ comparing ST2$^{-/-}$ mice with WT mice.

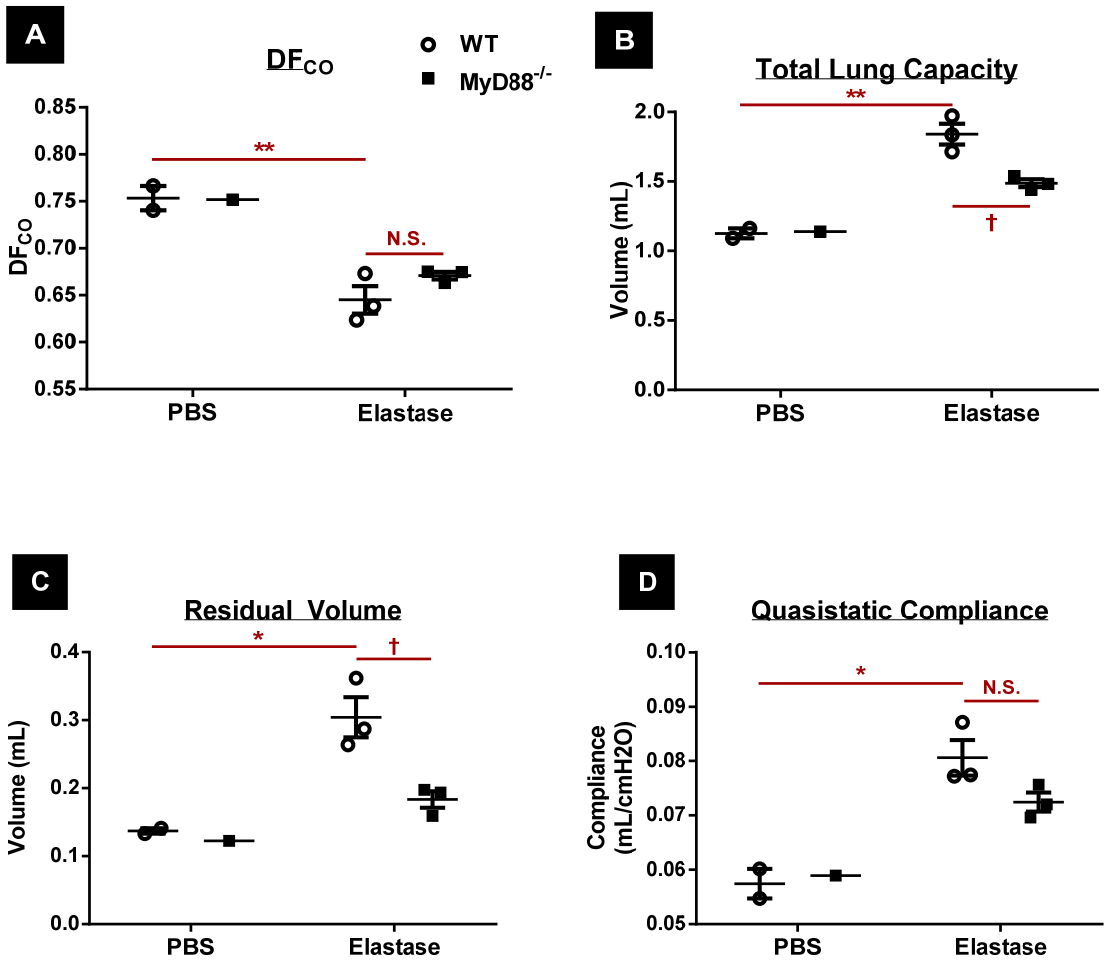

Figure 4.19 Properties of lungs from MyD88-deficient (C57BL/6 background) mice and C57BL/6J mice following 3U elastase. (A) Diffusion capacity (B) Total lung capacity (C) Residual volume and (D) Compliance of respiratory system of MyD88$^{-/-}$ and wild-type (WT) C57BL/6J mice on Day 21 after intratracheal administration of 3U elastase. (n = 1-3 mice per group). Two-way ANOVA analysis: * = $p < 0.05$, ** = $p < 0.01$ comparing elastase-treated group to PBS-treated animals on the same genotype. † = $p < 0.05$ comparing MyD88-defeicient mice with WT mice.

CHAPTER 5

Viral infection alters the sensitivity to elastase-induced emphysema

5.1 Abstract

Viral infection-induced exacerbation is common in COPD, and it critically impacts the progression of the disease. This viral infection potentially can modulate both the innate and adaptive immune responses in several ways, but little is known how these changes in the immune response impact the severity of emphysema outcomes. In the present study, we pre-infected both C57BL/6J and BALB/cJ mice with either vaccinia virus, influenza A virus, or their appropriate vehicle, followed by intratracheal challenging with elastase at 7 days (for vaccinia virus) or 14 days (for influenza virus) after viral inoculation to induce emphysematous changes in the lung. Our results showed that while vaccination with vaccinia one week prior to induction of emphysema exaggerated the extent of elastase-induced alveolar tissue destruction in C57BL/6J mice, it abrogated the disease in BALB/cJ mice. Examining the effect of pre-exposure of influenza A virus, we found no differences in the degree of emphysema caused by elastase between influenza-infected and non-infected in C57BL/6J mice. However, pronounced reduction in the severity of emphysema was observed in BALB/cJ animals exposed to influenza virus prior to elastase. Also, we found that this viral infection effect on susceptibility to emphysema was dependent on altered immune responses in certain critical time periods, with minimal effect outside of these critical periods. Overall, this study reveals that exposure to viral infection can modulate the pulmonary immune environment and subsequently impact the development of emphysema. This effect is both animal strain-dependent and time-sensitive.

5.2 Introduction

Chronic obstructive pulmonary disease (COPD) is characterized by progressive and usually irreversible airflow limitation and is a major cause of chronic morbidity and mortality world-wide [517]. Clinically, patients with COPD usually experience pathologic characteristics of both chronic inflammation in the airway (chronic bronchitis) and proteolytic destruction of alveolar wall tissue leading to permanent airspace enlargement (emphysema) [28, 29]. One of the major complications affecting the accelerated progression of COPD is acute exacerbation from bacterial or viral respiratory infections [266, 267]. Such exacerbations impact the nature of the pulmonary immune environment, which can subsequently affect the progression of COPD. Robust increases of inflammatory biomarkers (e.g. white blood cell counts, pro-inflammatory cytokines, chemokines and proteases) have always been detectable during such exacerbations. However, little is known about the underlying mechanisms linking the immune system changes induced by these infectious agents to the pathologic effects driving the progression of emphysema. Here, we selected two types of viruses, vaccinia and influenza A virus to study the role of viral infection on the progression of emphysema.

Vaccinia virus is a prototype member of the *Orthopoxvirus* genus, which is a group of large enveloped DNA viruses with ability to reproduce entirely within the cytoplasm of host cells [518]. Vaccination with vaccinia virus was used to eradicate human smallpox, another human pathogenic virus in the same genus. Recently, vaccinia has been employed as a promising viral vector to deliver immunotherapetics for targeting cancer cells including lung cancer [519-523]. Intranasal infection with modified vaccinia virus Ankara (MVA) strain has been shown to be able to effectively induce pulmonary immune responses, particularly Th1 effects

[524]. Pre-vaccination can induce Th1 responses and promote M1 macrophages. It also mitigates Th17 and M2 phenotypes in the lungs, resulting in a protective effect for bleomycin-induced pulmonary fibrosis [525]. Because of this effect on fibrosis, we sought to investigate if pre-exposure to vaccinia can similarly modulate the development of emphysema.

In contrast to vaccinia virus, influenza A viruses are in the group of *Orthomyxoviruses* and contain a negative-sense strand RNA in its genome [526]. They are categorized by 16 types of surface hemagglutinin (HA or H) together with 9 types of neuraminidase (NA or N) glycoproteins [526]. Influenza A viruses are some of the most important viral pathogen responsible for regular outbreaks worldwide, causing morbidity and mortality in human and animals [527, 528]. The most recent global pandemic in 2009 was caused by the influenza A H1N1 strain and was associated with more than 100,000 deaths worldwide, especially in children, young adults, and pregnant women [529, 530]. Moreover, several lines of epidemiological evidence indicate that influenza viruses are commonly found in COPD exacerbations and are the most common viruses associated with severe exacerbations requiring hospitalization [260, 531, 532]. Aberrant pulmonary immune responses, including striking elevation of numerous cytokines and chemokines, often called a "cytokine storm," has been well-documented during influenza virus infection in both humans and animal models [533-535]. Nevertheless, experimental studies linking this influenza-induced inflammation to the progression of emphysema have not been reported.

In this study, our main goal was to study whether an altered immune status in the lungs induced by either vaccinia virus or influenza A virus can change the susceptibility to emphysema in mice, using the intratracheal porcine pancreatic elastase model.

5.3 Results

5.3.1 Priming with vaccinia enhances the sensitivity to develop elastase-induced emphysema in C57BL/6J mice

To determine the effect of pre-exposure to vaccinia on the development of emphysema, we infected C57BL/6J mice by intranasal inoculation of two million vaccinia particles (Fig. 5.1A). The control group was treated with an equal volume of PBS. Seven days after vaccinia inoculation, the mice received either PBS (control) or porcine-derived pancreatic elastase at doses of 1.5, 3 or 6 enzymatic units (U) by the intratracheal route. When the mice were sacrificed at day 21 post-elastase challenge, we evaluated the degree of pulmonary emphysematous changes by measurement of diffusion capacity, pressure-volume relationship, and histological assessment. Fig. 5.1B-D shows that vaccinia alone did not change any pulmonary function measurement at the harvest day. As expected, increasing the dose of elastase resulted in more emphysematous changes in the lung as seen by dose-dependent decreases in DF_{CO}, and increases in TLC, RV, and compliance. Vaccinia-infected mice who received 1.5 and 3 U of elastase showed augmented changes in all measurements compared to the mock-infected mice given the same dose of elastase. However, vaccinia did not show any effect with the 6U dose of elastase. Histological examination of the lungs supported the pulmonary function tests, showing that vaccinia alone did not cause any observable pathology in the lungs, but induced more pronounced elastase-induced airspace enlargement (Fig. 5.2A). By morphometric analysis, compared to 3U elastase-treated mice,

mice infected with vaccinia and followed by 3U elastase exhibited significant increases in mean linear intercept (L_m) compared to 3U elastase without the early vaccinia infection (Fig. 5.2B).

5.3.2 Intranasal vaccinia treatment alters pulmonary immune cell profiles

We speculated that intranasal vaccinia treatment would change the pulmonary immune environment resulting in more susceptibility to elastase. C57BL/6J mice were either given vaccinia (2 x 10^6 pfu) or PBS, then all challenged with 3U elastase 7 days later. Then we harvested and analyzed the whole lung tissue for cellular profiles by flow cytometry at day 0, 2, 7 or 14 post-elastase challenge (Fig. 5.3A). We analyzed for polymorphonuclear cells (PMNs, $Ly6G^+$ $CD11b^+$ $Ly6C^+$), monocytes ($CD11b^+$ $CD64^+$ $Ly6C^+$), dendritic cells ($CD11b^+$ $CD11c^+$ $SiglecF^-$), macrophages ($CD11b^-$ $CD11c^+$ $SiglecF^+$), $CD4^+$ T cells ($B220^-$ $CD3^+$ $CD4^+$), $CD8^+$ T cells ($B220^-$ $CD3^+$ $CD8^+$), γδ T cells ($gdTCR^+$), B cells ($B220^+$ $CD3^-$), NK cells ($NKp46^+$ $CD3^-$ $CD49b^+$), and NKT cells ($NKp46^+$ $CD3^+$ $CD49b^+$). In term of myeloid populations (Fig. 5.3), vaccinia treated mice showed a much greater number of dendritic cells than mock treated animals at day 0 (7 days after vaccinia administration), with a gradual decrease over time. While there were more monocytes recruited into the lungs of vaccinia-treated mice at day 2 and day 7, the increases in number of macrophages seemed to be delayed and were not found significant until day 7 and day 14. However, vaccinia had no effect on the neutrophil count. Examining the lymphoid populations showed that vaccinia infected mice had greater numbers of $CD4^+$, $CD8^+$, γδ T cells, and NK cells on day 0 than PBS-treated mice. Although eventually there were decreases in the numbers of $CD4^+$ and $CD8^+$ T cells, the level of these cells in vaccinated mice remained significantly higher compared to control animals. In contrast, the elevated number of γδ T cells and NK cells

were only found in the lungs less than 7 days after elastase administration. There were slight increases in the number of NKT cells in vaccinia-treated mice from day 2 to day 7, but no differences in the number of B cells were detectable.

5.3.3 Effect of vaccinia on the sensitivity of elastase-induced emphysema is time-sensitive

Since the elevated number of immune cells peaked around 7 days after intranasal administration of vaccinia (the day of elastase challenge in the previous experiments), and then steadily declined after 7 days, we hypothesized that there was a critical period for the vaccinia effect on the alteration of elastase-induced emphysema. To test this proposition, we modified the treatment by giving vaccinia to C57BL/6J mice 21 days (instead of 7 days) prior to challenging with 3U elastase and observing the emphysema phenotypes at 21 days post-elastase challenge (Fig. 5.5). We found that, with this modified protocol, the effect of prior vaccinia infection on augmenting the severity of elastase-induced emphysema no longer existed. There were no differences in DF_{CO}, TLC, RV, or compliance between vaccinia-treated or mock-treated animals (Fig. 5.5B-E).

We then intratracheally instilled 3U elastase to C57BL/6J mice 7 days before intranasal infection with vaccinia and obtained the functional data on day 21 post-elastase instillation (Fig. 5.6). There were slight decreases in DF_{CO} and increases in TLC in the mice who received vaccinia compared to the ones who did not. However, these changes did not reach a significance level of 0.05. Only lung compliance was found to be significantly higher in vaccinia-treated mice compared to saline-treated mice.

5.3.4 Priming with vaccinia reduces the sensitivity to develop elastase-induced emphysema in BALB/cJ mice

Since it is known that BALB/c and C57BL/6 mice exhibit distinct responses to viral infection [536] as well as dissimilar sensitivity to developing elastase-induced emphysema (Chapter 3), we repeated experiments in BALB/c mice. BALB/cJ mice were infected with 2 x 10^6 pfu vaccinica by the intranasal route, and then instilled with either 1.5U, 3U or 6U of elastase seven days later. Twenty-one days after the treatment with elastase, animals were subjected to pulmonary function tests and their lung were collected to evaluate morphology (Fig. 5.7). Surprisingly, opposite results were obtained in the BALB/cJ strain, compared to C57BL/6 mice. Vaccinia-treated BALB/cJ mice who received 1.5 and 3 U elastase showed reduced degrees of emphysematous changes as observed by diminished TLC, RV, and compliance compared to mice without vaccinia who received the same dose of elastase. While all 10 BALB/cJ mice receiving 6U elastase were found dead within 48 hours after elastase administration, this mortality rate was significantly reduced to 40% in BALB/cJ pre-infected with vaccinia. Similar to C57BL/6J mice, vaccinia alone had no detectable effect on pulmonary function measurements. These functional data were supported by the histological sections (Fig. 5.8). BALB/cJ mice given vaccinia developed less severe elastase-induced alveolar damage than mice with no infection.

5.3.5 Pre-infection with influenza virus modifies the sensitivity to develop elastase-induced emphysema in BALB/cJ mice, but not in C57BL/6J mice

Because influenza virus is much more relevant to COPD patients than vaccinia virus, we also evaluated the effect of pre-infection with influenza virus on the development of elastase-induced pulmonary emphysema in both C57BL/6J and BALB/cJ mice. We

inoculated C57BL/6J and BALB/cJ mice via the intranasal route with mouse adapted influenza A virus H1N1/PR8 (50 $TCID_{50}$). All mock-infected mice received an equivalent volume of DMEM media. After 14 days of infection, either 3 units of porcine elastase or PBS was delivered to the mice via intratracheal route. The lung properties were measured and lung tissue was collected at day 21 post-elastase delivery. In contrast to vaccinia, influenza virus failed to enhance the severity of elastase-induced emphysema in C57BL/6J mice (Fig. 5.9). No significant differences were observed in DF_{CO}, TLC, RV, or compliance between influenza-infected and mocked-infected mice in both PBS and elastase groups. However, similar to vaccinia, pre-exposure to influenza in BALB/cJ mice significantly attenuated the increases in TLC, RV, and compliance following the elastase insult (Fig. 5.10). Comparable degree of emphysematous lesions were confirmed by histological assessment between elastase-treated C57BL/6J mice who were either pre-infected with influenza or not, whereas airspace enlargement caused by elastase was less conspicuous in influenza-exposed BALB/cJ mice (Fig. 5.11). Of note, the lung tissue sections from BALB/cJ mice in the influenza/PBS group displayed a noticeable degree of peribronchiolar and perivascular lymphoid tissues (Fig .5.11B). These changes were reflected by marginal drops in DF_{CO} and TLC when compared to PBS/Vehicle control animals (Fig. 5.10B-C).

5.4 Discussion

Exacerbation from respiratory bacterial/viral infection is a major concern for COPD/emphysema management, because such infections can impair patients' quality of life, decrease their health status, accelerate the progression of diseases and lead to life-threatening complications [31]. Although emphysema per se can develop in a sterile alveolar inflammation environment, and there is no evidence showing that pathogens can initiate the

destruction of alveolar ultrastructure leading to emphysema, we have investigated whether these infections can change the inflammatory milieu sufficiently to affect the development of emphysema initiated by other stimuli. Most of the studies on exacerbation of COPD in animal models focused on how host defenses respond to cigarette smoke, the primary etiological factor of COPD. These studies examined how the infection burdens impacts the clearance of pathogens and how combined cigarette smoke, combined with infection, impacts pulmonary inflammation ([338, 537-539]). On the other hand, few studies have examined how infection can modulate the functional progression of emphysema. To date, only Foronjy *et al.* and Ganesan *et al.* showed that respiratory syncytial virus and *Haemophilus influenzae* infection could augment the severity of chronic cigarette smoke-induced inflammation and emphysema in the lungs [339, 341]. Here, we have studied the effect of viral infection on the development of elastase-induced emphysema.

We first investigated the role of vaccinia virus on elastase-induced emphysema. Modified vaccinia virus Ankara (MVA) used in this study was originally adapted and derived by serial passage in chicken embryo fibroblast chicken [540]. During extended passage, MVA becomes a highly attenuated strain of vaccinia virus which contains multiple deletion and mutations in its genome compared to the parental strain, and it loses replication capacity in almost all mammalian cells, but it still contains some host immunomodulatory proteins found in wild-type orthopoxviruses, including complement control protein (virulence factor) [541-543]. We selected MVA vaccinia strain to use in this study because of its several advantages. First, it is safe to use in both humans and mice because of its defectiveness in propagation as seen by no detectable pathology in the lungs (Fig. 5.2, 5.8). Second, several investigations in both pre-clinical studies and clinical trials have used MVA vaccinia as a

target protein-expressing vector to develop vaccines for many cancers, including lung cancer which often co-exists with COPD/emphysema [523, 544-546]. Last, despite its loss of several factors during its long time passage, MVA retains its immunogeneticity, and its induction of immune responses remains potent and equivalent to a fully replicating vaccinia virus [547, 548]. Our data show opposite effects between C57BL/6J and BALB/cJ mice in the development of elastase-induced emphysema when the mice were pre-infected with vaccinia virus. It is well known that C57BL/6 display a Th1-biased immunity during infection [416, 417], and vaccinia virus can induce strong IFN-γ-producing Th1 responses as well as augmented NK cells [524]. In Chapter 3 and 4, we showed that there was an up-regulation of IFN-γ expression following to elastase administration in C57BL/6J mice, and IFN-$\gamma^{-/-}$ mice failed to develop emphysema induced by elastase. Also, we also identified marked increases of $CD4^+$, $CD8^+$ and NK cells that have the potential to produce IFN-γ shortly after elastase administration (Fig. 5.4). Collectively, we hypothesized that vaccinia virus elevated the level of IFN-γ which subsequently exacerbated the severity of emphysema induced by elastase. Conversely, BALB/c mice have considerably less ability to develop a Th1 response [549], and our data from Chapter 3 showed that the development of emphysema in BALB/cJ mice was more likely due to increased IL-17A production and MMP-producing alternatively activated macrophages, rather than IFN-γ. A previous study on vaccination and pulmonary fibrosis from our colleagues demonstrated that vaccinia reduced both Th17 and alternatively activated macrophages responses in the lungs post-bleomycin exposure [525]. We reasoned that decreases in the induction of IL-17 and M2 macrophages contributed to the protective effect on developing emphysema in vaccinated BALB/cJ mice.

We also examined the effect of a more relevant viral infection on elastase-induced emphysema using the influenza A virus strain H1N1/PR8. MVA vaccinia virus and PR8 influenza virus are different in several important ways. MVA vaccinia virus contains a DNA genome, has a lack of replication capacity in most of murine cells, and has relatively low virulence so it can be used under laboratory conditions at biosafety level 1. Conversely, influenza virus has RNA as a genome, and it can infect and reproduce in several cell types along the respiratory tract including ciliated/non-ciliated bronchial cells, alveolar epithelial type I cells, type II cells, and alveolar macrophages. Infection subsequently leads to pathologies such as marked bronchitis, alveolitis and mucus cell metaplasia, and the virus require handling at biosafety level 2 [550, 551]. Of note, due to its relatively high pathogenicity, intranasal inoculation of influenza virus causes loss about 20% of body weight at day 7 after inoculation, and administration of elastase on that day leads to almost 100% mortality of mice within 48 hours. Thus, we adapted the protocol to give elastase to the mice 14 days after this viral infection instead of the 7 days used with vaccinia.

Our results showed that previous infection with influenza virus 14 days beforehand did not alter elastase-induced emphysema in C57BL/6J mice. PR8 influenza virus can infect and rapidly replicate in the lung after intranasal administration. The virus titers reached a peak at 2-5 days post-inoculation and virus was cleared out by day 9 [552, 553]. The peak inflammatory cell infiltration together with the peak of IFN-γ expression were found close to the time of peak viral load in the lung, and the levels of most inflammatory cytokines (including IFN-γ) return to baseline levels within one week post-infection [553, 554]. Previously, in Chapter 3, we proposed that the pathology of emphysema in C57BL/6J was mediated by IFN-γ, and this is consistent with the observed increased level of IFN-γ induced

by the vaccinia infection. Perhaps most of the altered immune response from the viral infection might be so minimal at day 14 after infection, that it would have little effect on elastase-induced emphysema.

On the other hand, a prior influenza virus infection did abrogate the development of elastase-induced emphysema in BALB/cJ mice. Similar to vaccinia virus, intranasal inoculation of influenza H1N1/PR8 was found to significantly decrease pulmonary IL-17A level in BALB/c mice [555]. Influenza virus could also infect alveolar macrophages and, by tracking macrophage dynamics with in vivo labeling of lung resident macrophages, it was shown that more than 90% of alveolar macrophages were depleted (due to a cell death mechanism) by day 7 after sublethal PR8 influenza infection in this strain of mice [556]. Although this study showed that replenishment of macrophages was completed by day 11, another study demonstrated that the function of alveolar macrophages isolated after resolution of influenza infection did not return to the pre-infection state [557]. Desensitization of intracellular mechanisms, such as the NF-κB signaling pathway, was evident and sustained for several months even after viral clearance. We suspect that both a decline in IL-17 level and impaired function of alveolar macrophages in the lungs facilitated the lesser progressive emphysema induced by the acute elastase insult.

Overall, one of the most important finding of this study is the opposite responses of prior respiratory infection on the development of emphysema in the two mouse strain studied. This finding suggests a complex interaction between host genetic predisposition and environmental factors in determining the susceptibility to emphysema. This might be part of the reason why not all smokers with different infection history and with different genetic

backgrounds are equally susceptible to cigarette smoke. Since most of the studies on COPD exacerbation in animal models have been performed in only one genetically-identical animal strain (commonly the C57BL/6 strain), these published results thus might not be easily extrapolateable to humans.

In summary, we conclude that prior viral infection can impact the pulmonary immune environment, and in turn can modulate the susceptibility to emphysema. This effect can manifest itself differently in different genetic backgrounds, but the exact mechanisms underlying this phenomenon need further study.

5.5 Acknowledgements

I would like to thank Dr. Sam Collins, Dr. Maureen Horton and Dr. Jonathan Powell at the Johns Hopkins School of Medicine for providing the stock of vaccinia virus, Dr. Sabra Klein and Olivia Hall at the Johns Hopkins School of Public Health for providing the stock of influenza virus. All the flow cytometric analysis shown in Fig. 5.3 - 5.4 were performed with great help from Dr. Daniel Lagasse. All histological tissue preparation was assisted by Xin Guo and the quantitative morphometric analysis of lung tissues was done by Alexandra Kearson. This work was supported by National Heart, Lung, and Blood Institute Grant # P01HL10342.

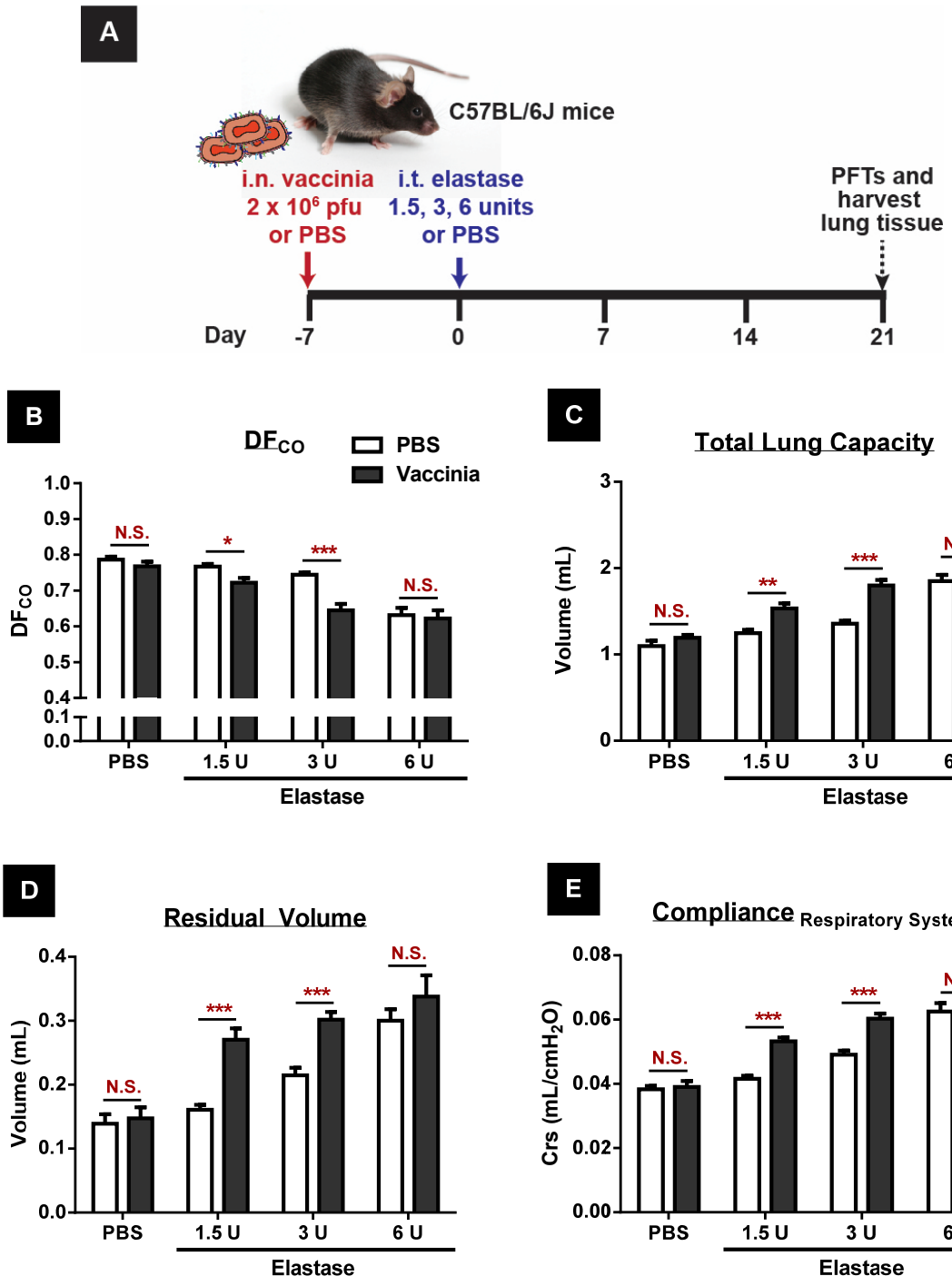

Figure 5.1 Effect of priming with vaccinia (1 week before) on pulmonary function and mechanics in elastase-induced emphysema in C57BL/6J mice. (A) Schematic of the experimental design showing pre-infection with vaccinia 7 days prior to elastase administration (B) DF_{CO} (C) TLC (D) RV and (E) Crs of C57BL/6J mice on Day 21 after elastase. (n = 5-15 mice per group). Unpaired *t*-test analysis: N.S. = not significant, * = $p < 0.05$, ** = $p < 0.01$, *** = $p < 0.001$ comparing vaccinated group to unvaccinated group at the same dose of elastase.

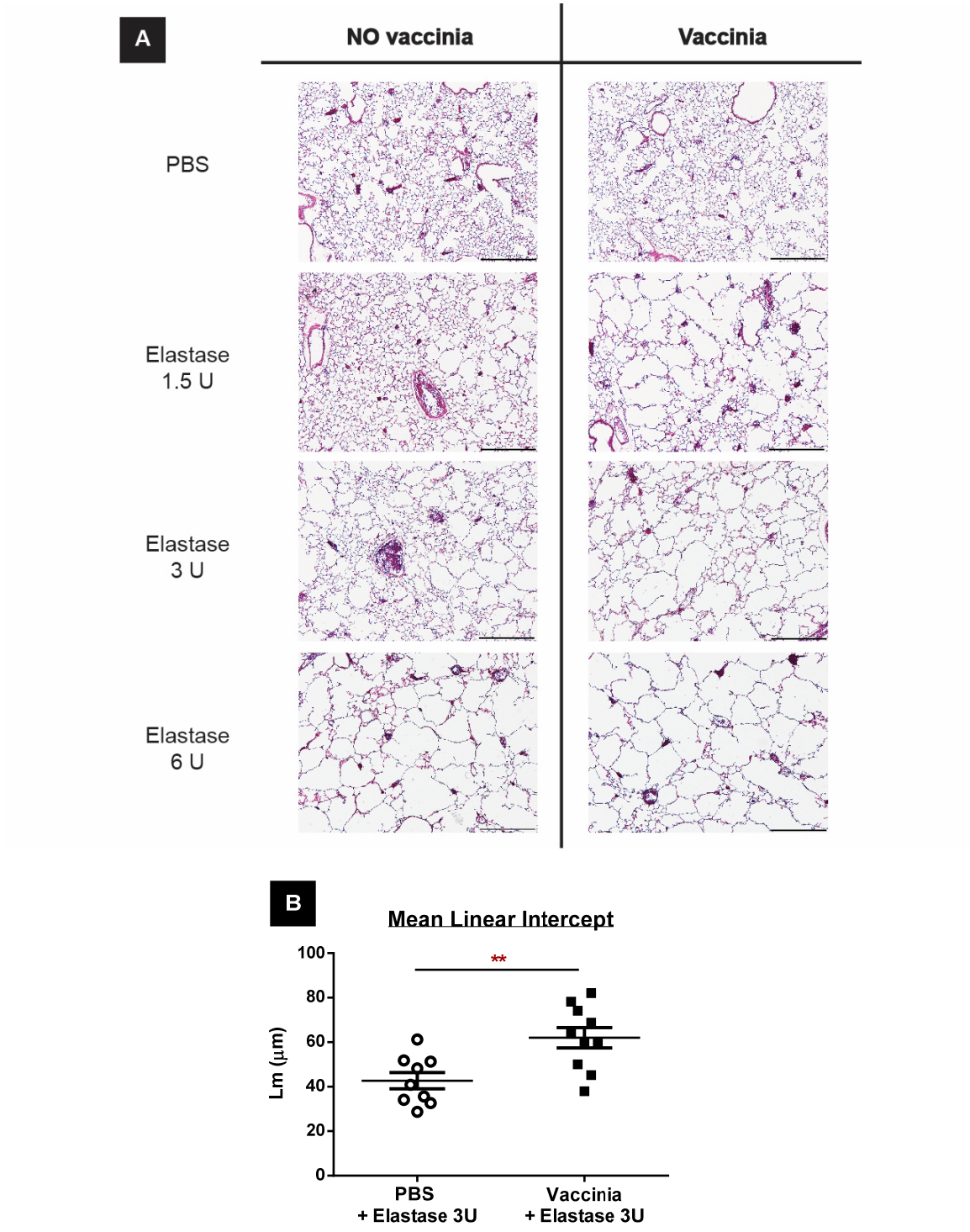

Figure 5.2 Effect of priming with vaccinia (1 week before) on histological assessment in elastase-induced emphysema in C57BL/6J mice. (A) Representative H&E-stained lung sections on day 21 post elastase administration from vaccinia-primed vs non-primed C57BL/6J mice given different doses of elastase or PBS. Original magnification x40. Scale bar = 500 µm. (B) Quantitative morphometric assessment of airspace enlargement. (n = 9 mice/group). ** = $p < 0.01$ (unpaired *t*-test)

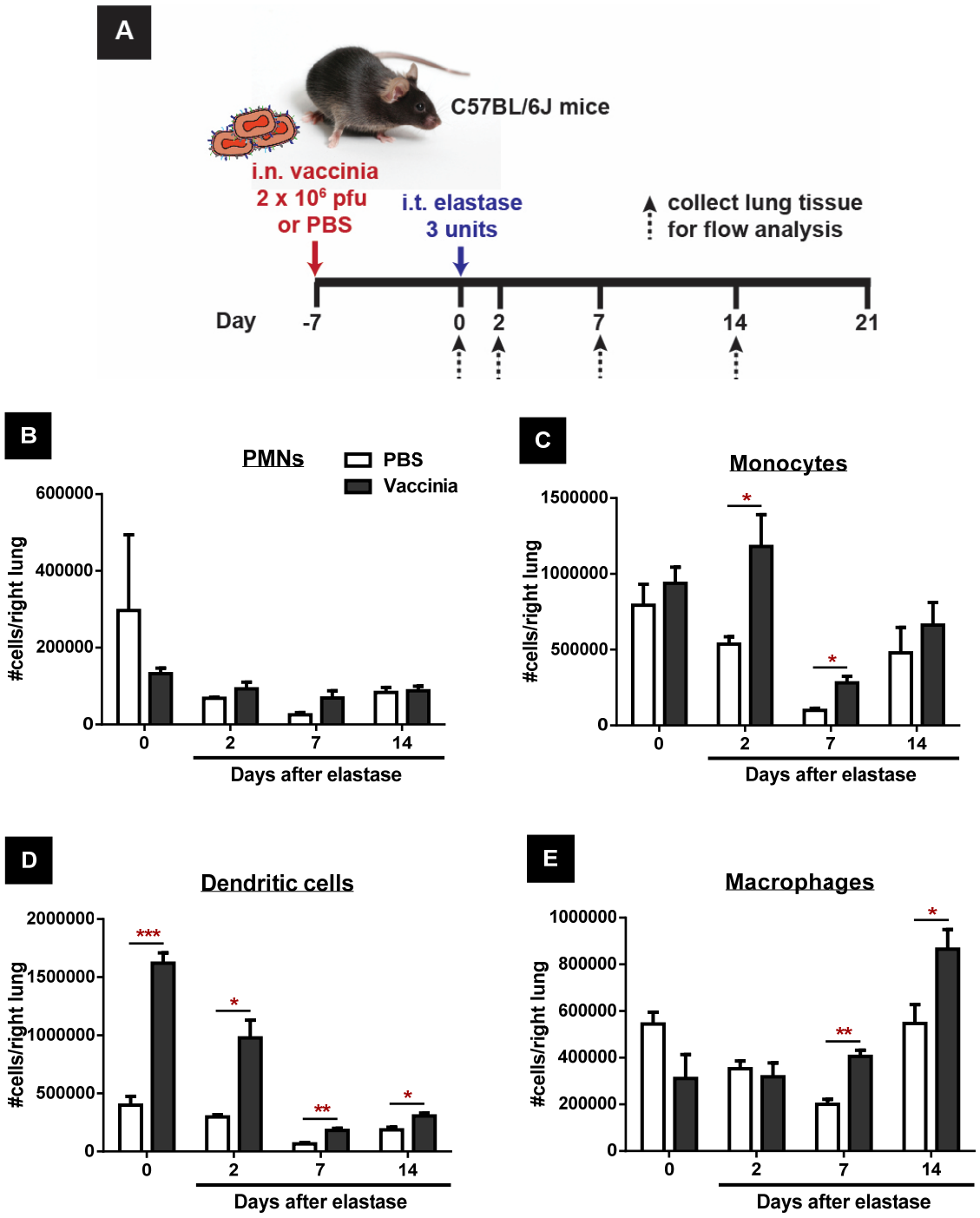

Figure 5.3 Effect of priming with vaccinia (1 week before) on granulocytes/myeloid cell populations in elastase-treated C57BL/6J mice. (A) Schematic of the experimental design showing either pre-infection with vaccinia or PBS 7 days prior to 3U elastase administration. Numbers of (B) Polymorphonuclear cells (C) Monocytes (D) Dendritic cells and (E) Macrophages per right lung of C57BL/6J mice on Day 0, 2, 7 and 14 after elastase. (n = 3). Unpaired *t*-test analysis: * = $p < 0.05$, ** = $p < 0.01$, *** = $p < 0.001$ comparing vaccinated group to unvaccinated group at the same time points.

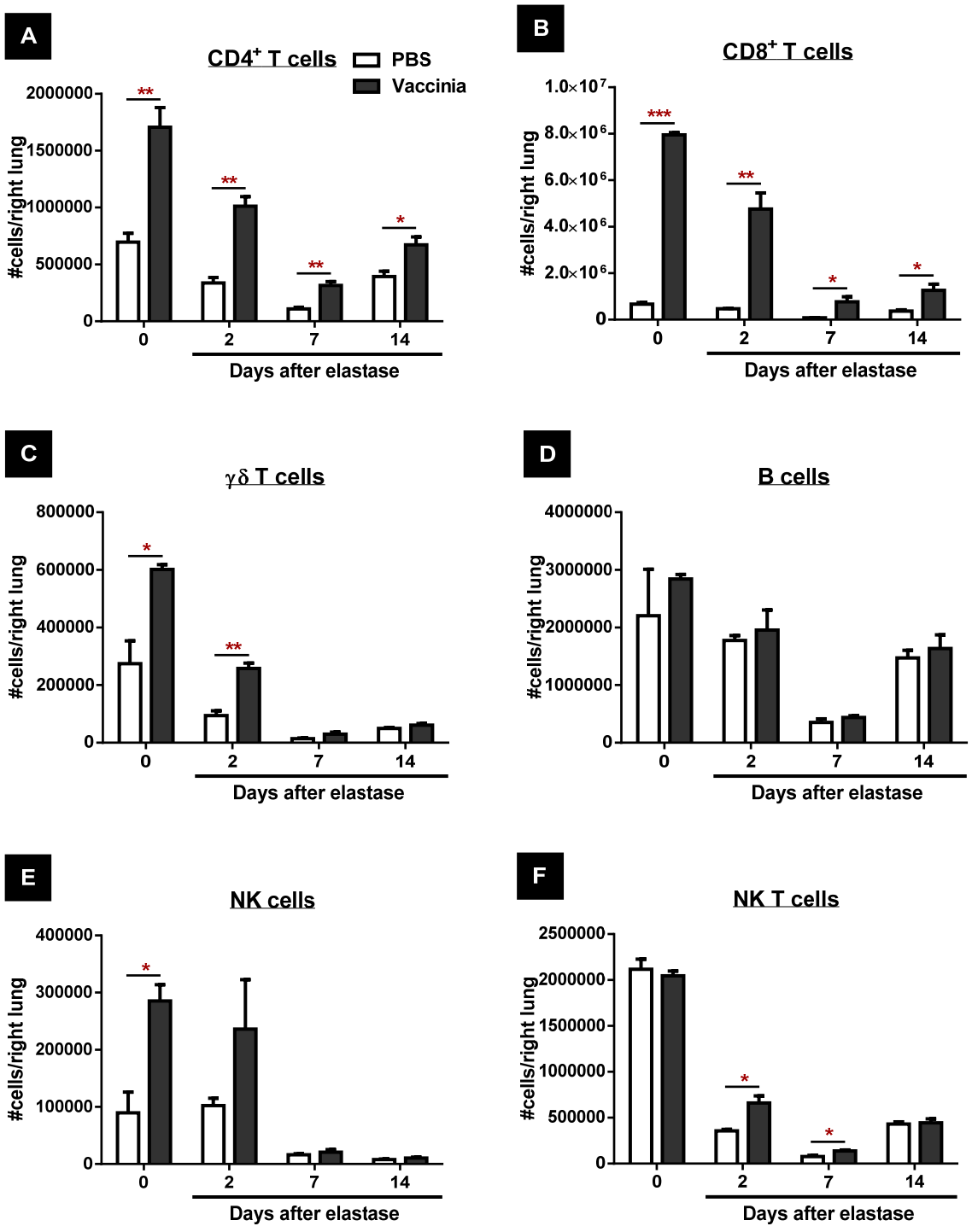

Figure 5.4 Effect of priming with vaccinia (1 week before) on lymphocyte populations in elastase-treated C57BL/6J mice. Numbers of (A) $CD4^+$ T cells (B) $CD8^+$ T cells (C) γδ T cells (D) B cells (E) NK cells and (F) NKT cells per right lung of C57BL/6J mice on Day 0, 2, 7 and 14 after elastase. (n = 3). Unpaired *t*-test analysis: * = $p < 0.05$, ** = $p < 0.01$, *** = $p < 0.001$ comparing vaccinated group to unvaccinated group at the same time points.

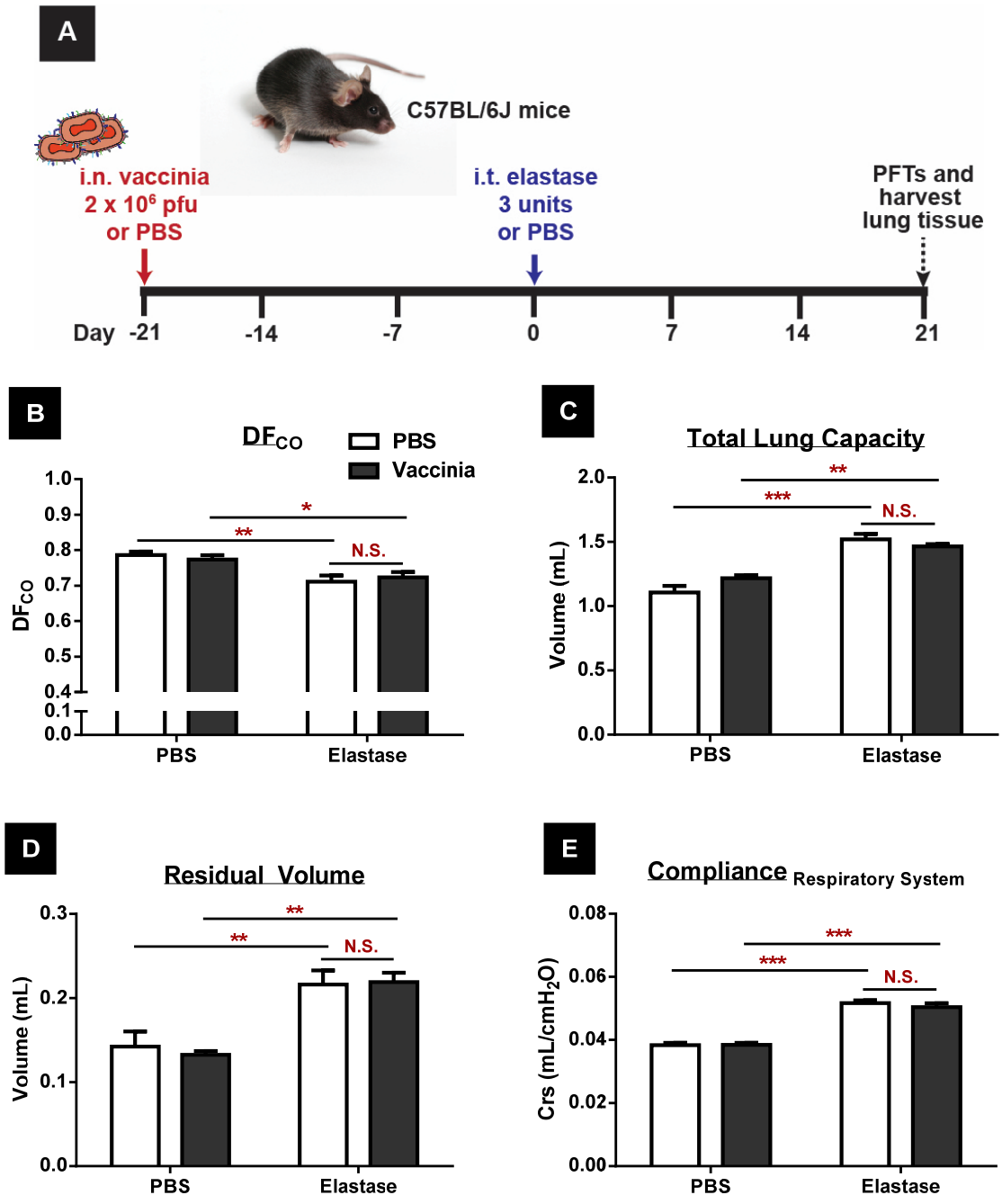

Figure 5.5 Effect of priming with vaccinia (3 weeks before) on elastase-induced emphysema in C57BL/6J mice. (A) Schematic of the experimental design showing pre-infection with vaccinia 21 days prior to 3U elastase administration (B) DF_{CO} (C) TLC (D) RV and (E) Crs of C57BL/6J mice on Day 21 after elastase. (n = 5 mice per group). Two-way ANOVA analysis: * = $p < 0.05$, ** = $p < 0.01$, *** = $p < 0.001$ comparing elastase-treated group to PBS control group. N.S. = no significant difference were observed between vaccinia and no vaccinia group.

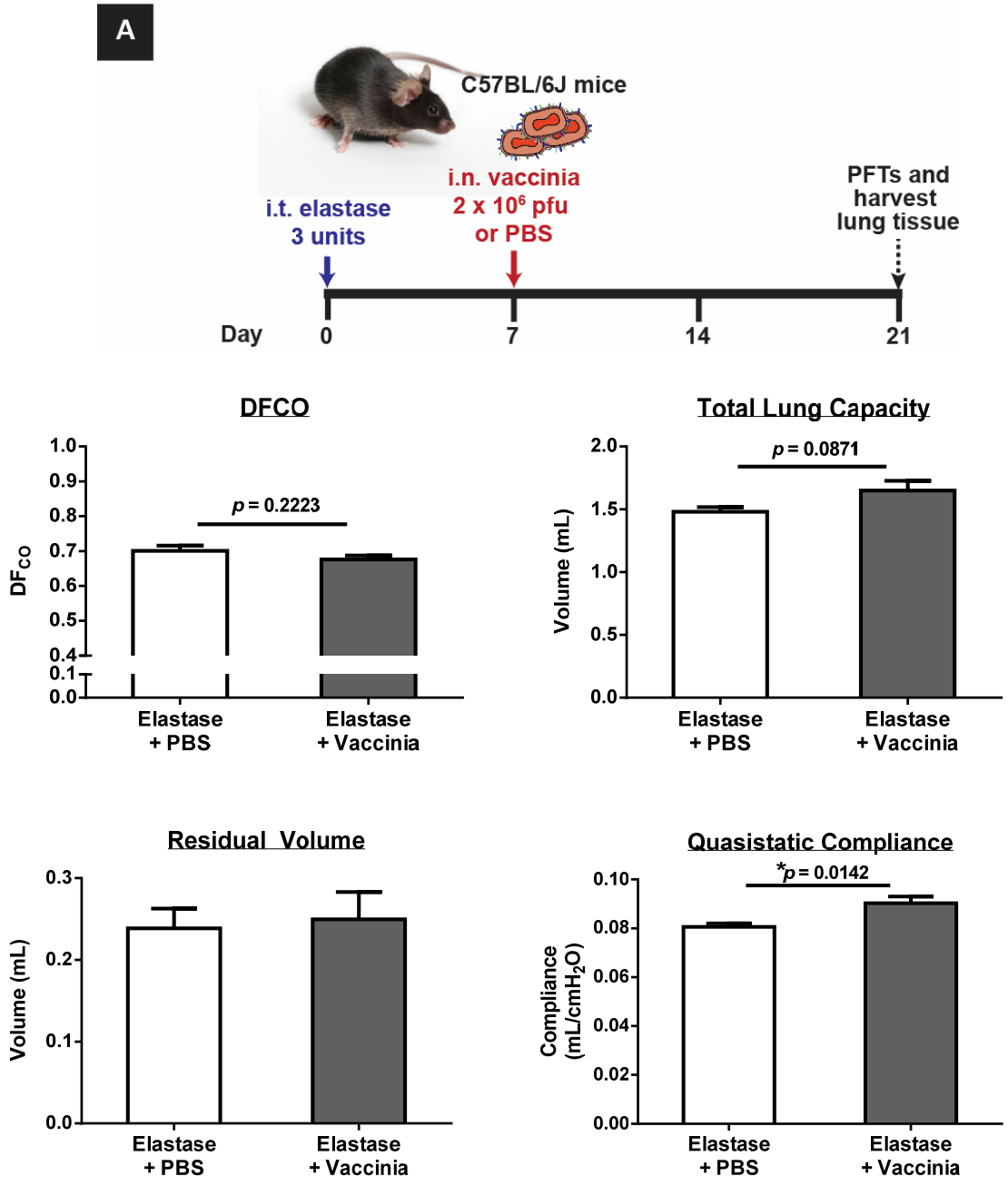

Figure 5.6 Effect of post-exposure with vaccinia (1 week after) on elastase-induced emphysema in C57BL/6J mice. (A) Schematic of the experimental design showing post-infection with vaccinia 7 days after 3U elastase administration (B) DF_{CO} (C) TLC (D) RV and (E) Crs of C57BL/6J mice on Day 21 after elastase. (n = 5 mice per group). Unpaired *t*-test analysis: * = $p < 0.05$, and *p*-values were indicated.

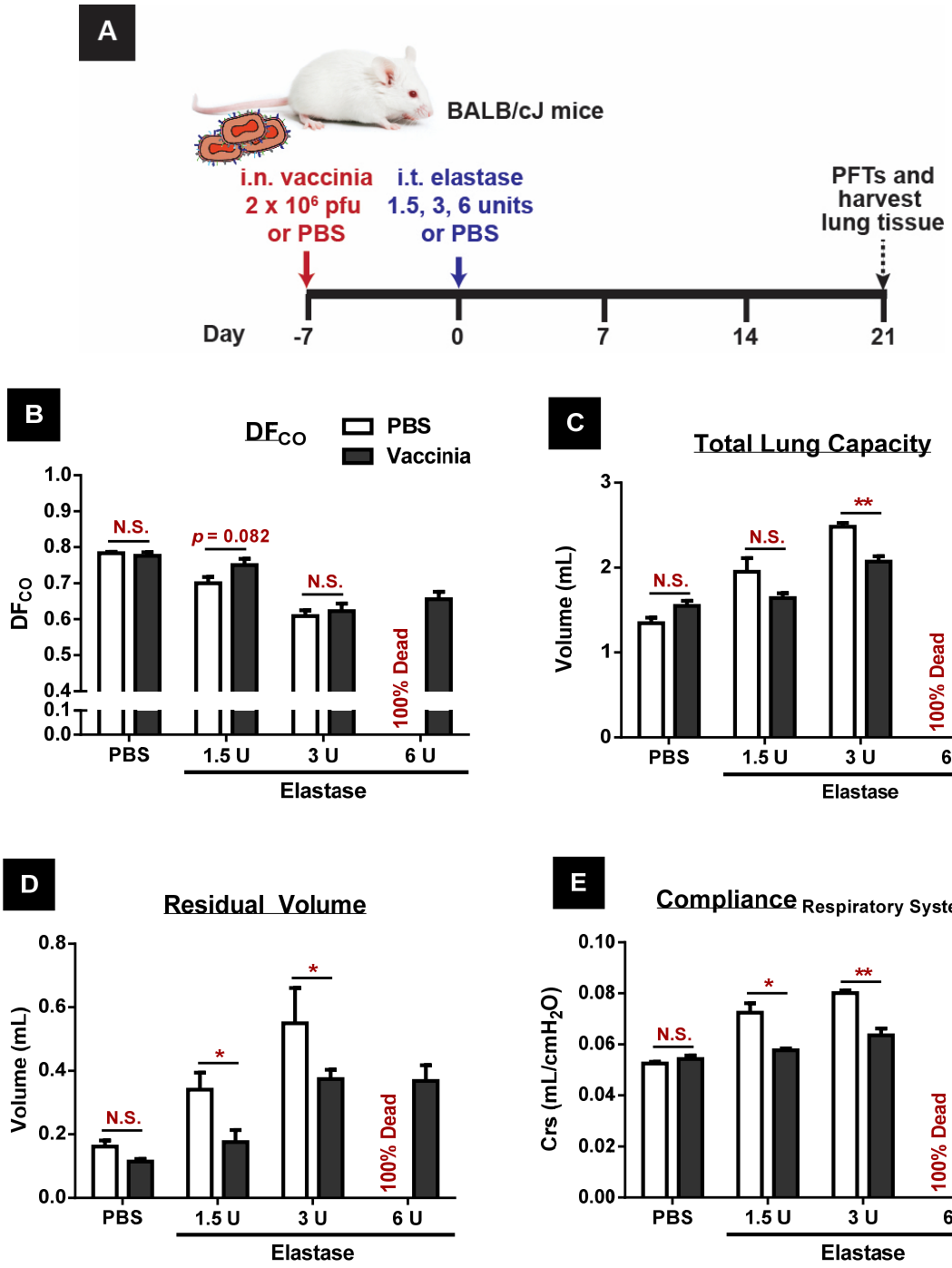

Figure 5.7 Effect of priming with vaccinia on pulmonary function and mechanics in elastase-induced emphysema in BALB/cJ mice. (A) Schematic of the experimental design showing pre-infection with vaccinia 7 days prior to elastase administration (B) DF_{CO} (C) TLC (D) RV and (E) Crs of BALB/cJ mice on Day 21 after elastase. (n = 5-15 mice per group). Unpaired *t*-test analysis: N.S. = not significant, * = $p < 0.05$, ** = $p < 0.01$ comparing vaccinated group to unvaccinated group at the same dose of elastase.

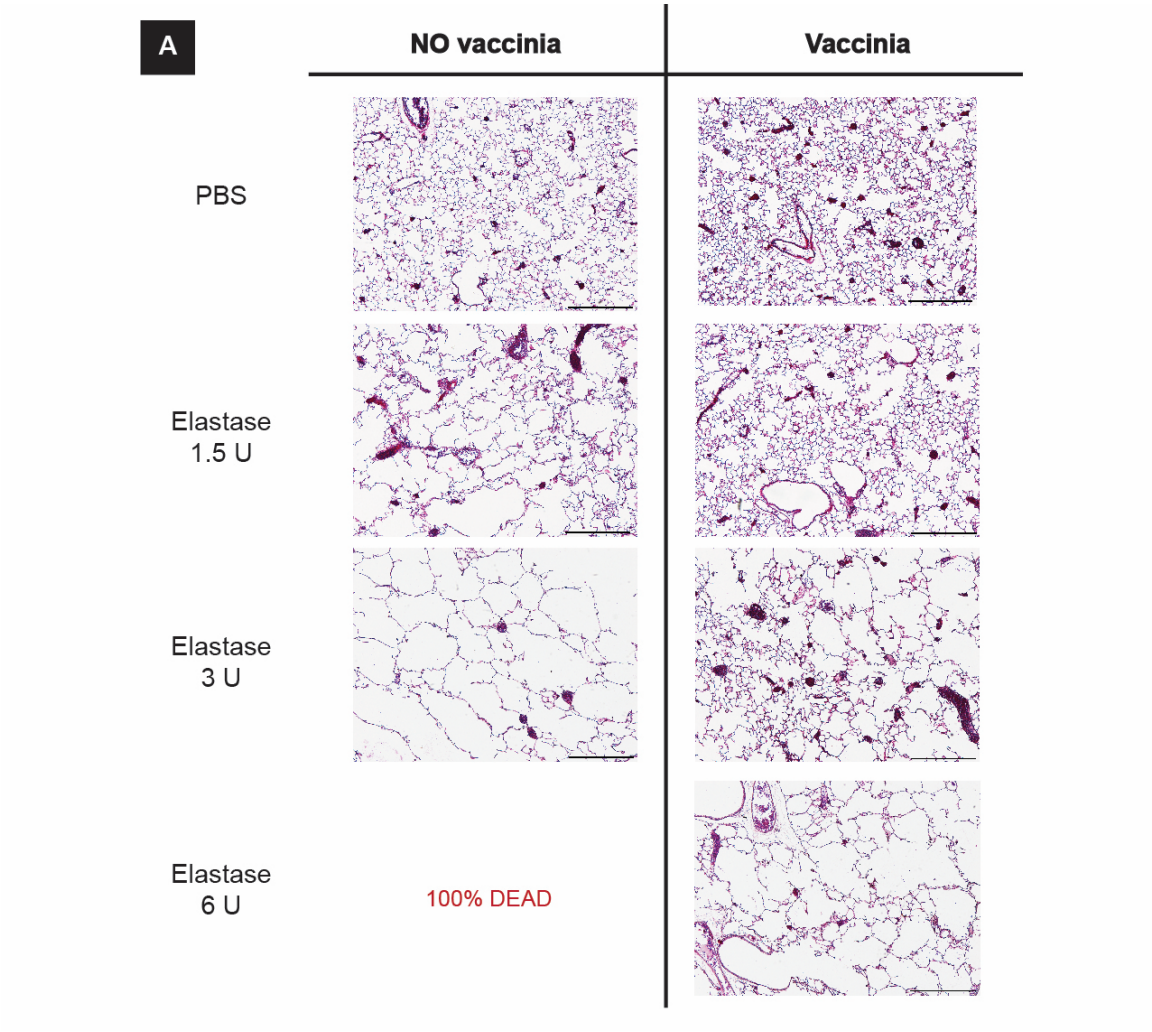

Figure 5.8 Effect of priming with vaccinia on histological assessment in elastase-induced emphysema in BALB/cJ mice. Representative H&E-stained lung sections from vaccinia-primed vs non-primed BALB/cJ mice given different doses of elastase or PBS on day 21 post elastase administration. Original magnification x40. Scale bar = 500 μm.

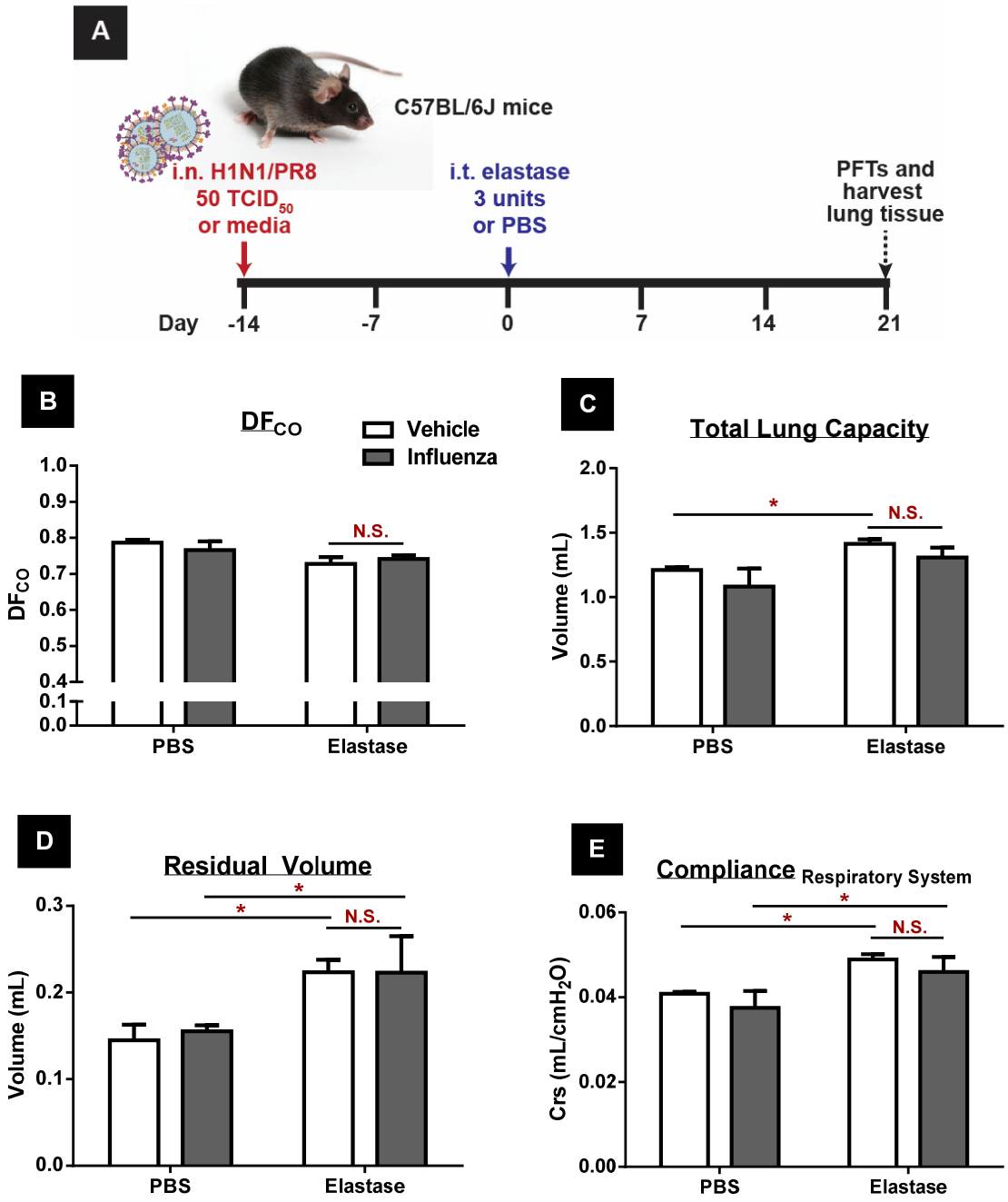

Figure 5.9 Effect of priming with influenza virus (2 weeks before) on elastase-induced emphysema in C57BL/6J mice. (A) Schematic of the experimental design showing pre-infection with influenza virus 14 days prior to 3U elastase administration (B) DF_{CO} (C) TLC (D) RV and (E) Crs of C57BL/6J mice on Day 21 after elastase. (n = 3-6 mice per group). Two-way ANOVA analysis: * = $p < 0.05$ comparing elastase-treated group to PBS control group. N.S. = no significant differences were observed between influenza-infection and no infection groups.

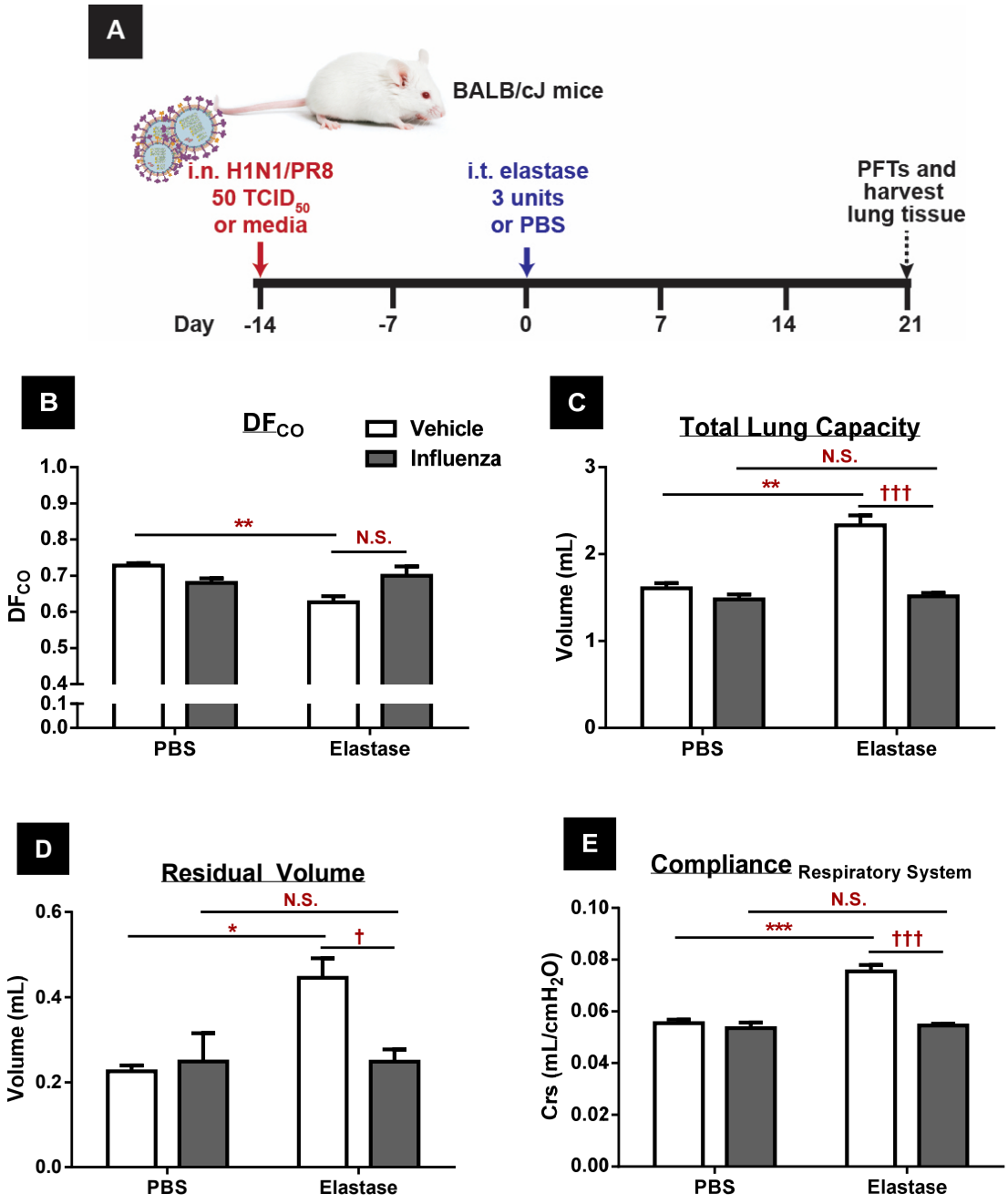

Figure 5.10 Effect of priming with influenza virus (2 weeks before) on elastase-induced emphysema in BALB/cJ mice. (A) Schematic of the experimental design showing pre-infection with influenza virus 14 days prior to 3U elastase administration (B) DF_{CO} (C) TLC (D) RV and (E) Crs of BALB/cJ mice on Day 21 after given elastase. (n = 3-6 mice per group). Two-way ANOVA analysis: N.S. = not significant, * = $p < 0.05$, ** = $p < 0.01$, *** = $p < 0.001$ comparing elastase-treated group to PBS control group. † = $p < 0.05$, ††† = $p < 0.001$ comparing influenza-infected mice with non-infected mice.

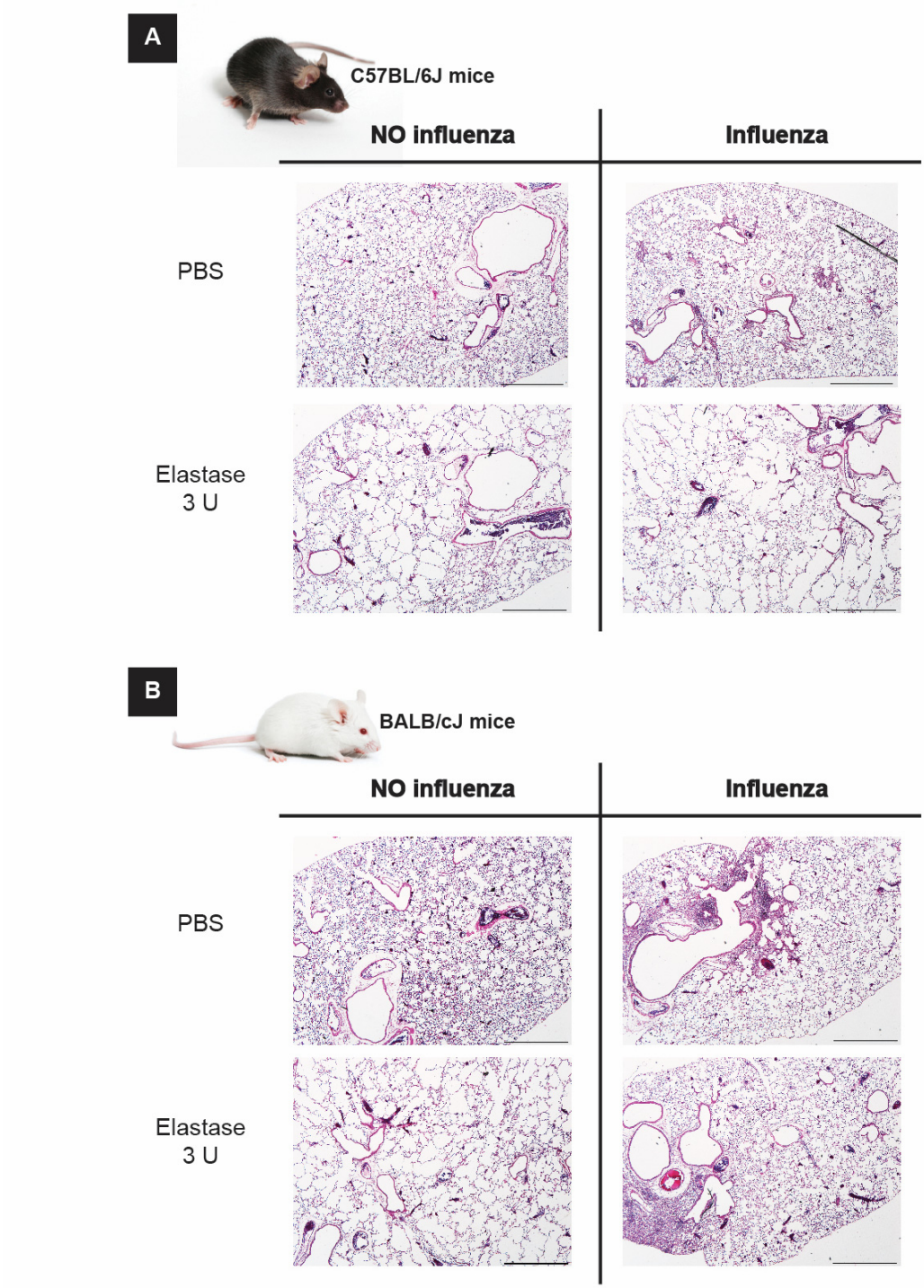

Figure 5.11 Effect of priming with influenza virus (2 weeks before) on histological assessment of elastase-induced emphysema in C57BL/6J and BALB/cJ mice. Representative H&E-stained lung sections from influenza-infected vs non-infected (A) C57BL/6J and (B) BALB/cJ mice given 3U elastase or PBS on day 21 post elastase administration. Original magnification x20. Scale bar = 1000 μm.

CHAPTER 6

GENERAL DISCUSSION

6.1 Summary

In the present study, we focused on the identification of immunological pathways that are involved in determining the susceptibility to emphysema in a mouse model of the disease. First, we compared the susceptibility to emphysema in two commonly used strains of mice, C57BL/6J and BALB/cJ, which have shown disparate phenotypic and immune responses in other disease models. We used pulmonary functional tests, lung mechanics, and lung histopathology to show that BALB/cJ mice were not only much more sensitive to pulmonary hemorrhage, edema, and alveolar tissue destruction, but also show an accelerated chronic progression of elastase-induced emphysema compared to C57BL/6J mice. This response to elastase by the BALB/cJ strain is consistent with the exacerbated phenotypes reported for other murine emphysema models, including chronic ozone and hookworm infection. We then showed how differences in the production of IFN-γ, IL-17A, and the activation status of macrophages between these two strains might contribute to the degree of pathology in the lung. While the resistant C57BL/6J strain had greater increases in the expression of IFN-γ, the sensitive BALB/cJ mice had a higher elevation of Th17-associated cytokine gene expression (IL-17A, IL-6, IL-1β and IL-18) and greater activation of macrophages (with both M1 and M2 markers), especially in the expression of the genes encoding the proteases MMP-2 and MMP-12.

To clarify the significance of these cytokines and their activation, studies were conducted using mice carrying targeted genetic manipulation of several key genes. We showed that deficiency of either IFN-γ or IL-17A ameliorated the severity of elastase-induced emphysema. These results indicate a potential contribution of these cytokines/signaling pathways in the general development of emphysema. Also, the data suggest that different

pathways in the two strains of mice might primarily drive elastase-induced emphysema, specifically by IFN-γ in C57BL/6J mice and by IL-17A in BALB/cJ mice.

Somewhat surprisingly, we found that systemic depletion of neutrophils or the lack of B and T lymphocytes in RAG-$1^{-/-}$ mice had no significant impact on the degree of elastase-induced emphysema. However, our data does suggest an important role for macrophages in the pathogenesis of elastase-induced emphysema. Mice deficient in key transcriptional regulators of alternative macrophage activation (i.e., STAT6 and STAT3) were moderately protected from elastase-induced emphysema. Given that BALB/cJ mice had a greater number of long-lived macrophages in the BAL and higher expression of activation markers including matrix-remodeling enzymes (MMP-2, MMP-12), these changes in macrophage activation might account for the BALB/cJ strain showing increased sensitivity to emphysema in both the acute and chronic disease stages.

Our experiments also showed a potential role for the IL-33/ST2/MyD88 signaling pathway in the progression of elastase-induced emphysema. IL-33 is released during necrotic cell death or epithelial damage and has been shown to enhance the alternative activation of macrophages [488]. We observed increased IL-33 and ST2 expression after elastase injury, which is consistent with previous data from our laboratory showing elevated IL-33 protein in the lungs following elastase challenge. Blockade of this IL-33/ST2/MyD88 axis by using mice lacking either the ST2 receptor or the MyD88 adaptor protein had a significant impact on elastase-induced emphysema by lessening the severity of pathology.

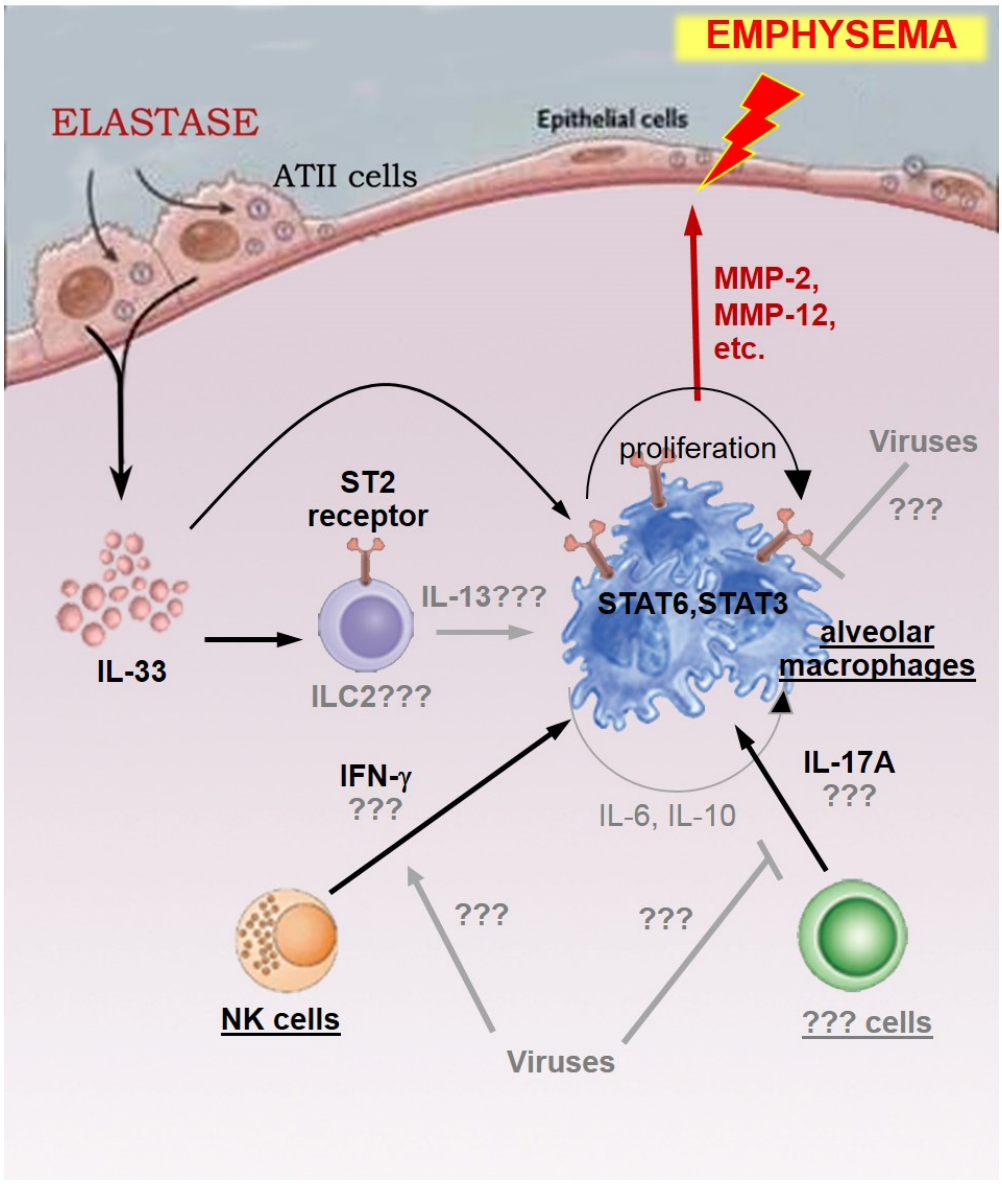

Figure 6.1 Proposed model for the pathogenesis of elastase-induced emphysema and the effects of viral infection. The data from this study and other previous studies are presented in dark black and red colors. Hypothesized pathways are illustrated in light grey.

Fig. 6-1 represents a mechanistic model for maintenance of progressive lung damage in elastase-induced experimental emphysema that summarizes the relevant signaling pathways supported by the data presented in this dissertation. This model places macrophages as the central effector cells, and their activation leads to the release of several extracellular matrix-degrading proteases (such as MMP-2, MMP-12) that subsequently contribute to the progression of emphysema. The activation of these deleterious macrophages is in part via STAT6 and STAT3 phosphorylation and can be triggered and modulated by several mediators such as IL-33, IL-17A, and IFN-γ. So with the initial acute elastase insult, there is damage of epithelial tissue, degradation of the extracellular matrix, and generation of cells undergoing necrotic and pyroptotic death, which serves to drive the release of the epithelial-derived alarmin, IL-33. We hypothesize that IL-33 binds directly to the ST2/IL1RAP receptor on the surface of alveolar macrophages and activates them toward a protease-secreting phenotype. Alternatively, IL-33 may bind to receptors on type 2 innate lymphoid cells (ILC2) causing them to release IL-13, which results in M2 activation of macrophages. These two modes of IL-33-meidated activation of macrophages are not mutually exclusive. In addition, lung macrophages also express the receptor for IL-17A. Elevated IL-17A, especially in BALB/cJ mice after elastase challenge, can enhance the production of MMPs by macrophages. The activated macrophages might also serve as autocrine sources of IL-6 and IL-10, which in turn promote STAT3 phosphorylation and perpetuate their own activation. Lastly, MMP expression in macrophages might be induced by IFN-γ following the administration of elastase, particularly in C57BL/6J mice. Although MMPs were shown to be induced in alternatively activated macrophages *in vitro*, some studies have suggested that IFN-γ, primarily an inducer of classical macrophage activation, can indirectly stimulate the production of several MMPs via the induction of CCR5 ligands *in vivo* [173, 511].

This hypothesized schematic pathway is supported by several human and animal studies. Patients with COPD/emphysema and animals exposed to cigarette smoke often have elevations of IFN-γ, IL-17A, as well as activated macrophages in the lungs [160, 167, 169, 181, 187, 464, 465, 475]. Overexpression of IFN-γ in the murine lung can induce MMP-12 production leading to pulmonary emphysema [173]. Lung specific, transgenic mice overexpressing-IL-17A had more BAL macrophages, greater MMP-12 expression, and had exaggerated emphysema when exposed to cigarette smoke [187]. Conversely, either IFN-γ or IL-17A deficient mice exposed to cigarette smoke had fewer numbers of BAL macrophages, reduced expression of MMP-12, and developed a lesser degree of emphysema compared to wild-type controls [187, 511].

The development, progression and severity of emphysema in humans is influence by a number of environmental factors. To provide evidence that environmental factors impact progression in the elastase-induced experimental emphysema model (Fig. 6-1), we utilized two viral infection models: vaccinia and influenza A. Vaccinia virus was selected because it has been shown to induce IFN-γ production and alternative macrophage activation while decreasing IL-17 production [525]. Our study is the first to show how a prior infection can affect the development of elastase-induced emphysema. Interestingly, pre-infection with vaccinia virus resulted in differential effects on elastase-induced emphysema between C57BL/6J and BALB/cJ mice. In C57BL/6J mice, prior vaccinia virus amplified the elastase-induced emphysematous changes, possibly due to the induction of IFN-γ by vaccinia virus in Th1-biased C57BL/6J mice. In contrast, in BALB/cJ mice vaccinia virus

prevented the development of emphysema, possibly due to the impaired production of IL-17 following vaccinia infection. We confirmed these results by using influenza A virus, a virus that is more relevant to humans. Similar to the vaccinia virus results, pre-inoculation of influenza A virus could ameliorate the severity of elastase-induced emphysema in BALB/cJ mice. However, we did not observe the significant impact of infection with influenza A virus (14 days prior to elastase challenge) on the development of emphysema in C57BL/6J mice. This lack of effect may have been caused by the increased (14 day) length of time post-infection when the mice were studied.

Overall, these results show that the underlying mechanisms of elastase-induced emphysema are quite complex and involve several types of immune cells and mediators beyond the proteolytic activity of exogenously-administered elastase. As such, emphysema can be considered as a disease that results from the outcome of multiple hits originating from a variety of initiating factors (e.g. cigarette smoke), with upstream and downstream modulation by a complex combination of both genetic and environmental factors.

An important finding from this thesis is that BALB/cJ mice are more sensitive to elastase-induced emphysema than C57BL/6J mice. This result is advantageous, since an understanding of the reasons for this differential sensitivity in the BALB/cJ strain might lead to mechanistic insights that could lead to new therapeutic interventions to delay or lessen the progression of emphysema. Another important (and perhaps related) finding is the differential effect in the two mouse strains when infected with virus prior to an elastase insult. Prior infection with vaccinia augmented the severity of the elastase-induced emphysema in C57BL/6J mice, but it significantly lessened the emphysematous outcome in

BALB/cJ mice. The implications of this could be profound, since many studies often use only one genetically identical inbred mouse strain (particularly C57BL/6J mice) to study emphysema, and it is now quite reasonable to question whether such published observations can be generally extrapolated to what might happen in the context of human emphysema. Studies utilizing just a single mouse strain may in fact be representative of only single individuals or groups of genetically similar individuals, and likely would not reflect the diversity of responsiveness you might expect to exist within a heterogeneous population. Ultimately, the data presented here might provide some insight as to why not all smokers develop emphysema. Furthermore, since many drugs have been shown to provide effective protection against emphysema in animal models, but have failed to translate successfully into the clinic, our results offer a possible explanation for this disparity. Even if a therapy holds promise for certain individuals, it may not be generally useful across a genetically diverse population.

A comment on the lung phenotyping approaches utilized in our mouse studies is also warranted here. One of the essential steps in the study of emphysema is an unbiased and accurate quantitative assessment of emphysematous changes to the lung. Although a careful quantitation of airspace size (L_m) should be mandatory to properly characterize changes to lung structure, an increase in L_m by itself does not always implicate the destruction of alveolar walls, because L_m is also a function of lung volume [558]. Many published studies fail to consider how changes in lung volume can affect L_m, and most studies do not measure lung volumes. Thus, there is an ongoing dispute over the most appropriate morphometric quantitative analyses for emphysematous changes in animal models and in humans [293, 558, 559]. Of importance, L_m is not used routinely to identify emphysema in humans. While most

investigators attempt to demonstrate emphysematous changes in animal models solely based on changes to L_m, one of the strengths of the studies presented here is the combination of quantitative assessments of histological sections used in conjunction with pulmonary function tests. The loss of alveolar walls (gas exchange surface area) and the subsequent loss of elastic recoil were quantified by DF_{CO} measurements and lung P-V curves to demonstrate phenotypic physiological changes during the progression of emphysema. Indeed, DF_{CO} is a functional test quite similar to what is more generally used in human subjects (DL_{CO}). Accurate phenotyping in mice provides animal studies with more meaningful data that can then be used to better link potential disease mechanisms and therapeutic interventions discovered in the lab to changes in lung structure and function observed in the clinic.

6.2 Limitations of the study

Although the elastase-induced emphysema model resembles human emphysema in many ways, thereby providing a good opportunity to study the progressive nature of the disease, this model has several important limitations. The elastase model can be considered one of chronic sterile inflammation, originating from a single insult which initially causes acute lung injury but subsequently triggers a mild degree of chronic inflammation that eventually leads to progressive emphysema. Most of the sustained elevation of immune cells following elastase injury in the lung is attributable to macrophages. Neutrophils and lymphocytes are recruited only during the first week of injury and are quickly cleared from the lungs. After much experimentation we could find no convincing contribution of these cells beyond the acute phase of disease onset. However, it would be presumptuous to entirely rule out the importance of neutrophils and lymphocytes in human emphysema. In humans, the onset of emphysema may involve the repetition of insults that result in the accumulation of

inflammatory cells including neutrophils and lymphocytes in the lung parenchyma and alveolar space. And if there were a long-term presence of neutrophils and lymphocytes in the lungs of patients with emphysema, particularly during infections, these cells might play a bigger role in the development of human emphysema than what we can accurately study following an acute elastase insult in our animal model.

To explore the immunological pathways involved in the pathogenesis of emphysema in Chapter 4, we utilized genetically-engineered mice with deletions of relevant immune genes. While knockout animal technology represents a valuable research tool, several concerns with such knockout mice should be addressed. One important drawback of using genetically engineered mice is that the absence of a specific gene itself might have some consequences, which affect either the expression or the function of other genes and could have secondary effects on the outcome of experiments and their subsequent interpretation. Also, redundant mechanisms might be activated to compensate for a specific gene deletion. Moreover, the mixed genetic background of the knockout mice may also impact the experimental results. Knockout mice were originally generated from 129/Sv embryonic stem cells, fused with C57BL/6J blastocysts, and then backcrossed for several generations onto the desired background strains. However, given the limitation of resources, it was not feasible to retrace the number of generations each of our knockout strains were backcrossed and thus how pure the present genetic background is. Furthermore, it should be noted that even ten generations of backcrossing might not be sufficient to adequately homogenize the genetic background, and thus sufficient backcrossing and colony maintenance represents a daunting task [560]. In this thesis we emphasize that there are different susceptibilities to emphysema between two strains of mice. However, if the knockout mice (particularly on the BALB/cJ

background) used in this study retained some degree of coding or regulatory content from other background strains, it might have a significant impact on our results. In practice, although often not achievable, it would be best to breed these genetically altered mice as heterozygous x heterozygous and use the littermate wild-types derived from the same parent strain that was originally used to backcross the mice as controls to avoid genetic background effects. Also, other approaches such as the recently described CRISPR/Cas9 knockout system and the targeting of specific cytokines or signaling pathways with neutralizing antibodies or specific inhibitors should be done to validate the results from conventional knockout animal experiments.

6.3 Moving forward: Future directions

While this dissertation has yielded several interesting results, there are many outstanding issues to be addressed.

(i) Contribution of macrophages to the development of emphysema. In this study, we identified a role for macrophages as key effector cells in the pathogenesis of emphysema. This speculation was based on data showing that macrophages can produce several tissue degrading enzymes. In addition, a deficiency of either STAT6 or STAT3, which can alter the activation of macrophages, offered some degree of protection from elastase-induced emphysema. However, these observations do not truly verify the contribution of macrophages, since these enzymes can also be produced by other cell types. Also, the $STAT6^{-/-}$ mice and Cre-Lyz/$STAT3^{fl/fl}$ mice we used for our studies do not lack these genes only in macrophages, but also in other cell types, which could act separately from macrophage activation. Other approaches, such as the depletion of macrophages, are

necessary in order to confirm the role of macrophages. Previous data by Dr. Daniel Lagassé, a former graduate student in our group, showed that the increasing number of macrophages in the lung following elastase treatment resulted from the proliferation of $CD11c^+$ alveolar macrophages residing in the lung, rather than from blood monocytes recruited from the peripheral circulation. This result adds the possibility of using transgenic mice containing the diphtheria toxin receptor gene under the CD11c promoter (CD11c-DTR mice) as an alternative way to deplete alveolar macrophages.

Although we have paid much attention here to alternatively activated macrophages, classically activated or regulatory macrophages might also play important roles in emphysema. There have been many studies looking at the activation status of macrophages in human COPD/emphysema. Some investigators have shown a predominance of M1 macrophages, whereas others have described the presence of M2 macrophages or macrophages that display a mix of the M1 and M2 phenotypes. One issue that further complicates this issue of macrophage activation is the inconsistent use of the markers used to characterize these cells across a number of these studies. Furthermore, M2 macrophages can be subdivided into several (not yet standardized) subtypes. A new concept of regulatory macrophages, distinct from classically and alternatively activated macrophages has also been proposed [561]. It is critical to this field to standardize the characterization of these cell types in order to provide consistency among investigators. A better understanding of macrophage heterogeneity in the pathogenesis of emphysema may reveal a better molecular target to develop new therapies for the disease.

Matrix metalloprotease-12 (MMP-12) is mainly produced by macrophages and is believed by many to account for the major matrix destruction in the lungs of mice. This hypothesis is based on several studies showing an association between the expression of lung MMP-12 and the severity of emphysema in experimental rodents. Unfortunately, although MMP-12 inhibitors have been developed, none of them have been successfully shown to be beneficial for treating emphysema in humans. This might result for several reasons. (i) There have been controversial reports in humans questioning whether MMP-12 is actually up-regulated in COPD patients [562]. (ii) MMP-12 in rodents has a pro-inflammatory effect, whereas MMP-12 in humans is not necessarily pro-inflammatory and actually inhibits neutrophil recruitment in certain scenarios. In general, it seems unlikely that the inhibition of one specific enzyme could be used as a broad-spectrum therapy to treat emphysema. A more realistic approach to treat emphysema might be to take advantage of the plasticity of macrophages to reprogram or shift their polarization status to a more beneficial phenotype.

(ii) Source of IL-17A. Our data showed a role of IL-17A in modulating the function of macrophages and determining the extent of elastase-induced emphysema. However, data obtained from RAG-1$^{-/-}$ in our model would seem to suggest that the critical source of IL-17A is not T cells - normally the primary source of IL-17A. So which cells might be producing this cytokine in response to elastase injury? Other cell types now shown to secrete IL-17A include type 3 innate lymphoid cells (ILC3s), NK cells, monocytes, and even alveolar macrophages [525, 563]. For example, Song *et al.* showed that IL-17A produced by alveolar macrophages can be mediated by allergic challenges [563]. We speculate that elevated IL-17A in our model might be coming from either alveolar macrophages or ILC3s. However, this assertion remains to be tested.

(iii) Significance of IL-33/ST2 and type 2 cytokines. One of the important findings in this dissertation is the significant role of the IL-33/ST2 axis in elastase-induced emphysema. Although IL-33 can stimulate activation markers in macrophages by itself [564], it is also well known to be able to amplify the alternative activation of macrophages by eliciting IL-13 secretion from ILC2s. It would be interesting to investigate whether the production of IL-13 by ILC2, as induced by IL-33, plays any role in the elastase-induced emphysema model. Even though we did not observe an increased expression of IL-13 in the lung after elastase administration, it is important to note that this effect was only shown at the mRNA level in the whole lung, and not in isolated cells or at the protein level. In addition, there are relatively few ILC2 cells in the lungs, so changes in their expression of IL-13 might be masked by changes in other more abundant cell types. Moreover, although we have emphasized an important contribution of IFN-γ and IL-17A, we have not entirely ruled out roles for type 2 cytokines (IL-4, IL-5 and IL-13). Indeed, we also observed an elevated expression level of IL-4 and IL-5 in response to elastase challenge at certain time points, so these cytokines might still play some role in the pathologic mechanism. .

Another unknown pertains to what forms of IL-33 are involved during elastase-induced emphysema. IL-33 is constitutively expressed particularly in Type II epithelial cells of the mouse lung as a 30 kDa full-length nuclear protein. After cellular injury, IL-33 can be released to the extracellular space where it is subjected to cleavage by several proteolytic enzymes into a variety of highly bioactive forms [565]. Given the fact that there are a number of proteases present in the alveolar space after elastase injury, it would be important to determine which enzymes are involved in the cleavage of pro-IL-33 and which bioactive

forms of IL-33 play the most important role in our model. Furthermore, the IL-33 receptor, ST2, also has two isoforms: a membrane-bound receptor form (known as ST2L) and a soluble ST2 form (sST2). The soluble ST2 form lacks the transmembrane domain and is proposed to be a decoy receptor with no intrinsic signaling ability. This raises the question whether the neutralization of IL-33 by administration of sST2 could possibly serve as a therapeutic intervention in emphysema.

(iv) Role of viral infection. Our data also show that the prior exposure to viruses can alter the severity of elastase-induced emphysema. However, the mechanisms underlying this effect are unclear, and it warrants further study. The levels of IFN-γ and IL-17A and the function of macrophages (including MMP-12 expression) need to be assessed following viral inoculation and elastase administration. Further experiments using knockout mice (e.g. IFN-$\gamma^{-/-}$ or IL-17A$^{-/-}$) and/or neutralizing antibodies should be performed to further clarify the mechanism.

REFERENCES

1. Weibel, E.R., *Chapter II - Organization of the Human Lung*, in *Morphometry of the Human Lung*, E.R. Weibel, Editor. 1963, Academic Press. p. 4-9.
2. Weibel, E.R., B. Sapoval, and M. Filoche, *Design of peripheral airways for efficient gas exchange.* Respir Physiol Neurobiol, 2005. **148**(1-2): p. 3-21.
3. Suarez, C.J., S.M. Dintzis, and C.W. Frevert, *9 - Respiratory*, in *Comparative Anatomy and Histology*, P.M.T.M. Dintzis, Editor. 2012, Academic Press: San Diego. p. 121-134.
4. Caduff, J.H., L.C. Fischer, and P.H. Burri, *Scanning electron microscope study of the developing microvasculature in the postnatal rat lung.* Anat Rec, 1986. **216**(2): p. 154-64.
5. Weibel, E.R., *What makes a good lung?* Swiss Med Wkly, 2009. **139**(27-28): p. 375-86.
6. Weibel, E.R., *Symmorphosis: On Form and Function in Shaping Life.* 2000: Harvard University Press.
7. Ochs, M., J.R. Nyengaard, A. Jung, L. Knudsen, M. Voigt, T. Wahlers, et al., *The Number of Alveoli in the Human Lung.* American Journal of Respiratory and Critical Care Medicine, 2004. **169**(1): p. 120-124.
8. Hasleton, P.S., *The internal surface area of the adult human lung.* J Anat, 1972. **112**(Pt 3): p. 391-400.
9. Wiebe, B.M. and H. Laursen, *Human lung volume, alveolar surface area, and capillary length.* Microsc Res Tech, 1995. **32**(3): p. 255-62.
10. Sacco, J.J., J. Botten, F. Macbeth, A. Bagust, and P. Clark, *The average body surface area of adult cancer patients in the UK: a multicentre retrospective study.* PLoS One, 2010. **5**(1): p. e8933.
11. Knust, J., M. Ochs, H.J. Gundersen, and J.R. Nyengaard, *Stereological estimates of alveolar number and size and capillary length and surface area in mice lungs.* Anat Rec (Hoboken), 2009. **292**(1): p. 113-22.
12. Barkauskas, C.E., M.J. Cronce, C.R. Rackley, E.J. Bowie, D.R. Keene, B.R. Stripp, et al., *Type 2 alveolar cells are stem cells in adult lung.* J Clin Invest, 2013. **123**(7): p. 3025-36.
13. Adamson, I.Y. and D.H. Bowden, *The pathogenesis of bleomycin-induced pulmonary fibrosis in mice.* Am J Pathol, 1974. **77**(2): p. 185-97.
14. Mason, R.J., *Biology of alveolar type II cells.* Respirology, 2006. **11 Suppl**: p. S12-5.
15. Matthay, M.A., L. Robriquet, and X. Fang, *Alveolar epithelium: role in lung fluid balance and acute lung injury.* Proc Am Thorac Soc, 2005. **2**(3): p. 206-13.
16. Hussell, T. and T.J. Bell, *Alveolar macrophages: plasticity in a tissue-specific context.* Nat Rev Immunol, 2014. **14**(2): p. 81-93.
17. Ely, K.H., T. Cookenham, A.D. Roberts, and D.L. Woodland, *Memory T cell populations in the lung airways are maintained by continual recruitment.* J Immunol, 2006. **176**(1): p. 537-43.

18. WH, O. *Global Health Estimates 2014 Summary Tables: Deaths by cause, age and sex, 2000–2012* Updated May 2014 [cited 2015 January].

19. Hoyert, D.L. and J. Xu, *Deaths: preliminary data for 2011.* Natl Vital Stat Rep, 2012. **61**(6): p. 1-51.

20. Horton, R., *GBD 2010: understanding disease, injury, and risk.* Lancet, 2012. **380**(9859): p. 2053-4.

21. Gershon, A.S., L. Warner, P. Cascagnette, J.C. Victor, and T. To, *Lifetime risk of developing chronic obstructive pulmonary disease: a longitudinal population study.* Lancet, 2011. **378**(9795): p. 991-6.

22. Guarascio, A.J., S.M. Ray, C.K. Finch, and T.H. Self, *The clinical and economic burden of chronic obstructive pulmonary disease in the USA.* Clinicoecon Outcomes Res, 2013. **5**: p. 235-45.

23. Yasothan, U. and S. Kar, *Therapies for COPD.* Nat Rev Drug Discov, 2008. **7**(4): p. 285-286.

24. Barnes, P.J., *New anti-inflammatory targets for chronic obstructive pulmonary disease.* Nat Rev Drug Discov, 2013. **12**(7): p. 543-59.

25. Vestbo, J.r., S.S. Hurd, A.G. Agust, P.W. Jones, C. Vogelmeier, A. Anzueto, et al., *Global Strategy for the Diagnosis, Management, and Prevention of Chronic Obstructive Pulmonary Disease.* American Journal of Respiratory and Critical Care Medicine, 2013. **187**(4): p. 347-365.

26. Hogg, J.C. and W. Timens, *The pathology of chronic obstructive pulmonary disease.* Annu Rev Pathol, 2009. **4**: p. 435-59.

27. Decramer, M., W. Janssens, and M. Miravitlles, *Chronic obstructive pulmonary disease.* Lancet, 2012. **379**(9823): p. 1341-51.

28. *Standards for the diagnosis and care of patients with chronic obstructive pulmonary disease. American Thoracic Society.* Am J Respir Crit Care Med, 1995. **152**(5 Pt 2): p. S77-121.

29. *The definition of emphysema. Report of a National Heart, Lung, and Blood Institute, Division of Lung Diseases workshop.* Am Rev Respir Dis, 1985. **132**(1): p. 182-5.

30. Pauwels, R.A., A.S. Buist, P.M. Calverley, C.R. Jenkins, S.S. Hurd, and G.S. Committee, *Global strategy for the diagnosis, management, and prevention of chronic obstructive pulmonary disease. NHLBI/WHO Global Initiative for Chronic Obstructive Lung Disease (GOLD) Workshop summary.* Am J Respir Crit Care Med, 2001. **163**(5): p. 1256-76.

31. Rabe, K.F., S. Hurd, A. Anzueto, P.J. Barnes, S.A. Buist, P. Calverley, et al., *Global strategy for the diagnosis, management, and prevention of chronic obstructive pulmonary disease: GOLD executive summary.* Am J Respir Crit Care Med, 2007. **176**(6): p. 532-55.

32. Lindberg, A., L.G. Larsson, E. Ronmark, A.C. Jonsson, K. Larsson, and B. Lundback, *Decline in FEV1 in relation to incident chronic obstructive pulmonary disease in a cohort with respiratory symptoms.* COPD, 2007. **4**(1): p. 5-13.

33. Lindberg, A., A. Bjerg, E. Ronmark, L.G. Larsson, and B. Lundback, *Prevalence and underdiagnosis of COPD by disease severity and the attributable fraction of smoking* Report *from*

the Obstructive Lung Disease in Northern Sweden Studies. Respir Med, 2006. **100**(2): p. 264-72.

34. Coultas, D.B., D. Mapel, R. Gagnon, and E. Lydick, *The health impact of undiagnosed airflow obstruction in a national sample of United States adults.* Am J Respir Crit Care Med, 2001. **164**(3): p. 372-7.

35. Menezes, A.M., R. Perez-Padilla, J.R. Jardim, A. Muino, M.V. Lopez, G. Valdivia, et al., *Chronic obstructive pulmonary disease in five Latin American cities (the PLATINO study): a prevalence study.* Lancet, 2005. **366**(9500): p. 1875-81.

36. Buist, A.S., M.A. McBurnie, W.M. Vollmer, S. Gillespie, P. Burney, D.M. Mannino, et al., *International variation in the prevalence of COPD (the BOLD Study): a population-based prevalence study.* Lancet, 2007. **370**(9589): p. 741-50.

37. O'Kelly, S., S.M. Smith, S. Lane, C. Teljeur, and T. O'Dowd, *Chronic respiratory disease and multimorbidity: prevalence and impact in a general practice setting.* Respir Med, 2011. **105**(2): p. 236-42.

38. Mannino, D.M., D.M. Homa, L.J. Akinbami, E.S. Ford, and S.C. Redd, *Chronic obstructive pulmonary disease surveillance--United States, 1971-2000.* Respir Care, 2002. **47**(10): p. 1184-99.

39. Bresnitz, E.A., *Epidemiology of advanced lung disease in the United States.* Clin Chest Med, 1997. **18**(3): p. 421-33.

40. General, U.S.P.H.S.O.o.t.S., *The Health Consequences of Smoking: Chronic Obstructive Lung Disease: A Report of the Surgeon General* D.R. Shopland, Editor. 1984.

41. Sethi, J.M. and C.L. Rochester, *Smoking and chronic obstructive pulmonary disease.* Clin Chest Med, 2000. **21**(1): p. 67-86, viii.

42. Salvi, S.S. and P.J. Barnes, *Chronic obstructive pulmonary disease in non-smokers.* Lancet, 2009. **374**(9691): p. 733-43.

43. Beyer, D., H. Mitfessel, and A. Gillissen, *Maternal smoking promotes chronic obstructive lung disease in the offspring as adults.* Eur J Med Res, 2009. **14 Suppl 4**: p. 27-31.

44. Hylkema, M.N. and M.J. Blacquiere, *Intrauterine effects of maternal smoking on sensitization, asthma, and chronic obstructive pulmonary disease.* Proc Am Thorac Soc, 2009. **6**(8): p. 660-2.

45. Sahebjami, H., *Emphysema-like changes in HIV.* Ann Intern Med, 1992. **116**(10): p. 876.

46. Taraseviciene-Stewart, L. and N.F. Voelkel, *Molecular pathogenesis of emphysema.* J Clin Invest, 2008. **118**(2): p. 394-402.

47. Dossing, M., J. Khan, and F. al-Rabiah, *Risk factors for chronic obstructive lung disease in Saudi Arabia.* Respir Med, 1994. **88**(7): p. 519-22.

48. Anderson, H.R., *Chronic lung disease in the Papua New Guinea Highlands.* Thorax, 1979. **34**(5): p. 647-53.

49. Dennis, R.J., D. Maldonado, S. Norman, E. Baena, and G. Martinez, *Woodsmoke exposure and risk for obstructive airways disease among women.* Chest, 1996. **109**(1): p. 115-9.

50. Kiraz, K., L. Kart, R. Demir, S. Oymak, I. Gulmez, M. Unalacak, et al., *Chronic pulmonary disease in rural women exposed to biomass fumes.* Clin Invest Med, 2003. **26**(5): p. 243-8.

51. Ekici, A., M. Ekici, E. Kurtipek, A. Akin, M. Arslan, T. Kara, et al., *Obstructive airway diseases in women exposed to biomass smoke.* Environ Res, 2005. **99**(1): p. 93-8.

52. Lamprecht, B., L. Schirnhofer, B. Kaiser, M. Studnicka, and A.S. Buist, *Farming and the prevalence of non-reversible airways obstruction: results from a population-based study.* Am J Ind Med, 2007. **50**(6): p. 421-6.

53. Organization, W.H., *Burden of disease from Household Air Pollution for 2012*. 2014.

54. in *Global Burden of Disease and Risk Factors*, A.D. Lopez, et al., Editors. 2006: Washington (DC).

55. Cox, D.W., S.L. Woo, and T. Mansfield, *DNA restriction fragments associated with alpha 1-antitrypsin indicate a single origin for deficiency allele PI Z.* Nature, 1985. **316**(6023): p. 79-81.

56. Seixas, S., O. Garcia, M.J. Trovoada, M.T. Santos, A. Amorim, and J. Rocha, *Patterns of haplotype diversity within the serpin gene cluster at 14q32.1: insights into the natural history of the alpha1-antitrypsin polymorphism.* Hum Genet, 2001. **108**(1): p. 20-30.

57. Blanco, I., F.J. de Serres, E. Fernandez-Bustillo, B. Lara, and M. Miravitlles, *Estimated numbers and prevalence of PI*S and PI*Z alleles of alpha1-antitrypsin deficiency in European countries.* Eur Respir J, 2006. **27**(1): p. 77-84.

58. Laurell, C.B. and S. Eriksson, *The electrophoretic a;1-globulin pattern of serum in a;1-antitrypsin deficiency.* Scandinavian Journal of Clinical and Laboratory Investigation, 1963. **15**(2): p. 132-140.

59. Wan, E.S. and E.K. Silverman, *Genetics of COPD and emphysema.* Chest, 2009. **136**(3): p. 859-66.

60. Silverman, E.K. and R.A. Sandhaus, *Clinical practice. Alpha1-antitrypsin deficiency.* N Engl J Med, 2009. **360**(26): p. 2749-57.

61. Lieberman, J., B. Winter, and A. Sastre, *Alpha 1-antitrypsin Pi-types in 965 COPD patients.* Chest, 1986. **89**(3): p. 370-3.

62. Wu, L., J. Chau, R.P. Young, V. Pokorny, G.D. Mills, R. Hopkins, et al., *Transforming growth factor-beta1 genotype and susceptibility to chronic obstructive pulmonary disease.* Thorax, 2004. **59**(2): p. 126-9.

63. Hersh, C.P., D.L. Demeo, C. Lange, A.A. Litonjua, J.J. Reilly, D. Kwiatkowski, et al., *Attempted replication of reported chronic obstructive pulmonary disease candidate gene associations.* Am J Respir Cell Mol Biol, 2005. **33**(1): p. 71-8.

64. Harrison, D.J., A.M. Cantlay, F. Rae, D. Lamb, and C.A. Smith, *Frequency of glutathione S-transferase M1 deletion in smokers with emphysema and lung cancer.* Hum Exp Toxicol, 1997. **16**(7): p. 356-60.

65. He, J.Q., J.E. Connett, N.R. Anthonisen, P.D. Pare, and A.J. Sandford, *Glutathione S-transferase variants and their interaction with smoking on lung function.* Am J Respir Crit Care Med, 2004. **170**(4): p. 388-94.

66. Guo, X., H.M. Lin, Z. Lin, M. Montano, R. Sansores, G. Wang, et al., *Surfactant protein gene A, B, and D marker alleles in chronic obstructive pulmonary disease of a Mexican population.* Eur Respir J, 2001. **18**(3): p. 482-90.

67. Ito, I., S. Nagai, Y. Hoshino, S. Muro, T. Hirai, M. Tsukino, et al., *Risk and severity of COPD is associated with the group-specific component of serum globulin 1F allele.* Chest, 2004. **125**(1): p. 63-70.

68. MacNee, W., *Pathogenesis of chronic obstructive pulmonary disease.* Proc Am Thorac Soc, 2005. **2**(4): p. 258-66; discussion 290-1.

69. Stoller, J.K. and L.S. Aboussouan, *Alpha1-antitrypsin deficiency.* Lancet, 2005. **365**(9478): p. 2225-36.

70. Snider, G.L. and C.B. Sherter, *A one-year study of the evolution of elastase-induced emphysema in hamsters.* J Appl Physiol Respir Environ Exerc Physiol, 1977. **43**(4): p. 721-9.

71. Gross, P., E.A. Pfitzer, E. Tolker, M.A. Babyak, and M. Kaschak, *Experimental Emphysema: Its Production with Papain in Normal and Silicotic Rats.* Arch Environ Health, 1965. **11**: p. 50-8.

72. Barnes, P.J., *Mediators of chronic obstructive pulmonary disease.* Pharmacol Rev, 2004. **56**(4): p. 515-48.

73. Gottlieb, D.J., P.J. Stone, D. Sparrow, M.E. Gale, S.T. Weiss, G.L. Snider, et al., *Urinary desmosine excretion in smokers with and without rapid decline of lung function: the Normative Aging Study.* Am J Respir Crit Care Med, 1996. **154**(5): p. 1290-5.

74. Huang, J.T., R. Chaudhuri, O. Albarbarawi, A. Barton, C. Grierson, P. Rauchhaus, et al., *Clinical validity of plasma and urinary desmosine as biomarkers for chronic obstructive pulmonary disease.* Thorax, 2012. **67**(6): p. 502-8.

75. Sayed, L., Y. Soha, R. Eman, and A. Ahmed, *Study of blood desmosine level in patients with COPD exacerbation in relation to severity.* Egyptian Journal of Chest Diseases and Tuberculosis, 2014. **63**(3).

76. Attia, A., E.l. Abd, A. Halim, E. Shebl, and A. Ali, *Utility of Total Desmosine as Biomarker for Chronic Obstructive Pulmonary Disease Patient.* J Pulm Respir Med 2013. **3**(152).

77. Owen, C.A., M.A. Campbell, S.S. Boukedes, and E.J. Campbell, *Cytokines regulate membrane-bound leukocyte elastase on neutrophils: a novel mechanism for effector activity.* Am J Physiol, 1997. **272**(3 Pt 1): p. L385-93.

78. Segal, A.W., *How neutrophils kill microbes.* Annu Rev Immunol, 2005. **23**: p. 197-223.

79. Papayannopoulos, V., K.D. Metzler, A. Hakkim, and A. Zychlinsky, *Neutrophil elastase and myeloperoxidase regulate the formation of neutrophil extracellular traps.* J Cell Biol, 2010. **191**(3): p. 677-91.

80. Senior, R.M., H. Tegner, C. Kuhn, K. Ohlsson, B.C. Starcher, and J.A. Pierce, *The induction of pulmonary emphysema with human leukocyte elastase.* Am Rev Respir Dis, 1977. **116**(3): p. 469-75.

81. Janoff, A., B. Sloan, G. Weinbaum, V. Damiano, R.A. Sandhaus, J. Elias, et al., *Experimental emphysema induced with purified human neutrophil elastase: tissue localization of the instilled protease.* Am Rev Respir Dis, 1977. **115**(3): p. 461-78.

82. Damiano, V.V., A. Tsang, U. Kucich, W.R. Abrams, J. Rosenbloom, P. Kimbel, et al., *Immunolocalization of elastase in human emphysematous lungs.* J Clin Invest, 1986. **78**(2): p. 482-93.

83. Shapiro, S.D., N.M. Goldstein, A.M. Houghton, D.K. Kobayashi, D. Kelley, and A. Belaaouaj, *Neutrophil elastase contributes to cigarette smoke-induced emphysema in mice.* Am J Pathol, 2003. **163**(6): p. 2329-35.

84. Cavarra, E., B. Bartalesi, M. Lucattelli, S. Fineschi, B. Lunghi, F. Gambelli, et al., *Effects of cigarette smoke in mice with different levels of alpha(1)-proteinase inhibitor and sensitivity to oxidants.* Am J Respir Crit Care Med, 2001. **164**(5): p. 886-90.

85. Takubo, Y., A. Guerassimov, H. Ghezzo, A. Triantafillopoulos, J.H. Bates, J.R. Hoidal, et al., *Alpha1-antitrypsin determines the pattern of emphysema and function in tobacco smoke-exposed mice: parallels with human disease.* Am J Respir Crit Care Med, 2002. **166**(12 Pt 1): p. 1596-603.

86. Kuna, P., M. Jenkins, C.D. O'Brien, and W.A. Fahy, *AZD9668, a neutrophil elastase inhibitor, plus ongoing budesonide/formoterol in patients with COPD.* Respir Med, 2012. **106**(4): p. 531-9.

87. Vogelmeier, C., T.O. Aquino, C.D. O'Brien, J. Perrett, and K.A. Gunawardena, *A randomised, placebo-controlled, dose-finding study of AZD9668, an oral inhibitor of neutrophil elastase, in patients with chronic obstructive pulmonary disease treated with tiotropium.* COPD, 2012. **9**(2): p. 111-20.

88. Luisetti, M., C. Sturani, D. Sella, E. Madonini, V. Galavotti, G. Bruno, et al., *MR889, a neutrophil elastase inhibitor, in patients with chronic obstructive pulmonary disease: a double-blind, randomized, placebo-controlled clinical trial.* Eur Respir J, 1996. **9**(7): p. 1482-6.

89. Groutas, W.C., D. Dou, and K.R. Alliston, *Neutrophil elastase inhibitors.* Expert Opin Ther Pat, 2011. **21**(3): p. 339-54.

90. Lucas, S.D., E. Costa, R.C. Guedes, and R. Moreira, *Targeting COPD: advances on low-molecular-weight inhibitors of human neutrophil elastase.* Med Res Rev, 2013. **33 Suppl 1**: p. E73-101.

91. Sekhon, B.S., *Matrix metalloproteinases – an overview.* Res Rep Biol, 2010. **2010**(1): p. 1-20.

92. Demedts, I.K., A. Morel-Montero, S. Lebecque, Y. Pacheco, D. Cataldo, G.F. Joos, et al., *Elevated MMP-12 protein levels in induced sputum from patients with COPD.* Thorax, 2006. **61**(3): p. 196-201.

93. Molet, S., C. Belleguic, H. Lena, N. Germain, C.P. Bertrand, S.D. Shapiro, et al., *Increase in macrophage elastase (MMP-12) in lungs from patients with chronic obstructive pulmonary disease.* Inflamm Res, 2005. **54**(1): p. 31-6.

94. Montano, M., C. Beccerril, V. Ruiz, C. Ramos, R.H. Sansores, and G. Gonzalez-Avila, *Matrix metalloproteinases activity in COPD associated with wood smoke.* Chest, 2004. **125**(2): p. 466-72.

95. Bezerra, F.S., S.S. Valenca, K.M. Pires, M. Lanzetti, W.A. Pimenta, A.C. Schmidt, et al., *Long-term exposure to cigarette smoke impairs lung function and increases HMGB-1 expression in mice.* Respir Physiol Neurobiol, 2011. **177**(2): p. 120-6.

96. Botelho, F.M., J.K. Nikota, C. Bauer, N.H. Davis, E.S. Cohen, I.K. Anderson, et al., *A mouse GM-CSF receptor antibody attenuates neutrophilia in mice exposed to cigarette smoke.* Eur Respir J, 2011. **38**(2): p. 285-94.

97. Pauwels, N.S., K.R. Bracke, T. Maes, G.R. Van Pottelberge, C. Garlanda, A. Mantovani, et al., *Cigarette smoke induces PTX3 expression in pulmonary veins of mice in an IL-1 dependent manner.* Respir Res, 2010. **11**: p. 134.

98. Xu, J., F. Xu, R. Wang, J. Seagrave, Y. Lin, and T.H. March, *Cigarette smoke-induced hypercapnic emphysema in C3H mice is associated with increases of macrophage metalloelastase and substance P in the lungs.* Exp Lung Res, 2007. **33**(5): p. 197-215.

99. da Hora, K., S.S. Valenca, and L.C. Porto, *Immunohistochemical study of tumor necrosis factor-alpha, matrix metalloproteinase-12, and tissue inhibitor of metalloproteinase-2 on alveolar macrophages of BALB/c mice exposed to short-term cigarette smoke.* Exp Lung Res, 2005. **31**(8): p. 759-70.

100. Bracke, K.R., I. D'Hulst A, T. Maes, K.B. Moerloose, I.K. Demedts, S. Lebecque, et al., *Cigarette smoke-induced pulmonary inflammation and emphysema are attenuated in CCR6-deficient mice.* J Immunol, 2006. **177**(7): p. 4350-9.

101. Churg, A., X. Wang, R.D. Wang, S.C. Meixner, E.L. Pryzdial, and J.L. Wright, *Alpha1-antitrypsin suppresses TNF-alpha and MMP-12 production by cigarette smoke-stimulated macrophages.* Am J Respir Cell Mol Biol, 2007. **37**(2): p. 144-51.

102. Hautamaki, R.D., D.K. Kobayashi, R.M. Senior, and S.D. Shapiro, *Requirement for macrophage elastase for cigarette smoke-induced emphysema in mice.* Science, 1997. **277**(5334): p. 2002-4.

103. Valenca, S.S., K. da Hora, P. Castro, V.G. Moraes, L. Carvalho, and L.C. Porto, *Emphysema and metalloelastase expression in mouse lung induced by cigarette smoke.* Toxicol Pathol, 2004. **32**(3): p. 351-6.

104. Aida, Y., Y. Shibata, S. Abe, S. Inoue, T. Kimura, A. Igarashi, et al., *Inhibition of elastase-pulmonary emphysema in dominant-negative MafB transgenic mice.* Int J Biol Sci, 2014. **10**(8): p. 882-94.

105. Tasaka, S., K. Inoue, K. Miyamoto, Y. Nakano, H. Kamata, H. Shinoda, et al., *Role of interleukin-6 in elastase-induced lung inflammatory changes in mice.* Exp Lung Res, 2010. **36**(6): p. 362-72.

106. Lourenco, J.D., L.P. Neves, C.R. Olivo, A. Duran, F.M. Almeida, P.M. Arantes, et al., *A treatment with a protease inhibitor recombinant from the cattle tick (Rhipicephalus Boophilus microplus) ameliorates emphysema in mice.* PLoS One, 2014. **9**(6): p. e98216.

107. Triantaphyllopoulos, K., F. Hussain, M. Pinart, M. Zhang, F. Li, I. Adcock, et al., *A model of chronic inflammation and pulmonary emphysema after multiple ozone exposures in mice.* Am J Physiol Lung Cell Mol Physiol, 2011. **300**(5): p. L691-700.

108. Marsland, B.J., M. Kurrer, R. Reissmann, N.L. Harris, and M. Kopf, *Nippostrongylus brasiliensis infection leads to the development of emphysema associated with the induction of alternatively activated macrophages.* Eur J Immunol, 2008. **38**(2): p. 479-88.

109. Churg, A., R. Wang, X. Wang, P.O. Onnervik, K. Thim, and J.L. Wright, *Effect of an MMP-9/MMP-12 inhibitor on smoke-induced emphysema and airway remodelling in guinea pigs.* Thorax, 2007. **62**(8): p. 706-13.

110. Imai, K., S.S. Dalal, E.S. Chen, R. Downey, L.L. Schulman, M. Ginsburg, et al., *Human collagenase (matrix metalloproteinase-1) expression in the lungs of patients with emphysema.* Am J Respir Crit Care Med, 2001. **163**(3 Pt 1): p. 786-91.

111. Finlay, G.A., L.R. O'Driscoll, K.J. Russell, E.M. D'Arcy, J.B. Masterson, M.X. FitzGerald, et al., *Matrix metalloproteinase expression and production by alveolar macrophages in emphysema.* Am J Respir Crit Care Med, 1997. **156**(1): p. 240-7.

112. Gosselink, J.V., S. Hayashi, W.M. Elliott, L. Xing, B. Chan, L. Yang, et al., *Differential expression of tissue repair genes in the pathogenesis of chronic obstructive pulmonary disease.* Am J Respir Crit Care Med, 2010. **181**(12): p. 1329-35.

113. Houghton, A.M., W.O. Hartzell, C.S. Robbins, F.X. Gomis-Ruth, and S.D. Shapiro, *Macrophage elastase kills bacteria within murine macrophages.* Nature, 2009. **460**(7255): p. 637-41.

114. Selman, M., M. Montano, C. Ramos, B. Vanda, C. Becerril, J. Delgado, et al., *Tobacco smoke-induced lung emphysema in guinea pigs is associated with increased interstitial collagenase.* Am J Physiol, 1996. **271**(5 Pt 1): p. L734-43.

115. Segura-Valdez, L., A. Pardo, M. Gaxiola, B.D. Uhal, C. Becerril, and M. Selman, *Upregulation of gelatinases A and B, collagenases 1 and 2, and increased parenchymal cell death in COPD.* Chest, 2000. **117**(3): p. 684-94.

116. Shiomi, T., Y. Okada, R. Foronjy, J. Schiltz, R. Jaenish, S. Krane, et al., *Emphysematous changes are caused by degradation of type III collagen in transgenic mice expressing MMP-1.* Exp Lung Res, 2003. **29**(1): p. 1-15.

117. D'Armiento, J., S.S. Dalal, Y. Okada, R.A. Berg, and K. Chada, *Collagenase expression in the lungs of transgenic mice causes pulmonary emphysema.* Cell, 1992. **71**(6): p. 955-61.

118. Betsuyaku, T., M. Nishimura, K. Takeyabu, M. Tanino, P. Venge, S. Xu, et al., *Neutrophil granule proteins in bronchoalveolar lavage fluid from subjects with subclinical emphysema.* Am J Respir Crit Care Med, 1999. **159**(6): p. 1985-91.

119. Vernooy, J.H., J.H. Lindeman, J.A. Jacobs, R. Hanemaaijer, and E.F. Wouters, *Increased activity of matrix metalloproteinase-8 and matrix metalloproteinase-9 in induced sputum from patients with COPD.* Chest, 2004. **126**(6): p. 1802-10.

120. Ilumets, H., P.H. Rytila, A.R. Sovijarvi, T. Tervahartiala, M. Myllarniemi, T.A. Sorsa, et al., *Transient elevation of neutrophil proteinases in induced sputum during COPD exacerbation.* Scand J Clin Lab Invest, 2008. **68**(7): p. 618-23.

121. Lee, E.J., K.H. In, J.H. Kim, S.Y. Lee, C. Shin, J.J. Shim, et al., *Proteomic analysis in lung tissue of smokers and COPD patients.* Chest, 2009. **135**(2): p. 344-52.

122. Cataldo, D., C. Munaut, A. Noel, F. Frankenne, P. Bartsch, J.M. Foidart, et al., *MMP-2- and MMP-9-linked gelatinolytic activity in the sputum from patients with asthma and chronic obstructive pulmonary disease.* Int Arch Allergy Immunol, 2000. **123**(3): p. 259-67.

123. Churg, A., R.D. Wang, H. Tai, X. Wang, C. Xie, and J.L. Wright, *Tumor necrosis factor-alpha drives 70% of cigarette smoke-induced emphysema in the mouse.* Am J Respir Crit Care Med, 2004. **170**(5): p. 492-8.

124. March, T.H., J.A. Wilder, D.C. Esparza, P.Y. Cossey, L.F. Blair, L.K. Herrera, et al., *Modulators of cigarette smoke-induced pulmonary emphysema in A/J mice.* Toxicol Sci, 2006. **92**(2): p. 545-59.

125. Ramos, C., J. Cisneros, G. Gonzalez-Avila, C. Becerril, V. Ruiz, and M. Montano, *Increase of matrix metalloproteinases in woodsmoke-induced lung emphysema in guinea pigs.* Inhal Toxicol, 2009. **21**(2): p. 119-32.

126. Culpitt, S.V., D.F. Rogers, S.L. Traves, P.J. Barnes, and L.E. Donnelly, *Sputum matrix metalloproteases: comparison between chronic obstructive pulmonary disease and asthma.* Respir Med, 2005. **99**(6): p. 703-10.

127. Xie, S.S., F. Hu, M. Tan, Y.X. Duan, X.L. Song, and C.H. Wang, *Relationship between expression of matrix metalloproteinase-9 and adenylyl cyclase-associated protein 1 in chronic obstructive pulmonary disease.* J Int Med Res, 2014. **42**(6): p. 1272-84.

128. Montano, M., R.H. Sansores, C. Becerril, J. Cisneros, G. Gonzalez-Avila, B. Sommer, et al., *FEV1 inversely correlates with metalloproteinases 1, 7, 9 and CRP in COPD by biomass smoke exposure.* Respir Res, 2014. **15**: p. 74.

129. Navratilova, Z., J. Zatloukal, E. Kriegova, V. Kolek, and M. Petrek, *Simultaneous up-regulation of matrix metalloproteinases 1, 2, 3, 7, 8, 9 and tissue inhibitors of metalloproteinases 1, 4 in serum of patients with chronic obstructive pulmonary disease.* Respirology, 2012. **17**(6): p. 1006-12.

130. Braber, S., P.J. Koelink, P.A. Henricks, P.L. Jackson, F.P. Nijkamp, J. Garssen, et al., *Cigarette smoke-induced lung emphysema in mice is associated with prolyl endopeptidase, an enzyme involved in collagen breakdown.* Am J Physiol Lung Cell Mol Physiol, 2011. **300**(2): p. L255-65.

131. Yao, H., I. Edirisinghe, S. Rajendrasozhan, S.R. Yang, S. Caito, D. Adenuga, et al., *Cigarette smoke-mediated inflammatory and oxidative responses are strain-dependent in mice.* Am J Physiol Lung Cell Mol Physiol, 2008. **294**(6): p. L1174-86.

132. Seagrave, J., E.B. Barr, T.H. March, and K.J. Nikula, *Effects of cigarette smoke exposure and cessation on inflammatory cells and matrix metalloproteinase activity in mice.* Exp Lung Res, 2004. **30**(1): p. 1-15.

133. Doz, E., N. Noulin, E. Boichot, I. Guenon, L. Fick, M. Le Bert, et al., *Cigarette smoke-induced pulmonary inflammation is TLR4/MyD88 and IL-1R1/MyD88 signaling dependent.* J Immunol, 2008. **180**(2): p. 1169-78.

134. Moreno, J.A., A. Ortega-Gomez, A. Rubio-Navarro, L. Louedec, B. Ho-Tin-Noe, G. Caligiuri, et al., *High-density lipoproteins potentiate alpha1-antitrypsin therapy in elastase-induced pulmonary emphysema.* Am J Respir Cell Mol Biol, 2014. **51**(4): p. 536-49.

135. Cheng, S.L., H.C. Wang, C.J. Yu, P.N. Tsao, P. Carmeliet, S.J. Cheng, et al., *Prevention of elastase-induced emphysema in placenta growth factor knock-out mice.* Respir Res, 2009. **10**: p. 115.

136. Foronjy, R., T. Nkyimbeng, A. Wallace, J. Thankachen, Y. Okada, V. Lemaitre, et al., *Transgenic expression of matrix metalloproteinase-9 causes adult-onset emphysema in mice associated with the loss of alveolar elastin.* Am J Physiol Lung Cell Mol Physiol, 2008. **294**(6): p. L1149-57.

137. Hunninghake, G.M., M.H. Cho, Y. Tesfaigzi, M.E. Soto-Quiros, L. Avila, J. Lasky-Su, et al., *MMP12, lung function, and COPD in high-risk populations.* N Engl J Med, 2009. **361**(27): p. 2599-608.

138. Joos, L., J.Q. He, M.B. Shepherdson, J.E. Connett, N.R. Anthonisen, P.D. Pare, et al., *The role of matrix metalloproteinase polymorphisms in the rate of decline in lung function.* Hum Mol Genet, 2002. **11**(5): p. 569-76.

139. Haq, I., S. Chappell, S.R. Johnson, J. Lotya, L. Daly, K. Morgan, et al., *Association of MMP-2 polymorphisms with severe and very severe COPD: a case control study of MMPs-1, 9 and 12 in a European population.* BMC Med Genet, 2010. **11**: p. 7.

140. Pons, A.R., J. Sauleda, A. Noguera, J. Pons, B. Barcelo, A. Fuster, et al., *Decreased macrophage release of TGF-beta and TIMP-1 in chronic obstructive pulmonary disease.* Eur Respir J, 2005. **26**(1): p. 60-6.

141. Wang, Y., N.X. Su, Z.Q. Chen, Z. Wang, and S.F. Zhang, *Effects of Fengbaisan on the expression of matrix metalloproteinase-9 and tissue inhibitor of metalloproteinase-1 in lung tissue of rats with chronic obstructive pulmonary disease.* Chin J Integr Med, 2014. **20**(3): p. 224-31.

142. Yao, H., J.W. Hwang, I.K. Sundar, A.E. Friedman, M.W. McBurney, L. Guarente, et al., *SIRT1 redresses the imbalance of tissue inhibitor of matrix metalloproteinase-1 and matrix metalloproteinase-9 in the development of mouse emphysema and human COPD.* Am J Physiol Lung Cell Mol Physiol, 2013. **305**(9): p. L615-24.

143. Hirano, K., T. Sakamoto, Y. Uchida, Y. Morishima, K. Masuyama, Y. Ishii, et al., *Tissue inhibitor of metalloproteinases-2 gene polymorphisms in chronic obstructive pulmonary disease.* Eur Respir J, 2001. **18**(5): p. 748-52.

144. Lacoste, J.Y., J. Bousquet, P. Chanez, T. Van Vyve, J. Simony-Lafontaine, N. Lequeu, et al., *Eosinophilic and neutrophilic inflammation in asthma, chronic bronchitis, and chronic obstructive pulmonary disease.* J Allergy Clin Immunol, 1993. **92**(4): p. 537-48.

145. Keatings, V.M., P.D. Collins, D.M. Scott, and P.J. Barnes, *Differences in interleukin-8 and tumor necrosis factor-alpha in induced sputum from patients with chronic obstructive pulmonary disease or asthma.* Am J Respir Crit Care Med, 1996. **153**(2): p. 530-4.

146. Stanescu, D., A. Sanna, C. Veriter, S. Kostianev, P.G. Calcagni, L.M. Fabbri, et al., *Airways obstruction, chronic expectoration, and rapid decline of FEV1 in smokers are associated with increased levels of sputum neutrophils.* Thorax, 1996. **51**(3): p. 267-71.

147. Sparrow, D., R.J. Glynn, M. Cohen, and S.T. Weiss, *The relationship of the peripheral leukocyte count and cigarette smoking to pulmonary function among adult men.* Chest, 1984. **86**(3): p. 383-6.

148. Tanino, M., T. Betsuyaku, K. Takeyabu, Y. Tanino, E. Yamaguchi, K. Miyamoto, et al., *Increased levels of interleukin-8 in BAL fluid from smokers susceptible to pulmonary emphysema.* Thorax, 2002. **57**(5): p. 405-11.

149. Kostikas, K., M. Gaga, G. Papatheodorou, T. Karamanis, D. Orphanidou, and S. Loukides, *Leukotriene B4 in exhaled breath condensate and sputum supernatant in patients with COPD and asthma.* Chest, 2005. **127**(5): p. 1553-9.

150. Beeh, K.M., O. Kornmann, R. Buhl, S.V. Culpitt, M.A. Giembycz, and P.J. Barnes, *Neutrophil chemotactic activity of sputum from patients with COPD: role of interleukin 8 and leukotriene B4.* Chest, 2003. **123**(4): p. 1240-7.

151. Traves, S.L., S.V. Culpitt, R.E. Russell, P.J. Barnes, and L.E. Donnelly, *Increased levels of the chemokines GROalpha and MCP-1 in sputum samples from patients with COPD.* Thorax, 2002. **57**(7): p. 590-5.

152. Basu, S., G. Hodgson, M. Katz, and A.R. Dunn, *Evaluation of role of G-CSF in the production, survival, and release of neutrophils from bone marrow into circulation.* Blood, 2002. **100**(3): p. 854-61.

153. Meagher, L.C., J.S. Savill, A. Baker, R.W. Fuller, and C. Haslett, *Phagocytosis of apoptotic neutrophils does not induce macrophage release of thromboxane B2.* J Leukoc Biol, 1992. **52**(3): p. 269-73.

154. Zhang, J., J. He, J. Xia, Z. Chen, and X. Chen, *Delayed apoptosis by neutrophils from COPD patients is associated with altered Bak, Bcl-xl, and Mcl-1 mRNA expression.* Diagn Pathol, 2012. **7**: p. 65.

155. Shim, Y.M., M. Paige, H. Hanna, S.H. Kim, M.D. Burdick, and R.M. Strieter, *Role of LTB(4) in the pathogenesis of elastase-induced murine pulmonary emphysema.* Am J Physiol Lung Cell Mol Physiol, 2010. **299**(6): p. L749-59.

156. Ofulue, A.F. and M. Ko, *Effects of depletion of neutrophils or macrophages on development of cigarette smoke-induced emphysema.* Am J Physiol, 1999. **277**(1 Pt 1): p. L97-105.

157. Ishii, T., R.T. Abboud, A.M. Wallace, J.C. English, H.O. Coxson, R.J. Finley, et al., *Alveolar macrophage proteinase/antiproteinase expression in lung function and emphysema.* Eur Respir J, 2014. **43**(1): p. 82-91.

158. Punturieri, A., S. Filippov, E. Allen, I. Caras, R. Murray, V. Reddy, et al., *Regulation of elastinolytic cysteine proteinase activity in normal and cathepsin K-deficient human macrophages.* J Exp Med, 2000. **192**(6): p. 789-99.

159. Retamales, I., W.M. Elliott, B. Meshi, H.O. Coxson, P.D. Pare, F.C. Sciurba, et al., *Amplification of inflammation in emphysema and its association with latent adenoviral infection.* Am J Respir Crit Care Med, 2001. **164**(3): p. 469-73.

160. Pesci, A., B. Balbi, M. Majori, G. Cacciani, S. Bertacco, P. Alciato, et al., *Inflammatory cells and mediators in bronchial lavage of patients with chronic obstructive pulmonary disease.* Eur Respir J, 1998. **12**(2): p. 380-6.

161. Di Stefano, A., A. Capelli, M. Lusuardi, P. Balbo, C. Vecchio, P. Maestrelli, et al., *Severity of airflow limitation is associated with severity of airway inflammation in smokers.* Am J Respir Crit Care Med, 1998. **158**(4): p. 1277-85.

162. Hashimoto, D., A. Chow, C. Noizat, P. Teo, M.B. Beasley, M. Leboeuf, et al., *Tissue-resident macrophages self-maintain locally throughout adult life with minimal contribution from circulating monocytes.* Immunity, 2013. **38**(4): p. 792-804.

163. Tomita, K., G. Caramori, S. Lim, K. Ito, T. Hanazawa, T. Oates, et al., *Increased p21(CIP1/WAF1) and B cell lymphoma leukemia-x(L) expression and reduced apoptosis in alveolar macrophages from smokers.* Am J Respir Crit Care Med, 2002. **166**(5): p. 724-31.

164. Traves, S.L., S.J. Smith, P.J. Barnes, and L.E. Donnelly, *Specific CXC but not CC chemokines cause elevated monocyte migration in COPD: a role for CXCR2.* J Leukoc Biol, 2004. **76**(2): p. 441-50.

165. Hoogsteden, H.C., P.T. van Hal, J.M. Wijkhuijs, W. Hop, A.P. Verkaik, and C. Hilvering, *Expression of the CD11/CD18 cell surface adhesion glycoprotein family on alveolar macrophages in smokers and nonsmokers.* Chest, 1991. **100**(6): p. 1567-71.

166. Ofulue, A.F., M. Ko, and R.T. Abboud, *Time course of neutrophil and macrophage elastinolytic activities in cigarette smoke-induced emphysema.* Am J Physiol, 1998. **275**(6 Pt 1): p. L1134-44.

167. Hodge, G., J. Nairn, M. Holmes, P.N. Reynolds, and S. Hodge, *Increased intracellular T helper 1 proinflammatory cytokine production in peripheral blood, bronchoalveolar lavage and intraepithelial T cells of COPD subjects.* Clin Exp Immunol, 2007. **150**(1): p. 22-9.

168. Grumelli, S., D.B. Corry, L.Z. Song, L. Song, L. Green, J. Huh, et al., *An immune basis for lung parenchymal destruction in chronic obstructive pulmonary disease and emphysema.* PLoS Med, 2004. **1**(1): p. e8.

169. Majori, M., M. Corradi, A. Caminati, G. Cacciani, S. Bertacco, and A. Pesci, *Predominant TH1 cytokine pattern in peripheral blood from subjects with chronic obstructive pulmonary disease.* J Allergy Clin Immunol, 1999. **103**(3 Pt 1): p. 458-62.

170. Barczyk, A., W. Pierzchala, O.M. Kon, B. Cosio, I.M. Adcock, and P.J. Barnes, *Cytokine production by bronchoalveolar lavage T lymphocytes in chronic obstructive pulmonary disease.* J Allergy Clin Immunol, 2006. **117**(6): p. 1484-92.

171. Vargas-Rojas, M.I., A. Ramirez-Venegas, L. Limon-Camacho, L. Ochoa, R. Hernandez-Zenteno, and R.H. Sansores, *Increase of Th17 cells in peripheral blood of patients with chronic obstructive pulmonary disease.* Respir Med, 2011. **105**(11): p. 1648-54.

172. Barnes, P.J., *The cytokine network in chronic obstructive pulmonary disease.* Am J Respir Cell Mol Biol, 2009. **41**(6): p. 631-8.

173. Wang, Z., T. Zheng, Z. Zhu, R.J. Homer, R.J. Riese, H.A. Chapman, Jr., et al., *Interferon gamma induction of pulmonary emphysema in the adult murine lung.* J Exp Med, 2000. **192**(11): p. 1587-600.

174. Fujita, M., J.M. Shannon, C.G. Irvin, K.A. Fagan, C. Cool, A. Augustin, et al., *Overexpression of tumor necrosis factor-alpha produces an increase in lung volumes and pulmonary hypertension.* Am J Physiol Lung Cell Mol Physiol, 2001. **280**(1): p. L39-49.

175. Lucey, E.C., J. Keane, P.P. Kuang, G.L. Snider, and R.H. Goldstein, *Severity of elastase-induced emphysema is decreased in tumor necrosis factor-alpha and interleukin-1beta receptor-deficient mice.* Lab Invest, 2002. **82**(1): p. 79-85.

176. Couillin, I., V. Vasseur, S. Charron, P. Gasse, M. Tavernier, J. Guillet, et al., *IL-1R1/MyD88 signaling is critical for elastase-induced lung inflammation and emphysema.* J Immunol, 2009. **183**(12): p. 8195-202.

177. Churg, A., S. Zhou, X. Wang, R. Wang, and J.L. Wright, *The role of interleukin-1beta in murine cigarette smoke-induced emphysema and small airway remodeling.* Am J Respir Cell Mol Biol, 2009. **40**(4): p. 482-90.

178. Zheng, T., Z. Zhu, Z. Wang, R.J. Homer, B. Ma, R.J. Riese, Jr., et al., *Inducible targeting of IL-13 to the adult lung causes matrix metalloproteinase- and cathepsin-dependent emphysema.* J Clin Invest, 2000. **106**(9): p. 1081-93.

179. Jones, C.E. and K. Chan, *Interleukin-17 stimulates the expression of interleukin-8, growth-related oncogene-alpha, and granulocyte-colony-stimulating factor by human airway epithelial cells.* Am J Respir Cell Mol Biol, 2002. **26**(6): p. 748-53.

180. Vanaudenaerde, B.M., W.A. Wuyts, L.J. Dupont, D.E. Van Raemdonck, M.M. Demedts, and G.M. Verleden, *Interleukin-17 stimulates release of interleukin-8 by human airway smooth muscle cells in vitro: a potential role for interleukin-17 and airway smooth muscle cells in bronchiolitis obliterans syndrome.* J Heart Lung Transplant, 2003. **22**(11): p. 1280-3.

181. Di Stefano, A., G. Caramori, I. Gnemmi, M. Contoli, C. Vicari, A. Capelli, et al., *T helper type 17-related cytokine expression is increased in the bronchial mucosa of stable chronic obstructive pulmonary disease patients.* Clin Exp Immunol, 2009. **157**(2): p. 316-24.

182. Chang, Y., J. Nadigel, N. Boulais, J. Bourbeau, F. Maltais, D.H. Eidelman, et al., *CD8 positive T cells express IL-17 in patients with chronic obstructive pulmonary disease.* Respir Res, 2011. **12**: p. 43.

183. Zhang, J., S. Chu, X. Zhong, Q. Lao, Z. He, and Y. Liang, *Increased expression of CD4+IL-17+ cells in the lung tissue of patients with stable chronic obstructive pulmonary disease (COPD) and smokers.* Int Immunopharmacol, 2013. **15**(1): p. 58-66.

184. Eustace, A., L.J. Smyth, L. Mitchell, K. Williamson, J. Plumb, and D. Singh, *Identification of cells expressing IL-17A and IL-17F in the lungs of patients with COPD.* Chest, 2011. **139**(5): p. 1089-100.

185. Park, H., Z. Li, X.O. Yang, S.H. Chang, R. Nurieva, Y.H. Wang, et al., *A distinct lineage of CD4 T cells regulates tissue inflammation by producing interleukin 17.* Nat Immunol, 2005. **6**(11): p. 1133-41.

186. Chen, K., D.A. Pociask, J.P. McAleer, Y.R. Chan, J.F. Alcorn, J.L. Kreindler, et al., *IL-17RA is required for CCL2 expression, macrophage recruitment, and emphysema in response to cigarette smoke.* PLoS One, 2011. **6**(5): p. e20333.

187. Shan, M., X. Yuan, L.Z. Song, L. Roberts, N. Zarinkamar, A. Seryshev, et al., *Cigarette smoke induction of osteopontin (SPP1) mediates T(H)17 inflammation in human and experimental emphysema.* Sci Transl Med, 2012. **4**(117): p. 117ra9.

188. Kurimoto, E., N. Miyahara, A. Kanehiro, K. Waseda, A. Taniguchi, G. Ikeda, et al., *IL-17A is essential to the development of elastase-induced pulmonary inflammation and emphysema in mice.* Respir Res, 2013. **14**: p. 5.

189. Brucklacher-Waldert, V., E.J. Carr, M.A. Linterman, and M. Veldhoen, *Cellular Plasticity of CD4+ T Cells in the Intestine.* Front Immunol, 2014. **5**: p. 488.

190. Agusti, A., W. MacNee, K. Donaldson, and M. Cosio, *Hypothesis: does COPD have an autoimmune component?* Thorax, 2003. **58**(10): p. 832-4.

191. Cosio, M.G., M. Saetta, and A. Agusti, *Immunologic Aspects of Chronic Obstructive Pulmonary Disease.* New England Journal of Medicine, 2009. **360**(23): p. 2445-2454.

192. van der Strate, B.W., D.S. Postma, C.A. Brandsma, B.N. Melgert, M.A. Luinge, M. Geerlings, et al., *Cigarette smoke-induced emphysema: A role for the B cell?* Am J Respir Crit Care Med, 2006. **173**(7): p. 751-8.

193. Kheradmand, F., M. Shan, C. Xu, and D.B. Corry, *Autoimmunity in chronic obstructive pulmonary disease: clinical and experimental evidence.* Expert Rev Clin Immunol, 2012. **8**(3): p. 285-92.

194. Lee, S.H., S. Goswami, A. Grudo, L.Z. Song, V. Bandi, S. Goodnight-White, et al., *Antielastin autoimmunity in tobacco smoking-induced emphysema.* Nat Med, 2007. **13**(5): p. 567-9.

195. Rinaldi, M., A. Lehouck, N. Heulens, R. Lavend'homme, V. Carlier, J.M. Saint-Remy, et al., *Antielastin B-cell and T-cell immunity in patients with chronic obstructive pulmonary disease.* Thorax, 2012. **67**(8): p. 694-700.

196. Greene, C.M., T.B. Low, S.J. O'Neill, and N.G. McElvaney, *Anti-proline-glycine-proline or antielastin autoantibodies are not evident in chronic inflammatory lung disease.* Am J Respir Crit Care Med, 2010. **181**(1): p. 31-5.

197. Devasagayam, T.P., J.C. Tilak, K.K. Boloor, K.S. Sane, S.S. Ghaskadbi, and R.D. Lele, *Free radicals and antioxidants in human health: current status and future prospects.* J Assoc Physicians India, 2004. **52**: p. 794-804.

198. Pinamonti, S., M. Leis, A. Barbieri, D. Leoni, M. Muzzoli, S. Sostero, et al., *Detection of xanthine oxidase activity products by EPR and HPLC in bronchoalveolar lavage fluid from patients with chronic obstructive pulmonary disease.* Free Radic Biol Med, 1998. **25**(7): p. 771-9.

199. Rahman, I., A.A. van Schadewijk, A.J. Crowther, P.S. Hiemstra, J. Stolk, W. MacNee, et al., *4-Hydroxy-2-nonenal, a specific lipid peroxidation product, is elevated in lungs of patients with chronic obstructive pulmonary disease.* Am J Respir Crit Care Med, 2002. **166**(4): p. 490-5.

200. Kharitonov, S.A. and P.J. Barnes, *Exhaled markers of pulmonary disease.* Am J Respir Crit Care Med, 2001. **163**(7): p. 1693-722.

201. Antczak, A. and P. Gorski, *Markers of pulmonary diseases in exhaled breath condensate.* Int J Occup Med Environ Health, 2002. **15**(4): p. 317-23.

202. Dekhuijzen, P.N., K.K. Aben, I. Dekker, L.P. Aarts, P.L. Wielders, C.L. van Herwaarden, et al., *Increased exhalation of hydrogen peroxide in patients with stable and unstable chronic obstructive pulmonary disease.* Am J Respir Crit Care Med, 1996. **154**(3 Pt 1): p. 813-6.

203. Rahman, I., D. Morrison, K. Donaldson, and W. MacNee, *Systemic oxidative stress in asthma, COPD, and smokers.* Am J Respir Crit Care Med, 1996. **154**(4 Pt 1): p. 1055-60.

204. Pratico, D., S. Basili, M. Vieri, C. Cordova, F. Violi, and G.A. Fitzgerald, *Chronic obstructive pulmonary disease is associated with an increase in urinary levels of isoprostane F2alpha-III, an index of oxidant stress.* Am J Respir Crit Care Med, 1998. **158**(6): p. 1709-14.

205. Pryor, W.A. and K. Stone, *Oxidants in cigarette smoke. Radicals, hydrogen peroxide, peroxynitrate, and peroxynitrite.* Ann N Y Acad Sci, 1993. **686**: p. 12-27; discussion 27-8.

206. Rahman, I. and W. MacNee, *Role of oxidants/antioxidants in smoking-induced lung diseases.* Free Radic Biol Med, 1996. **21**(5): p. 669-81.

207. Corradi, M., R. Alinovi, M. Goldoni, M. Vettori, G. Folesani, P. Mozzoni, et al., *Biomarkers of oxidative stress after controlled human exposure to ozone.* Toxicol Lett, 2002. **134**(1-3): p. 219-25.

208. Bayram, H., R.J. Sapsford, M.M. Abdelaziz, and O.A. Khair, *Effect of ozone and nitrogen dioxide on the release of proinflammatory mediators from bronchial epithelial cells of nonatopic nonasthmatic subjects and atopic asthmatic patients in vitro.* J Allergy Clin Immunol, 2001. **107**(2): p. 287-94.

209. Gilmour, P.S., I. Rahman, K. Donaldson, and W. MacNee, *Histone acetylation regulates epithelial IL-8 release mediated by oxidative stress from environmental particles.* Am J Physiol Lung Cell Mol Physiol, 2003. **284**(3): p. L533-40.

210. Schaberg, T., H. Haller, M. Rau, D. Kaiser, M. Fassbender, and H. Lode, *Superoxide anion release induced by platelet-activating factor is increased in human alveolar macrophages from smokers.* Eur Respir J, 1992. **5**(4): p. 387-93.

211. Ludwig, P.W. and J.R. Hoidal, *Alterations in leukocyte oxidative metabolism in cigarette smokers.* Am Rev Respir Dis, 1982. **126**(6): p. 977-80.

212. Hoidal, J.R., R.B. Fox, P.A. LeMarbe, R. Perri, and J.E. Repine, *Altered oxidative metabolic responses in vitro of alveolar macrophages from asymptomatic cigarette smokers.* Am Rev Respir Dis, 1981. **123**(1): p. 85-9.

213. Zhu, A., D. Ge, J. Zhang, Y. Teng, C. Yuan, M. Huang, et al., *Sputum myeloperoxidase in chronic obstructive pulmonary disease.* Eur J Med Res, 2014. **19**: p. 12.

214. Seimetz, M., N. Parajuli, A. Pichl, F. Veit, G. Kwapiszewska, F.C. Weisel, et al., *Inducible NOS inhibition reverses tobacco-smoke-induced emphysema and pulmonary hypertension in mice.* Cell, 2011. **147**(2): p. 293-305.

215. Lannan, S., K. Donaldson, D. Brown, and W. MacNee, *Effect of cigarette smoke and its condensates on alveolar epithelial cell injury in vitro.* Am J Physiol, 1994. **266**(1 Pt 1): p. L92-100.

216. Hayashi, A., A. Ryu, T. Suzuki, A. Kawada, and S. Tajima, *In vitro degradation of tropoelastin by reactive oxygen species.* Arch Dermatol Res, 1998. **290**(9): p. 497-500.

217. Yao, H., G. Arunachalam, J.W. Hwang, S. Chung, I.K. Sundar, V.L. Kinnula, et al., *Extracellular superoxide dismutase protects against pulmonary emphysema by attenuating oxidative fragmentation of ECM.* Proc Natl Acad Sci U S A, 2010. **107**(35): p. 15571-6.

218. Torres-Ramos, Y.D., M.L. Garcia-Guillen, I.M. Olivares-Corichi, and J.J. Hicks, *Correlation of Plasma Protein Carbonyls and C-Reactive Protein with GOLD Stage Progression in COPD Patients.* Open Respir Med J, 2009. **3**: p. 61-6.

219. Janoff, A. and H. Carp, *Possible mechanisms of emphysema in smokers: cigarette smoke condensate suppresses protease inhibition in vitro.* Am Rev Respir Dis, 1977. **116**(1): p. 65-72.

220. Gadek, J.E., G.A. Fells, and R.G. Crystal, *Cigarette smoking induces functional antiprotease deficiency in the lower respiratory tract of humans.* Science, 1979. **206**(4424): p. 1315-6.

221. Asami, S., H. Manabe, J. Miyake, Y. Tsurudome, T. Hirano, R. Yamaguchi, et al., *Cigarette smoking induces an increase in oxidative DNA damage, 8-hydroxydeoxyguanosine, in a central site of the human lung.* Carcinogenesis, 1997. **18**(9): p. 1763-6.

222. Yoshida, T. and R.M. Tuder, *Pathobiology of cigarette smoke-induced chronic obstructive pulmonary disease.* Physiol Rev, 2007. **87**(3): p. 1047-82.

223. Rahman, I., S.R. Yang, and S.K. Biswas, *Current concepts of redox signaling in the lungs.* Antioxid Redox Signal, 2006. **8**(3-4): p. 681-9.

224. MacNee, W., *Oxidants/antioxidants and COPD.* Chest, 2000. **117**(5 Suppl 1): p. 303S-17S.

225. Foronjy, R.F., O. Mirochnitchenko, O. Propokenko, V. Lemaitre, Y. Jia, M. Inouye, et al., *Superoxide dismutase expression attenuates cigarette smoke- or elastase-generated emphysema in mice.* Am J Respir Crit Care Med, 2006. **173**(6): p. 623-31.

226. Sussan, T.E., T. Rangasamy, D.J. Blake, D. Malhotra, H. El-Haddad, D. Bedja, et al., *Targeting Nrf2 with the triterpenoid CDDO-imidazolide attenuates cigarette smoke-induced emphysema and cardiac dysfunction in mice.* Proc Natl Acad Sci U S A, 2009. **106**(1): p. 250-5.

227. Suzuki, M., T. Betsuyaku, Y. Ito, K. Nagai, N. Odajima, C. Moriyama, et al., *Curcumin attenuates elastase- and cigarette smoke-induced pulmonary emphysema in mice.* Am J Physiol Lung Cell Mol Physiol, 2009. **296**(4): p. L614-23.

228. Rubio, M.L., M.C. Martin-Mosquero, M. Ortega, G. Peces-Barba, and N. Gonzalez-Mangado, *Oral N-acetylcysteine attenuates elastase-induced pulmonary emphysema in rats.* Chest, 2004. **125**(4): p. 1500-6.

229. Kirkham, P.A. and P.J. Barnes, *Oxidative stress in COPD.* Chest, 2013. **144**(1): p. 266-73.

230. Rahman, I., *Pharmacological antioxidant strategies as therapeutic interventions for COPD.* Biochim Biophys Acta, 2012. **1822**(5): p. 714-28.

231. Tuder, R.M. and I. Petrache, *Pathogenesis of chronic obstructive pulmonary disease.* J Clin Invest, 2012. **122**(8): p. 2749-55.

232. Kasahara, Y., R.M. Tuder, C.D. Cool, D.A. Lynch, S.C. Flores, and N.F. Voelkel, *Endothelial cell death and decreased expression of vascular endothelial growth factor and vascular endothelial growth factor receptor 2 in emphysema.* Am J Respir Crit Care Med, 2001. **163**(3 Pt 1): p. 737-44.

233. Imai, K., B.A. Mercer, L.L. Schulman, J.R. Sonett, and J.M. D'Armiento, *Correlation of lung surface area to apoptosis and proliferation in human emphysema.* Eur Respir J, 2005. **25**(2): p. 250-8.

234. Yokohori, N., K. Aoshiba, A. Nagai, and J. Respiratory Failure Research Group in, *Increased levels of cell death and proliferation in alveolar wall cells in patients with pulmonary emphysema.* Chest, 2004. **125**(2): p. 626-32.

235. Kasahara, Y., R.M. Tuder, L. Taraseviciene-Stewart, T.D. Le Cras, S. Abman, P.K. Hirth, et al., *Inhibition of VEGF receptors causes lung cell apoptosis and emphysema.* J Clin Invest, 2000. **106**(11): p. 1311-9.

236. Tang, K., H.B. Rossiter, P.D. Wagner, and E.C. Breen, *Lung-targeted VEGF inactivation leads to an emphysema phenotype in mice.* J Appl Physiol (1985), 2004. **97**(4): p. 1559-66; discussion 1549.

237. Stanley, S.E., J.J. Chen, J.D. Podlevsky, J.K. Alder, N.N. Hansel, R.A. Mathias, et al., *Telomerase mutations in smokers with severe emphysema.* J Clin Invest, 2014.

238. Aoshiba, K., N. Yokohori, and A. Nagai, *Alveolar wall apoptosis causes lung destruction and emphysematous changes.* Am J Respir Cell Mol Biol, 2003. **28**(5): p. 555-62.

239. Tsuji, T., K. Aoshiba, and A. Nagai, *Alveolar cell senescence in patients with pulmonary emphysema.* Am J Respir Crit Care Med, 2006. **174**(8): p. 886-93.

240. Morla, M., X. Busquets, J. Pons, J. Sauleda, W. MacNee, and A.G. Agusti, *Telomere shortening in smokers with and without COPD.* Eur Respir J, 2006. **27**(3): p. 525-8.

241. Alder, J.K., N. Guo, F. Kembou, E.M. Parry, C.J. Anderson, A.I. Gorgy, et al., *Telomere length is a determinant of emphysema susceptibility.* Am J Respir Crit Care Med, 2011. **184**(8): p. 904-12.

242. Tsuji, T., K. Aoshiba, and A. Nagai, *Cigarette smoke induces senescence in alveolar epithelial cells.* Am J Respir Cell Mol Biol, 2004. **31**(6): p. 643-9.

243. Muller, K.C., L. Welker, K. Paasch, B. Feindt, V.J. Erpenbeck, J.M. Hohlfeld, et al., *Lung fibroblasts from patients with emphysema show markers of senescence in vitro.* Respir Res, 2006. **7**: p. 32.

244. Holz, O., I. Zuhlke, E. Jaksztat, K. Muller, L. Welker, M. Nakashima, et al., *Lung fibroblasts from patients with emphysema show a reduced proliferation rate in culture.* Eur Respir J, 2004. **24**: p. 575 - 579.

245. Baraldo, S., G. Turato, F. Lunardi, E. Bazzan, M. Schiavon, I. Ferrarotti, et al., *Immune Activation in alpha-1antitrypsin Deficiency Emphysema: Beyond the Protease/Antiprotease Paradigm.* Am J Respir Crit Care Med, 2014.

246. Rahman, I. and I.M. Adcock, *Oxidative stress and redox regulation of lung inflammation in COPD.* Eur Respir J, 2006. **28**(1): p. 219-42.

247. Taggart, C., D. Cervantes-Laurean, G. Kim, N.G. McElvaney, N. Wehr, J. Moss, et al., *Oxidation of either methionine 351 or methionine 358 in alpha 1-antitrypsin causes loss of anti-neutrophil elastase activity.* J Biol Chem, 2000. **275**(35): p. 27258-65.

248. Hunninghake, G.W., J.M. Davidson, S. Rennard, S. Szapiel, J.E. Gadek, and R.G. Crystal, *Elastin fragments attract macrophage precursors to diseased sites in pulmonary emphysema.* Science, 1981. **212**(4497): p. 925-7.

249. Senior, R.M., G.L. Griffin, and R.P. Mecham, *Chemotactic activity of elastin-derived peptides.* J Clin Invest, 1980. **66**(4): p. 859-62.

250. Thimmulappa, R.K., X. Gang, J.H. Kim, T.E. Sussan, J.L. Witztum, and S. Biswal, *Oxidized phospholipids impair pulmonary antibacterial defenses: evidence in mice exposed to cigarette smoke.* Biochem Biophys Res Commun, 2012. **426**(2): p. 253-9.

251. Vandivier, R.W., P.M. Henson, and I.S. Douglas, *Burying the dead: the impact of failed apoptotic cell removal (efferocytosis) on chronic inflammatory lung disease.* Chest, 2006. **129**(6): p. 1673-82.

252. Marwick, J.A., C.S. Stevenson, J. Giddings, W. MacNee, K. Butler, I. Rahman, et al., *Cigarette smoke disrupts VEGF165-VEGFR-2 receptor signaling complex in rat lungs and patients with COPD: morphological impact of VEGFR-2 inhibition.* Am J Physiol Lung Cell Mol Physiol, 2006. **290**(5): p. L897-908.

253. Petrache, I., I. Fijalkowska, T.R. Medler, J. Skirball, P. Cruz, L. Zhen, et al., *alpha-1 antitrypsin inhibits caspase-3 activity, preventing lung endothelial cell apoptosis.* Am J Pathol, 2006. **169**(4): p. 1155-66.

254. Tuder, R.M., J.A. Kern, and Y.E. Miller, *Senescence in chronic obstructive pulmonary disease.* Proc Am Thorac Soc, 2012. **9**(2): p. 62-3.

255. Tsuji, T., K. Aoshiba, and A. Nagai, *Alveolar cell senescence exacerbates pulmonary inflammation in patients with chronic obstructive pulmonary disease.* Respiration, 2010. **80**(1): p. 59-70.

256. Soler-Cataluna, J.J., M.A. Martinez-Garcia, P. Roman Sanchez, E. Salcedo, M. Navarro, and R. Ochando, *Severe acute exacerbations and mortality in patients with chronic obstructive pulmonary disease.* Thorax, 2005. **60**(11): p. 925-31.

257. Gibson, P.G., J.H. Wlodarczyk, A.J. Wilson, and A. Sprogis, *Severe exacerbation of chronic obstructive airways disease: health resource use in general practice and hospital.* J Qual Clin Pract, 1998. **18**(2): p. 125-33.

258. Warren, P.M., D.C. Flenley, J.S. Millar, and A. Avery, *Respiratory failure revisited: acute exacerbations of chronic bronchitis between 1961-68 and 1970-76.* Lancet, 1980. **1**(8166): p. 467-70.

259. Gunen, H., S.S. Hacievliyagil, F. Kosar, L.C. Mutlu, G. Gulbas, E. Pehlivan, et al., *Factors affecting survival of hospitalised patients with COPD.* Eur Respir J, 2005. **26**(2): p. 234-41.

260. Celli, B.R. and P.J. Barnes, *Exacerbations of chronic obstructive pulmonary disease.* Eur Respir J, 2007. **29**(6): p. 1224-38.

261. Rodriguez-Roisin, R., *Toward a consensus definition for COPD exacerbations.* Chest, 2000. **117**(5 Suppl 2): p. 398S-401S.

262. Burge, S. and J.A. Wedzicha, *COPD exacerbations: definitions and classifications.* Eur Respir J Suppl, 2003. **41**: p. 46s-53s.

263. Wier, L.M., A. Elixhauser, A. Pfuntner, and D.H. Au, *Overview of Hospitalizations among Patients with COPD, 2008: Statistical Brief #106*, in *Healthcare Cost and Utilization Project (HCUP) Statistical Briefs.* 2011: Rockville (MD).

264. Yu, A.P., H. Yang, E.Q. Wu, J. Setyawan, M. Mocarski, and S. Blum, *Incremental third-party costs associated with COPD exacerbations: a retrospective claims analysis.* J Med Econ, 2011. **14**(3): p. 315-23.

265. Price, D.B., B.P. Yawn, and R.C. Jones, *Improving the differential diagnosis of chronic obstructive pulmonary disease in primary care.* Mayo Clin Proc, 2010. **85**(12): p. 1122-9.

266. Sethi, S. and T.F. Murphy, *Infection in the pathogenesis and course of chronic obstructive pulmonary disease.* N Engl J Med, 2008. **359**(22): p. 2355-65.

267. Papi, A., C.M. Bellettato, F. Braccioni, M. Romagnoli, P. Casolari, G. Caramori, et al., *Infections and airway inflammation in chronic obstructive pulmonary disease severe exacerbations.* Am J Respir Crit Care Med, 2006. **173**(10): p. 1114-21.

268. Rosell, A., E. Monso, N. Soler, F. Torres, J. Angrill, G. Riise, et al., *Microbiologic determinants of exacerbation in chronic obstructive pulmonary disease.* Arch Intern Med, 2005. **165**(8): p. 891-7.

269. Bandi, V., M.A. Apicella, E. Mason, T.F. Murphy, A. Siddiqi, R.L. Atmar, et al., *Nontypeable Haemophilus influenzae in the lower respiratory tract of patients with chronic bronchitis.* Am J Respir Crit Care Med, 2001. **164**(11): p. 2114-9.

270. Sethi, S., R. Sethi, K. Eschberger, P. Lobbins, X. Cai, B.J. Grant, et al., *Airway bacterial concentrations and exacerbations of chronic obstructive pulmonary disease.* Am J Respir Crit Care Med, 2007. **176**(4): p. 356-61.

271. Sethi, S., N. Evans, B.J. Grant, and T.F. Murphy, *New strains of bacteria and exacerbations of chronic obstructive pulmonary disease.* N Engl J Med, 2002. **347**(7): p. 465-71.

272. Murphy, T.F., A.L. Brauer, S. Sethi, M. Kilian, X. Cai, and A.J. Lesse, *Haemophilus haemolyticus: a human respiratory tract commensal to be distinguished from Haemophilus influenzae.* J Infect Dis, 2007. **195**(1): p. 81-9.

273. Murphy, T.F., A.L. Brauer, B.J. Grant, and S. Sethi, *Moraxella catarrhalis in chronic obstructive pulmonary disease: burden of disease and immune response.* Am J Respir Crit Care Med, 2005. **172**(2): p. 195-9.

274. Murphy, T.F., A.L. Brauer, K. Eschberger, P. Lobbins, L. Grove, X. Cai, et al., *Pseudomonas aeruginosa in chronic obstructive pulmonary disease.* Am J Respir Crit Care Med, 2008. **177**(8): p. 853-60.

275. Patel, I.S., T.A. Seemungal, M. Wilks, S.J. Lloyd-Owen, G.C. Donaldson, and J.A. Wedzicha, *Relationship between bacterial colonisation and the frequency, character, and severity of COPD exacerbations.* Thorax, 2002. **57**(9): p. 759-64.

276. Seemungal, T., R. Harper-Owen, A. Bhowmik, I. Moric, G. Sanderson, S. Message, et al., *Respiratory viruses, symptoms, and inflammatory markers in acute exacerbations and stable chronic obstructive pulmonary disease.* Am J Respir Crit Care Med, 2001. **164**(9): p. 1618-23.

277. Rohde, G., A. Wiethege, I. Borg, M. Kauth, T.T. Bauer, A. Gillissen, et al., *Respiratory viruses in exacerbations of chronic obstructive pulmonary disease requiring hospitalisation: a case-control study.* Thorax, 2003. **58**(1): p. 37-42.

278. Falsey, A.R., P.A. Hennessey, M.A. Formica, C. Cox, and E.E. Walsh, *Respiratory syncytial virus infection in elderly and high-risk adults.* N Engl J Med, 2005. **352**(17): p. 1749-59.

279. Hamelin, M.E., S. Cote, J. Laforge, N. Lampron, J. Bourbeau, K. Weiss, et al., *Human metapneumovirus infection in adults with community-acquired pneumonia and exacerbation of chronic obstructive pulmonary disease.* Clin Infect Dis, 2005. **41**(4): p. 498-502.

280. Anderson, H.R., C. Spix, S. Medina, J.P. Schouten, J. Castellsague, G. Rossi, et al., *Air pollution and daily admissions for chronic obstructive pulmonary disease in 6 European cities: results from the APHEA project.* Eur Respir J, 1997. **10**(5): p. 1064-71.

281. Wordley, J., S. Walters, and J.G. Ayres, *Short term variations in hospital admissions and mortality and particulate air pollution.* Occup Environ Med, 1997. **54**(2): p. 108-16.

282. Donaldson, G.C., T. Seemungal, D.J. Jeffries, and J.A. Wedzicha, *Effect of temperature on lung function and symptoms in chronic obstructive pulmonary disease.* Eur Respir J, 1999. **13**(4): p. 844-9.

283. Biernacki, W.A., S.A. Kharitonov, and P.J. Barnes, *Increased leukotriene B4 and 8-isoprostane in exhaled breath condensate of patients with exacerbations of COPD.* Thorax, 2003. **58**(4): p. 294-8.

284. Gerritsen, W.B., J. Asin, P. Zanen, J.M. van den Bosch, and F.J. Haas, *Markers of inflammation and oxidative stress in exacerbated chronic obstructive pulmonary disease patients.* Respir Med, 2005. **99**(1): p. 84-90.

285. Gan, W.Q., S.F. Man, A. Senthilselvan, and D.D. Sin, *Association between chronic obstructive pulmonary disease and systemic inflammation: a systematic review and a meta-analysis.* Thorax, 2004. **59**(7): p. 574-80.

286. Dev, D., E. Wallace, R. Sankaran, J. Cunniffe, J.R. Govan, C.G. Wathen, et al., *Value of C-reactive protein measurements in exacerbations of chronic obstructive pulmonary disease.* Respir Med, 1998. **92**(4): p. 664-7.

287. Saldias, P.F., P.O. Diaz, D.J. Dreyse, B.A. Gaggero, A.C. Sandoval, and B.C. Lisboa, *[Etiology and biomarkers of systemic inflammation in mild to moderate COPD exacerbations].* Rev Med Chil, 2012. **140**(1): p. 10-8.

288. Seemungal, T.A., R. Harper-Owen, A. Bhowmik, D.J. Jeffries, and J.A. Wedzicha, *Detection of rhinovirus in induced sputum at exacerbation of chronic obstructive pulmonary disease.* Eur Respir J, 2000. **16**(4): p. 677-83.

289. Bhowmik, A., T.A. Seemungal, R.J. Sapsford, and J.A. Wedzicha, *Relation of sputum inflammatory markers to symptoms and lung function changes in COPD exacerbations.* Thorax, 2000. **55**(2): p. 114-20.

290. Banerjee, D., O.A. Khair, and D. Honeybourne, *Impact of sputum bacteria on airway inflammation and health status in clinical stable COPD.* Eur Respir J, 2004. **23**(5): p. 685-91.

291. Sethi, S., J. Maloney, L. Grove, C. Wrona, and C.S. Berenson, *Airway inflammation and bronchial bacterial colonization in chronic obstructive pulmonary disease.* Am J Respir Crit Care Med, 2006. **173**(9): p. 991-8.

292. Mercer, P.F., J.K. Shute, A. Bhowmik, G.C. Donaldson, J.A. Wedzicha, and J.A. Warner, *MMP-9, TIMP-1 and inflammatory cells in sputum from COPD patients during exacerbation.* Respir Res, 2005. **6**: p. 151.

293. Kang, M.J., C.G. Lee, J.Y. Lee, C.S. Dela Cruz, Z.J. Chen, R. Enelow, et al., *Cigarette smoke selectively enhances viral PAMP- and virus-induced pulmonary innate immune and remodeling responses in mice.* J Clin Invest, 2008. **118**(8): p. 2771-84.

294. Hayes, J.A., A. Korthy, and G.L. Snider, *The pathology of elastase-induced panacinar emphysema in hamsters.* J Pathol, 1975. **117**(1): p. 1-14.

295. Kaplan, P.D., C. Kuhn, and J.A. Pierce, *The induction of emphysema with elastase. I. The evolution of the lesion and the influence of serum.* J Lab Clin Med, 1973. **82**(3): p. 349-56.

296. Kuraki, T., M. Ishibashi, M. Takayama, M. Shiraishi, and M. Yoshida, *A novel oral neutrophil elastase inhibitor (ONO-6818) inhibits human neutrophil elastase-induced emphysema in rats.* Am J Respir Crit Care Med, 2002. **166**(4): p. 496-500.

297. Lafuma, C., E. Frisdal, A. Harf, L. Robert, and W. Hornebeck, *Prevention of leucocyte elastase-induced emphysema in mice by heparin fragments.* Eur Respir J, 1991. **4**(8): p. 1004-9.

298. Snider, G.L., C.B. Sherter, K.W. Koo, J.B. Karlinsky, J.A. Hayes, and C. Franzblau, *Respiratory mechanics in hamsters following treatment with endotracrael elastase or collagenase.* J Appl Physiol Respir Environ Exerc Physiol, 1977. **42**(2): p. 206-15.

299. Kao, R.C., N.G. Wehner, K.M. Skubitz, B.H. Gray, and J.R. Hoidal, *Proteinase 3. A distinct human polymorphonuclear leukocyte proteinase that produces emphysema in hamsters.* J Clin Invest, 1988. **82**(6): p. 1963-73.

300. Lesser, M., M.L. Padilla, and C. Cardozo, *Induction of emphysema in hamsters by intratracheal instillation of cathepsin B.* Am Rev Respir Dis, 1992. **145**(3): p. 661-8.

301. Snider, G.L., E.C. Lucey, and P.J. Stone, *Animal models of emphysema.* Am Rev Respir Dis, 1986. **133**(1): p. 149-69.

302. Snider, G.L., *Emphysema: the first two centuries--and beyond. A historical overview, with suggestions for future research: Part 2.* Am Rev Respir Dis, 1992. **146**(6): p. 1615-22.

303. Shapiro, S.D., *Animal models for COPD.* Chest, 2000. **117**(5 Suppl 1): p. 223S-7S.

304. Kuhn, C., 3rd and F. Tavassoli, *The scanning electron microscopy of elastase-induced emphysema. A comparison with emphysema in man.* Lab Invest, 1976. **34**(1): p. 2-9.

305. Trocme, C., C. Deffert, J. Cachat, Y. Donati, C. Tissot, S. Papacatzis, et al., *Macrophage-specific NOX2 contributes to the development of lung emphysema through modulation of SIRT1/MMP-9 pathways.* J Pathol, 2015. **235**(1): p. 65-78.

306. Ishii, Y., K. Itoh, Y. Morishima, T. Kimura, T. Kiwamoto, T. Iizuka, et al., *Transcription factor Nrf2 plays a pivotal role in protection against elastase-induced pulmonary inflammation and emphysema.* J Immunol, 2005. **175**(10): p. 6968-75.

307. Stone, P.J., E.C. Lucey, J.D. Calore, M.P. McMahon, G.L. Snider, and C. Franzblau, *Defenses of the hamster lung against human neutrophil and porcine pancreatic elastase.* Respiration, 1988. **54**(1): p. 1-15.

308. Gudapaty, S.R., I.E. Liener, J.R. Hoidal, R.V. Padmanabhan, D.E. Niewoehner, and J. Abel, *The prevention of elastase-induced emphysema in hamsters by the intratracheal administration of a synthetic elastase inhibitor bound to albumin microspheres.* Am Rev Respir Dis, 1985. **132**(1): p. 159-63.

309. Kleinerman, J., V. Ranga, D. Rynbrandt, J. Sorensen, and J.C. Powers, *The effect of the specific elastase inhibitor, alanyl alanyl prolyl alanine chloromethylketone, on elastase-induced emphysema.* Am Rev Respir Dis, 1980. **121**(2): p. 381-7.

310. Stone, P.J., E.C. Lucey, J.D. Calore, G.L. Snider, C. Franzblau, M.J. Castillo, et al., *The moderation of elastase-induced emphysema in the hamster by intratracheal pretreatment or post-treatment with succinyl alanyl alanyl prolyl valine chloromethyl ketone.* Am Rev Respir Dis, 1981. **124**(1): p. 56-9.

311. Rutgers, S.R., D.S. Postma, N.H. ten Hacken, H.F. Kauffman, T.W. van Der Mark, G.H. Koeter, et al., *Ongoing airway inflammation in patients with COPD who do not currently smoke.* Thorax, 2000. **55**(1): p. 12-8.

312. Mohamed Hoesein, F.A., P. Zanen, P.A. de Jong, B. van Ginneken, H.M. Boezen, H.J. Groen, et al., *Rate of progression of CT-quantified emphysema in male current and ex-smokers: a follow-up study.* Respir Res, 2013. **14**: p. 55.

313. Ito, S., E.P. Ingenito, K.K. Brewer, L.D. Black, H. Parameswaran, K.R. Lutchen, et al., *Mechanics, nonlinearity, and failure strength of lung tissue in a mouse model of emphysema: possible role of collagen remodeling.* J Appl Physiol (1985), 2005. **98**(2): p. 503-11.

314. Takahashi, A., A. Majumdar, H. Parameswaran, E. Bartolak-Suki, and B. Suki, *Proteoglycans maintain lung stability in an elastase-treated mouse model of emphysema.* Am J Respir Cell Mol Biol, 2014. **51**(1): p. 26-33.

315. Hamakawa, H., E. Bartolak-Suki, H. Parameswaran, A. Majumdar, K.R. Lutchen, and B. Suki, *Structure-function relations in an elastase-induced mouse model of emphysema.* Am J Respir Cell Mol Biol, 2011. **45**(3): p. 517-24.

316. Hou, H.H., S.L. Cheng, H.T. Liu, F.Z. Yang, H.C. Wang, and C.J. Yu, *Elastase induced lung epithelial cell apoptosis and emphysema through placenta growth factor.* Cell Death Dis, 2013. **4**: p. e793.

317. Lanzetti, M., C.A. da Costa, R.T. Nesi, M.V. Barroso, V. Martins, T. Victoni, et al., *Oxidative stress and nitrosative stress are involved in different stages of proteolytic pulmonary emphysema.* Free Radic Biol Med, 2012. **53**(11): p. 1993-2001.

318. Massaro, G.D. and D. Massaro, *Retinoic acid treatment abrogates elastase-induced pulmonary emphysema in rats.* Nat Med, 1997. **3**(6): p. 675-7.

319. Antunes, M.A. and P.R. Rocco, *Elastase-induced pulmonary emphysema: insights from experimental models.* An Acad Bras Cienc, 2011. **83**(4): p. 1385-96.

320. Vlahos, R. and S. Bozinovski, *Recent advances in pre-clinical mouse models of COPD.* Clin Sci (Lond), 2014. **126**(4): p. 253-65.

321. Wright, J.L. and A. Churg, *Animal models of cigarette smoke-induced chronic obstructive pulmonary disease.* Expert Rev Respir Med, 2010. **4**(6): p. 723-34.

322. Hele, D., *First Siena International Conference on animal models of chronic obstructive pulmonary disease, Certosa di Pontignano, University of Siena, Italy, September 30-October 2, 2001.* Respir Res, 2002. **3**: p. 12.

323. Huber, G.L., P. Davies, G.R. Zwilling, V.E. Pochay, W.C. Hinds, H.A. Nicholas, et al., *A morphologic and physiologic bioassay for quantifying alterations in the lung following experimental chronic inhalation of tobacco smoke.* Bull Eur Physiopathol Respir, 1981. **17**(2): p. 269-327.

324. Zheng, H., Y. Liu, T. Huang, Z. Fang, G. Li, and S. He, *Development and characterization of a rat model of chronic obstructive pulmonary disease (COPD) induced by sidestream cigarette smoke.* Toxicol Lett, 2009. **189**(3): p. 225-34.

325. Xu, L., B.Q. Cai, and Y.J. Zhu, *Pathogenesis of cigarette smoke-induced chronic obstructive pulmonary disease and therapeutic effects of glucocorticoids and N-acetylcysteine in rats.* Chin Med J (Engl), 2004. **117**(11): p. 1611-9.

326. Xue, Y., M.D. Haub, B.W. Smith, and R.C. Baybutt, *Decreases in bone mineral content by dietary all-trans retinoic acid precede decreases in bone mineral density in a weanling rat model of cigarette smoke-induced lung injuries.* Int J Vitam Nutr Res, 2011. **81**(1): p. 5-11.

327. Zhou, Y., X. Tan, W. Kuang, L. Liu, and L. Wan, *Erythromycin ameliorates cigarette-smoke-induced emphysema and inflammation in rats.* Transl Res, 2012. **159**(6): p. 464-72.

328. Rinaldi, M., K. Maes, S. De Vleeschauwer, D. Thomas, E.K. Verbeken, M. Decramer, et al., *Long-term nose-only cigarette smoke exposure induces emphysema and mild skeletal muscle dysfunction in mice.* Dis Model Mech, 2012. **5**(3): p. 333-41.

329. Cendon, S.P., C. Battlehner, G. Lorenzi Filho, M. Dohlnikoff, P.M. Pereira, G.M. Conceicao, et al., *Pulmonary emphysema induced by passive smoking: an experimental study in rats.* Braz J Med Biol Res, 1997. **30**(10): p. 1241-7.

330. Wright, J.L. and A. Churg, *Cigarette smoke causes physiologic and morphologic changes of emphysema in the guinea pig.* Am Rev Respir Dis, 1990. **142**(6 Pt 1): p. 1422-8.

331. Nemmar, A., H. Raza, D. Subramaniyan, A. John, M. Elwasila, B.H. Ali, et al., *Evaluation of the pulmonary effects of short-term nose-only cigarette smoke exposure in mice.* Exp Biol Med (Maywood), 2012. **237**(12): p. 1449-56.

332. Nemmar, A., H. Raza, D. Subramaniyan, J. Yasin, A. John, B.H. Ali, et al., *Short-term systemic effects of nose-only cigarette smoke exposure in mice: role of oxidative stress.* Cell Physiol Biochem, 2013. **31**(1): p. 15-24.

333. Stinn, W., A. Buettner, H. Weiler, B. Friedrichs, S. Luetjen, F. van Overveld, et al., *Lung inflammatory effects, tumorigenesis, and emphysema development in a long-term inhalation study with cigarette mainstream smoke in mice.* Toxicol Sci, 2013. **131**(2): p. 596-611.

334. Atkinson, J.J., B.A. Lutey, Y. Suzuki, H.M. Toennies, D.G. Kelley, D.K. Kobayashi, et al., *The role of matrix metalloproteinase-9 in cigarette smoke-induced emphysema.* Am J Respir Crit Care Med, 2011. **183**(7): p. 876-84.

335. Obot, C., K. Lee, A. Fuciarelli, R. Renne, and W. McKinney, *Characterization of mainstream cigarette smoke-induced biomarker responses in ICR and C57Bl/6 mice.* Inhal Toxicol, 2004. **16**(10): p. 701-19.

336. Chen, Y., M. Hanaoka, P. Chen, Y. Droma, N.F. Voelkel, and K. Kubo, *Protective effect of beraprost sodium, a stable prostacyclin analog, in the development of cigarette smoke extract-induced emphysema.* Am J Physiol Lung Cell Mol Physiol, 2009. **296**(4): p. L648-56.

337. Gualano, R.C., M.J. Hansen, R. Vlahos, J.E. Jones, R.A. Park-Jones, G. Deliyannis, et al., *Cigarette smoke worsens lung inflammation and impairs resolution of influenza infection in mice.* Respir Res, 2008. **9**: p. 53.

338. Bauer, C.M., C.C. Zavitz, F.M. Botelho, K.N. Lambert, E.G. Brown, K.L. Mossman, et al., *Treating viral exacerbations of chronic obstructive pulmonary disease: insights from a mouse model of cigarette smoke and H1N1 influenza infection.* PLoS One, 2010. **5**(10): p. e13251.

339. Foronjy, R.F., A.J. Dabo, C.C. Taggart, S. Weldon, and P. Geraghty, *Respiratory syncytial virus infections enhance cigarette smoke induced COPD in mice.* PLoS One, 2014. **9**(2): p. e90567.

340. Tanabe, N., Y. Hoshino, S. Marumo, H. Kiyokawa, S. Sato, D. Kinose, et al., *Thioredoxin-1 protects against neutrophilic inflammation and emphysema progression in a mouse model of chronic obstructive pulmonary disease exacerbation.* PLoS One, 2013. **8**(11): p. e79016.

341. Ganesan, S., A.T. Comstock, B. Kinker, P. Mancuso, J.M. Beck, and U.S. Sajjan, *Combined exposure to cigarette smoke and nontypeable Haemophilus influenzae drives development of a COPD phenotype in mice.* Respir Res, 2014. **15**: p. 11.

342. Wright, J.L., M. Cosio, and A. Churg, *Animal models of chronic obstructive pulmonary disease.* Am J Physiol Lung Cell Mol Physiol, 2008. **295**(1): p. L1-15.

343. Churg, A., D.D. Sin, and J.L. Wright, *Everything prevents emphysema: are animal models of cigarette smoke-induced chronic obstructive pulmonary disease any use?* Am J Respir Cell Mol Biol, 2011. **45**(6): p. 1111-5.

344. Motz, G.T., B.L. Eppert, G. Sun, S.C. Wesselkamper, M.J. Linke, R. Deka, et al., *Persistence of lung CD8 T cell oligoclonal expansions upon smoking cessation in a mouse model of cigarette smoke-induced emphysema.* J Immunol, 2008. **181**(11): p. 8036-43.

345. Hu, G., Y. Zhou, W. Hong, J. Tian, J. Hu, G. Peng, et al., *Development and systematic oxidative stress of a rat model of chronic bronchitis and emphysema induced by biomass smoke.* Exp Lung Res, 2013. **39**(6): p. 229-40.

346. Fidan, F., M. Unlu, M. Sezer, O. Sahin, C. Tokyol, and H. Esme, *Acute effects of environmental tobacco smoke and dried dung smoke on lung histopathology in rabbits.* Pathology, 2006. **38**(1): p. 53-7.

347. Lal, K., U. Mani, R. Pandey, N. Singh, A.K. Singh, D.K. Patel, et al., *Multiple approaches to evaluate the toxicity of the biomass fuel cow dung (kanda) smoke.* Ecotoxicol Environ Saf, 2011. **74**(7): p. 2126-32.

348. (EPA), U.S.E.P.A. *What Are the Six Common Air Pollutants?* 2014 [cited 2015 January]; Available from: http://www.epa.gov/oaqps001/urbanair/.

349. Gleason, J.A., L. Bielory, and J.A. Fagliano, *Associations between ozone, PM2.5, and four pollen types on emergency department pediatric asthma events during the warm season in New Jersey: a case-crossover study.* Environ Res, 2014. **132**: p. 421-9.

350. Delamater, P.L., A.O. Finley, and S. Banerjee, *An analysis of asthma hospitalizations, air pollution, and weather conditions in Los Angeles County, California.* Sci Total Environ, 2012. **425**: p. 110-8.

351. Strickland, M.J., L.A. Darrow, M. Klein, W.D. Flanders, J.A. Sarnat, L.A. Waller, et al., *Short-term associations between ambient air pollutants and pediatric asthma emergency department visits.* Am J Respir Crit Care Med, 2010. **182**(3): p. 307-16.

352. Kariisa, M., R. Foraker, M. Pennell, T. Buckley, P. Diaz, G.J. Criner, et al., *Short- and long-term effects of ambient ozone and fine particulate matter on the respiratory health of chronic obstructive pulmonary disease subjects.* Arch Environ Occup Health, 2015. **70**(1): p. 56-62.

353. Cho, H.Y., L.Y. Zhang, and S.R. Kleeberger, *Ozone-induced lung inflammation and hyperreactivity are mediated via tumor necrosis factor-alpha receptors.* Am J Physiol Lung Cell Mol Physiol, 2001. **280**(3): p. L537-46.

354. Koto, H., M. Salmon, B. Haddad el, T.J. Huang, J. Zagorski, and K.F. Chung, *Role of cytokine-induced neutrophil chemoattractant (CINC) in ozone-induced airway inflammation and hyperresponsiveness.* Am J Respir Crit Care Med, 1997. **156**(1): p. 234-9.

355. Williams, A.S., J.A. Mathews, D.I. Kasahara, L. Chen, A.P. Wurmbrand, H. Si, et al., *Augmented pulmonary responses to acute ozone exposure in obese mice: roles of TNFR2 and IL-13.* Environ Health Perspect, 2013. **121**(5): p. 551-7.

356. Wiegman, C.H., F. Li, C.J. Clarke, E. Jazrawi, P. Kirkham, P.J. Barnes, et al., *A comprehensive analysis of oxidative stress in the ozone-induced lung inflammation mouse model.* Clin Sci (Lond), 2014. **126**(6): p. 425-40.

357. Li, F., C. Wiegman, J.M. Seiffert, J. Zhu, C. Clarke, Y. Chang, et al., *Effects of N-acetylcysteine in ozone-induced chronic obstructive pulmonary disease model.* PLoS One, 2013. **8**(11): p. e80782.

358. Camberis, M., G. Le Gros, and J. Urban, Jr., *Animal model of Nippostrongylus brasiliensis and Heligmosomoides polygyrus.* Curr Protoc Immunol, 2003. **Chapter 19**: p. Unit 19 12.

359. Finkelman, F.D., T. Shea-Donohue, S.C. Morris, L. Gildea, R. Strait, K.B. Madden, et al., *Interleukin-4- and interleukin-13-mediated host protection against intestinal nematode parasites.* Immunol Rev, 2004. **201**: p. 139-55.

360. Ogilvie, B.M., *Nippostrongylus brasiliensis in mice: an explanation for the failure to induce worm expulsion from passively immunized animals.* Int J Parasitol, 1971. **1**(2): p. 161-7.

361. Allen, J.E. and R.M. Maizels, *Diversity and dialogue in immunity to helminths.* Nat Rev Immunol, 2011. **11**(6): p. 375-88.

362. Min, B., M. Prout, J. Hu-Li, J. Zhu, D. Jankovic, E.S. Morgan, et al., *Basophils produce IL-4 and accumulate in tissues after infection with a Th2-inducing parasite.* J Exp Med, 2004. **200**(4): p. 507-17.

363. Voehringer, D., K. Shinkai, and R.M. Locksley, *Type 2 immunity reflects orchestrated recruitment of cells committed to IL-4 production.* Immunity, 2004. **20**(3): p. 267-77.

364. Nair, M.G., I.J. Gallagher, M.D. Taylor, P. Loke, P.S. Coulson, R.A. Wilson, et al., *Chitinase and Fizz family members are a generalized feature of nematode infection with selective*

upregulation of Ym1 and Fizz1 by antigen-presenting cells. Infect Immun, 2005. **73**(1): p. 385-94.

365. Reece, J.J., M.C. Siracusa, and A.L. Scott, *Innate immune responses to lung-stage helminth infection induce alternatively activated alveolar macrophages.* Infect Immun, 2006. **74**(9): p. 4970-81.

366. Marsland, B.J., M. Camberis, and G. Le Gros, *Secretory products from infective forms of Nippostrongylus brasiliensis induce a rapid allergic airway inflammatory response.* Immunol Cell Biol, 2005. **83**(1): p. 40-7.

367. Heitmann, L., R. Rani, L. Dawson, C. Perkins, Y. Yang, J. Downey, et al., *TGF-beta-responsive myeloid cells suppress type 2 immunity and emphysematous pathology after hookworm infection.* Am J Pathol, 2012. **181**(3): p. 897-906.

368. Morrison, N.J., R.T. Abboud, F. Ramadan, R.R. Miller, N.N. Gibson, K.G. Evans, et al., *Comparison of single breath carbon monoxide diffusing capacity and pressure-volume curves in detecting emphysema.* Am Rev Respir Dis, 1989. **139**(5): p. 1179-87.

369. Gould, G.A., A.T. Redpath, M. Ryan, P.M. Warren, J.J. Best, D.C. Flenley, et al., *Lung CT density correlates with measurements of airflow limitation and the diffusing capacity.* Eur Respir J, 1991. **4**(2): p. 141-6.

370. Bates, D.V., *Revisiting "respiratory function in emphysema in relation to prognosis".* Can Respir J, 2000. **7**(3): p. 271-9.

371. Fallica, J., S. Das, M. Horton, and W. Mitzner, *Application of carbon monoxide diffusing capacity in the mouse lung.* J Appl Physiol (1985), 2011. **110**(5): p. 1455-9.

372. Limjunyawong, N., J. Fallica, A. Ramakrishnan, K. Datta, M. Gabrielson, M. Horton, et al., *Phenotyping mouse pulmonary function in vivo with the lung diffusing capacity.* J Vis Exp, 2015(95).

373. Pare, P.D. and W. Mitzner, *Airway-parenchymal interdependence.* Compr Physiol, 2012. **2**(3): p. 1921-35.

374. O'Donnell, D.E., *Hyperinflation, dyspnea, and exercise intolerance in chronic obstructive pulmonary disease.* Proc Am Thorac Soc, 2006. **3**(2): p. 180-4.

375. Papandrinopoulou, D., V. Tzouda, and G. Tsoukalas, *Lung compliance and chronic obstructive pulmonary disease.* Pulm Med, 2012. **2012**: p. 542769.

376. Soutiere, S.E. and W. Mitzner, *On defining total lung capacity in the mouse.* J Appl Physiol (1985), 2004. **96**(5): p. 1658-64.

377. Limjunyawong, N., J. Fallica, M.R. Horton, and W. Mitzner, *Measurement of the Pressure-volume Curve in Mouse Lungs.* J Vis Exp, 2015(95).

378. Hsia, C.C., D.M. Hyde, M. Ochs, E.R. Weibel, and A.E.J.T.F.o.Q.A.o.L. Structure, *An official research policy statement of the American Thoracic Society/European Respiratory Society: standards for quantitative assessment of lung structure.* Am J Respir Crit Care Med, 2010. **181**(4): p. 394-418.

379. Campbell, H. and S.I. Tomkeieff, *Calculation of the internal surface of a lung.* Nature, 1952. **170**(4316): p. 116-7.

380. Dunnill, M.S., *Quantitative methods in the study of pulmonary pathology.* Thorax, 1962. **17**(4): p. 320-28.

381. Knudsen, L., E.R. Weibel, H.J. Gundersen, F.V. Weinstein, and M. Ochs, *Assessment of air space size characteristics by intercept (chord) measurement: an accurate and efficient stereological approach.* J Appl Physiol (1985), 2010. **108**(2): p. 412-21.

382. Thurlbeck, W.M., *Measurement of distal airspace size.* Thorax, 1994. **49**(6): p. 625.

383. Heemskerk-Gerritsen, B.A., J.H. Dijkman, and A.A. Ten Have-Opbroek, *Stereological methods: a new approach in the assessment of pulmonary emphysema.* Microsc Res Tech, 1996. **34**(6): p. 556-62.

384. Wiebe, B.M. and H. Laursen, *Lung morphometry by unbiased methods in emphysema: bronchial and blood vessel volume, alveolar surface area and capillary length.* APMIS, 1998. **106**(6): p. 651-6.

385. Muhlfeld, C. and M. Ochs, *Quantitative microscopy of the lung: a problem-based approach. Part 2: stereological parameters and study designs in various diseases of the respiratory tract.* Am J Physiol Lung Cell Mol Physiol, 2013. **305**(3): p. L205-21.

386. Gurney, J.W., K.K. Jones, R.A. Robbins, G.L. Gossman, K.J. Nelson, D. Daughton, et al., *Regional distribution of emphysema: correlation of high-resolution CT with pulmonary function tests in unselected smokers.* Radiology, 1992. **183**(2): p. 457-63.

387. Munoz-Barrutia, A., M. Ceresa, X. Artaechevarria, L.M. Montuenga, and C. Ortiz-de-Solorzano, *Quantification of lung damage in an elastase-induced mouse model of emphysema.* Int J Biomed Imaging, 2012. **2012**: p. 734734.

388. Vasilescu, D.M., C. Klinge, L. Knudsen, L. Yin, G. Wang, E.R. Weibel, et al., *Stereological assessment of mouse lung parenchyma via nondestructive, multiscale micro-CT imaging validated by light microscopic histology.* J Appl Physiol (1985), 2013. **114**(6): p. 716-24.

389. Quintana, H.K., C. Cannet, S. Zurbruegg, F.X. Ble, J.R. Fozard, C.P. Page, et al., *Proton MRI as a noninvasive tool to assess elastase-induced lung damage in spontaneously breathing rats.* Magn Reson Med, 2006. **56**(6): p. 1242-50.

390. Olsson, L.E., M. Lindahl, P.O. Onnervik, L.B. Johansson, M. Palmer, M.K. Reimer, et al., *Measurement of MR signal and T2* in lung to characterize a tight skin mouse model of emphysema using single-point imaging.* J Magn Reson Imaging, 2007. **25**(3): p. 488-94.

391. Chen, X.J., L.W. Hedlund, H.E. Moller, M.S. Chawla, R.R. Maronpot, and G.A. Johnson, *Detection of emphysema in rat lungs by using magnetic resonance measurements of 3He diffusion.* Proc Natl Acad Sci U S A, 2000. **97**(21): p. 11478-81.

392. Peces-Barba, G., J. Ruiz-Cabello, Y. Cremillieux, I. Rodriguez, D. Dupuich, V. Callot, et al., *Helium-3 MRI diffusion coefficient: correlation to morphometry in a model of mild emphysema.* Eur Respir J, 2003. **22**(1): p. 14-9.

393. Iguchi, S., H. Imai, Y. Hori, J. Nakajima, A. Kimura, and H. Fujiwara, *Direct imaging of hyperpolarized 129Xe alveolar gas uptake in a mouse model of emphysema.* Magn Reson Med, 2013. **70**(1): p. 207-15.

394. Jobse, B.N., R.G. Rhem, I.Q. Wang, W.B. Counter, M.R. Stampfli, and N.R. Labiris, *Detection of lung dysfunction using ventilation and perfusion SPECT in a mouse model of chronic cigarette smoke exposure.* J Nucl Med, 2013. **54**(4): p. 616-23.

395. Townsend, M.J., P.G. Fallon, D.J. Matthews, H.E. Jolin, and A.N. McKenzie, *T1/ST2-deficient mice demonstrate the importance of T1/ST2 in developing primary T helper cell type 2 responses.* J Exp Med, 2000. **191**(6): p. 1069-76.

396. Mangan, N.E., A. Dasvarma, A.N. McKenzie, and P.G. Fallon, *T1/ST2 expression on Th2 cells negatively regulates allergic pulmonary inflammation.* Eur J Immunol, 2007. **37**(5): p. 1302-12.

397. Nakae, S., Y. Komiyama, A. Nambu, K. Sudo, M. Iwase, I. Homma, et al., *Antigen-specific T cell sensitization is impaired in Il-17-deficient mice, causing suppression of allergic cellular and humoral responses.* Immunity, 2002. **17**(3): p. 375-387.

398. Earl, P.L., N. Cooper, L.S. Wyatt, B. Moss, and M.W. Carroll, *Preparation of cell cultures and vaccinia virus stocks.* Curr Protoc Protein Sci, 2001. **Chapter 5**: p. Unit5 12.

399. Lorenzo, M.E., A. Hodgson, D.P. Robinson, J.B. Kaplan, A. Pekosz, and S.L. Klein, *Antibody responses and cross protection against lethal influenza A viruses differ between the sexes in C57BL/6 mice.* Vaccine, 2011. **29**(49): p. 9246-55.

400. Ewart, S., R. Levitt, and W. Mitzner, *Respiratory system mechanics in mice measured by end-inflation occlusion.* J Appl Physiol (1985), 1995. **79**(2): p. 560-6.

401. Hantos, Z., B. Daroczy, B. Suki, S. Nagy, and J.J. Fredberg, *Input impedance and peripheral inhomogeneity of dog lungs.* J Appl Physiol (1985), 1992. **72**(1): p. 168-78.

402. Scherle, W., *A simple method for volumetry of organs in quantitative stereology.* Mikroskopie, 1970. **26**(1): p. 57-60.

403. Kakhniashvili, D.G., L.A. Bulla, Jr., and S.R. Goodman, *The human erythrocyte proteome: analysis by ion trap mass spectrometry.* Mol Cell Proteomics, 2004. **3**(5): p. 501-9.

404. Boehm, D. and A. Bell, *Simply red: A novel spectrophotometric erythroid proliferation assay as a tool for erythropoiesis and erythrotoxicity studies.* Biotechnology Reports, 2014. **4**: p. 34-41.

405. Livak, K.J. and T.D. Schmittgen, *Analysis of relative gene expression data using real-time quantitative PCR and the 2(-Delta Delta C(T)) Method.* Methods, 2001. **25**(4): p. 402-8.

406. Siracusa, M.C., J.J. Reece, J.F. Urban, Jr., and A.L. Scott, *Dynamics of lung macrophage activation in response to helminth infection.* J Leukoc Biol, 2008. **84**(6): p. 1422-33.

407. Fischer, B.M., E. Pavlisko, and J.A. Voynow, *Pathogenic triad in COPD: oxidative stress, protease-antiprotease imbalance, and inflammation.* Int J Chron Obstruct Pulmon Dis, 2011. **6**: p. 413-21.

408. Fletcher, C. and R. Peto, *The natural history of chronic airflow obstruction.* Br Med J, 1977. **1**(6077): p. 1645-8.

409. Mahadeva, R. and S.D. Shapiro, *Chronic obstructive pulmonary disease * 3: Experimental animal models of pulmonary emphysema.* Thorax, 2002. **57**(10): p. 908-14.

410. Guerassimov, A., Y. Hoshino, Y. Takubo, A. Turcotte, M. Yamamoto, H. Ghezzo, et al., *The development of emphysema in cigarette smoke-exposed mice is strain dependent.* Am J Respir Crit Care Med, 2004. **170**(9): p. 974-80.

411. Johnson, M., *Laboratory Mice and Rats.* Labome.com: MATER METHODS, 2012. **2**: p. 113.

412. Mosmann, T.R. and R.L. Coffman, *TH1 and TH2 cells: different patterns of lymphokine secretion lead to different functional properties.* Annu Rev Immunol, 1989. **7**: p. 145-73.

413. Gueders, M.M., G. Paulissen, C. Crahay, F. Quesada-Calvo, J. Hacha, C. Van Hove, et al., *Mouse models of asthma: a comparison between C57BL/6 and BALB/c strains regarding bronchial responsiveness, inflammation, and cytokine production.* Inflamm Res, 2009. **58**(12): p. 845-54.

414. Filbey, K.J., J.R. Grainger, K.A. Smith, L. Boon, N. van Rooijen, Y. Harcus, et al., *Innate and adaptive type 2 immune cell responses in genetically controlled resistance to intestinal helminth infection.* Immunol Cell Biol, 2014. **92**(5): p. 436-48.

415. Sun, B., L.V. Rizzo, S.H. Sun, C.C. Chan, B. Wiggert, R.L. Wilder, et al., *Genetic susceptibility to experimental autoimmune uveitis involves more than a predisposition to generate a T helper-1-like or a T helper-2-like response.* J Immunol, 1997. **159**(2): p. 1004-11.

416. Reiner, S.L. and R.M. Locksley, *The regulation of immunity to Leishmania major.* Annu Rev Immunol, 1995. **13**: p. 151-77.

417. Muller, I., U. Fruth, and J.A. Louis, *Immunobiology of experimental leishmaniasis.* Med Microbiol Immunol, 1992. **181**(1): p. 1-12.

418. Schulte, S., G.K. Sukhova, and P. Libby, *Genetically programmed biases in Th1 and Th2 immune responses modulate atherogenesis.* Am J Pathol, 2008. **172**(6): p. 1500-8.

419. Santos, J.L., A.A. Andrade, A.A. Dias, C.A. Bonjardim, L.F. Reis, S.M. Teixeira, et al., *Differential sensitivity of C57BL/6 (M-1) and BALB/c (M-2) macrophages to the stimuli of IFN-gamma/LPS for the production of NO: correlation with iNOS mRNA and protein expression.* J Interferon Cytokine Res, 2006. **26**(9): p. 682-8.

420. Mills, C.D., K. Kincaid, J.M. Alt, M.J. Heilman, and A.M. Hill, *M-1/M-2 macrophages and the Th1/Th2 paradigm.* J Immunol, 2000. **164**(12): p. 6166-73.

421. Tumitan, A.R., L.G. Monnazzi, F.R. Ghiraldi, E.M. Cilli, and B.M. Machado de Medeiros, *Pattern of macrophage activation in yersinia-resistant and yersinia-susceptible strains of mice.* Microbiol Immunol, 2007. **51**(10): p. 1021-8.

422. Kovtunovych, G., M.A. Eckhaus, M.C. Ghosh, H. Ollivierre-Wilson, and T.A. Rouault, *Dysfunction of the heme recycling system in heme oxygenase 1-deficient mice: effects on macrophage viability and tissue iron distribution.* Blood, 2010. **116**(26): p. 6054-62.

423. Lalor, S.J., L.S. Dungan, C.E. Sutton, S.A. Basdeo, J.M. Fletcher, and K.H. Mills, *Caspase-1-processed cytokines IL-1beta and IL-18 promote IL-17 production by gammadelta and CD4 T cells that mediate autoimmunity.* J Immunol, 2011. **186**(10): p. 5738-48.

424. Bettelli, E., Y. Carrier, W. Gao, T. Korn, T.B. Strom, M. Oukka, et al., *Reciprocal developmental pathways for the generation of pathogenic effector TH17 and regulatory T cells.* Nature, 2006. **441**(7090): p. 235-8.

425. Martinez, F.O. and S. Gordon, *The M1 and M2 paradigm of macrophage activation: time for reassessment.* F1000Prime Rep, 2014. **6**: p. 13.

426. Snelgrove, R.J., J. Goulding, A.M. Didierlaurent, D. Lyonga, S. Vekaria, L. Edwards, et al., *A critical function for CD200 in lung immune homeostasis and the severity of influenza infection.* Nat Immunol, 2008. **9**(9): p. 1074-83.

427. Jenmalm, M.C., H. Cherwinski, E.P. Bowman, J.H. Phillips, and J.D. Sedgwick, *Regulation of myeloid cell function through the CD200 receptor.* J Immunol, 2006. **176**(1): p. 191-9.

428. Zuo, W., T. Zhang, D.Z. Wu, S.P. Guan, A.A. Liew, Y. Yamamoto, et al., *p63(+)Krt5(+) distal airway stem cells are essential for lung regeneration.* Nature, 2015. **517**(7536): p. 616-20.

429. Le, H., W. Kim, J. Kim, H.R. Cho, and B. Kwon, *Interleukin-33: a mediator of inflammation targeting hematopoietic stem and progenitor cells and their progenies.* Front Immunol, 2013. **4**: p. 104.

430. Borzone, G., L. Liberona, P. Olmos, C. Saez, M. Meneses, T. Reyes, et al., *Rat and hamster species differences in susceptibility to elastase-induced pulmonary emphysema relate to differences in elastase inhibitory capacity.* Am J Physiol Regul Integr Comp Physiol, 2007. **293**(3): p. R1342-9.

431. Borzone, G.R., L.F. Liberona, A.P. Bustamante, C.G. Saez, P.R. Olmos, A. Vecchiola, et al., *Differences in lung glutathione metabolism may account for rodent susceptibility in elastase-induced emphysema development.* Am J Physiol Regul Integr Comp Physiol, 2009. **296**(4): p. R1113-23.

432. Vecchiola, A., J.F. de la Llera, R. Ramirez, P. Olmos, C.I. Herrera, and G. Borzone, *Differences in acute lung response to elastase instillation in two rodent species may determine differences in severity of emphysema development.* Am J Physiol Regul Integr Comp Physiol, 2011. **301**(1): p. R148-58.

433. Ewart, S.L., D. Kuperman, E. Schadt, C. Tankersley, A. Grupe, D.M. Shubitowski, et al., *Quantitative trait loci controlling allergen-induced airway hyperresponsiveness in inbred mice.* Am J Respir Cell Mol Biol, 2000. **23**(4): p. 537-45.

434. Nadziejko, C., K. Fang, A. Bravo, and T. Gordon, *Susceptibility to pulmonary hypertension in inbred strains of mice exposed to cigarette smoke.* J Appl Physiol (1985), 2007. **102**(5): p. 1780-5.

435. Bartalesi, B., E. Cavarra, S. Fineschi, M. Lucattelli, B. Lunghi, P.A. Martorana, et al., *Different lung responses to cigarette smoke in two strains of mice sensitive to oxidants.* Eur Respir J, 2005. **25**(1): p. 15-22.

436. Kang, M.J., J.M. Choi, B.H. Kim, C.M. Lee, W.K. Cho, G. Choe, et al., *IL-18 induces emphysema and airway and vascular remodeling via IFN-gamma, IL-17A, and IL-13.* Am J Respir Crit Care Med, 2012. **185**(11): p. 1205-17.

437. Murray, P.J. and T.A. Wynn, *Protective and pathogenic functions of macrophage subsets.* Nat Rev Immunol, 2011. **11**(11): p. 723-37.

438. Page-McCaw, A., A.J. Ewald, and Z. Werb, *Matrix metalloproteinases and the regulation of tissue remodelling.* Nat Rev Mol Cell Biol, 2007. **8**(3): p. 221-33.

439. Sorsa, T., L. Tjaderhane, Y.T. Konttinen, A. Lauhio, T. Salo, H.M. Lee, et al., *Matrix metalloproteinases: contribution to pathogenesis, diagnosis and treatment of periodontal inflammation.* Ann Med, 2006. **38**(5): p. 306-21.

440. Murphy, G., V. Knauper, S. Atkinson, G. Butler, W. English, M. Hutton, et al., *Matrix metalloproteinases in arthritic disease.* Arthritis Res, 2002. **4 Suppl 3**: p. S39-49.

441. Sunil, V.R., K. Patel-Vayas, J. Shen, J.D. Laskin, and D.L. Laskin, *Classical and alternative macrophage activation in the lung following ozone-induced oxidative stress.* Toxicol Appl Pharmacol, 2012. **263**(2): p. 195-202.

442. Yuan, F., X. Fu, H. Shi, G. Chen, P. Dong, and W. Zhang, *Induction of murine macrophage M2 polarization by cigarette smoke extract via the JAK2/STAT3 pathway.* PLoS One, 2014. **9**(9): p. e107063.

443. Gebel, S., B. Gerstmayer, P. Kuhl, J. Borlak, K. Meurrens, and T. Muller, *The kinetics of transcriptomic changes induced by cigarette smoke in rat lungs reveals a specific program of defense, inflammation, and circadian clock gene expression.* Toxicol Sci, 2006. **93**(2): p. 422-31.

444. Kunz, L.I., T.S. Lapperre, J.B. Snoeck-Stroband, S.E. Budulac, W. Timens, S. van Wijngaarden, et al., *Smoking status and anti-inflammatory macrophages in bronchoalveolar lavage and induced sputum in COPD.* Respir Res, 2011. **12**: p. 34.

445. Ichinose, M., H. Sugiura, S. Yamagata, A. Koarai, and K. Shirato, *Increase in reactive nitrogen species production in chronic obstructive pulmonary disease airways.* Am J Respir Crit Care Med, 2000. **162**(2 Pt 1): p. 701-6.

446. van Straaten, J.F., D.S. Postma, W. Coers, J.A. Noordhoek, H.F. Kauffman, and W. Timens, *Macrophages in lung tissue from patients with pulmonary emphysema express both inducible and endothelial nitric oxide synthase.* Mod Pathol, 1998. **11**(7): p. 648-55.

447. Maestrelli, P., C. Paska, M. Saetta, G. Turato, Y. Nowicki, S. Monti, et al., *Decreased haem oxygenase-1 and increased inducible nitric oxide synthase in the lung of severe COPD patients.* Eur Respir J, 2003. **21**(6): p. 971-6.

448. Ito, K. and P.J. Barnes, *COPD as a disease of accelerated lung aging.* Chest, 2009. **135**(1): p. 173-80.

449. Demirjian, L., R.T. Abboud, H. Li, and V. Duronio, *Acute effect of cigarette smoke on TNF-alpha release by macrophages mediated through the erk1/2 pathway.* Biochim Biophys Acta, 2006. **1762**(6): p. 592-7.

450. Yang, S.R., A.S. Chida, M.R. Bauter, N. Shafiq, K. Seweryniak, S.B. Maggirwar, et al., *Cigarette smoke induces proinflammatory cytokine release by activation of NF-kappaB and posttranslational modifications of histone deacetylase in macrophages.* Am J Physiol Lung Cell Mol Physiol, 2006. **291**(1): p. L46-57.

451. Chu, C.T. and S.V. Pizzo, *alpha 2-Macroglobulin, complement, and biologic defense: antigens, growth factors, microbial proteases, and receptor ligation.* Lab Invest, 1994. **71**(6): p. 792-812.

452. Rehman, A.A., H. Ahsan, and F.H. Khan, *alpha-2-Macroglobulin: a physiological guardian.* J Cell Physiol, 2013. **228**(8): p. 1665-75.

453. Martorana, P.A., T. Brand, C. Gardi, P. van Even, M.M. de Santi, P. Calzoni, et al., *The pallid mouse. A model of genetic alpha 1-antitrypsin deficiency.* Lab Invest, 1993. **68**(2): p. 233-41.

454. Cavarra, E., P.A. Martorana, F. Gambelli, M. de Santi, P. van Even, and G. Lungarella, *Neutrophil recruitment into the lungs is associated with increased lung elastase burden, decreased lung elastin, and emphysema in alpha 1 proteinase inhibitor-deficient mice.* Lab Invest, 1996. **75**(2): p. 273-80.

455. Marcelino, M.Y., N.L. Fuoco, C.A. de Faria, L. Kozma Rde, L.F. Marques, and J.T. Ribeiro-Paes, *Animal models in chronic obstructive pulmonary disease-an overview.* Exp Lung Res, 2014. **40**(6): p. 259-71.

456. Lane, N., R.A. Robins, J. Corne, and L. Fairclough, *Regulation in chronic obstructive pulmonary disease: the role of regulatory T-cells and Th17 cells.* Clin Sci (Lond), 2010. **119**(2): p. 75-86.

457. Meijer, M., G.T. Rijkers, and F.J. van Overveld, *Neutrophils and emerging targets for treatment in chronic obstructive pulmonary disease.* Expert Rev Clin Immunol, 2013. **9**(11): p. 1055-68.

458. Terashima, T., M.E. Klut, D. English, J. Hards, J.C. Hogg, and S.F. van Eeden, *Cigarette smoking causes sequestration of polymorphonuclear leukocytes released from the bone marrow in lung microvessels.* Am J Respir Cell Mol Biol, 1999. **20**(1): p. 171-7.

459. Wilgus, T.A., S. Roy, and J.C. McDaniel, *Neutrophils and Wound Repair: Positive Actions and Negative Reactions.* Adv Wound Care (New Rochelle), 2013. **2**(7): p. 379-388.

460. Kolaczkowska, E. and P. Kubes, *Neutrophil recruitment and function in health and inflammation.* Nat Rev Immunol, 2013. **13**(3): p. 159-75.

461. Donnelly, L.E. and P.J. Barnes, *Defective phagocytosis in airways disease.* Chest, 2012. **141**(4): p. 1055-62.

462. Henson, P.M., G.P. Cosgrove, and R.W. Vandivier, *State of the art. Apoptosis and cell homeostasis in chronic obstructive pulmonary disease.* Proc Am Thorac Soc, 2006. **3**(6): p. 512-6.

463. Brinkmann, V. and A. Zychlinsky, *Neutrophil extracellular traps: is immunity the second function of chromatin?* J Cell Biol, 2012. **198**(5): p. 773-83.

464. Saetta, M., A. Di Stefano, P. Maestrelli, A. Ferraresso, R. Drigo, A. Potena, et al., *Activated T-lymphocytes and macrophages in bronchial mucosa of subjects with chronic bronchitis.* Am Rev Respir Dis, 1993. **147**(2): p. 301-6.

465. Chung, K.F. and I.M. Adcock, *Multifaceted mechanisms in COPD: inflammation, immunity, and tissue repair and destruction.* Eur Respir J, 2008. **31**(6): p. 1334-56.

466. Finkelstein, R., R.S. Fraser, H. Ghezzo, and M.G. Cosio, *Alveolar inflammation and its relation to emphysema in smokers.* Am J Respir Crit Care Med, 1995. **152**(5 Pt 1): p. 1666-72.

467. Meshi, B., T.Z. Vitalis, D. Ionescu, W.M. Elliott, C. Liu, X.D. Wang, et al., *Emphysematous lung destruction by cigarette smoke. The effects of latent adenoviral infection on the lung inflammatory response.* Am J Respir Cell Mol Biol, 2002. **26**(1): p. 52-7.

468. Hodge, S., G. Matthews, V. Mukaro, J. Ahern, A. Shivam, G. Hodge, et al., *Cigarette smoke-induced changes to alveolar macrophage phenotype and function are improved by treatment with procysteine.* Am J Respir Cell Mol Biol, 2011. **44**(5): p. 673-81.

469. Shaykhiev, R., A. Krause, J. Salit, Y. Strulovici-Barel, B.G. Harvey, T.P. O'Connor, et al., *Smoking-dependent reprogramming of alveolar macrophage polarization: implication for pathogenesis of chronic obstructive pulmonary disease.* J Immunol, 2009. **183**(4): p. 2867-83.

470. Maziak, W., S. Loukides, S. Culpitt, P. Sullivan, S.A. Kharitonov, and P.J. Barnes, *Exhaled nitric oxide in chronic obstructive pulmonary disease.* Am J Respir Crit Care Med, 1998. **157**(3 Pt 1): p. 998-1002.

471. Hogg, J.C., F. Chu, S. Utokaparch, R. Woods, W.M. Elliott, L. Buzatu, et al., *The nature of small-airway obstruction in chronic obstructive pulmonary disease.* N Engl J Med, 2004. **350**(26): p. 2645-53.

472. Maeno, T., A.M. Houghton, P.A. Quintero, S. Grumelli, C.A. Owen, and S.D. Shapiro, *CD8+ T Cells are required for inflammation and destruction in cigarette smoke-induced emphysema in mice.* J Immunol, 2007. **178**(12): p. 8090-6.

473. Zhou, H., W. Hua, Y. Jin, C. Zhang, L. Che, L. Xia, et al., *Tc17 cells are associated with cigarette smoke-induced lung inflammation and emphysema.* Respirology, 2015.

474. Duan, M.C., H.J. Tang, X.N. Zhong, and Y. Huang, *Persistence of Th17/Tc17 cell expression upon smoking cessation in mice with cigarette smoke-induced emphysema.* Clin Dev Immunol, 2013. **2013**: p. 350727.

475. Harrison, O.J., J. Foley, B.J. Bolognese, E. Long, 3rd, P.L. Podolin, and P.T. Walsh, *Airway infiltration of CD4+ CCR6+ Th17 type cells associated with chronic cigarette smoke induced airspace enlargement.* Immunol Lett, 2008. **121**(1): p. 13-21.

476. Bettelli, E., T. Korn, M. Oukka, and V.K. Kuchroo, *Induction and effector functions of T(H)17 cells.* Nature, 2008. **453**(7198): p. 1051-7.

477. Shan, M., H.F. Cheng, L.Z. Song, L. Roberts, L. Green, J. Hacken-Bitar, et al., *Lung myeloid dendritic cells coordinately induce TH1 and TH17 responses in human emphysema.* Sci Transl Med, 2009. **1**(4): p. 4ra10.

478. Mombaerts, P., J. Iacomini, R.S. Johnson, K. Herrup, S. Tonegawa, and V.E. Papaioannou, *RAG-1-deficient mice have no mature B and T lymphocytes.* Cell, 1992. **68**(5): p. 869-77.

479. Takeda, K., T. Tanaka, W. Shi, M. Matsumoto, M. Minami, S. Kashiwamura, et al., *Essential role of Stat6 in IL-4 signalling.* Nature, 1996. **380**(6575): p. 627-30.

480. Weng, M., D. Huntley, I.F. Huang, O. Foye-Jackson, L. Wang, A. Sarkissian, et al., *Alternatively activated macrophages in intestinal helminth infection: effects on concurrent bacterial colitis.* J Immunol, 2007. **179**(7): p. 4721-31.

481. Reece, J.J., M.C. Siracusa, T.L. Southard, C.F. Brayton, J.F. Urban, Jr., and A.L. Scott, *Hookworm-induced persistent changes to the immunological environment of the lung.* Infect Immun, 2008. **76**(8): p. 3511-24.

482. Lang, R., D. Patel, J.J. Morris, R.L. Rutschman, and P.J. Murray, *Shaping gene expression in activated and resting primary macrophages by IL-10.* J Immunol, 2002. **169**(5): p. 2253-63.

483. Fernando, M.R., J.L. Reyes, J. Iannuzzi, G. Leung, and D.M. McKay, *The pro-inflammatory cytokine, interleukin-6, enhances the polarization of alternatively activated macrophages.* PLoS One, 2014. **9**(4): p. e94188.

484. Milovanovic, M., V. Volarevic, G. Radosavljevic, I. Jovanovic, N. Pejnovic, N. Arsenijevic, et al., *IL-33/ST2 axis in inflammation and immunopathology.* Immunol Res, 2012. **52**(1-2): p. 89-99.

485. Lefrancais, E. and C. Cayrol, *Mechanisms of IL-33 processing and secretion: differences and similarities between IL-1 family members.* Eur Cytokine Netw, 2012. **23**(4): p. 120-7.

486. Neill, D.R., S.H. Wong, A. Bellosi, R.J. Flynn, M. Daly, T.K. Langford, et al., *Nuocytes represent a new innate effector leukocyte that mediates type-2 immunity.* Nature, 2010. **464**(7293): p. 1367-70.

487. Mizutani, N., T. Nabe, and S. Yoshino, *Interleukin-33 and alveolar macrophages contribute to the mechanisms underlying the exacerbation of IgE-mediated airway inflammation and remodelling in mice.* Immunology, 2013. **139**(2): p. 205-18.

488. Kurowska-Stolarska, M., B. Stolarski, P. Kewin, G. Murphy, C.J. Corrigan, S. Ying, et al., *IL-33 amplifies the polarization of alternatively activated macrophages that contribute to airway inflammation.* J Immunol, 2009. **183**(10): p. 6469-77.

489. Beers, M.F., C.Y. Kim, C. Dodia, and A.B. Fisher, *Localization, synthesis, and processing of surfactant protein SP-C in rat lung analyzed by epitope-specific antipeptide antibodies.* J Biol Chem, 1994. **269**(32): p. 20318-28.

490. Daley, J.M., A.A. Thomay, M.D. Connolly, J.S. Reichner, and J.E. Albina, *Use of Ly6G-specific monoclonal antibody to deplete neutrophils in mice.* J Leukoc Biol, 2008. **83**(1): p. 64-70.

491. Henderson, R.B., J.A. Hobbs, M. Mathies, and N. Hogg, *Rapid recruitment of inflammatory monocytes is independent of neutrophil migration.* Blood, 2003. **102**(1): p. 328-35.

492. Geissmann, F., S. Jung, and D.R. Littman, *Blood monocytes consist of two principal subsets with distinct migratory properties.* Immunity, 2003. **19**(1): p. 71-82.

493. Nakano, H., M. Yanagita, and M.D. Gunn, *CD11c(+)B220(+)Gr-1(+) cells in mouse lymph nodes and spleen display characteristics of plasmacytoid dendritic cells.* J Exp Med, 2001. **194**(8): p. 1171-8.

494. Palamara, F., S. Meindl, M. Holcmann, P. Luhrs, G. Stingl, and M. Sibilia, *Identification and characterization of pDC-like cells in normal mouse skin and melanomas treated with imiquimod.* J Immunol, 2004. **173**(5): p. 3051-61.

495. Matsuzaki, J., T. Tsuji, K. Chamoto, T. Takeshima, F. Sendo, and T. Nishimura, *Successful elimination of memory-type CD8+ T cell subsets by the administration of anti-Gr-1 monoclonal antibody in vivo.* Cell Immunol, 2003. **224**(2): p. 98-105.

496. Tumpey, T.M., S.H. Chen, J.E. Oakes, and R.N. Lausch, *Neutrophil-mediated suppression of virus replication after herpes simplex virus type 1 infection of the murine cornea.* J Virol, 1996. **70**(2): p. 898-904.

497. Kidokoro, Y., T.C. Kravis, K.M. Moser, J.C. Taylor, and I.P. Crawford, *Relationship of leukocyte elastase concentration to severity of emphysema in homozygous alpha1-antitrypsin-deficient persons.* Am Rev Respir Dis, 1977. **115**(5): p. 793-803.

498. Churg, A., R.D. Wang, C. Xie, and J.L. Wright, *alpha-1-Antitrypsin ameliorates cigarette smoke-induced emphysema in the mouse.* Am J Respir Crit Care Med, 2003. **168**(2): p. 199-207.

499. D'Hulst A, I., T. Maes, K.R. Bracke, I.K. Demedts, K.G. Tournoy, G.F. Joos, et al., *Cigarette smoke-induced pulmonary emphysema in scid-mice. Is the acquired immune system required?* Respir Res, 2005. **6**: p. 147.

500. Gordon, S. and P.R. Taylor, *Monocyte and macrophage heterogeneity.* Nat Rev Immunol, 2005. **5**(12): p. 953-64.

501. Mackaness, G.B., *Cellular resistance to infection.* J Exp Med, 1962. **116**: p. 381-406.

502. Stein, M., S. Keshav, N. Harris, and S. Gordon, *Interleukin 4 potently enhances murine macrophage mannose receptor activity: a marker of alternative immunologic macrophage activation.* J Exp Med, 1992. **176**(1): p. 287-92.

503. Murray, P.J., J.E. Allen, S.K. Biswas, E.A. Fisher, D.W. Gilroy, S. Goerdt, et al., *Macrophage activation and polarization: nomenclature and experimental guidelines.* Immunity, 2014. **41**(1): p. 14-20.

504. Nelson, M.P., B.S. Christmann, C.W. Dunaway, A. Morris, and C. Steele, *Experimental Pneumocystis lung infection promotes M2a alveolar macrophage-derived MMP12 production.* Am J Physiol Lung Cell Mol Physiol, 2012. **303**(5): p. L469-75.

505. Sica, A. and A. Mantovani, *Macrophage plasticity and polarization: in vivo veritas.* J Clin Invest, 2012. **122**(3): p. 787-95.

506. Lanone, S., T. Zheng, Z. Zhu, W. Liu, C.G. Lee, B. Ma, et al., *Overlapping and enzyme-specific contributions of matrix metalloproteinases-9 and -12 in IL-13-induced inflammation and remodeling.* J Clin Invest, 2002. **110**(4): p. 463-74.

507. Kim, H.Y., Y.J. Chang, S. Subramanian, H.H. Lee, L.A. Albacker, P. Matangkasombut, et al., *Innate lymphoid cells responding to IL-33 mediate airway hyperreactivity independently of adaptive immunity.* J Allergy Clin Immunol, 2012. **129**(1): p. 216-27 e1-6.

508. Martinez, F.O., L. Helming, and S. Gordon, *Alternative activation of macrophages: an immunologic functional perspective.* Annu Rev Immunol, 2009. **27**: p. 451-83.

509. Bowie, A. and L.A. O'Neill, *The interleukin-1 receptor/Toll-like receptor superfamily: signal generators for pro-inflammatory interleukins and microbial products.* J Leukoc Biol, 2000. **67**(4): p. 508-14.

510. Mauer, J., B. Chaurasia, J. Goldau, M.C. Vogt, J. Ruud, K.D. Nguyen, et al., *Signaling by IL-6 promotes alternative activation of macrophages to limit endotoxemia and obesity-associated resistance to insulin.* Nat Immunol, 2014. **15**(5): p. 423-30.

511. Ma, B., M.J. Kang, C.G. Lee, S. Chapoval, W. Liu, Q. Chen, et al., *Role of CCR5 in IFN-gamma-induced and cigarette smoke-induced emphysema.* J Clin Invest, 2005. **115**(12): p. 3460-72.

512. Pinart, M., M. Zhang, F. Li, F. Hussain, J. Zhu, C. Wiegman, et al., *IL-17A modulates oxidant stress-induced airway hyperresponsiveness but not emphysema.* PLoS One, 2013. **8**(3): p. e58452.

513. Linden, A., M. Laan, and G.P. Anderson, *Neutrophils, interleukin-17A and lung disease.* Eur Respir J, 2005. **25**(1): p. 159-72.

514. Iwakura, Y., H. Ishigame, S. Saijo, and S. Nakae, *Functional specialization of interleukin-17 family members.* Immunity, 2011. **34**(2): p. 149-62.

515. Harris, T.J., J.F. Grosso, H.R. Yen, H. Xin, M. Kortylewski, E. Albesiano, et al., *Cutting edge: An in vivo requirement for STAT3 signaling in TH17 development and TH17-dependent autoimmunity.* J Immunol, 2007. **179**(7): p. 4313-7.

516. Cua, D.J. and C.M. Tato, *Innate IL-17-producing cells: the sentinels of the immune system.* Nat Rev Immunol, 2010. **10**(7): p. 479-89.

517. Hurd, S., *The impact of COPD on lung health worldwide: epidemiology and incidence.* Chest, 2000. **117**(2 Suppl): p. 1S-4S.

518. Moss, B., *Poxvirus DNA replication.* Cold Spring Harb Perspect Biol, 2013. **5**(9).

519. Bell, J.C., K.A. Garson, B.D. Lichty, and D.F. Stojdl, *Oncolytic viruses: programmable tumour hunters.* Curr Gene Ther, 2002. **2**(2): p. 243-54.

520. Lin, E. and J. Nemunaitis, *Oncolytic viral therapies.* Cancer Gene Ther, 2004. **11**(10): p. 643-64.

521. Guo, Z.S. and D.L. Bartlett, *Vaccinia as a vector for gene delivery.* Expert Opin Biol Ther, 2004. **4**(6): p. 901-17.

522. Essajee, S. and H.L. Kaufman, *Poxvirus vaccines for cancer and HIV therapy.* Expert Opin Biol Ther, 2004. **4**(4): p. 575-88.

523. Wang, L.C., R.C. Lynn, G. Cheng, E. Alexander, V. Kapoor, E.K. Moon, et al., *Treating tumors with a vaccinia virus expressing IFNbeta illustrates the complex relationships between oncolytic ability and immunogenicity.* Mol Ther, 2012. **20**(4): p. 736-48.

524. Weidinger, G., M. Ohlmann, B. Schlereth, G. Sutter, and S. Niewiesk, *Vaccination with recombinant modified vaccinia virus Ankara protects against measles virus infection in the mouse and cotton rat model.* Vaccine, 2001. **19**(20-22): p. 2764-8.

525. Collins, S.L., Y. Chan-Li, R.W. Hallowell, J.D. Powell, and M.R. Horton, *Pulmonary vaccination as a novel treatment for lung fibrosis.* PLoS One, 2012. **7**(2): p. e31299.

526. Lamb, R.A. and R.M. Krug, *Orthomyxoviridae: the viruses and their replication.*, in *Fields Virology*, D.M. Knipe and P.M. Howley, Editors. 2001, Lippincott Williams & Wilkins: Philadelphia, USA. p. 1487–1531.

527. Itoh, Y., K. Shinya, M. Kiso, T. Watanabe, Y. Sakoda, M. Hatta, et al., *In vitro and in vivo characterization of new swine-origin H1N1 influenza viruses.* Nature, 2009. **460**(7258): p. 1021-5.

528. Kuiken, T., B. Riteau, R.A. Fouchier, and G.F. Rimmelzwaan, *Pathogenesis of influenza virus infections: the good, the bad and the ugly.* Curr Opin Virol, 2012. **2**(3): p. 276-86.

529. Simonsen, L., P. Spreeuwenberg, R. Lustig, R.J. Taylor, D.M. Fleming, M. Kroneman, et al., *Global mortality estimates for the 2009 Influenza Pandemic from the GLaMOR project: a modeling study.* PLoS Med, 2013. **10**(11): p. e1001558.

530. Dawood, F.S., A.D. Iuliano, C. Reed, M.I. Meltzer, D.K. Shay, P.Y. Cheng, et al., *Estimated global mortality associated with the first 12 months of 2009 pandemic influenza A H1N1 virus circulation: a modelling study.* Lancet Infect Dis, 2012. **12**(9): p. 687-95.

531. Zwaans, W.A., P. Mallia, M.E. van Winden, and G.G. Rohde, *The relevance of respiratory viral infections in the exacerbations of chronic obstructive pulmonary disease-a systematic review.* J Clin Virol, 2014. **61**(2): p. 181-8.

532. Wu, X., D. Chen, X. Gu, X. Su, Y. Song, and Y. Shi, *Prevalence and risk of viral infection in patients with acute exacerbation of chronic obstructive pulmonary disease: a meta-analysis.* Mol Biol Rep, 2014. **41**(7): p. 4743-51.

533. Cilloniz, C., K. Shinya, X. Peng, M.J. Korth, S.C. Proll, L.D. Aicher, et al., *Lethal influenza virus infection in macaques is associated with early dysregulation of inflammatory related genes.* PLoS Pathog, 2009. **5**(10): p. e1000604.

534. Kobasa, D., S.M. Jones, K. Shinya, J.C. Kash, J. Copps, H. Ebihara, et al., *Aberrant innate immune response in lethal infection of macaques with the 1918 influenza virus.* Nature, 2007. **445**(7125): p. 319-23.

535. Arankalle, V.A., K.S. Lole, R.P. Arya, A.S. Tripathy, A.Y. Ramdasi, M.S. Chadha, et al., *Role of host immune response and viral load in the differential outcome of pandemic H1N1 (2009) influenza virus infection in Indian patients.* PLoS One, 2010. **5**(10).

536. Kohyama, S., S. Ohno, A. Isoda, O. Moriya, M.L. Belladonna, H. Hayashi, et al., *IL-23 enhances host defense against vaccinia virus infection via a mechanism partly involving IL-17.* J Immunol, 2007. **179**(6): p. 3917-25.

537. Han, Y., M.T. Ling, H. Mao, J. Zheng, M. Liu, K.T. Lam, et al., *Influenza virus-induced lung inflammation was modulated by cigarette smoke exposure in mice.* PLoS One, 2014. **9**(1): p. e86166.

538. Gaschler, G.J., C.C. Zavitz, C.M. Bauer, and M.R. Stampfli, *Mechanisms of clearance of nontypeable Haemophilus influenzae from cigarette smoke-exposed mouse lungs.* Eur Respir J, 2010. **36**(5): p. 1131-42.

539. Yageta, Y., Y. Ishii, Y. Morishima, H. Masuko, S. Ano, T. Yamadori, et al., *Role of Nrf2 in host defense against influenza virus in cigarette smoke-exposed mice.* J Virol, 2011. **85**(10): p. 4679-90.

540. Mayr, A., V. Hochstein-Mintzel, and H. Stickl, *Abstammung, Eigenschaften und Verwendung des attenuierten Vaccinia-Stammes MVA.* Infection, 1975. **3**(1): p. 6-14.

541. Seet, B.T., J.B. Johnston, C.R. Brunetti, J.W. Barrett, H. Everett, C. Cameron, et al., *Poxviruses and immune evasion.* Annu Rev Immunol, 2003. **21**: p. 377-423.

542. Isaacs, S.N., G.J. Kotwal, and B. Moss, *Vaccinia virus complement-control protein prevents antibody-dependent complement-enhanced neutralization of infectivity and contributes to virulence.* Proc Natl Acad Sci U S A, 1992. **89**(2): p. 628-32.

543. McFadden, G., *Poxvirus tropism.* Nat Rev Microbiol, 2005. **3**(3): p. 201-13.

544. Acres, B., *Cancer immunotherapy: phase II clinical studies with TG4010 (MVA-MUC1-IL2).* J BUON, 2007. **12 Suppl 1**: p. S71-5.

545. Carroll, M.W., W.W. Overwijk, R.S. Chamberlain, S.A. Rosenberg, B. Moss, and N.P. Restifo, *Highly attenuated modified vaccinia virus Ankara (MVA) as an effective recombinant vector: a murine tumor model.* Vaccine, 1997. **15**(4): p. 387-94.

546. Liu, M., B. Acres, J.M. Balloul, N. Bizouarne, S. Paul, P. Slos, et al., *Gene-based vaccines and immunotherapeutics.* Proc Natl Acad Sci U S A, 2004. **101 Suppl 2**: p. 14567-71.

547. Sutter, G. and B. Moss, *Nonreplicating vaccinia vector efficiently expresses recombinant genes.* Proc Natl Acad Sci U S A, 1992. **89**(22): p. 10847-51.

548. Ramirez, J.C., M.M. Gherardi, and M. Esteban, *Biology of attenuated modified vaccinia virus Ankara recombinant vector in mice: virus fate and activation of B- and T-cell immune responses in comparison with the Western Reserve strain and advantages as a vaccine.* J Virol, 2000. **74**(2): p. 923-33.

549. Yoshida, A., Y. Koide, M. Uchijima, and T.O. Yoshida, *Dissection of strain difference in acquired protective immunity against Mycobacterium bovis Calmette-Guerin bacillus (BCG). Macrophages regulate the susceptibility through cytokine network and the induction of nitric oxide synthase.* J Immunol, 1995. **155**(4): p. 2057-66.

550. Tate, M.D., H.C. Schilter, A.G. Brooks, and P.C. Reading, *Responses of mouse airway epithelial cells and alveolar macrophages to virulent and avirulent strains of influenza A virus.* Viral Immunol, 2011. **24**(2): p. 77-88.

551. Loosli, C.G., S.F. Stinson, D.P. Ryan, M.S. Hertweck, J.D. Hardy, and R. Serebrin, *The destruction of type 2 pneumocytes by airborne influenza PR8-A virus; its effect on surfactant and lecithin content of the pneumonic lesions of mice.* Chest, 1975. **67**(2 Suppl): p. 7S-14S.

552. Ayala, V.I., J.R. Teijaro, D.L. Farber, S.G. Dorsey, and N.H. Carbonetti, *Bordetella pertussis infection exacerbates influenza virus infection through pertussis toxin-mediated suppression of innate immunity.* PLoS One, 2011. **6**(4): p. e19016.

553. Armstrong, R., S. Jordan, J. Carter, A. Rowles, K. Meecham, and D. Rodgers, *Assessment of viral load and time course of pulmonary inflammation in a murine model of H1N1 (PR8) influenza virus infection.* European Respiratory Journal, 2014. **44**(Suppl 58).

554. Davidson, S., S. Crotta, T.M. McCabe, and A. Wack, *Pathogenic potential of interferon alphabeta in acute influenza infection.* Nat Commun, 2014. **5**: p. 3864.

555. Lv, J., D. Wang, Y.H. Hua, S.J. Pei, J. Wang, W.W. Hu, et al., *Pulmonary immune responses to 2009 pandemic influenza A (H1N1) virus in mice.* BMC Infect Dis, 2014. **14**: p. 197.

556. Ghoneim, H.E., P.G. Thomas, and J.A. McCullers, *Depletion of alveolar macrophages during influenza infection facilitates bacterial superinfections.* J Immunol, 2013. **191**(3): p. 1250-9.

557. Didierlaurent, A., J. Goulding, S. Patel, R. Snelgrove, L. Low, M. Bebien, et al., *Sustained desensitization to bacterial Toll-like receptor ligands after resolution of respiratory influenza infection.* J Exp Med, 2008. **205**(2): p. 323-9.

558. Mitzner, W., *Use of mean airspace chord length to assess emphysema.* J Appl Physiol (1985), 2008. **105**(6): p. 1980-1.

559. Weibel, E.R., *Morphological quantitation of emphysema: a debate.* J Appl Physiol (1985), 2006. **100**(4): p. 1419-20; author reply 1420-1.

560. Holmdahl, R. and B. Malissen, *The need for littermate controls.* Eur J Immunol, 2012. **42**(1): p. 45-7.

561. Fleming, B.D. and D.M. Mosser, *Regulatory macrophages: setting the threshold for therapy.* Eur J Immunol, 2011. **41**(9): p. 2498-502.

562. Churg, A., S. Zhou, and J.L. Wright, *Series "matrix metalloproteinases in lung health and disease": Matrix metalloproteinases in COPD.* Eur Respir J, 2012. **39**(1): p. 197-209.

563. Song, C., L. Luo, Z. Lei, B. Li, Z. Liang, G. Liu, et al., *IL-17-producing alveolar macrophages mediate allergic lung inflammation related to asthma.* J Immunol, 2008. **181**(9): p. 6117-24.

564. Yang, Z., V. Grinchuk, J.F. Urban, Jr., J. Bohl, R. Sun, L. Notari, et al., *Macrophages as IL-25/IL-33-responsive cells play an important role in the induction of type 2 immunity.* PLoS One, 2013. **8**(3): p. e59441.

565. Lefrancais, E., S. Roga, V. Gautier, A. Gonzalez-de-Peredo, B. Monsarrat, J.P. Girard, et al., *IL-33 is processed into mature bioactive forms by neutrophil elastase and cathepsin G.* Proc Natl Acad Sci U S A, 2012. **109**(5): p. 1673-8.

CURRICULUM VITAE

NATHACHIT LIMJUNYAWONG
500 W. University Pkwy, Apt 4D
Baltimore, MD 21210
(443)-310-9913
nlimjun1@jhu.edu, nlimjunyawong@gmail.com

EDUCATION

2010 -2015 **Doctoral of Philosophy**
Johns Hopkins Bloomberg School of Public Health • Baltimore, MD, USA
Department of Environmental Health Sciences
Dissertation: "Pulmonary Immune Environment Determines the Manifestation of Experimental Emphysema"

2005 - 2009 **Bachelor of Science**
Chulalongkorn University • Bangkok, THAILAND
Major: Biology
1st Class Honors with academic golden medal

SCHOLARSHIPS

2010 – 2015 **Graduate study**: Scholarship from Anandamahidol Foundation, Thailand (King Rama VIII's scholarship)

2005 – 2008 **Undergraduate study**: Scholarship from the Science Human Resource Development Project, Office of the Higher Education Commission, Ministry of Education, Thailand

RESEARCH EXPERIENCE

2011 – 2015 Doctoral and collaborative research, Laboratory of Dr. Wayne Mitzner
Johns Hopkins Bloomberg School of Public Health • Baltimore, MD, USA

- Explored the susceptibility and mechanisms underlying the pathogenesis of lung diseases (COPD, asthma, pulmonary fibrosis and acute lung injury), including pathophysiology, molecular and immunological mechanisms, and epigenetic alteration (microRNAs and methylation) in animal models.

2008 – 2009 Undergraduate research, Laboratory of Dr. Suchinda Malaivijitnond
Primate Research Unit, Chulalongkorn University • Bangkok, Thailand

- Studied the effects of *Pueraria mirifica* (a Thai phytoestrogen-rich herb) on mouse alveolar tissue regeneration after ovariectomy-induced airspace enlargement.

2008 Summer internship research, Young Scientist and Technologist Programme, Laboratory of Dr. Sutipa Tanapongpipat
National Science and Technology Development Agency, Pathumthani, Thailand

- Characterized a new yeast strain isolated in Thailand for its potential as a new protein expression host.

2007 Junior student mini-project research, Laboratory of Dr. Suchinda Malaivijitnond
Science Human Resource Development Project, Bangkok, Thailand.

- Studied the effects of phytoestrogens (puerarin and genistein) on changes of estrus cycle in immature female rats.

TEACHING EXPERIENCE

2012-2014 **Graduate Teaching Assistant**
"Fundamentals of Human Physiology" (terms 2 & 4)
Johns Hopkins Bloomberg School of Public Health

2009 **Teaching Assistant**
"Animal Physiology Laboratory" for Thailand Biology Olympiad (TBO) camp
Chulalongkorn University

PUBLICATIONS

Collin SL, Chan-Li Y, Oh M, Vigeland CL, **Limjunyawong N**, Mitzner W, Powell JD and Horton MR. 2015. Vaccination induced tissue resident memory cells arrest and reverse pulmonary fibrosis. (in review).

Lagassé HAD, Anidi IU, Craig JM, **Limjunyawong N**, Mitzner W and Scott AL. 2015. Recruited monocytes limit malaria-induced lung injury through CD36-mediated clearance of sequestered infected erythrocytes. (in review).

Limjunyawong N, Mock JR and Mitzner W. 2015. Instillation and fixation methods useful in mouse lung cancer research. (accepted, *J. Vis. Exp., 1, 2015*).

Alder JK, Barkauskas CE, **Limjunyawong N**, Kembou F, Tuder RM, Stanley SE, Mitzner W and Armanios M. 2015. Telomere dysfunction causes alveolar stem cell failure. *Proc. Natl. Acad. Sci. U.S.A., 2015*. (Apr 3) [Epub ahead of print].

Limjunyawong N, Fallica J, Horton M and Mitzner W. 2015. Measurement of the Pressure-Volume Curve in Mouse Lungs. *J. Vis. Exp.,* (95), e52376, doi: 10.3791/52376.

Limjunyawong N, Fallica J, Ramakrishnan A, Datta K, Gabrielson M, Horton M and Mitzner W. 2015. Phenotyping mouse pulmonary function *in vivo* with the lung diffusing capacity. *J. Vis. Exp.,* (95), e52216, doi:10.3791/52216.

Limjunyawong N, Kearson A, Das S and Mitzner W. 2014. Effect of point sampling density in quantifying mouse lung emphysema. *Anat. Rec.*, doi:10.1002/ar.23085.

Mock JR, Garibaldi BT, Aggarwal NR, Jenkins J, **Limjunyawong N**, Singer BD, Chau E, Rabold R, Files DC, Sidhaye V, Mitzner W, Wagner EM, King LS and D'Alessio FR. 2014. Foxp3+ regulatory T cells promote lung epithelial proliferation. *Mucosal Immunol.*, 7 (6): 1440-51.

Limjunyawong N, Mitzner W and Horton MR. 2014. A mouse model of chronic idiopathic pulmonary fibrosis. *Physiol. Rep.*, 25;2 (2): e00249.

Cheng RY, Shang Y, **Limjunyawong N**, Dao T, Das S, Rabold R, Sham JS, Mitzner W and Tang WY. 2014. Alterations of the lung methylome in allergic airway hyper-responsiveness. *Environ. Mol. Mutagen.*, 55 (3): 244-55.

Malaivijitnond S, Tungmunnithum D, Gittarasanee S, Kawin K and **Limjunyawong N**. 2010. Puerarin exhibits weak estrogenic activity in female rats. *Fitoterapia.*, 81 (6): 569-76.

ABSTRACTS & PRESENTATIONS

Limjunyawong N, Craig JM, Scott A and Mitzner W. (Poster Presentation)
STAT3 signaling in myeloid cells promotes elastase-induced emphysema
May 2014 • American Thoracic Society 2014 International Conference

Craig JM, **Limjunyawong N**, Scott A and Mitzner W. (Poster Presentation)
ST2-deficiency attenuates the severity of elastase-induced emphysema
May 2014 • American Thoracic Society 2014 International Conference

Bradley CC, Craig JM, **Limjunyawong N**, Lagassé, HAD, Mitzner W and Scott A. (Poster Presentation)
The dynamics and depletion of neutrophils in an elastase model of emphysema
May 2014 • American Thoracic Society 2014 International Conference

Limjunyawong N, D'Alessio F and Mitzner W. (Poster Presentation)
Protective role of miR-146a in LPS-induced acute lung injury
February 2014 • Delta Omega Scientific Poster Competition 2014

Limjunyawong N, D'Alessio F and Mitzner W. (Poster Presentation)
Protective role of miR-146a in LPS-induced acute lung injury
January 2014 • Environmental Health Sciences Departmental Research Retreat 2014

Limjunyawong N, Rivers J, Horton MR and Mitzner W. (Poster Presentation)
A mouse model of chronic interstitial pulmonary fibrosis
May 2013 • American Thoracic Society 2013 International Conference

Tankersley CG, Tang WY, Rabold R, **Limjunyawong N** and Mitzner W. (Poster Presentation)
Ozone-induced lung resistance differs among pre-pubescent leptin deficient mice
May 2013 • American Thoracic Society 2013 International Conference

Kearson A, **Limjunyawong N**, Das S, and Mitzner W. (Poster Presentation)
Effect of point sampling density in quantifying mouse lung emphysema
May 2013 • American Thoracic Society 2013 International Conference

Limjunyawong N, and Mitzner W. (Poster Presentation)
Role of Nrf2 transcription factor in ozone-induced emphysema in mice
April 2013 • Experimental Biology 2013 Conference

Limjunyawong N, Das S, Tang WY and Mitzner W. (Poster Presentation)
Gender difference in lung miR-146a expression in elastase-induced emphysema mice
May 2012 • American Thoracic Society 2013 International Conference

Limjunyawong N, Malaivijitnond S, and Srisuma S. (Poster Presentation)
Effects of *Pueraria mirifica* herb on mouse alveolar regeneration after ovariectomy-induced airspace enlargement
June 2009 • 16th International Congress of Comparative Endocrinology 2009

Limjunyawong N, Malaivijitnond S, and Srisuma S. (Oral Presentation)
Effects of *Pueraria mirifica* herb on mouse alveolar regeneration after ovariectomy
March 2009 • Science Forum 2009, Faculty of Science, Chulalongkorn University

OTHER AWARDS

2014	1st place award for poster presentation, Environmental Health Sciences Departmental Research Retreat 2014
2009	Travel award from the International Brain Research Organization-Asia Pacific Regional Committee (IBRO-APRC) Associate School
2009	Best academic performance in the Faculty of Science (Professor Dr. Tab Nilanithi Medal)
2009	Travel award for Exchange Student Program at the Laboratory of Veterinary Physiology, Tokyo University of Agriculture and Technology, Japan
2009	1st place award for oral presentation in Biological Sciences, the Hitachi Trophy 2009, the 17th Science Forum, Faculty of Science, Chulalongkorn University
2008	2nd place award for oral presentation, the Chulabhorn Graduate Institute (CGI) Award for Young Scientists 2008
2008	Summer internship training grants of the "Young Scientist and Technologist Programme: YSTP" for summer research training, National Science and Technology Development Agency (NSTDA), Thailand

LABORATORY SKILLS

- Animal (mouse and rat) and infectious agents handling, ovariectomy, evaluation of estrous cycle, pulmonary functional tests, bronchoalveolar lavage, bone marrow isolation and adoptive transfer of immune cells
- Bacterial and yeast cell culture, mammalian cell culture (primary and cell lines), transfection of siRNA
- DNA/RNA/miRNA/protein isolation and purification, nuclear protein extraction, standard and real-time PCR, western blotting, ELISAs
- Tissue preparation for histological processing, immunohistochemistry and immunofluorescence microscopy
- Recombinant DNA cloning, electroporation, transformation, protein expression and purification
- Multicolor flow cytometry and intracellular staining
- DNA methylation and hydroxymethylation quantification, methylation-specific PCR (MSPCR) and bisulfite genomic sequencing